Study of High Packing Density and High Transfer Rate Encoder/Decoder

ORION PRODUCTS, INC.
SUNNYVALE, CALIFORNIA

STUDY OF HIGH PACKING DENSITY/HIGH TRANSFER RATE ENCODER/DECODER

by

John Wood
Orion Products Inc.

Prepared for
Massachusetts Institute of Technology
Lincoln Laboratory

PRIME CONTRACT AF 19(628)-5167

FOREWORD

This final report culminates work performed in accordance with purchase order No. CC-975, issued by Massachusetts Institute of Technology (Lincoln Laboratory) dated 1 April, 1966. This purchase order was issued in response to a proposal prepared by John F. Wood and submitted by Orion Associates dated 31 December, 1965.

SUMMARY

Orion Products, Inc. (formerly Orion Associates) herein submits a final report for the evaluation of a narrow band/phase modulated (NB/PM) digital encoding/decoding technique.

The report covering the NB/PM encoder/decoding technique deals primarily with the evaluation of this system in terms of digital bit error rates as a function of digital bit packing density. The evaluation is based on a series of comprehensive tests conducted by controlled procedures.

A working breadboard of the encoder/decoder system consisted of the NB/PM encoder and the signal processing, decoder and data reconstitution circuitry. The NB/PM encoder is designed to accept standard formatted NRZ digital data and transform this data into an encoded narrow band/phase modulated signal. This signal is then recorded and processed through a standard magnetic tape recorder. In reprocessing the data off the tape, the signal is fed to the decoder and conditioned, decoded and reconstituted into the original NRZ data format. Schematics of the Encoder/Decoder used for these tests are shown at the back of the report.

The analysis and evaluation of this NB/PM encoding/decoding system consisted of running tests that compared the fidelity of the recovered data off tape with that originally recorded. Prime consideration was given to insuring that the ultimate results were

meaningful with respect to the possibility of applying this technique to any existing tape recording system. To this end, special test equipment was designed and built which permitted the actual testing of this system to be conducted under realistic operation conditions and in a comprehensive manner. In addition, the test equipment and the criteria used for testing permitted the accumulation of test data that was adequate and sufficient to allow for thorough analysis of the system.

A pseudo-random code generator that is in effect a digital pseudo-random noise generator was used as the final data generator for generating a digital code pattern test. To permit an analysis and evaluation of the system using worse-case codes, a recirculating 8- or 16-bit static word generator was used. The checkout portion of the system consisted of a digital bit-error detector that permitted the detection of bit errors on a continuous bit-for-bit basis.

The error checkout portion of the test equipments primary function consisted of detecting bit errors and accumulating these errors in a totalizing counter. The totalized errors were periodically recorded on an incremental sampling basis for ultimate reduction and presentation in the form of a graphic display. The graphic displays consist of bit-error profile curves in addition to a Poisson distribution plot of the number of bit errors vs the number of error totalizing samples. The displays are graphic presentations showing the performance of the system both on a quantitative and qualitative basis. The collated results of all the tests are presented in graphical form to show quantitatively the overall performance of this system in a statistical manner.

Accepted for the Air Force
Franklin C. Hudson
Chief, Lincoln Laboratory Office

CONTENTS

ILLUSTRATIONS

TABLES

INTRODUCTION

As digital data processing systems become increasingly sophisticated greater demands are being made on the technology of data storage devices. As the sophistication of these data processing systems increase their field of application and utilization keep expanding. This inevitably results in increasing demand for larger and more efficient bulk storage devices. This demand is manifested primarily in the areas of increased data packing densities, high data transfer rates and lower data error rates. The limiting factor in most of these data processing systems at present is the data storage devices. As the overall efficiency and reliability of data storage devices increase the overall operating efficiency of most data processing systems will increase automatically.

Considerable development effort has been expended toward increasing the data storage capacity of bulk storage devices and toward improving the fidelity of the data as it is being processed on and off the storage media. The two primary parameters of interest are data packing densities and data error rates. The major contributing factors that have heretofore prevented any significant improvement in these areas have been the lack of a perfect media upon which to store the data and the intrinsic imperfections of the basic mechanism used to transport this media during the processing of the data.

Most of the effort to improve the overall performance level of the two basic parameters, information packing density and information fidelity, has been concentrated primarily in the area of "brute-forcing" the performance level of the operating parameters of the media (magnetic tape or magnetic surface) and that of the magnetic media transport mechanism. Very little effort has gone into attempting to extend the performance level of magnetic media transport mechanisms with respect to these basic parameters by designing the signal processing system as an integral and operational part of the media transport mechanism. The obvious exception to this has been in the area of rotary head television tape recorders. In these rotary head recording systems, complex as they are, the signal processing system becomes somewhat of an integral part of the mechanism in that it compensates and corrects for a great many of the system deficiencies resulting from mechanically induced distortions.

The digital encoding/decoding system described in this report is a significant step in that direction as it has, to a very large degree, overcome several of the more obvious deficiencies of the tape mechanism in recording digital data at very high bit packing densities. This encoding/decoding system in addition to improving the overall information storage efficiency of a tape recording system increases the overall performance level with respect to data fidelity. This NB/PM Encoding/Decoding system allows a significant improvement of the overall performance level of any digital recording system.

DATA ENCODER AND DATA FORMAT

The narrow band/phase modulated (NB/PM) encoder accepts standard NRZ encoded digital data and transforms the data into a format having these discrete frequency components. The intervals between the data transitions out of the encoder that contain information are held at a discrete 2-3-4 ratio in relation to the basic clock repetition rate. These transitions contain the information in a relatively narrow frequency band regardless of the incoming data code pattern. The lowest frequency in this band is (2f) while the highest is (4f) where (4f) is equal to the data clock frequency. This compares with any random NRZ code pattern covering a frequency spectrum from dc (all digital logic "0"s) to data clock (all digital logic "1"s).

The idea of transforming or generating digital data into a relatively narrow frequency spectrum is not particularly new or unique, (Fig. 1). Most other narrow band systems require one cycle (two transitions of quiescent state or two flux reversals on tape) to define a digital logic bit. The systems described here contain twice the data per cycle of information. This can be noted by comparing the waveforms of (B) and (D) with that of waveform (E) (Fig. 1). The energy spectrum of data clock that is contained in the encoded data format out of the NB/PM encoder is higher and relatively flat over the frequency spectrum compared to that of a random code pattern having an NRZ format. This high energy content permits the extraction of data clock with relative ease from the recovered NB/PM encoded data regardless of code pattern.

The incoming data of a typical random pattern, in a standard NRZ format, is shown in waveform (A) of Fig. 2. Data two-phase clock is shown above in waveform C1 and $C1_D$. The primary function of the NB/PM encoder is to detect the presence of two or more consecutive digital logic "0"s in the incoming code pattern. Once two or more digital logic "0"s have been detected, transitions (flux reversals) are inserted 180° out of phase with data clock, (which is normally phase synchronous with digital logic "1"s) starting one and one-half bit periods after the digital logic "1" that precedes the two detected logic "0"s during the period that the logic "0"s continue,up until one and one-half bit periods preceding the following digital logic "1". This implies that the encoder must delay, store and interrogate three consecutive data bits for the decision period. The NB/PM data out of the encoder shown in Fig. 2 waveform (H) is delayed one and one-half bit periods relative to the incoming NRZ data.

The function of the NB/PM encoder in Fig. 2 is as follows. The incoming data clock is fed to a delay circuit which generates a two-phase clock signal 180° out of phase, and synchronous with incoming data. The incoming data is fed into the four-bit shift register. The respective outputs of register, A, B, and C is shown in waveforms A, B, and C. The outputs A, B, and C of the three registers are ANDed as are their complements $\overline{A}$, $\overline{B}$, and $\overline{C}$. The outputs of these two AND gates are NORed to give $\overline{A} \cdot \overline{B} \cdot C + \overline{A} \cdot \overline{B} \cdot \overline{C}$ as shown in waveform (D). The output of this NORed gate is used to activate an AND gate whose other input is one phase of the two-phase clock. This phase of the two-phase clock,waveform (E), is 180° out of phase with the delayed data.

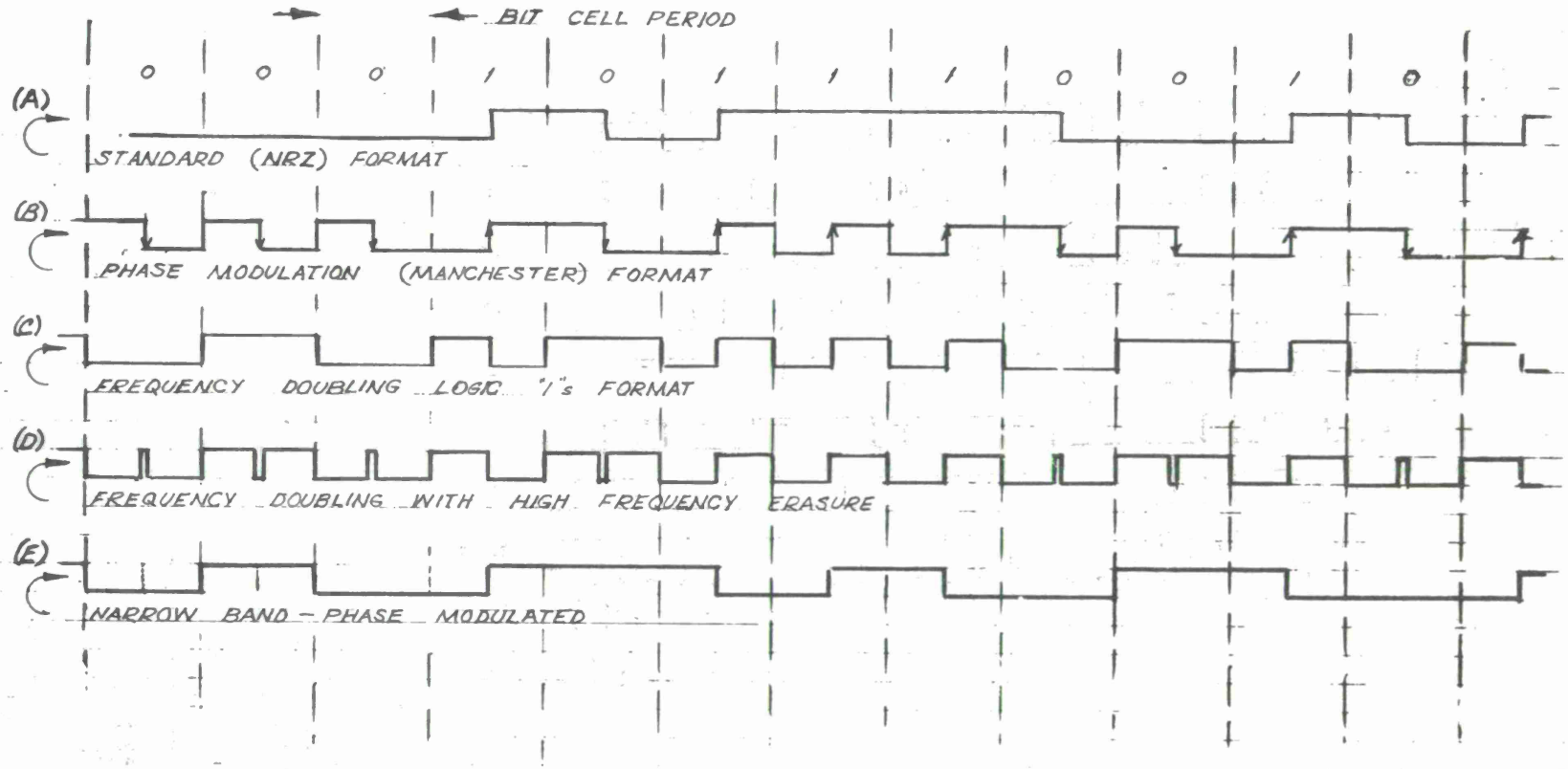

Fig. 1 Various Narrow Band Encoding Formats

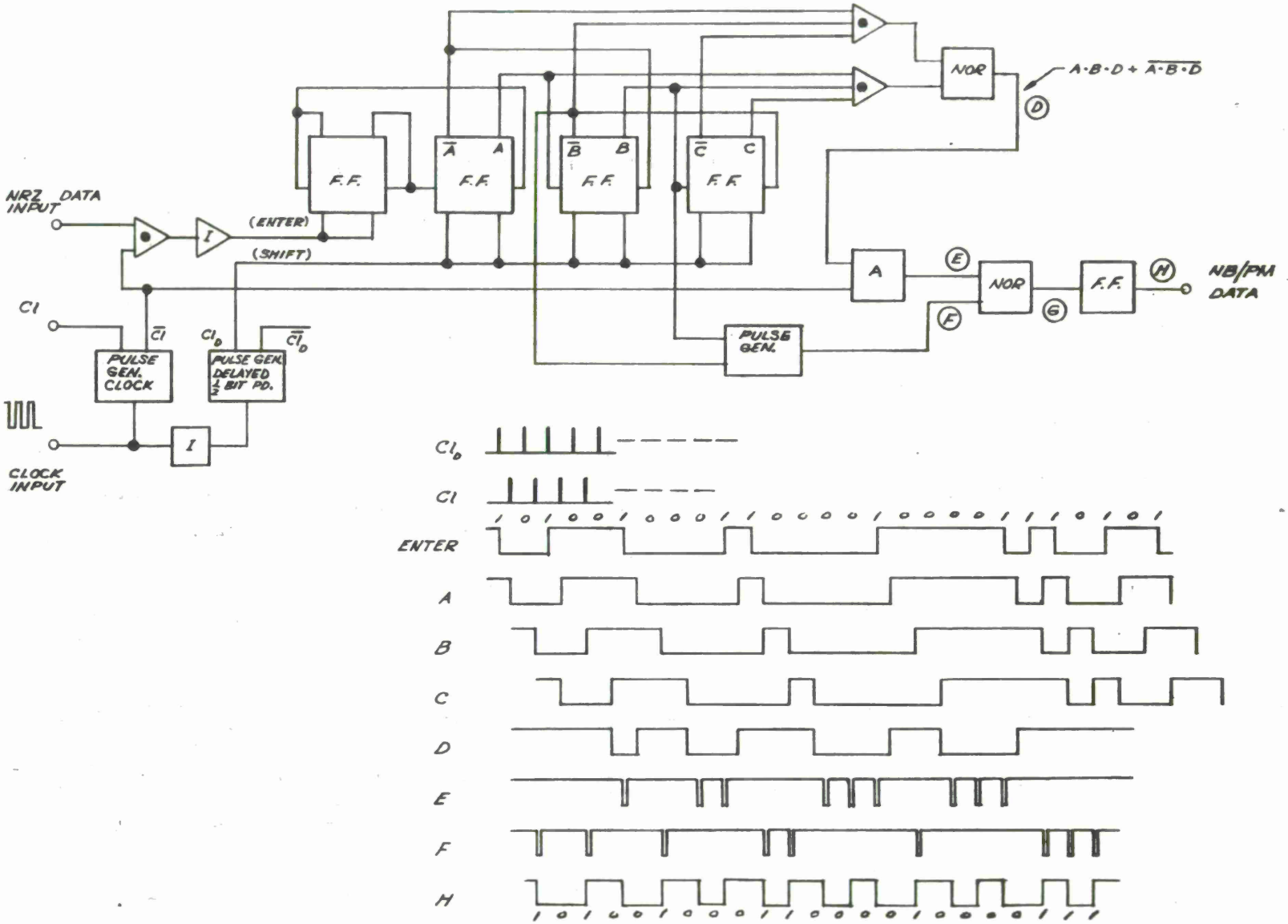

Fig. 2 NB/PM Encoder Block Diagram

The output of the second shift register (B) together with its complement ($\overline{B}$) drives a pulse generator that generates pulses synchronous with the positive and negative going NRZ transitions. The output of this pulse generator is shown in waveform (F). Both (E) and (F) are NORed to give waveform (G). This signal drives a bi-stable flip-flop (FF) whose output waveform (H) is the NB/PM encoded data.

The encoded NB/PM digital data format has distinct advantages over other narrow band digital formats when utilized as a self-clocking encoded system. Other narrow band digital encoding schemes contain clock information. However, when clock extracting circuits, such as a phase-lock oscillator (PLO) are used to extract data clock from a random generated code pattern,a clock synchronization pattern must be inserted to force the PLO to lock in the proper phase relative to the data. This usually places a limitation on the data acquisition portion of a system in that the data link must be broken periodically to insert a clock synchronization pattern. This can be shown in the following example. If one were to traverse a random narrow band generated code pattern such as waveform (B) or (C) in Fig. 1 with an "optical window" (interrogation gate) it would be impossible to tell which phase to synchronize to for the purpose of strobing the intelligence from the encoded waveform unless one were first "mentally" phase coherent and synchronized to the data intelligence.

The NB/PM encoded data format shown in waveform (E) contains clock and phase coherent synchronous information. This phase coherent information is contained in every digital logic "1-0-1" code pattern. This encoded three-bit code pattern provides a

"signature" that allows us to recognize and detect, if properly interrogated, a phase synchronous signal. At the instant of detection and recognition we are able to phase align to the intelligence in the encoded data. A description of this "1-0-1" code pattern recognition circuit is described in the signal decoder and reconstitution section.

An extension of the NB/PM encoder is shown in Fig. 3. The waveform timing diagram for this version of the encoder is shown in Fig. 4. This version of the encoder contains the head current modulator with associated logic.

The head current modulator is used primarily to provide pre-emphasis of the recorded signal at the higher bit packing densities. At the higher data packing densities, the frequency response of the record/reproduce system drops off in both linear record/reproduce systems and direct (saturation) record/reproduce systems. In a linear system this decrease in amplitude manifests itself as noise in the recovered reproduced signal off tape (Fig. 5a). In a direct (saturation) record/reproduce system this loss in response of the higher frequency components (self-erasure of adjacent bit cells) is manifested as a d-c shift in the recovered signal zero crossovers. See Fig. 5b. The recovered information is contained in the zero crossovers. In Fig. 5b we see that a saturation recorded signal shows the zero crossover has a d-c shift component that is a function of the frequency components contained in the encoded data pattern. The head current modulator helps to compensate for these effects by providing a degree of pre-emphasis during the record mode.

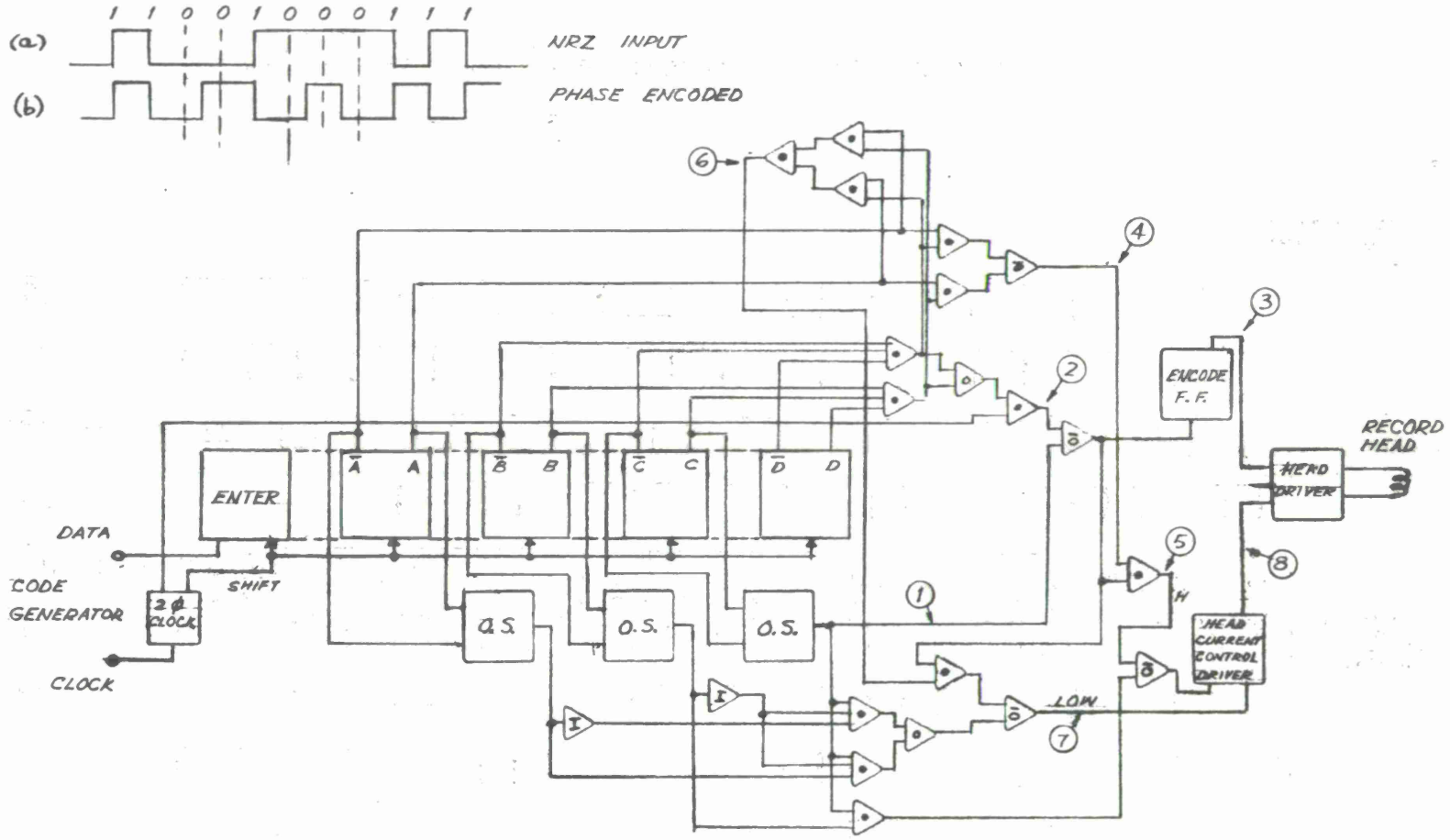

Fig. 3 NB/PM Encoder and Head Current Modulator - Block Diagram

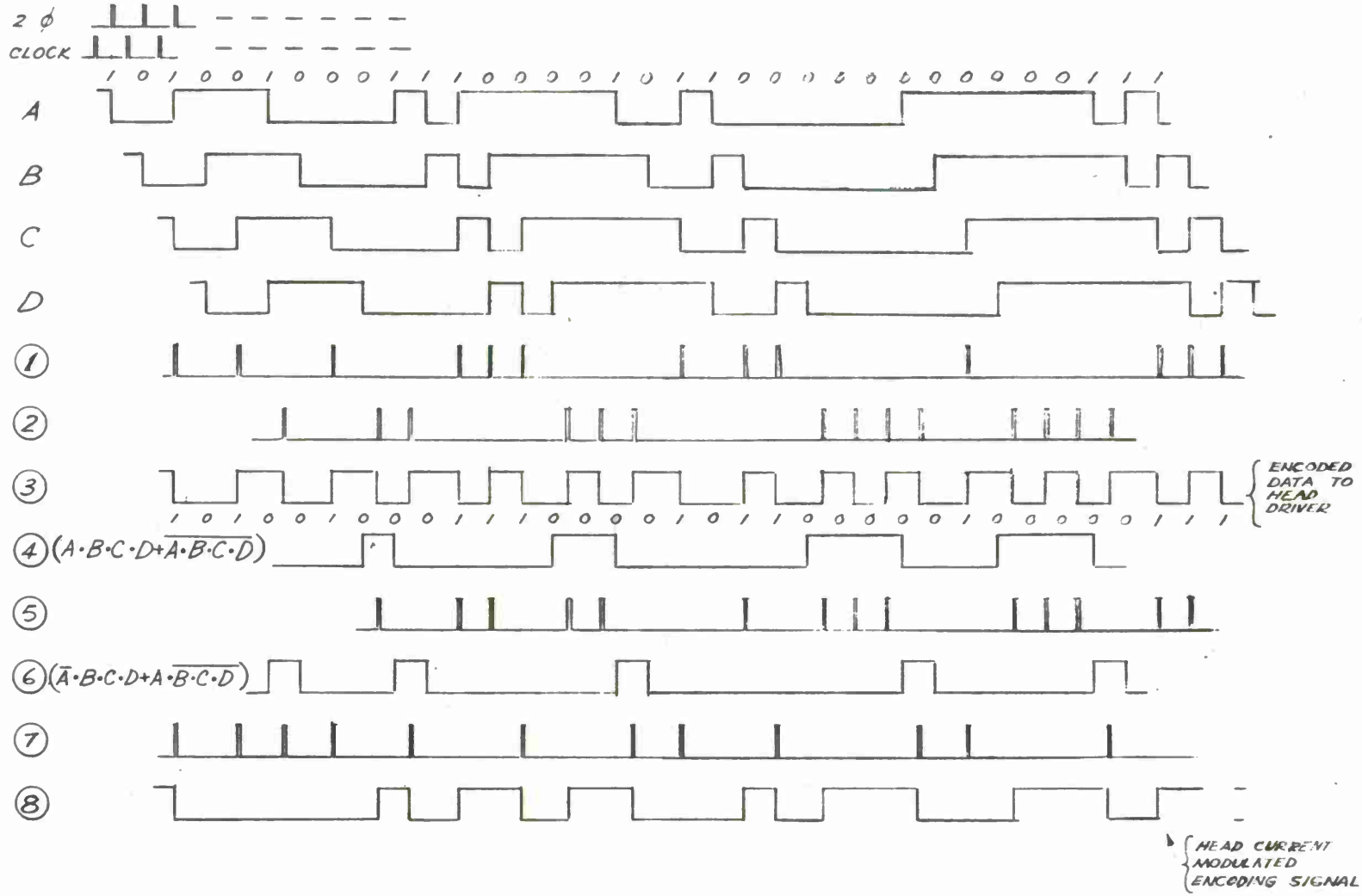

Fig. 4 Waveform Timing Diagram for NB/PM Encoder

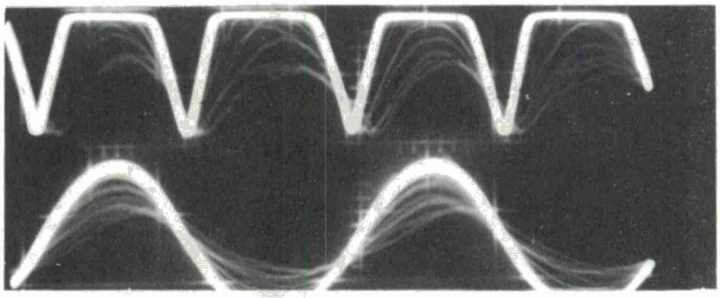

(a) AM Noise in Zero Crossovers of Signal from Linear Systems

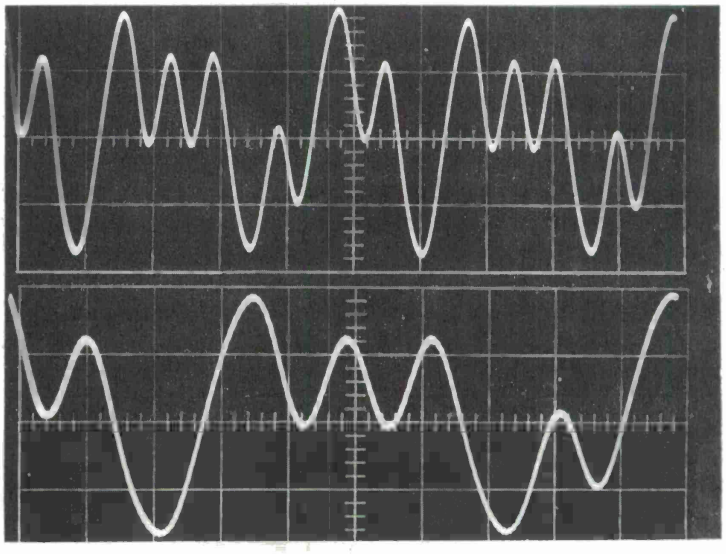

(b) d-c Shift Effect of Zero Crossovers in Saturation Record System

Fig. 5 Photographs of Signals from Saturation and Linear Record Systems

The head current modulator operates on the following basis. For an encoding pattern containing low frequency components the head current is adjusted to some optimum value of "x". The three distinct encoding patterns where this occurs are, "1-0-1", "1-0-0" and a "0-0-1". For those remaining encoding patterns containing higher frequency components, the head current is switched to some value greater than "x". These latter encoding patterns contain all digital logic "0"s or "1"s and consist of either of the two clock phases. Usually the head current is adjusted to give a maximum output at the higher frequencies (data clock rate) and the head current for the lower frequency components adjusted to optimize and normalize the reproduced output during periods when a combination of such encoding patterns occur.

The encoder portion is the same as that shown in Fig. 2 with the exception of the additional logic for the head current modulator. The function of the head current modulator logic is to provide a "high head current gate" at the instant when either a "0-0-0" or "1-1-1" encoding pattern is detected and a "low head current gate" at the instant that either a "1-0-1", "1-0-0" or a "0-0-1" encoding pattern is detected. The "high head current gate" is generated whenever the Boolean algebraic equation $\left[(A \cdot B \cdot C \cdot D) + \overline{(A \cdot B \cdot C \cdot D)}\right]$ is satisfied while the "low head current gate" is generated whenever the Boolean algebraic equation $\left[(\bar{A} \cdot B \cdot C \cdot D) + (A \cdot \overline{B \cdot C \cdot D})\right]$ is satisfied. These two gates are generated at points (4) and (6) respectively. The outputs of these two gates are ANDed with both phases of data clock and both AND gate outputs used respectively as "Set" and "Reset" signals of the head current FF driver. The output waveform of this head current driver is shown at point (8).

DECODER AND DATA RECONSTITUTION SYSTEM

The block diagram of the decoder and data reconstitution circuitry is shown in Fig. 6. The block diagram can be separated into three specific functions:

(1) Signal processing

(2) Decoder

(3) Data reconstitution

The signal processing portion conditions the reproduced signal from the recorder prior to decoding. Since the error rate tests were conducted using a linear (direct record/reproduce) system the signal processing portion of the decoder/data reconstitution circuitry conditions the signal via linear passive elements. The direct record/reproduce signal from the recorder is first fed to a filter having a corner at approximately 300 cps and 1.5 mc. The signal out of the filter looks into a wideband operational amplifier. The transfer function of the amplifier is adjustable over the data transfer rates of interest to compensate for (and to equalize) the recovered signal off tape. This conditioned signal is then fed to a wideband limiter to recover the encoded information in the zero crossovers. The dynamic gain of the limiter used in this system was approximately 20 db. The gain of the limiter, as well as the compensation and equalization, is to a large degree a critical part of the system relative to errors. This is particularly true for those sources of errors that are induced as a function of excessive amplitude modulation of off-tape signals. Since the on/off tape process is not a true linear system, the compensation and equalization are primarily to correct for the amplitude and phase distortions

introduced through the system. The main function of the limiter is to maximize the recovered signal symmetrically around a very narrow a-c zero threshold reference. See Fig. 7.

The decoding portion of the circuitry extracts the original digital generated data from the recovered NB/PM encoded signal in an RZ format. The recovered signal after limiting drives two one-shot multivibrators. The duration of the pulse out of one-shot #2, refer to Fig. 6, is adjusted for some optimum value that is dependent upon the bit packing density and the accumulative peak-to-peak timebase error difference (TBED). The pulse out of this one shot is one input to an interrogation AND gate. The other input to this AND gate is the reconstituted data clock. The duration of the clock strobe pulse, as with the zero crossover pulses, are adjusted for some optimum value dependent on the bit packing density as well as the accumulative peak-to-peak TBED of the system. See Fig. 7 (a) and (b).

The waveforms (e), (g) and (h) of Fig. 7(a) show the zero crossover pulses, point (e) Fig. 6; reconsituted clock point (g) Fig. 6 and reconstituted RZ digital logic "1"s point (h) Fig. 6 respectively. The duration of the data clock gate shown in (g) of Fig. 7(a) is sufficient to strobe all of the encoded digital logic "1" information contained in the zero crossovers that were inserted 180^{o} out of phase in the encoder. It can be noted that the first zero crossover pulse of waveform (e) lines up slightly to the left of center of the second clock strobe pulse of waveform (g). The second zero crossover waveform (e) is somewhat to the right of center of the third clock strobe pulse, and appears in waveform (h) to be inhibiting approximately

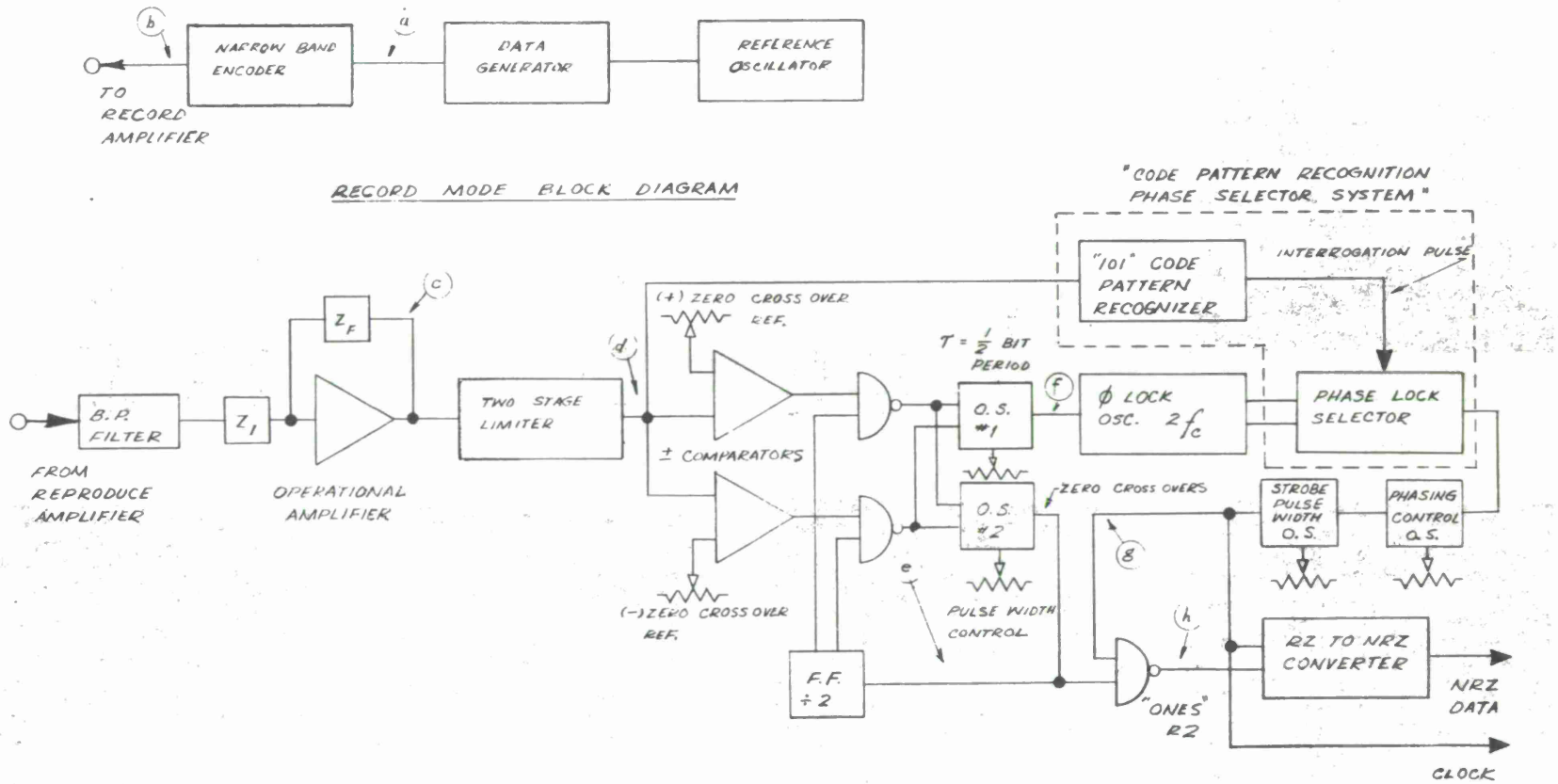

Fig. 6 Decoder and Data Reconstitution Block Diagram

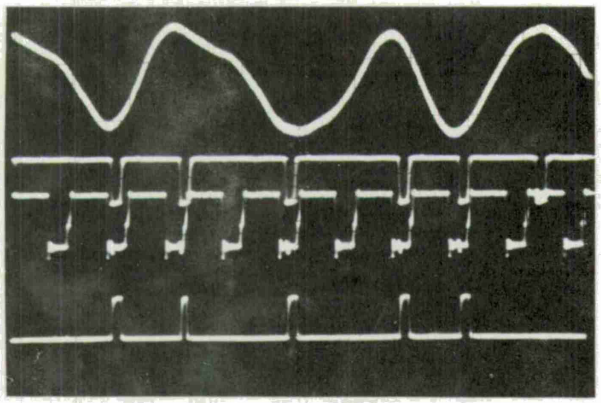

(a)

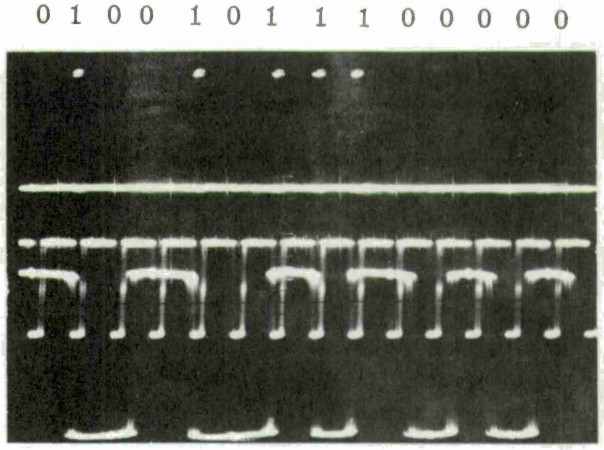

(b)

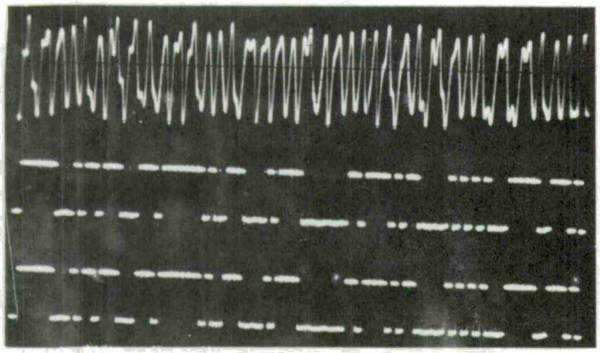

(c)

c Recovered Signal off Tape

Reconstituted Data in NRZ Format Delayed 8 Bits

Output Data from Pseudo-Random - Code Generator

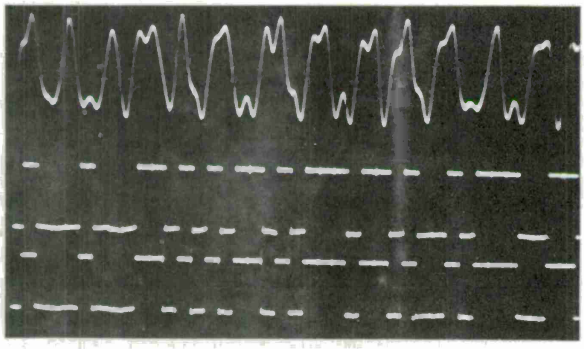

(d)

c Same Waveforms shown in (c) above - Expanded Sweep

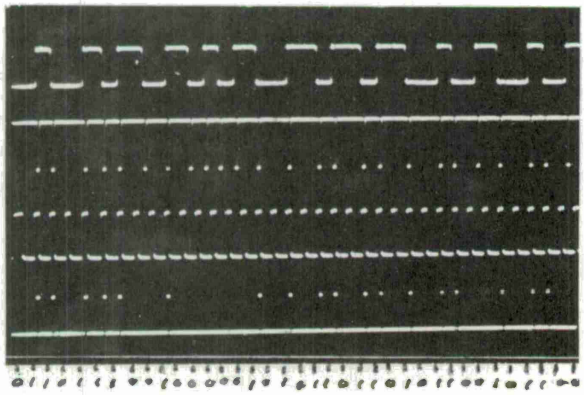

(e)

d Output Signal from Limiter

e Zero Crossover Pulses

g Reconstituted Data Clock Strobe Pulse

h Reconstituted Data in RZ Format

Fig. 7 Waveforms at Various Points in the Decoder/Reconstitution Circuit

30% of the zero crossover pulse. The sixth zero crossover pulse of waveform (e) is unsymmetrically balanced to the left of center between the inhibit portion between the ninth and tenth clock strobe pulse and is approaching the trailing edge of the ninth clock strobe pulse. This nonsymmetry of the zero crossover data relative to reconstituted clock is the result of the amplitude and phase distortions introduced in the on/off tape process. The photo of the waveforms shown in Fig. 7 (a) was taken with a time exposure of one timebase sweep period of approximately 16 us. The TBED of the information during this period is negligible. The photo in Fig. 7 (b) was taken using an exposure of approximately 10 ms with the sweep externally synchronized to clock. This photo displays the timebase error difference (TBED) relative to reconstituted clock during this 10-ms period and, in effect, shows the measurable peak-to-peak TBED of the system. This TBED figure is approximately $\pm$ 10% of a bit period for this example. Therefore, if the clock strobe pulse is adjusted to approximately 35% of a bit period and the peak-to-peak TBED of the system (during any 10-ms period) is $\pm$ 10% of a bit period this would allow for a total amplitude and phase distortion figure of slightly less than 15% of a bit period before error dropouts or dropins occur.

This would indicate that the example shown in Fig. 7(a) is marginal. Actually the system is well within the marginal limits since the value given in the above example for the peak-to-peak TBED is erroneous and does not apply in the actual system used for these error-rate tests. The frequency response (tracking response) and the dynamic range of the PLO used for these tests was more than adequate for the timebase perturbations typically experienced (with the exception of

extreme or unusual cases) with the type of tape transport used for these tests.

The data obtained at point (h), refer to Fig. 7, after strobing is recovered digital logic "1"s in an RZ format. This data together with reconstituted clock is fed to a data format converter that reconstitutes the data into an NRZ format. The data at this point, including clock, is fed into the bit-error detector and error totalizer.

The data clock reconstitution portion of the decoder includes a PLO, a code pattern recognization detector and a phase lock selector. The PLO used for these error rate tests utilized a commercially available product. The unit incorporates standard techniques in the area of providing a phase locked loop/voltage controlled oscillator (VCO) signal. The input to the PLO is the output of a one-shot multivibrator that is activated by the positive and negative data zero crossover transitions out of the signal limiter amplifier. The period of the one-shot is adjusted to one-half the period of the recorded data clock period. This gives frequency components of 4f, 6f and 8f, where 4f is the basic data clock. The frequency contains a fundamental component with even order subharmonics that maintains a phase integrity relationship with the VCO in the feedback of the PLO regardless of the recorded code pattern. The quiescent VCO frequency is set at or near twice the data clock rate (8f) and will synchronously phase lock with the higher frequency component of the incoming data (8f). There is, however, a 50% probability the VCO in the feedback loop of the PLO will phase lock 180^{o} out of phase with the encoded information in the NB/PM data. The means to provide a coherent phase

lock relationship of the reconstituted data clock with the encoded intelligence is provided via a code pattern recognization detector.

Block diagrams of the "Code Pattern Recognition Phase Selector" systems (CPR) together with the timing diagram waveforms are shown in Fig. 8 and Fig. 9. When a phase lock oscillator (PLO), typical of that with this encoding scheme is used to derive a synchronous self-clocking strobe gate this "pattern recognition" technique becomes an integral part of the encoding/decoding scheme.

The particular data encoding format that was selected for this evaluation program was so done for several reasons. We are able to obtain two data bits of information per recorded cycle of data, or essentially twice that of other narrow band schemes. In addition, clock is inherent in data and the code pattern is unique in that it generates a distinct data code pattern. This code pattern allows for the recognition and detection of the proper clock phasing with respect to the digital intelligence contained in the recovered signal. Once the code pattern is detected a command pulse selects the proper clock phase coherent with encoded intelligence.

This recognizable code pattern occurs in data whenever an encoded digital logic "1-0-1" is present. It is apparent from the encoded data that if one were to arbitrarily try to determine or extract data from the encoded data format, one would not know where to phase lock the oscillator until a "1-0-1" encoded data pattern was recognized. It can be seen that a string of encoded digital logic "0"s looks, and is in fact, the same encoding pattern as a string of encoded digital logic "1"s. The duration between transitions in an all digital logic "0" pattern is the same as that for an all digital logic "1" pattern. The

difference is that the transitions in the all "0"s pattern are 180° out of phase with the correct data intelligence. If one were to mentally phase lock and synchronize on all encoded data "0"s and repetitively strobe all following data, it is obvious that the strobe would be out of phase with the correct data intelligence.

If one were to arbitrarily phase lock and synchronize to an encoded data pattern containing a digital data logic sequence of "1-0-0-1-0-0-1--------" there is a 50% probability that we would be out of phase with the correct data intelligence. The duration between transitions in this encoded pattern is 1.5 times that for an all digital logic "1"s or clock pattern. Every other transition is alternately in and out of phase with the correct data intelligence because each alternate transition falls in the center of a bit-cell period.

An encoded data pattern of "1-0-1" is the only format in this encoding scheme that allows for a signature, upon which one may recognize and detect the phase relationship of data intelligence relative to clock. The duration between these transitions is twice that of data clock and both transitions occur in phase with the correct data intelligence, digital logic "1"s. Thus, the information is contained in the encoded data that will allow for the extraction of a coherent phase lock clock from recovered data.

The purpose of the PLO is to extract from the reproduced data a reference frequency, clock, phased locked and synchronous with data. This reference frequency, since it is instantaneously synchronous with data, will provide clock information for the strobing of the conditioned reproduced data to give reconstituted data in an RZ format.

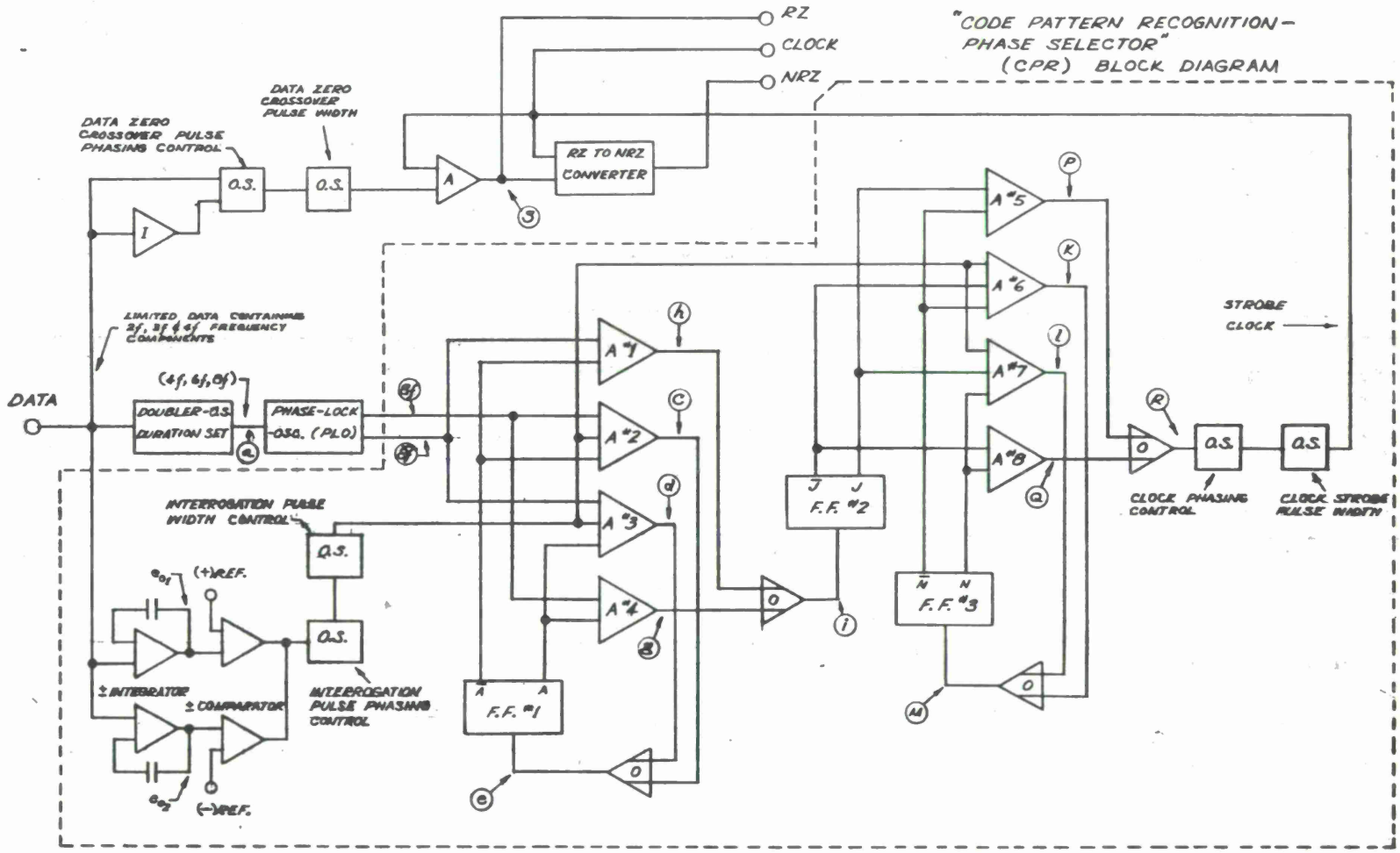

Fig. 8 Code Pattern Recognition Phase Selector (CPR)
Block Diagram

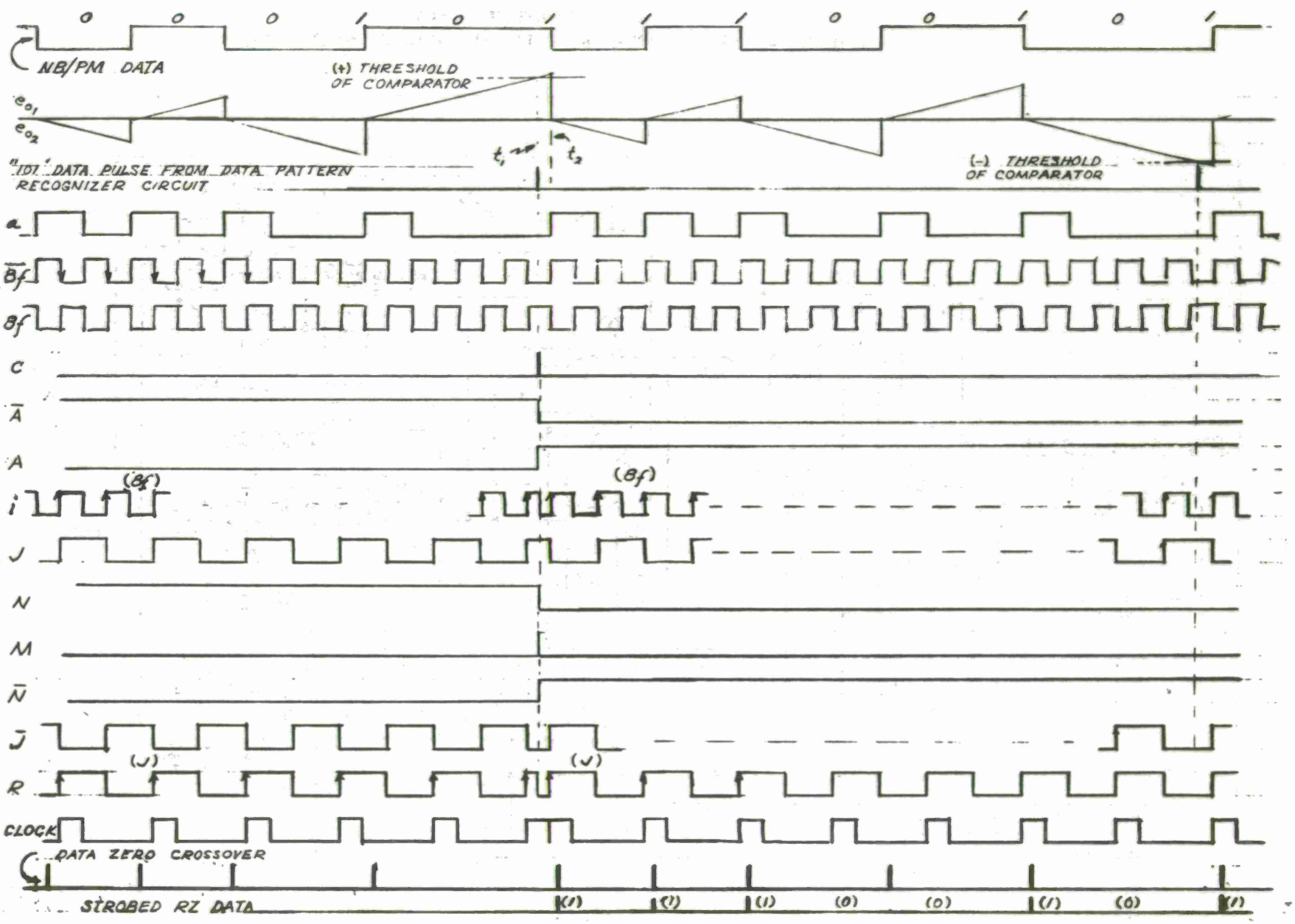

Fig. 9 Waveform Timing Diagram for (CPR)

Because of the nature in which the data is encoded it is possible during playback for the PLO to be synchronous with data but phase locked to those frequency components that are 180^{o} out of phase with the data intelligence. Or the oscillator could be phase locked with the data intelligence but 180^{o} out of phase relative to data intelligence or both. It is possible during the initial lock up period to force the PLO into the proper phase lock condition. However should loss of data momentarily cauase the PLO to lose lock, the chance of the PLO pulling in and locking on to the proper phase condition, with the CPR loop open, is one in four.

The logic sequence shown in the block diagram Fig. 8 together with the waveform timing diagram Fig. 9 is a "code pattern recognition and phase detector" that forces the output of the PLO to be in phase with, and synchronous with the correct intelligence in the recovered data. Basically, the circuit detects the presence of a data bit-code pattern of "1-0-1" and generates a recognition pulse just prior to the third data bit of the "1-0-1" pattern (a digital data logic one). This recognition pulse simultaneously interrogates the instantaneous phasing out of the phase lock oscillator in AND gates #2 and #3, and the phasing condition of the binary divider, FF #2, via AND gates #6 and #7. Since it has been confirmed via the recognition pulse that the next information bit could be a ditial data logic "1" bit the steering gates (AND gates #1 and #4 and #5 and #8) are selectively gated via their respective steering control flip-flops (FF) #1 and #3 to force the proper clock phase relationship at point (R).

The logic sequence, following the timing diagram and referring to the system block diagram, is as follows. The recovered data off tape is conditioned and at a point in the process (the output of the signal limiter) the recovered data is shown as the top waveform in the timing diagram with the appropriate assigned encoded data intelligence. This signal is fed to two linear integrators whose outputs look into plus and minus threshold comparators. One integrator integrates during the interval when the signal is in a negative state, the other when the signal is in a positive state. The rate of integration of both integrators are equal and are set at some arbitrary value of (X) volts/sec. The plus and minus reference voltages for the threshold comparators are set to a value slightly less than the time interval of two data clock periods (equivalent to the interval of a "1-0-1" data code period in the encoded waveform). When the output of either integrator reaches this value the output of the comparator generates a pulse, appropriately called an interrogation pulse, just prior to an actual digital data logic "1" in the recovered waveform. This pulse then allows for the interrogation of the synchronous relationship of the clock out of the PLO with respect to the intelligence in the recovered waveform as well as the phase relationship of the clock strobe pulse relative to a digital data logic "1".

In the example shown in the timing waveform diagram, at time (t_1) the output of the positive integrator has reached the threshold reference level of the positive threshold comparator. This generates the digital data logic "1" interrogation pulse. This pulse interrogates, simultaneously, AND gates #2, #3, #6 and #7 and detects that the wrong phase of the clock out of the PLO is being fed to the divider,

FF #2. In this example the inputs to AND gate #2 are coincident with the interrogation pulse as shown by ANDing the interrogation pulse, the signal out of the PLO (8f) and the steering control signal ($\bar{A}$). The resultant output is shown at point (C) which in turn is fed through the OR gate, signal (e), which toggles the steering control FF #1 to steer the correct clock phase out of the PLO through AND gate #4 to the input of the clock divider FF #2. The resultant waveform at point (i) at the instant (t_1) is shown to change phase just prior to the oncoming digital data logic "1" bit.

Simultaneously the interrogation pulse samples the condition of the phase of the resultant clock out of FF #2 via AND gates #6 and #7. In this example coincidence is detected in AND gate #7 with the steering control signal (N) and the clock phase signal (J). The resultant signal is shown at point (1) which is ORed through at point (M) to toggle the steering control FF #3. This signal activates AND gate #5. The correct clock phase, point (J) is then properly steered through the OR gate to give the resultant waveform at point (R). This signal activates a monostable that is used for the phasing control of the clock. The trailing edge out of this one-shot activates a clock monostable multivibrator whose pulse width is adjusted for the proper strobe period. This strobe pulse is fed to the data reconstitution strobe AND gate. The other input to this AND gate is extracted zero crossover pulses from the processed recovered waveform. The resultant output at (S) is reconstituted digital data logic "1"s in an RZ format. This RZ data together with clock is then converted to an NRZ format.

It appears that we are reaching the limitation of the encoding/decoding system using the particular recorder used to run these error-rate tests. The incremental timebase perturbation characteristics of this machine introduce incremental varying frequency components into the recorded and reproduced data during both the record and reproduce periods. The total effects on the reproduced data is cumulative. The incremental rate of change and deviation of these incremental frequency components, at times force the reproduced data beyond the linear limit tolerances required for adequate phase synchronization with the PLO. The synchronization of recovered information with recovered data clock is also critical to the deviation difference from a known frequency reference and the period during this deviation difference. The former requires a tight loop PLO while the latter requires a PLO with sufficient dynamic range. The ability to satisfy extremes of both cases is not compatible in any feedback loop type system. Therefore, a satisfactory compromise must be found for a system exhibiting timebase perturbation characteristics. The PLO we are using performs admirably, considering the operational characteristics under which it is forced to work.

The term "incremental frequency components" as it is used here is a catch-all phrase that has been erroneously referred to in the past as flutter. It may be more accurately referred to as "timebase error difference" (TBED). This can basically be defined as the timebase error with respect to a known reference (recorded data clock) that is introduced over some fixed known incremental period (τ). The incremental rate of change $[\Delta$ (TBED)/ Δ t$]$ defines the highest frequency components within the spectrum. The ratio (TBED / τ) defines the dynamic range for a given period.

Errors drived from the rate of change of incremental TBED variations usually result in bit errors due to incremental phase shift differences between the reconstituted data clock and the processed recovered waveform at the instant it is being strobed to decode and reconstitute data. Otherwise the distortion introduced into the recovered data at these higher bit packing densities forces the phase lock oscillator to lose lock, thus, causing data bit errors during the induced distortion period. This situation is aggravated at the higher bit packing densities as the transducer-gap-to-wavelength ratio rapidly approaches unity. This introduces additional distortion in the recovered signal off tape.

Small incremental TBED will result in a small number of bit errors while the larger TBED will produce rather large "clumps" of errors. Typical numbers resulting from the former are one to ten while the latter will show fifty to a hundred or more. These will be apparent on the bit error profile curves at the higher bit packing densities.

At the lower data bit packing densities where TBED variations have little effect on errors, almost all bit errors can be attributed to a head-to-tape separation phenomenon typically caused by dirt, head clogging, tape surface nonuniformities, etc. While those occuring at the higher bit packing densities are attributable to the recorder TBED characteristics.

ERROR RATE TEST SETUP AND TECHNIQUES

A block diagram of the error-rate test setup is shown in Fig. 10. A block diagram of the Bit Error Detector and Pseudo-Random Code Generator is shown in Fig. 11. A recirculating 8-bit feedback shift register generates a repetitive 255-bit pseudo-noise, code pattern. This data is reformatted in the NB/PM encoder and recorded on tape. When reproduced off tape, this data is fed into the decoder. The decoder extracts the information and reconstitutes the data into its original format together with reconstituted data clock. This reconstituted data together with recovered clock is fed to an 8-bit shift register. The outputs from each FF in the shift register is ANDed with a two-position toggle switch. The combined outputs from all eight AND gates are ORed to give an 8-bit word recognization pulse coincident with that determined by the position of the eight toggle switches. This coincidence pulse (id pulse) is used to reset all of the registers in the pseudo-random code generator (PRCG) coincident with the reconstituted 8-bit word within the recovered pseudo-noise data pattern. This insures that synchronization of the (PRCG) generator to the recovered data pseudo-random code pattern is maintained for every cycle of the PRCG code pattern (255 bits).

The outputs of the two last FF's in both the (PRCG) and the incoming data shift register are ANDed for detection coincidence. The absence of coincidence during any bit period is detected and a bit-error pulse is generated. These pulses are fed to a totalizing counter to register the accumulated bit errors. During any appropriate error

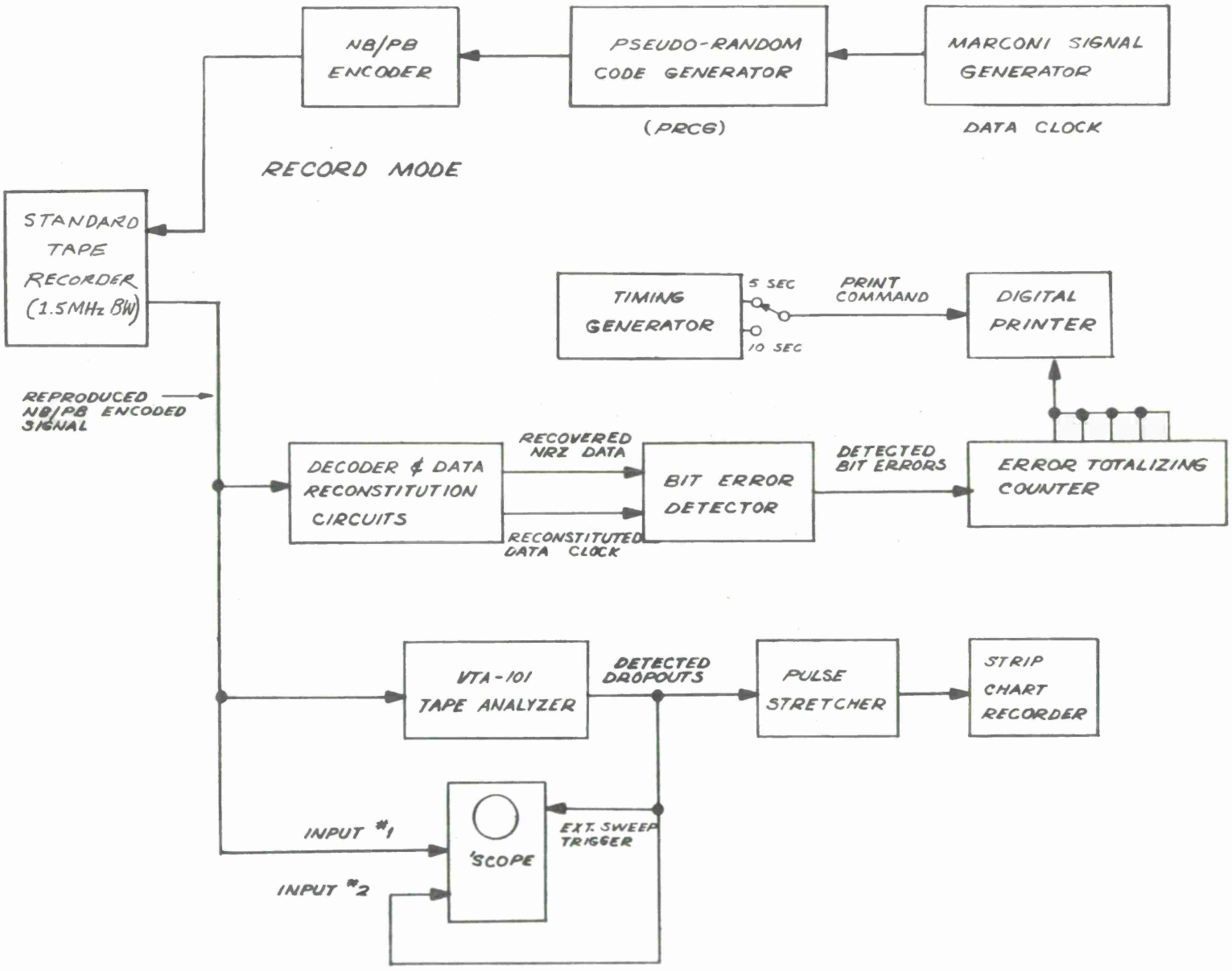

Fig. 10 Error Test Setup - Block Diagram

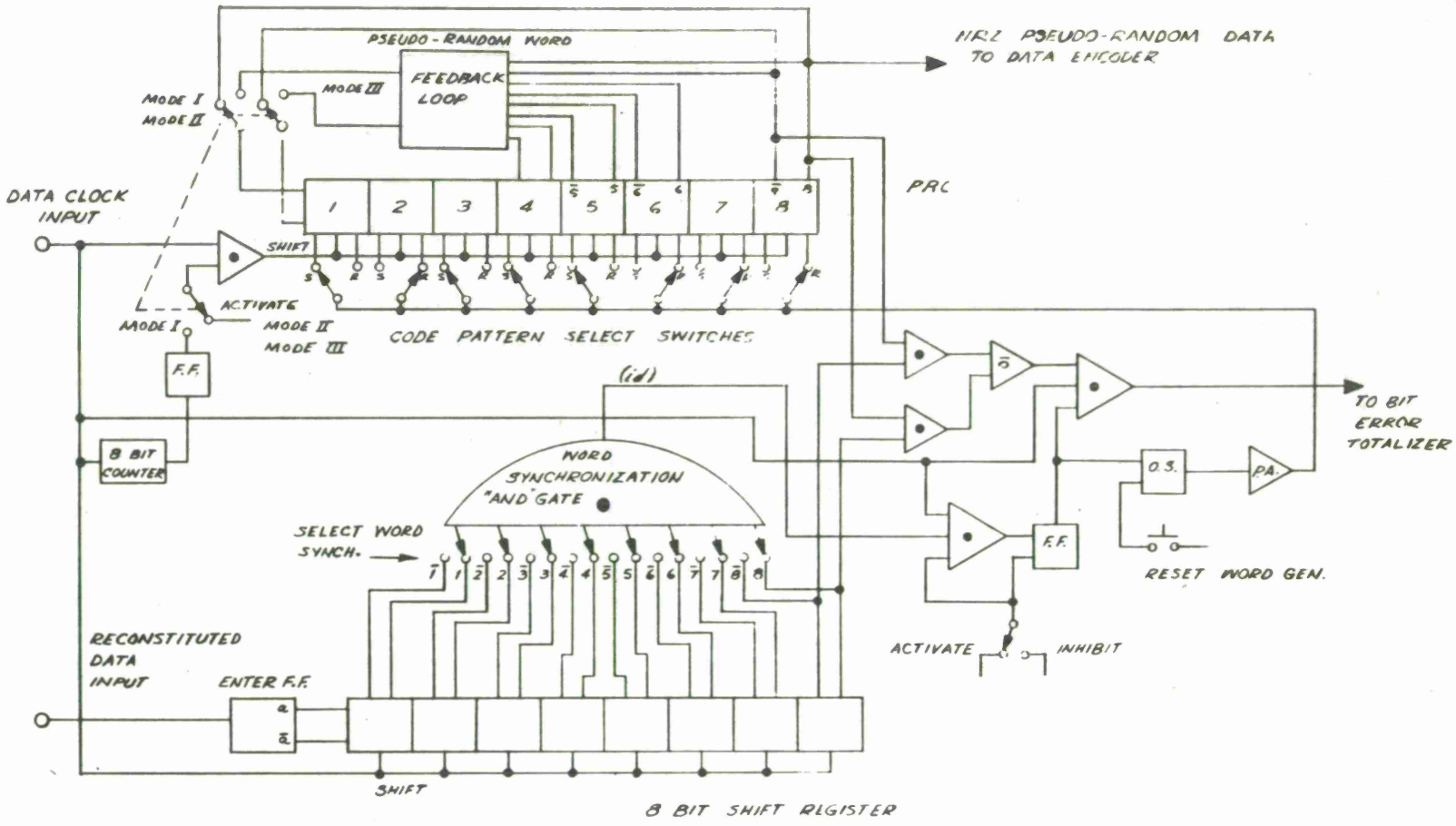

Fig. 11 Pseudo-Random Code Generator and Bit Error Detector - Block Diagram

totalizing period the bit-error accumulated count is read and recorded or printed out on a digital printer. This data is then used to graphically present the bit dropout profile in terms of the detected bit errors vs number of sampling periods.

If only the loss of recovered data occurs the bit errors totalized will then be those that do not correspond with the synchronous data from the PRCG. In almost all cases where loss of information is detected the clock out of the PLO maintains the PRCG in time synchronization with the recovered data during this period. Should the loss of information occur over an appreciable period that might force the data clock to slip for a bit period or some period less than a PRCG code pattern cycle (255 bits),the totalized bit errors will accumulate during the remainder of the 255-bit pseudo-noise code pattern cycle. A code pattern cycle is defined as that period between consecutive 8-bit word recognization coincidence (id) pulses; $2^n - 1$ (or 255 for n = 8) bits. This phenomenon results during loss of data clock because it forces the PRCG out of synchronization with the recovered data until the 8-bit word recognization (id) pulse resynchronizes the PRCG coincident with the recovered data code pattern. It is therefore possible in this system to lose one period of clock, hence obtaining one real bit error, but result in detection and registration of a total of $(2^n - 1)$ or 255 bit errors. No adjustment has been made in the error rate test results that have been conducted for these sources of error.

The primary instrumentation and test equipment used for these tests (Fig.10) consisted of a Commercial (1.5 MHz BW) recorder/reproducer, the pseudo-noise code pattern generator (PRCG) and bit error detector(described above), a Marconi Model No. TF 144H/4

signal generator (for data clock source), a CMC digital printer (when available), an Orion Products designed tape evaluation dropout detector (VTA-101) and the encoder/decoder under evaluation. The magnetic tape used during these tests was standard, commercially available tape from three of the major tape manufacturers. With the exception of the higher bit packing densities, the tape selected for a particular error rate test was on a random basis.

No special precautions were taken on either the selection of a particular reel of magnetic tape or the magnetic tape transport upon which the tests were to be conducted. Nor were any special calibration procedures performed on either the tape transport or the transport signal processing systems to insure optimum performance relative to these tests. The reason for this was to perform the error-rate test on equipments and components typical of those equipments commercially available and already existing in the field. In this way the test results that were obtained are both realistic and meaningful. This is particularly true for the purpose of evaluating this NB/PM encoding/decoding system on the basis of possible immediate application to existing installations. However, those sources of errors that were extraneous to the NB/PM encoding/decoding electronics, to the extent that they reflected on the overall performance of the systems under test were, isolated and identified whenever possible.

These tests were conducted in the following sequence. Data was recorded and reproduced in accordance to Table I. The recovered data was reproduced at a transfer rate compatible with the particular PLO used in the data clock reconstitution portion of the decoder/reconstitution circuitry. This PLO had an operatable

TABLE 1

BIT PACKING DENSITY (Kbpi)	RECORD TAPE VELOCITY (ips)	RECORD DATA TRANSFER RATE (megabits/sec)	REPRODUCE TAPE VELOCITY (ips)	REPRODUCE DATA TRANSFER RATE (Kbps)
10	120	1.2	60	600
15	120	1.8	60	900
18	30	0.54	30	540
18	120	2.16	30	540
20	120	2.4	30	600
22	120	2.64	30	660
24	60	1.44	30	720

bandwidth limit of 1.0 megabit per sec to approximately 1.6 megabits per sec.

During the error test runs, the detected data bit errors were fed to an error totalizing counter. These totalized errors were then recorded periodically every ten seconds (five seconds in some cases) and then plotted to give an error profile curve. The data was then recollated and plotted to quantitatively show the overall performance of the system in a statistical manner. This is displayed graphically as Poisson Distribution plots. The number of discrete data blocks for a given error test run is presented along the "x" axis. (Some error test runs were conducted using 10-sec data blocks while others were conducted using 5-sec blocks). The number of digital bit errors detected and accumulated during any given data block period is presented along the "y" axis.

During many of these error test runs, a special piece of test equipment, video-tape analyzer VTA-101, was used to obtain correlation between detected errors and loss of signal or signal dropouts. This piece of test equipment was designed several months ago by Orion Products as a commercial product for evaluating video tape. However the VTA-101 test equipment is directly applicable to the evaluation of any tape, digital as well as instrumentation. Basically the instrument detects loss of signal based on two parameters, signal dropout amplitude (db below some reference level) and the duration of the dropout at that level. A description of this equipment is included. See Appendix.

The recovered signal off tape was fed to the input of the tape analyzer. The Dropout Depth attenuator was set to -18db below the normal signal reference and the Dropout Duration adjustment was set at approximately 1 μs. The output of the tunnel diode threshold detector activated a one-shot monostable whose output pulse duration was adjusted to cause the pen of a strip chart to respond to a detected dropout. During a test run if any signal dropout was detected, an indication was made on the strip chart. After the test run, the time of these detected dropouts as indicated on the strip chart, was correlated against the time of occurance of detected digital bit errors. In addition, the output of the tunnel diode detector was used to trigger the linear sweep trace of an oscilloscope and was fed to one input of a dual-trace input. The other input of the vertical amplifier scope input was connected to the recovered signal off tape. These detected signal dropouts could then be observed and photographed on the scope. Correlation of signal dropouts with detected digital bit errors at the instant of occurance was immediately observable. Typical photos of detected dropouts are shown in Fig. 12. The lower trace of each photo shows the output of the tunnel diode detector while the upper trace is that of the recovered signal off tape showing detected signal dropouts of -18 db and larger.

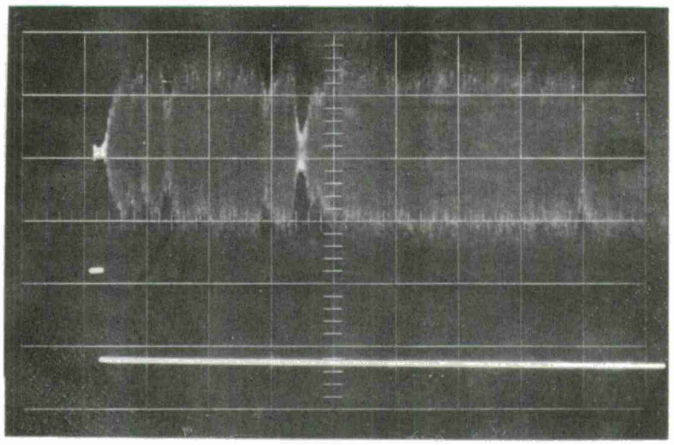

(a)

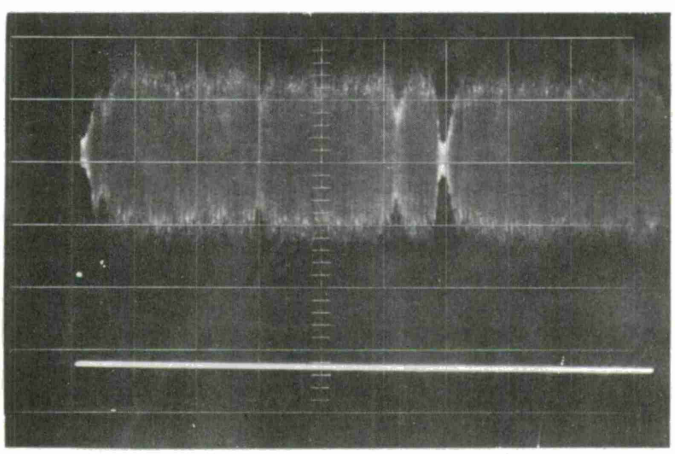

(b)

Fig. 12 Photographs of Detected Information Dropouts in Reproduced Signal

DATA GENERATOR AND BIT ERROR DETECTOR

Two functions are provided by the Data Generator/Error Detector. These are generation of a serial digitally coded pulse train, and error detection between processed test data and reference values.

These functions are performed independently. As a data generator, a pulse train is provided from an externally clocked register. This pulse train is coupled to the unit under test. The data generator has three modes of operation. The first mode, Mode I, generates an 8-bit word determined by the Code Pattern Select Switches followed by an 8-bit interword gap of all digital logic "0"s. This code pattern is continuously recycled. Any 8-bit code pattern combination may be selected and changed by resetting the Code Pattern Select Switches and activating the "Reset" switch. Mode II generates a repetitive 8-bit preselected word. Again any 8-bit code pattern may be selected via the code pattern select switches. The Mode III position of operation generates a recirculating $(2^n - 1)$ bit pseudo-random code pattern ($n = 8$). Operating in the error check mode, the stored test data is coupled to the data error generators incoming data register.

The contents of the incoming register is compared to programmed values and identity generates a word sync pulse. The clock pulse following the word sync initiates the count of the data generating register. The output of the latter, now in sync with the test data, is compared on a bit-by-bit basis with the incoming test data. For each error detected, an output pulse is generated.

When operating in the bit-error detection mode, the code pattern generator will still retain all three operating modes specified above. The incoming data shift register will drive a word sync AND gate. When a coincidence is detected in this gate the output from the gate activates a "Reset" one-shot pulse generator. The "Reset" pulse sets the word generator to the particular pattern determined by the code pattern select switches. This assures that the pseudo-random generator is synchronized every $(2^n - 1)^{th}$ bit.

Data Generator Mode Word Formats

Fixed data

A continuously recirculating 8-bit word is generated with data content set by front panel controls.

Interword gap

The same data as in fixed data mode is generated, and an 8-bit gap consisting of all "0"s is transmitted between each word.

Pseudo-random data

A known pseudo-random sequence of $(2^n - 1)$ bits in length is generated from the 8-stage register and recycled continuously.

Error Checking Mode

Incoming test data is checked bit-for-bit with the output of the data generating register (in any of the three-word formats) and an error pulse is generated for each deviation from sequence.

Word sync

Word sync is achieved when any front panel selected 8-bit word is present in the incoming data register. The data generating register is set to count data as programmed by front panel control by the word

sync pulse. The sequence is started with the next clock pulse.

Clock Rate, Input and Output

External clock: (3mc Maximum) Requires a positive pulse approximately 100 ns in duration with less than 25 ns rise. The amplitude is +5v ± 10% with baseline at ground ± 0.1v.

Data input

Requires NRZC-1 data. Amplitude: +5v ± 10%, Baseline: Ground ± 0.1v.

Data output

NRZC-1 Form: Approximately 20 ns transition time, Amplitude: +12v ± 10%, Baseline: Ground ± 0.1v, Source impedance: 100 ± 10%.

Error output:

Positive pulse occuring for each error detection. Amplitude: +12v ± 10%. Risetime: Approximately 20 ns, Pulse Width: Approximately 100 ns (approximately same as clock in) Baseline: Ground ± 0.1v. Source impedance: 100 ± 10%.

Word sync output:

Generated only in error checking mode when input register contains a word set by front panel controls. Amplitude: +12v ± 10%. Risetime: Approximately 20 ns. Pulse width: Approximately 100 ns (approximately same as clock in) Baseline: Ground ± 0.1v. Source impedance: 100 ± 10%.

Panel Controls and Connectors:

Word format select:

Three position switch labeled "Fixed Data, Interword Gap and Pseudo-Random Data".

Code pattern select:

Eight toggle switches select register pattern at reset.

Register reset switch:

Resets data generating register to the first bit of the selected code pattern.

Error output switch:

Inhibits error output until word sync is achieved.

Word recognition select:

Eight toggle switches determine bit content of the reference word used in establishing word sync.

Pulse connectors:

Shall be BNC type labeled and mounted as follows:

LABEL	LOCATIONS
Clock In	Front Panel
Data In	Front Panel
Data Out	Front Panel
Error Out	Front Panel
Sync Out	Front Panel

Circuitry:

Plug in digital logic modules. Transistors and diodes are high-speed silicon planar devices which provide reliable operation over a range of OC to 50^{O} C.

SOURCE OF ERRORS

The errors that were detected during our error test runs are the result of and can be separated into four definite categories:

(1) Errors resulting from reaching the limitations of the encoder/decoder as used in existing test setup. (These sources of errors consist primarily of the accumulative effects of amplitude and phase distortion and system-introduced timebase errors on the recovered off-tape signal).

(2) Transport induced errors, excluding those mentioned above.

(3) Tape imperfections

(4) Extraneous errors

Errors resulting from the first three causes are, in almost all cases, traceable to and identifiable with the specific source. The characteristics of the errors caused by these sources are recognizable and can, in most cases be isolated, detected and monitored. The sources of errors that make up the fourth category are varied in number and in almost all cases are completely random in nature. The bulk of these random errors can usually be traced directly to such causes as clogging of the transducer gaps (usually with excessive binder), loose dirt particles resulting in head-to-tape separation, line voltage variations causing excessive timebase perturbations, noise transients on the 60 cps line resulting in excessive noise on the signal, ground loop noise, etc.

The errors resulting from the digital HPD/HTR encoder/decoder combination are primarily due to the phase linearity of the direct record system and the signal-to-noise ratio of the system. This is best explained by referring to Fig. 13. The waveform at point d Fig. 13(a), (b) is the reproduced waveform of the recovered narrow band encoded data after limiting. (Fig. 6). If the tape transport were an ideal, unity gain, infinite band width, noise free passive element memory the output waveform at point d, Fig. 13(a) would be the mirror image of the narrow band data out of the encoder at the time of recording. However, the gain/phase nonlinearities of the system as the data bit packing density is increased results in an amplitude and phase distorted waveform. These nonlinearities manifest themselves as noise in the zero crossovers of the recovered signal.

In addition, the noise of the system is introduced and added to the processed recovered signal. The resulting limited waveform is typical of that shown in Fig. 13(b), point d. It is noted that the phase relationship of the zero crossovers from the recovered data relative to the recorded data is distorted in the time domain. The degree of accumulative phase distortion in terms of percent of a bit period determines the limitations of this encoding/decoding system. A standard commercial transport system with a direct record signal system was used which has a S/N specification of 20 db P-P/rms and a flutter specification of 0.25% at 120 ips. It was found that the total accumulative phase distortions of this system was approximately 250 ns peak-to-peak or approximately 25% of a bit period at the higher bit packing densities.

The derived data clock for the reproduced narrow band encoded data is used to strobe the limited waveform of the reproduced narrow band data to extract the encoded intelligence. This extracted intelligence is in an RZ format with digital logic "1"s presented as RZ pulse information and digital logic "0"s represented by the absence of pulses. This RZ digital logic "1" data is then reconstituted into an NRZ format compatible with that generated in the pseudo-random code generator.

The circuit used to extract data clock from the reproduced narrow band data is a phase-lock-oscillator (PLO) incorporating a filtered analog feedback loop. The dynamic delay introduced in this portion of the decoder/reconstitution circuitry relative to the frequency spectrum of the timebase errors introduced in the limited narrow band data is reflected in the overall system error rate limitations.

The reconstituted data clock out of the PLO is used to strobe the recovered, limited narrow band data. Thus, as the data bit packing density is increased (wavelengths on tape become shorter) and the S/N remains the same, the strobing and interrogation period in terms of percentage of a bit period becomes less. This is shown in Fig. 13 (a) and (b).

The waveforms of Fig. 13(a) were taken at relatively low bit packing densities while those in Fig. 13(b) represent the same waveforms taken at higher data bit packing densities. The waveforms in both figures represent the same points in the decoding/reconstitution system showing (h) reconstituted data in an RZ format, (g) reconstituted data clock and (d) the recovered narrow band/phase modulated signal

at the output of the limiter (Fig. 6 Decoder/Reconstitution Block Diagram). These waveforms were taken using a shutter exposure of 10 ms. The scope was triggered from reconstituted clock. The point of interest in these oscillograms lies in the comparison between the timebase deviation of the recovered zero crossovers in terms of percent of a bit period as a function of bit packing density. This time-base deviation is primarily the accumulative effects of S/N, tape transport timebase perturbations, amplitude and phase distortions and dynamic delays inherent in the decoder/reconstitution circuitry.

In Fig. 13(a) it can be seen that the timebase variation of the zero crossovers in terms of percent of a bit period is very small. It is, in fact, very small in comparison to the clock strobe period. The chances of a zero crossover deviating outside of a clock strobe pulse (digital logic "1"s) thus generating a digital logic "0" error, is very slight. Conversely the chance of a zero crossover deviating (and leaking) into a clock strobe pulse thus generating a digital logic "1" error is slight. With the same accumulative time base errors but at higher bit packing densities as in Fig. 13(b), however, the chances of errors resulting from digital logic "1" zero crossovers falling outside of a clock strobe pulse or of zero crossovers "leaking" into a clock strobe pulse generating false logic "1" are much greater. Therefore the limitation of this NB/PM encoding/decoding system as used with the equipments in these tests is a direct function of the overall systems accumulative timebase error difference (TBED) including the PLO tracking response and linear dynamic range.

Tape transport induced errors are, to a large extent covered in the accumulative timebase errors described above. These

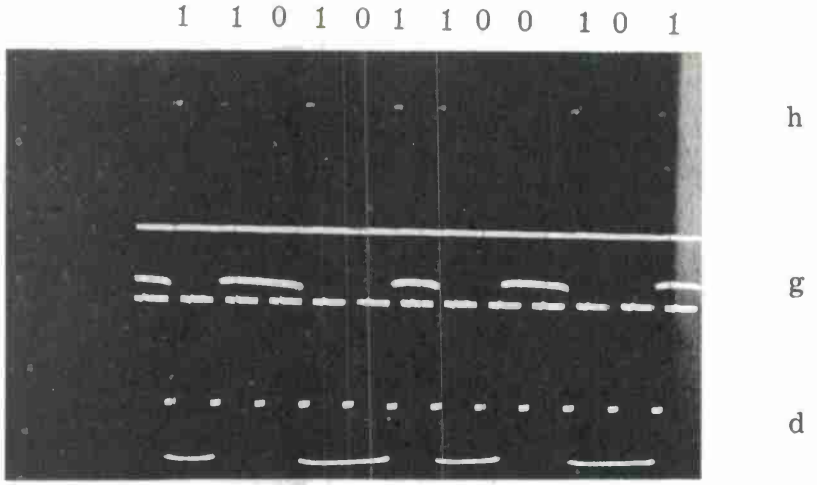

(a)

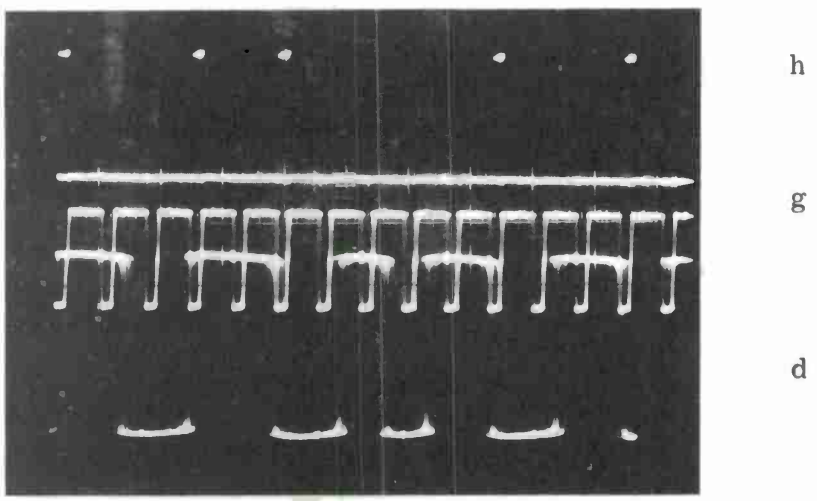

(b)

Fig. 13 Photographs of Decoder/Reconstituted Waveforms at two Different Digital Bit Packing Densities.

timebase errors exclude errors resulting, or caused by what is commonly called flutter. They are concerned primarily with machine induced timebase errors (TBE) and timebase error difference (TBED). TBE, as measured in this evaluation, is defined as the timebase error measured over a fixed period from some reference point. The TBE is usually the result of relative tape speed variations. In more absolute terms the TBE is equal to the time integral of flutter. The time increment (Δt) being the fixed period. The TBED that we are concerned with here is the measured peak-to-peak timebase error over some referenced period. The flutter that we are concerned with here is the tape-speed variation during the reproduce mode from that used during record mode. For most transport systems, including the Ampex FR 1400 used for these tests, the flutter can be considered random and as such has a zero mean value over relatively long periods. Excessive machine flutter will force a PLO out of lock. At the higher bit packing densities, it is desirable that the PLO have a high feedback loop gain. Since the dynamic range of the PLO is inversely proportional to the loop gain the tracking range for a higher bit packing density system, assuming the same flutter figure, will be less than for lower bit packing densities. The characteristics of the PLO used for these tests was more than adequate over the bit packing densities used during these tests. The machine flutter would periodically exceed the specifications however, forcing the PLO to lose phase-lock.

Magnetic tape imperfections as they affected these error rate tests usually involved such detectable characteristics as: gross variations in relative outputs resulting from non-homogeneity of oxide/binder combination, excessive binder coagulation resulting in "gunked"

heads (causing loss of signal) and tape surface nonuniformities resulting in either loss of recording and/or loss of signal during reproduce as a result of head-to-tape separation. With the exception of binder coagulation shunting the head gap and dirt particles, which results in very few actual errors, the other causes of error are consistent and can be isolated, detected and identified.

Extraneous sources of errors on the order of magnitude we are concerned with are usually very difficult to isolate, detect and identify. The buildup of excessive binder and foreign dirt particles on the tape oxide surface can be included in these sources. In general, once we became intimately familiar with all of the equipment associated with the test setup, including those equipments and items being tested, we know the sources of the great majority of these errors. Once detected the characterisitcs of these errors are of such a nature that one intuitively recognizes the source. The other sources, few as they might be, usually take a great deal of time and effort to trace, isolate and identify. Our fair share of these sources of errors were experienced during these error rate tests. The great bulk of them will be explained and justified on the basis of being classified as extraneous.

RESULTS AND INTERPRETATION OF ERROR RATE TESTS

The results of the error rate tests are shown in Figs. 14 through 76 inclusively. The data for these tests was accumulated in the following manner. Where available, a digital printer was used to print out the accumulated bit errors from the error totalizing counter. The digital printer was connected to the error totalizing counter, (Fig. 10). An external timing print command signal was generated to transfer the updated totalized error count to the printer and then into hard copy. The periodic print command signal was adjusted to either five-second or ten-second increments. When a digital printer was not available an operator continuously monitored the error totalizing counter and an accurate timing indicator (a watch with a second hand). Every time the readout of the error totalizing counter changed, the operator recorded both the time and the updated totalized bit error count.

A word error totalizing counter, based on eight bits per word, was used at the beginning of these tests; however, this was later abandoned for several reasons. The detected bit errors were of such a nature that in almost all cases we could observe the bit error rate profile curves and obtain the word error profile. By adding the numeral "one" to the integer obtained from $(^{n}/8)$ where (n) is the number of bit errors during any error totalizing period, we, in effect, obtain the number of word errors. Where $(1 < n \leq 8)$ assume two word errors and where $(n = 1)$ the word error would be

the same. The bit errors that were detected during any sampling increment invariably occurred in consecutive order.

The detected bit errors accumulated for each error test run were assembled and collated in order that they may be graphically displayed in two different formats. One graphical plot was made with each incremental error totalizing sampling period, where errors were detected, represented by a dot. The position of this dot relative to the ordinate axis represents the total number of errors detected during the incremental error totalizing period. The point in time that those errors were detected within a particular data block period is represented on the abscissa axis.

The same data recollated is presented in a form that allows a qualitative analysis of the data on the basis of performance level of the total system in a statistical manner. The recollated data of each error test run is presented in the form of Poisson distribution plots.

The logical questions that arise in the final analysis of the system with respect to these error rate test results is, are these detected error rates indicative of magnetic tape imperfections, do they represent errors introduced as a result of operating characteristic peculiarities of the tape recorder, are they extraneously introduced or are they a true representation of errors introduced via the NB/PM encoder/decoder as detected in this test setup?

We can largely isolate and identify those errors generated as a result of magnetic tape imperfections. Correlation of these induced errors is available by rerunning error rate tests over the same regions on tape where it is suspected that tape imperfections exist. In all error rate tests two or more runs were made over the same area on tape. Care was taken to insure that the start and finish of each error rate run fell approximately within the same region on tape. By overlaying the plotted dropout profile of these error runs correlation of errors as a function of position on tape is visible. Subsequent analysis of individual error rate runs will reveal direct correlation of detected errors relative to physical location on tape. In the overall analysis these errors will, in most cases, be excluded where conclusive evidence is available that they were tape induced.

Those errors introduced, as a result of random peculiarities of the operating characteristics of the transport, are very difficult to ascertain. We could usually identify these sources of errors only through an intimate working knowledge of all the equipment involved in the tests. We usually intuitively recognized the source of these errors at the time of occurrence. We were able to monitor one or more operating parameters of the equipment during the tests and detect these sources of errors at the instant these parameters exceed operating limits during the testing period.

Errors introduced extraneous to the test setup were traced and eliminated by the inevitable "brute force" technique. This is usually a time consuming, laborious process. Again only after we became intimately familiar with the test setup as well as the eviron under which the tests are being conducted can we intuitively recognize these sources of errors. After determining that a large percentage

of errors were being generated extraneously most of the error rate test runs were made in the evenings, after normal working hours or during periods when most local industrial operations and equipments were either inoperative or shutdown.

The error rate tests for bit packing densities of 10 Kbpi are shown in Fig. 14 through Fig. 25. The first two test runs, conducted using relatively old tape, showed a large percentage of the run consisting of amplitude modulation resulting from head-to-tape separations. The magnitude of these modulation dropouts were typical of those shown in Fig. 12. The purpose of this was to determine the sensitivity of the decoder/reconstitution circuitry to dropout levels and durations. The two error runs were made on the same reel of tape and over the same area of the tape. By overlaying the two bit-error profile plots, it was apparent that errors occurred at approximately the same times relative to each other. This is a valid indication of tape induced errors. This was further evidenced and substantiated by rerunning over the same area several times and monitoring the recovered signal envelop for loss of signal.

The following results of the four error rate test runs at 10 Kbpi, Fig. 18 through Fig. 25, revealed that at approximately 15 minutes into each test run a tape imperfection existed. This was also evidenced through monitoring the recovered signal off tape. These test runs were made on a new reel of tape.

Figures 26 through 35 display the results of error rate tests at bit packing densities of 15 Kbpi. The first two test runs, Figs. 26 through 29, revealed that at approximately five minutes into

the run, a tape imperfection existed. In addition to detecting that a tape imperfection existed by monitoring the reproduced signal the fact that these detected errors were tape induced is further substantiated by the fact that the totalized error count at those points are within 4% of each other. Similarly the results of error test runs, Figs. 32 through 35, reveal that at approximately 2.5, 4, 7, and 9.5 minutes into the error rate test run tape errors existed. The magnitude of the number of errors at each point approximated each other. These two test runs were made using the same reel of tape used on the first two runs with the exception that the test runs were made on an edge track.

In the second and third error rate test runs at 18 Kbpi, Figs. 40 through 43, correlated tape induced errors were introduced at times 1.5, 10 and 20.75 minutes from start of each test run. On the fourth test run (Fig. 42) it appeared that the head gap was shunted by loose or excessive tape binder at approximately 24.5 minutes into the tape.

The three 20 Kbpi error test runs (Figs. 50 through 55) were run on the same reel of tape. The results of these tests show no correlation of detected errors with tape imperfections. During the running of those tests shown in Figs. 44 through 49, however, it was found that the tape was shedding an excessive amount of binder/oxide. The excess binder/oxide was building up on the guides and heads thus causing complete loss of signal. This reel of tape had gone through many passes and had reached its useful end of life. The three error test runs at 20 Kbpi shown in Figs. 50 through 55 show definite correlation of tape induced errors on all three runs. This correlation occurs at approximately eight minutes from the start of each run.

In all the error test runs made at bit packing densities of 24 Kbpi, Figs. 62 through 73, it is obvious that this reel of tape contained a bad section at approximately 26 to 29 minutes into the tape. This was definitely confirmed by visually observing the recovered signall off tape during every run.

Table 2 is a tabloid of the pertinent information and test results of all the accumulated error tests shown in Fig. 14 through 73. For each specific test the table shows the digital bit packing density at which the data was recorded, the total number of digital data bits recorded on tape, the data bit transfer rate during record, the total number of detected errors (corrected for substantiated tape induced errors) and the overall digital bit error rate figure for each specific error test run. Table 3 is a tabloid of all the recollated test results taken from the Poisson error distribution graphs.

The values for the bar graphs shown in Figs. 74 and 75 were derived from the collated data in Table 3. The mean average percentage figures from Table 3 were calculated and presented in Table 4. These same results presented in Table 4 are graphically displayed in Fig. 76. The mean average bit error rate figure of all the error test runs for a specific packing density are shown in Fig. 77. Since the bit error rate figure at a 10 Kbpi packing density was zero, this curve is shown having any asymptote approaching the finite value zero.

The graphical photos in Figs. 14 through 77 represents the results of the error rate tests at various data packing densities. The results of each individual test are presented in two forms. One form shows the bit error rate profile as a function of time for a specific digital bit packing density. The results of each test are then recollated and this information is presented in the form of a bar chart showing the number of data blocks as a function of the number of detected bit errors. This collated data presented in this form quantitatively describes the performance in a statistical manner.

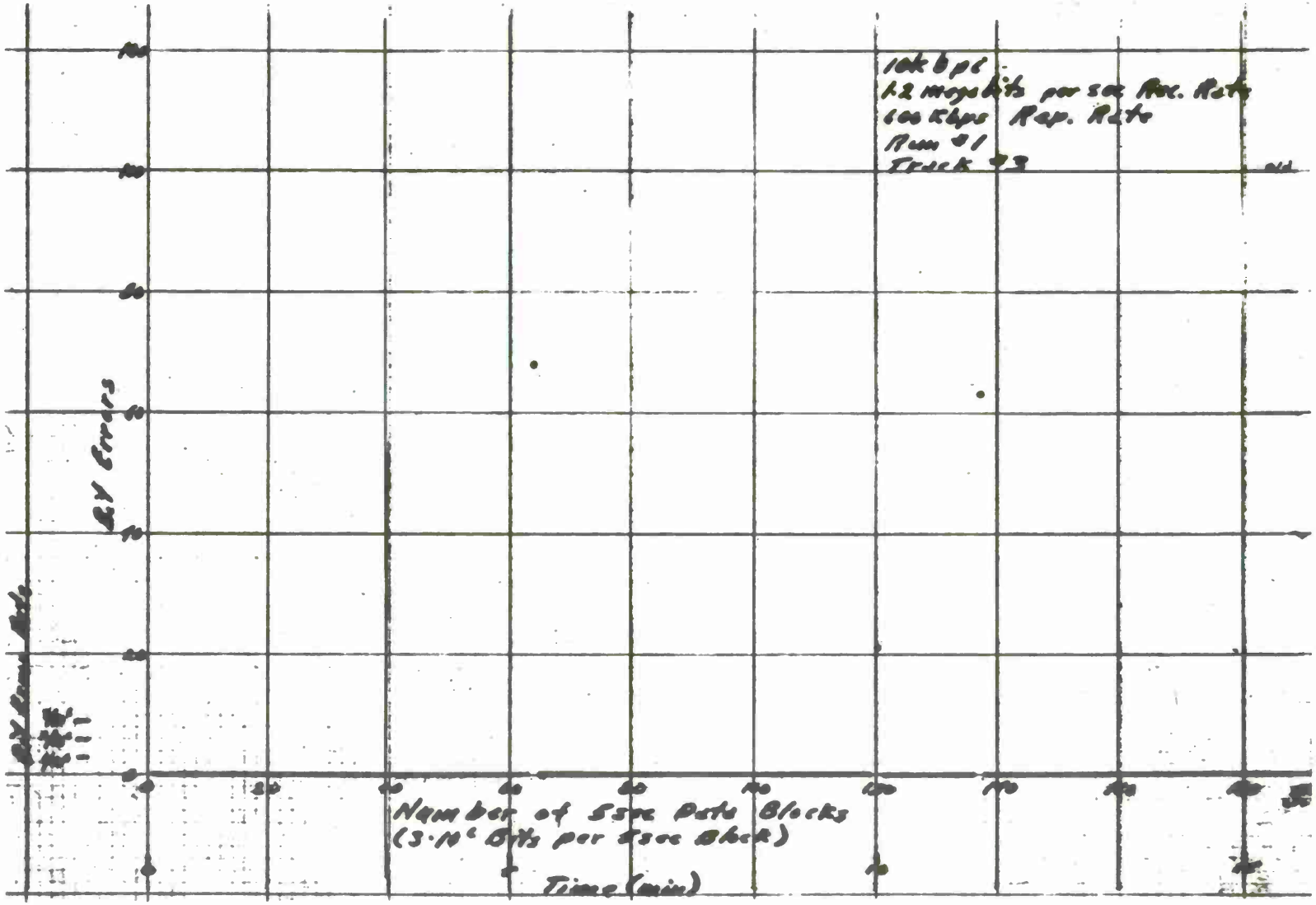
16k bpi
1.2 megabits per sec Rec. Rate
60 kbps Rep. Rate
Run #1
Track #3
Number of 5sec Data Blocks
(3.4 Mbits per 5sec Block)
Time (min)

Fig. 14

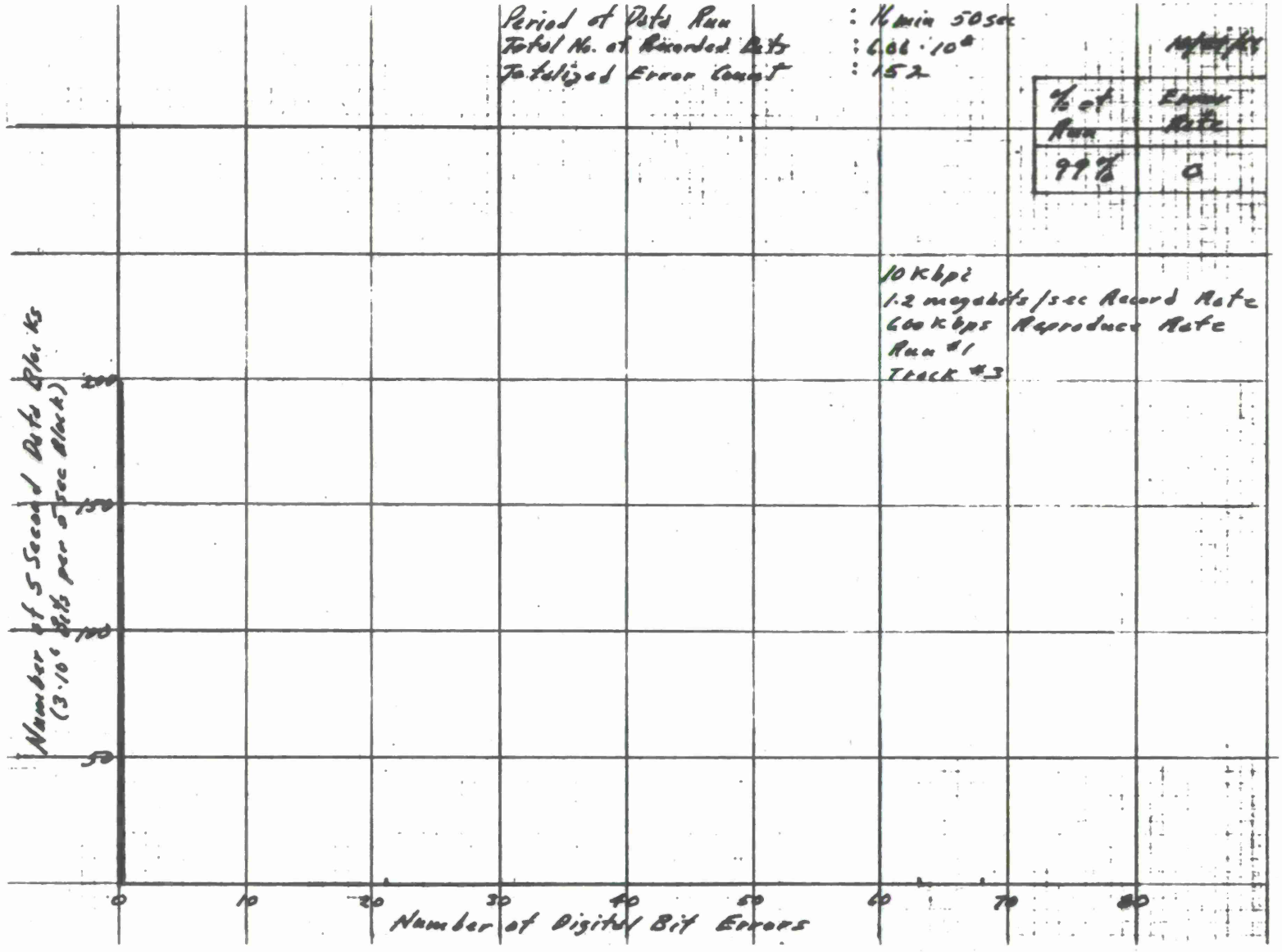
Period of Data Run : 4 min 50 sec
Total No. of Recorded Bits : 6.06 · 10⁸
Totalized Error Count : 152
% of Run
99 %
10 Kbpi
1.2 megabits/sec Record Rate
60 Kbps Reproduce Rate
Run #1
Track #3
Number of 5 Second Data Blocks (3·10⁶ Bits per 5 sec Block)
200
150
100
50
0
10
20
30
40
50
60
70
80
Number of Digital Bit Errors

Fig. 15

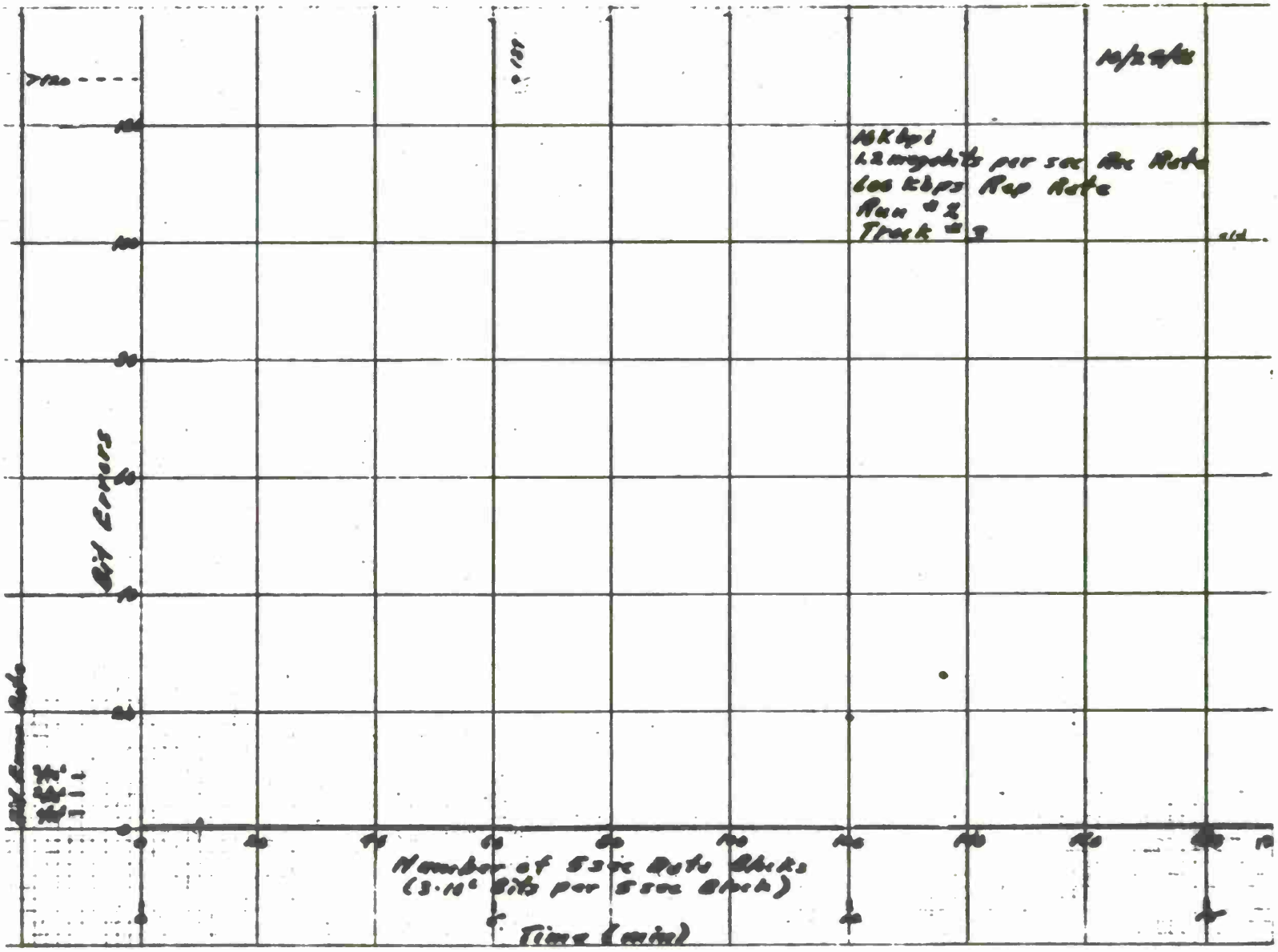
Bit Errors
Number of 512 Byte Blocks
(3.10⁶ Bits per 512 Block)
Time (min)

Fig. 16

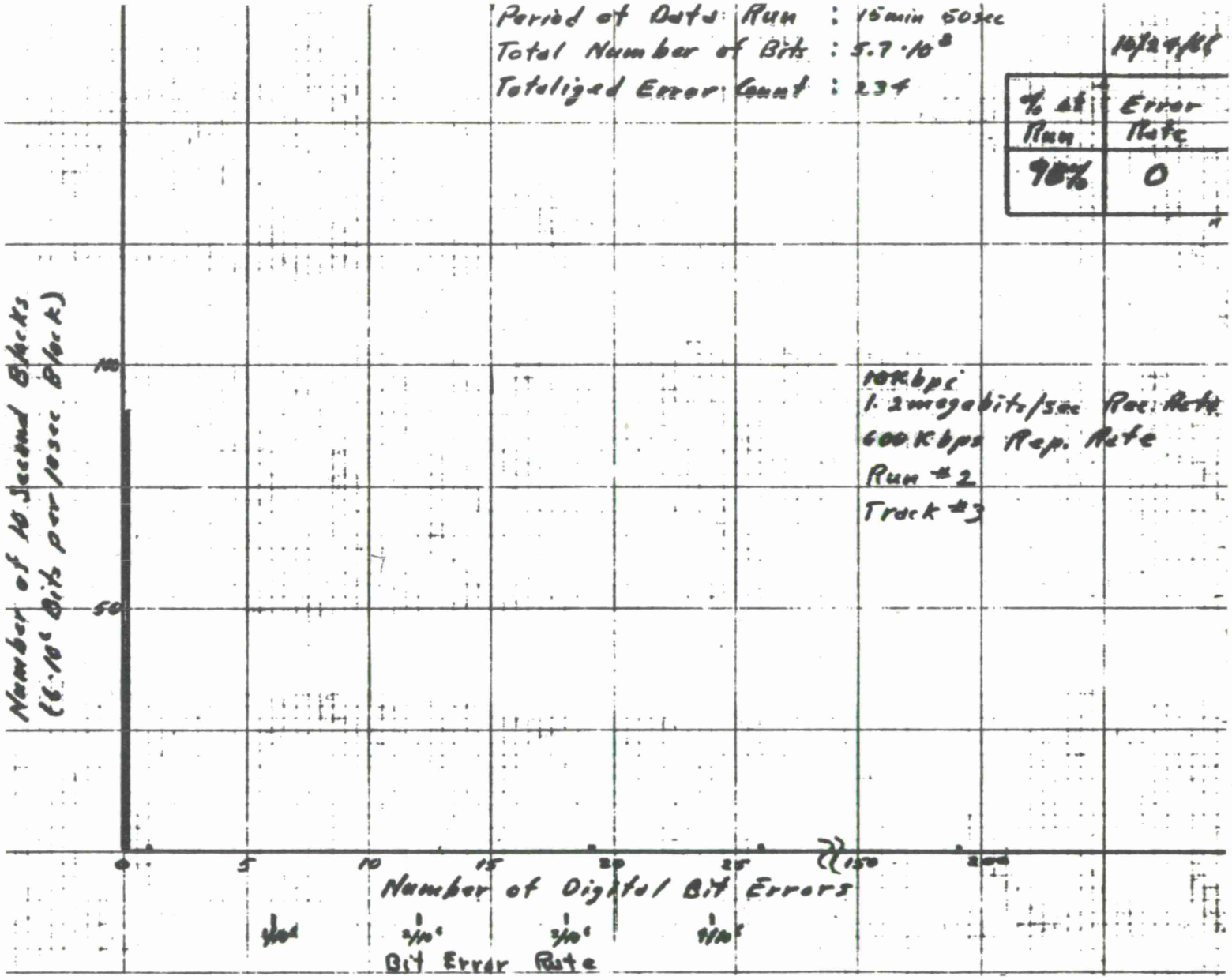
Period of Data Run : 15min 50sec
Total Number of Bits : 5.7·10⁸
Totaliged Error Count : 234
% of Run
Error Rate
98%
0
100 Kbps
1.2 megabits/sec Rec. Rate
600 K bps Rep. Rate
Run #2
Track #3
Number of 10 Second Blocks (5·10⁶ Bits per 10sec Block)
100
50
0
5
10
15
20
25
150
Number of Digital Bit Errors
Bit Error Rate

Fig. 17

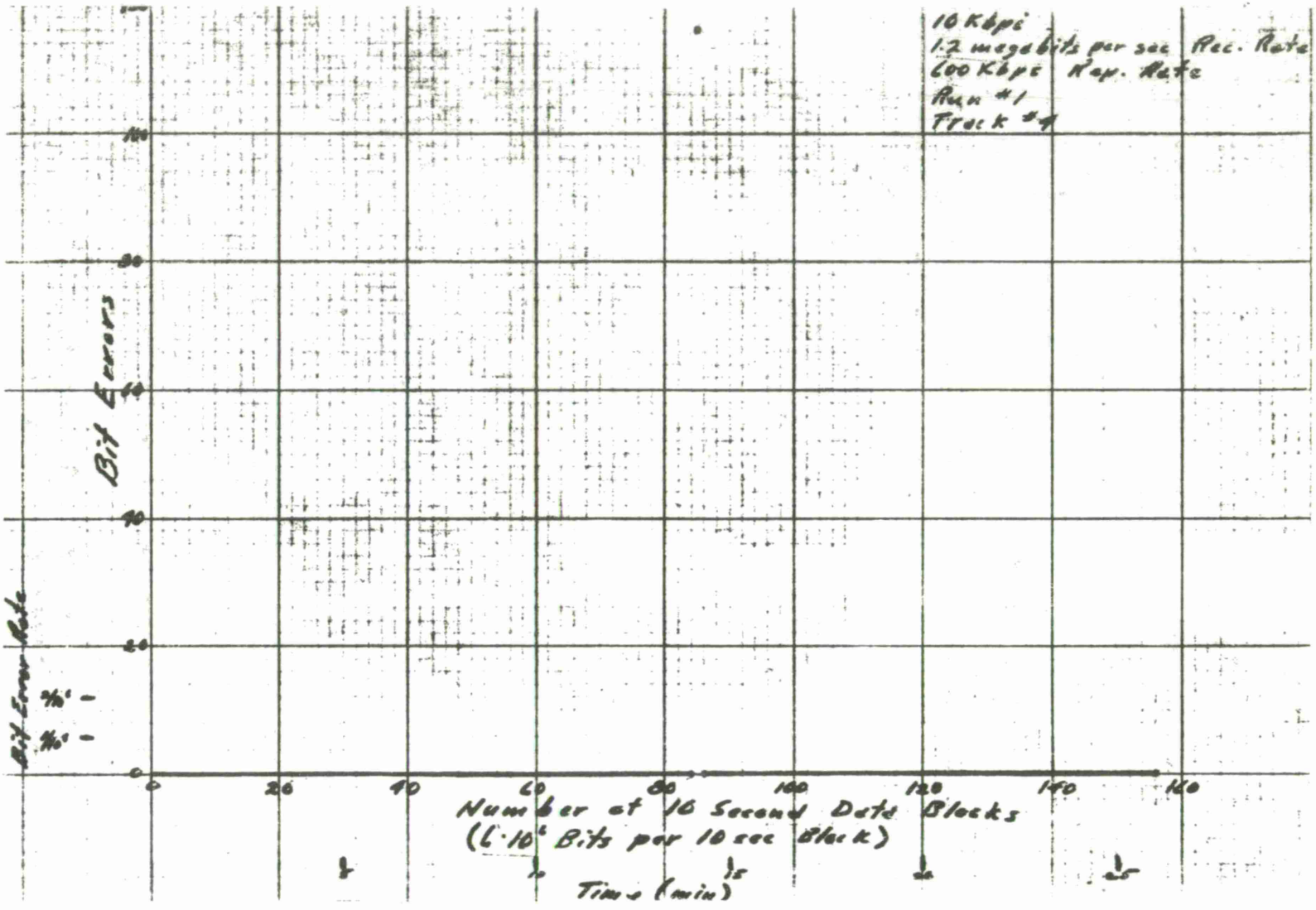
10 Kbpi
1.2 megabits per sec Rec. Rate
600 Kbpi Rep. Rate
Run #1
Track #4
Bit Errors
Bit Error Rate
Number of 10 Second Data Blocks
(1·10⁶ Bits per 10 sec Block)
Time (min)

Fig. 18

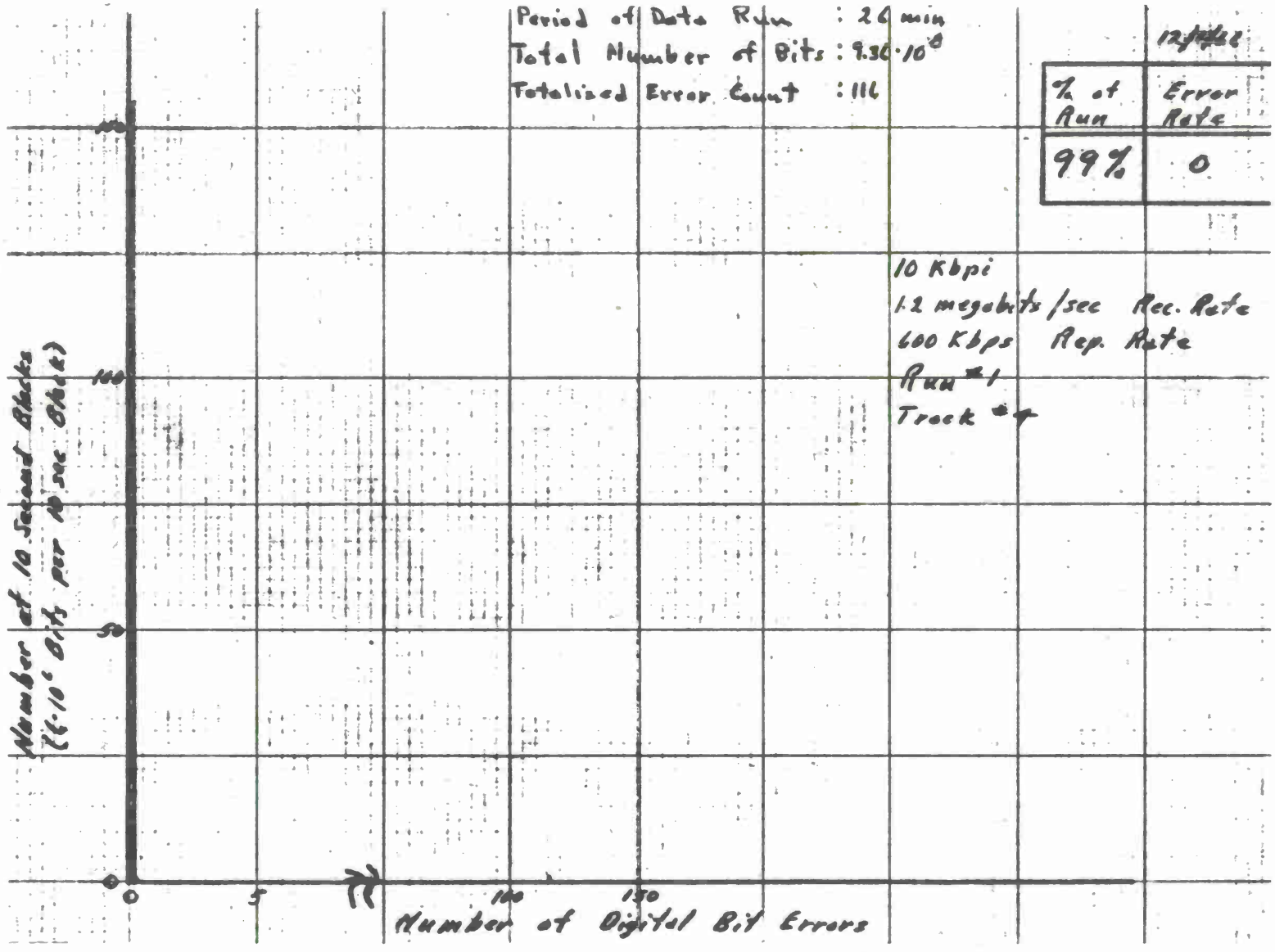
Period of Data Run : 24 min
Total Number of Bits : 9.36·10^8
Totalized Error Count : 116
% of Run
Error Rate
99%
0
10 Kbpi
1.2 megabits/sec Rec. Rate
600 Kbps Rep. Rate
Run #1
Track #4
Number of Digital Bit Errors
Number of 10 Second Blocks (1·10^7 Bits per 10 sec Block)
0
5
100
150

Fig. 19

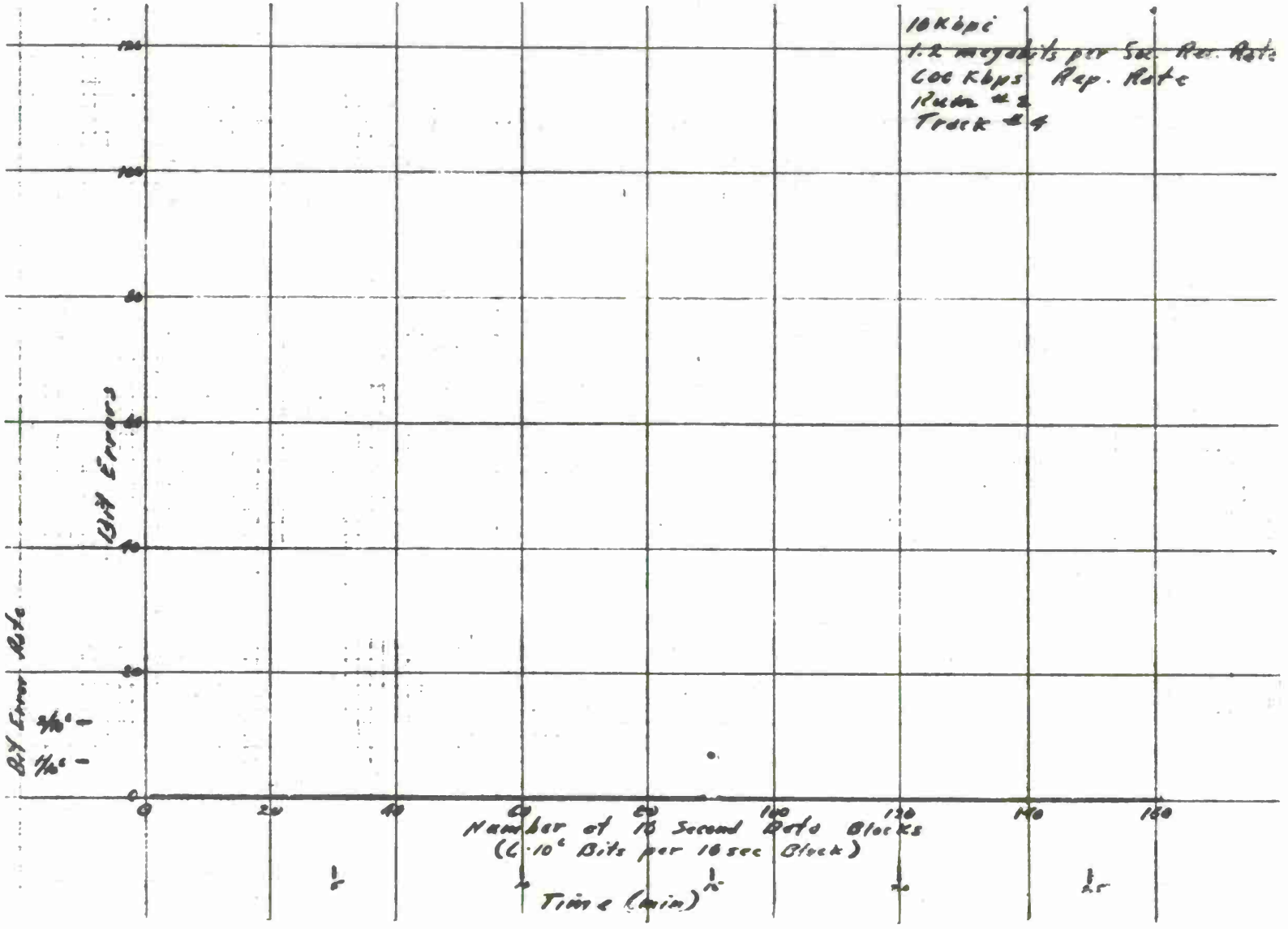
10 Kbpc
1.2 megabits per Sec Rec. Rate
600 Kbps Rep. Rate
Run # 2
Track # 4
Bit Errors
Bit Error Rate
Number of 10 Second Data Blocks
(C·10⁶ Bits per 10 sec Block)
Time (min)

Fig. 20

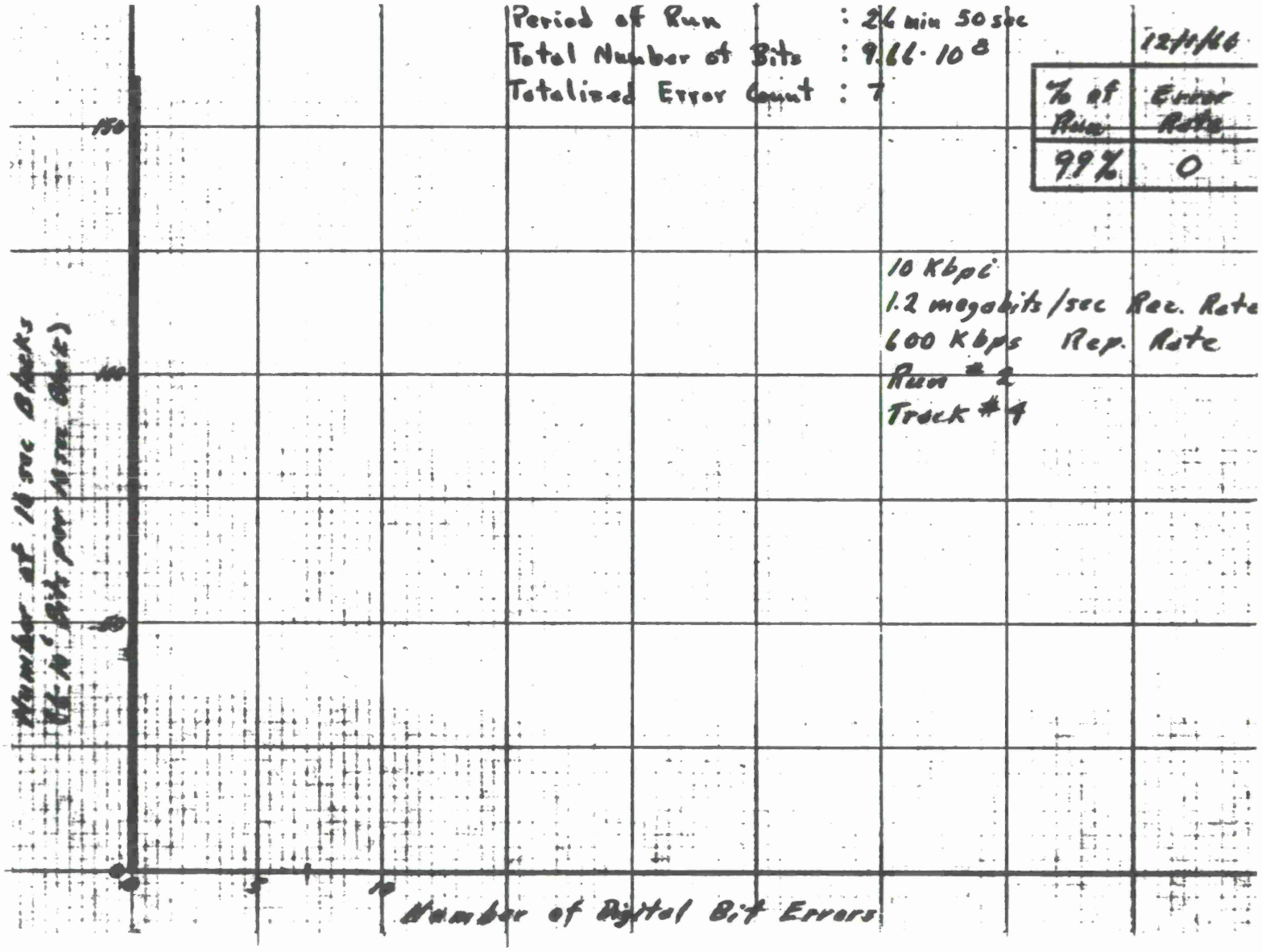
Period of Run : 24 min 50 sec
Total Number of Bits : 9.66 · 10^8
Totalized Error Count : 7
12/1/66
% of Run
Error Rate
99%
0
10 Kbpi
1.2 megabits/sec Rec. Rate
600 Kbps Rep. Rate
Run # 2
Track # 4
150
100
50
0
5
10
Number of Digital Bit Errors

Fig. 21

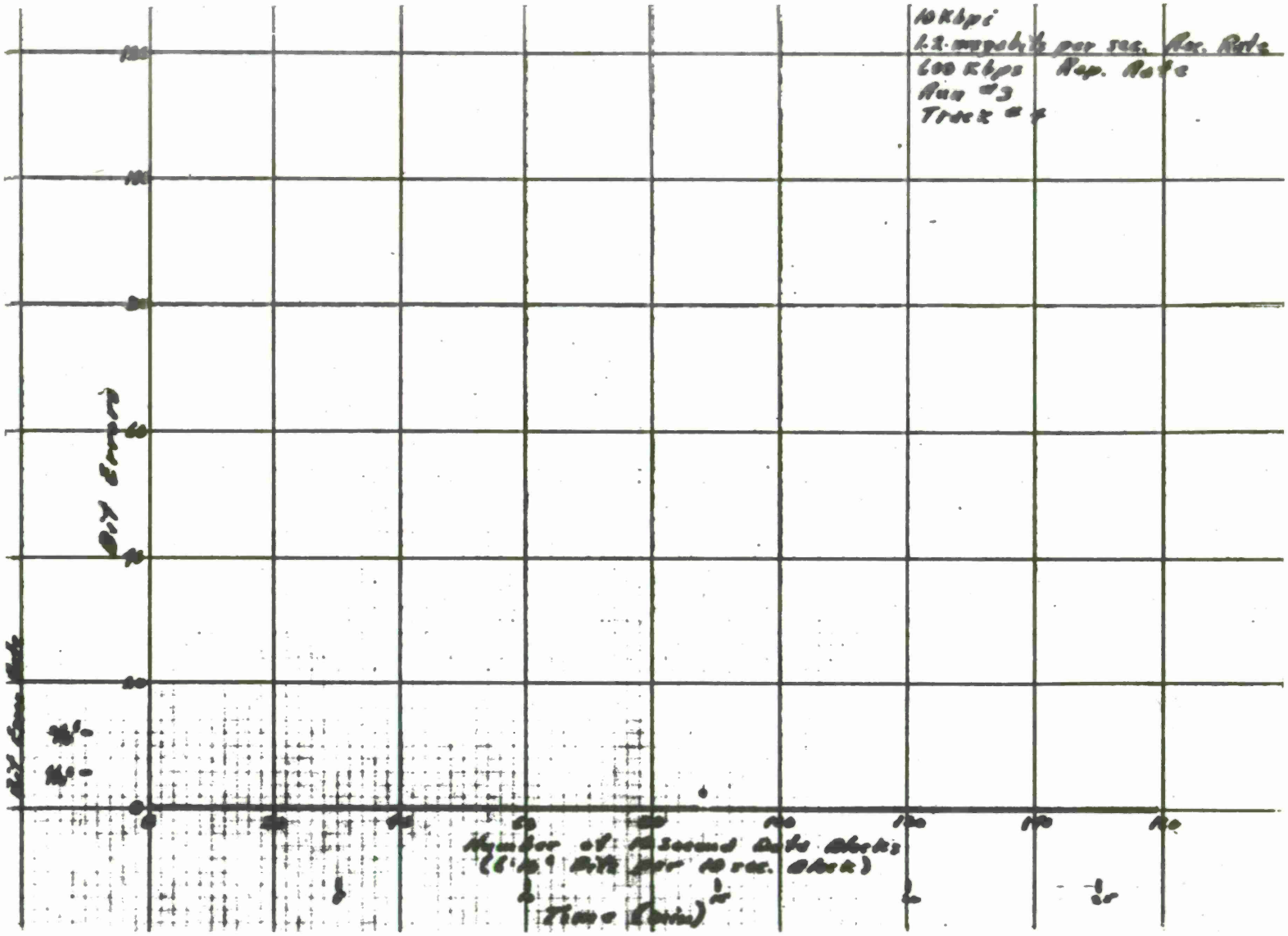

Fig. 22

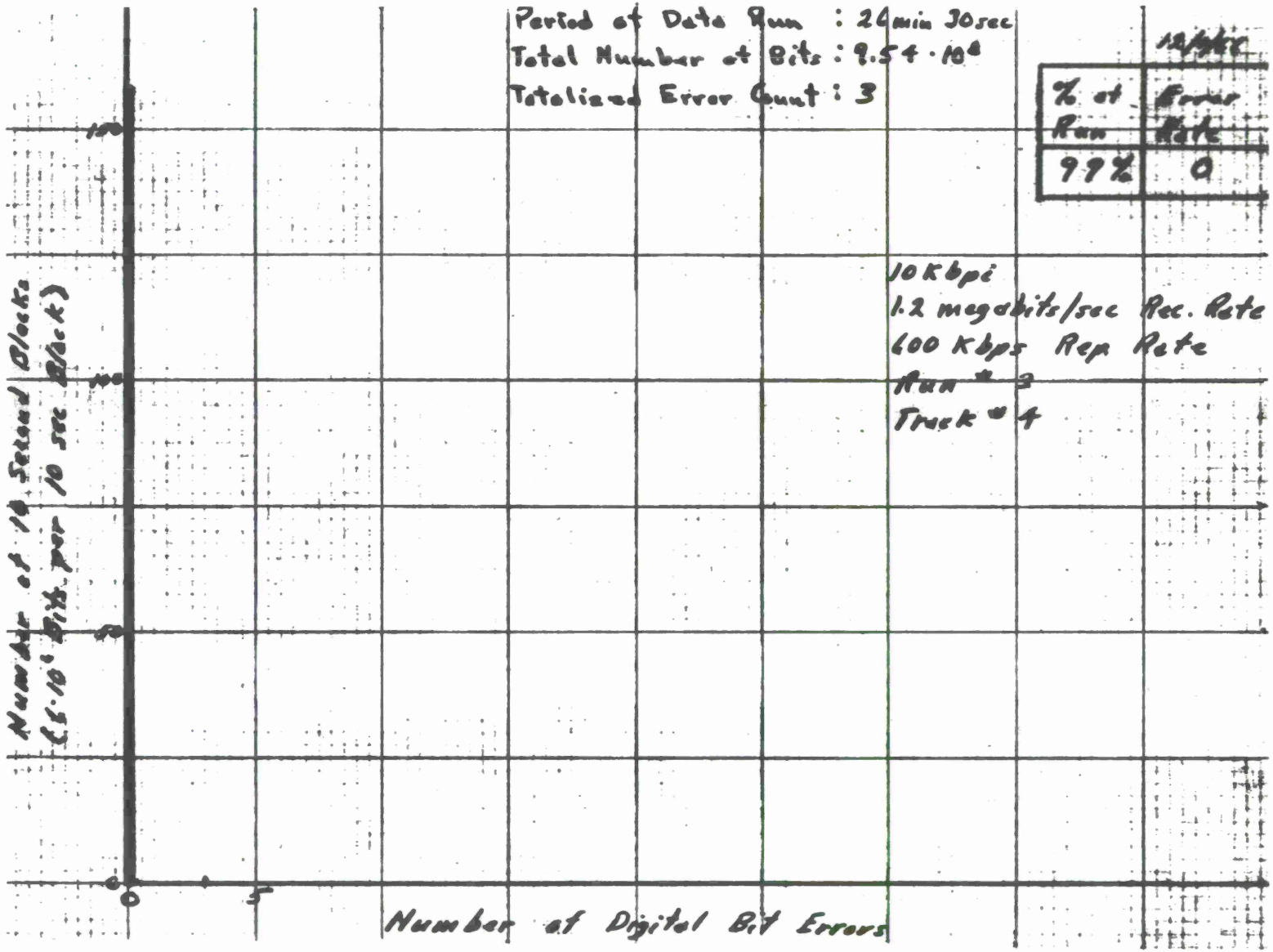
Period of Data Run : 24 min 30 sec
Total Number of Bits : 9.54 · 10⁸
Totalized Error Count : 3
% of Run
99%
Error Rate
0
10 Kbpi
1.2 megabits/sec Rec. Rate
600 Kbps Rep Rate
Run # 2
Track # 4
Number of 10 Second Blocks (1.5·10⁷ Bits per 10 sec Block)
Number of Digital Bit Errors

Fig. 23

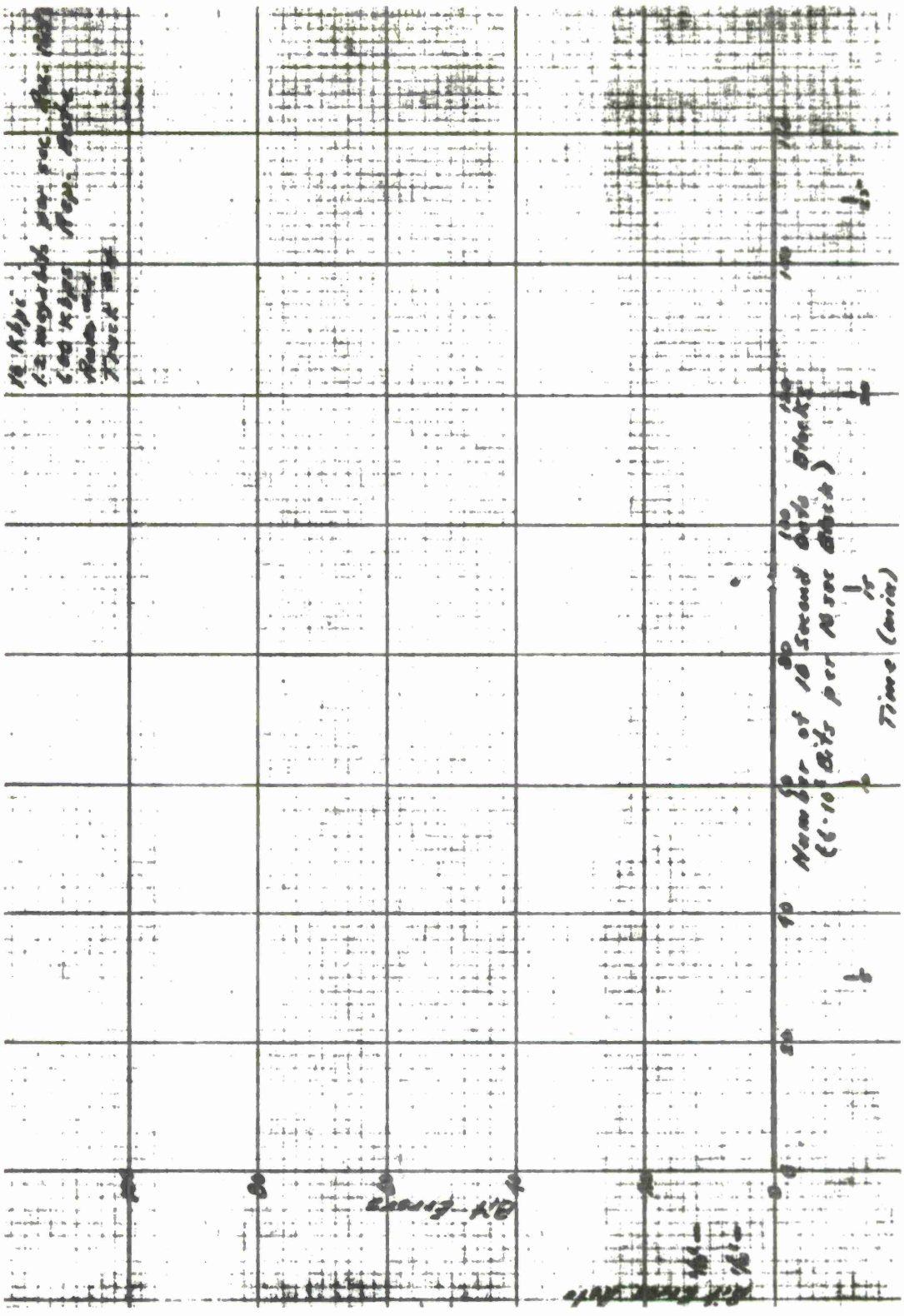

Fig. 24

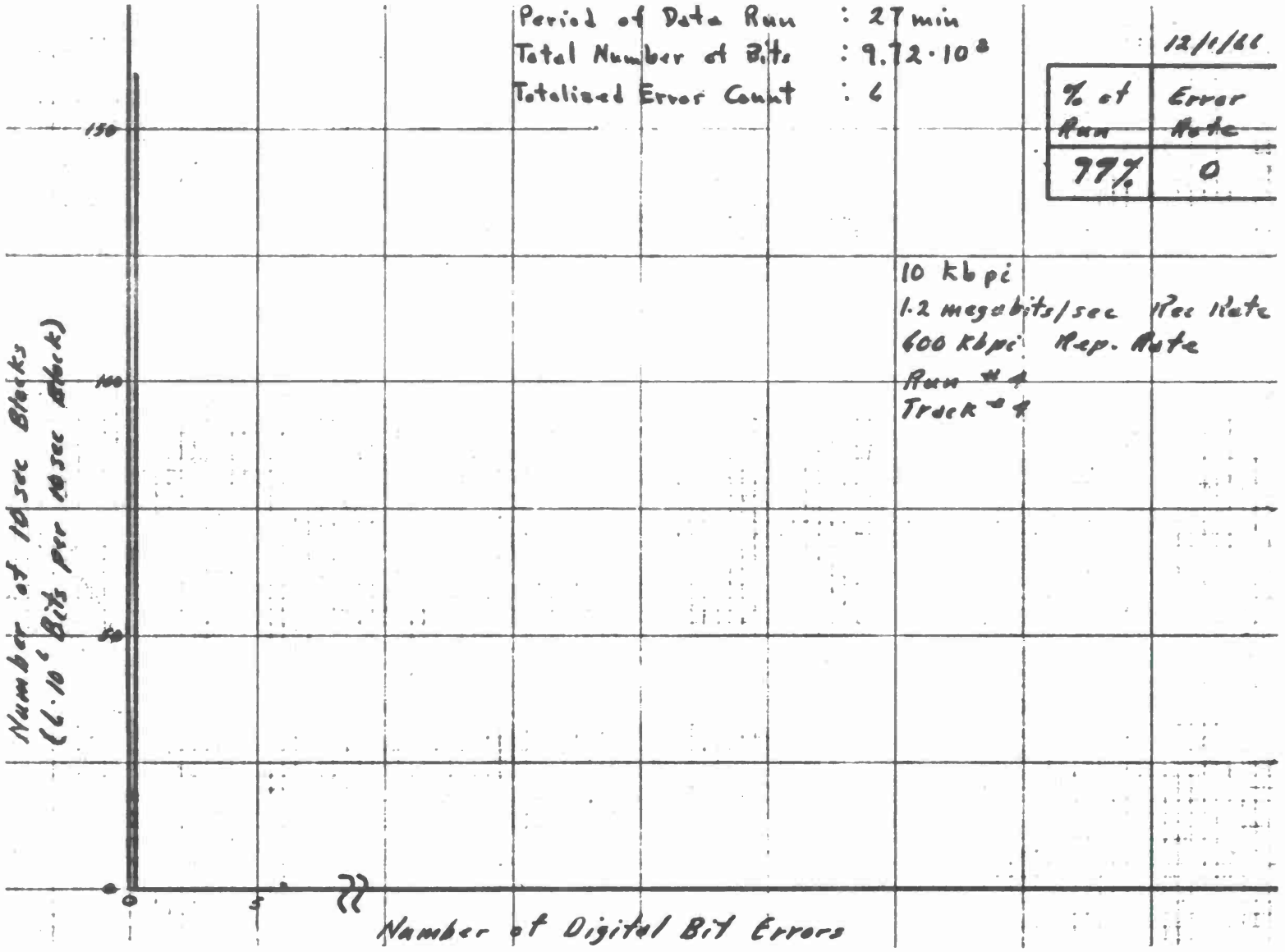
Period of Data Run : 27 min
Total Number of Bits : 9.72·10⁸
Totalized Error Count : 6
12/1/66
% of Run
Error Rate
99%
0
10 kb pi
1.2 megabits/sec Rec Rate
600 Kbpi Rep. Rate
Run #4
Track #4
Number of 10 sec Blocks
(1.10⁷ Bits per 10 sec Block)
150
100
50
0
5
Number of Digital Bit Errors

Fig. 25

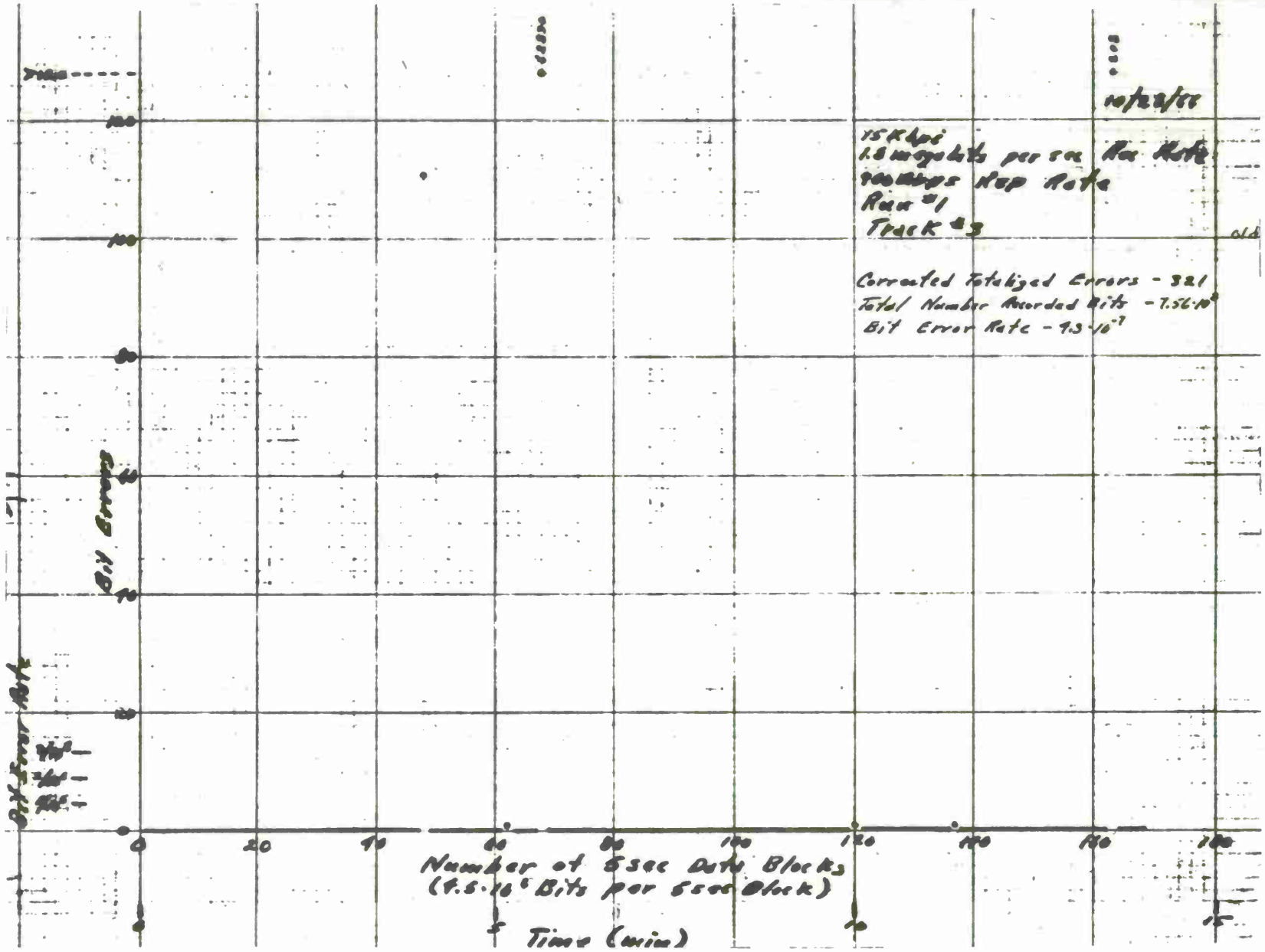
15 Kbps
1.5 megabits per sec Bit Rate
Recording Tape Rate
Run #1
Track #3
Corrected Totalized Errors - 321
Total Number Recorded Bits - 7.56·10⁸
Bit Error Rate - 4.3·10⁻⁷
Bit Errors
Bit Error Rate
Number of 5 sec Data Blocks
(4.5·10⁶ Bits per 5 sec Block)
Time (min)

Fig. 26

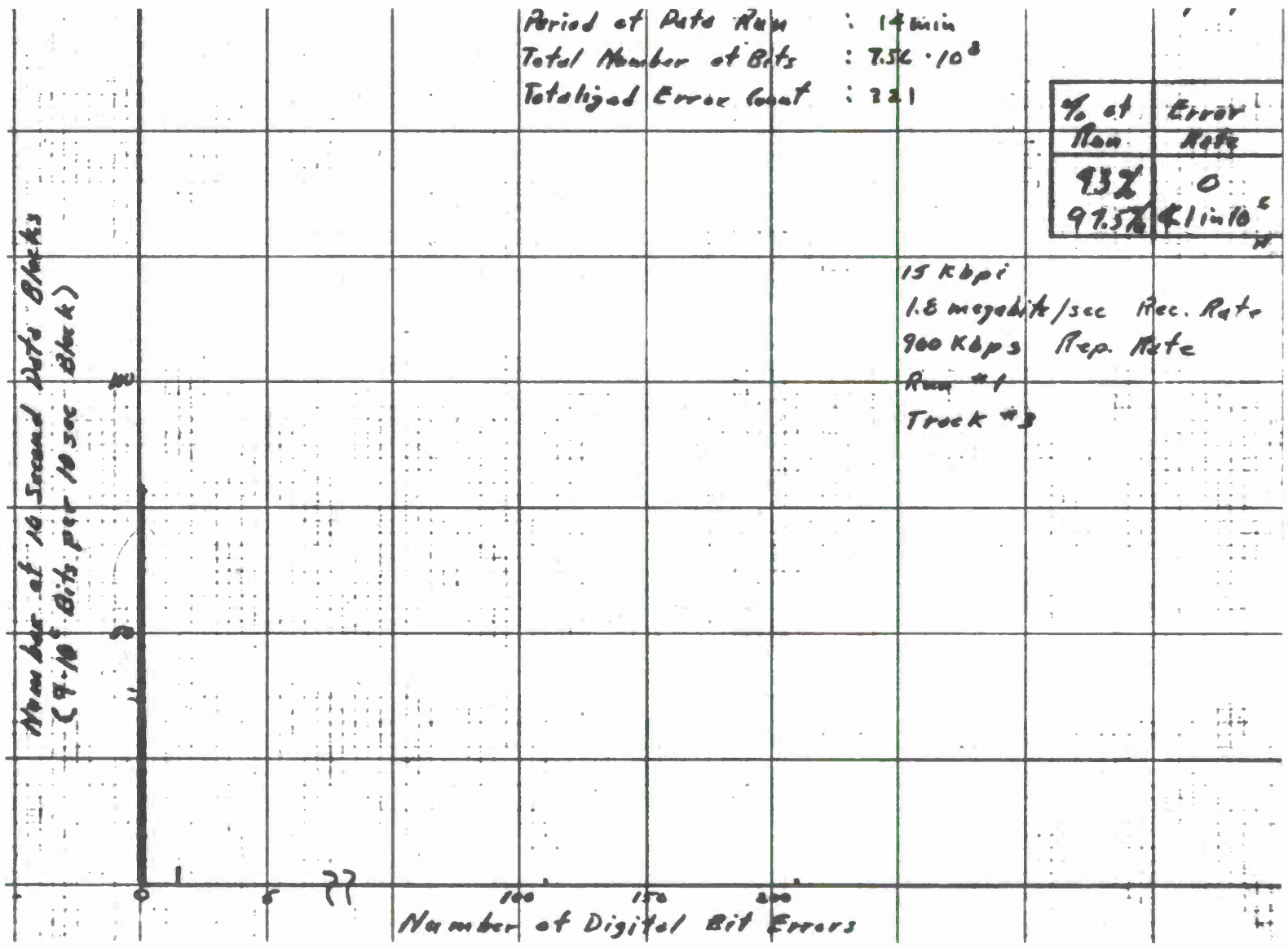
Period of Data Run : 14 min
Total Number of Bits : 7.5K · 10^8
Totalized Error Count : 221
% of Run
Error Rate
93%
0
97.5%
≤ 1 in 10^6
15 Kbpi
1.8 megabit/sec Rec. Rate
900 Kbps Rep. Rate
Run #1
Track #3
Number of 10 Second Data Blocks
(9·10^6 Bits per 10 sec Block)
0
1
77
100
150
200
Number of Digital Bit Errors

Fig. 27

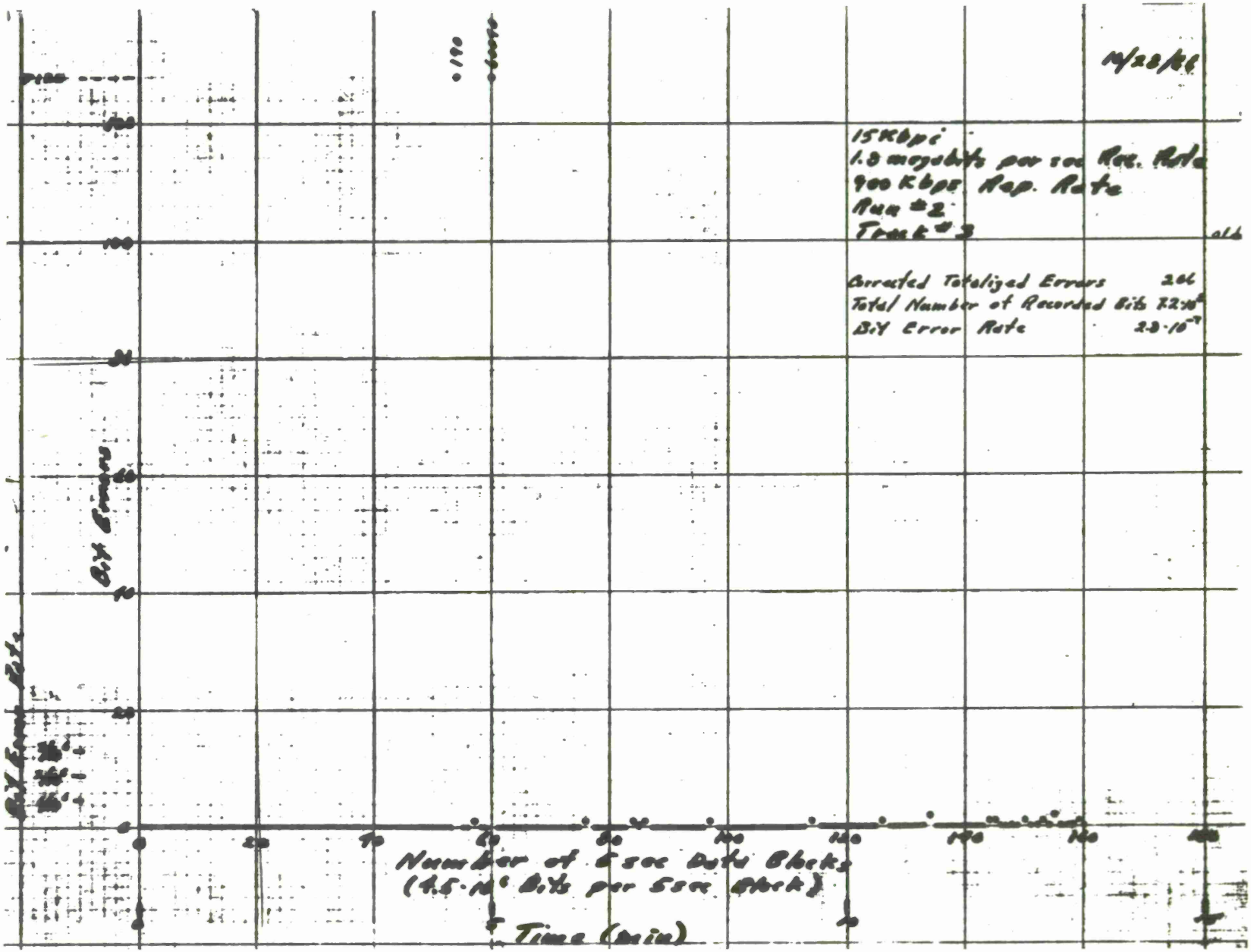
15 Kbpi
1.2 megabits per sec Rec. Rate
900 Kbps Rep. Rate
Run #2
Track #3
Corrected Totalized Errors 2.0L
Total Number of Recorded Bits 7.2×10⁶
Bit Error Rate 2.8·10⁻⁷
Bit Errors
Number of 4 sec Data Blocks
(4.5·10⁶ Bits per 5 sec Block)
Time (min)

Fig. 28

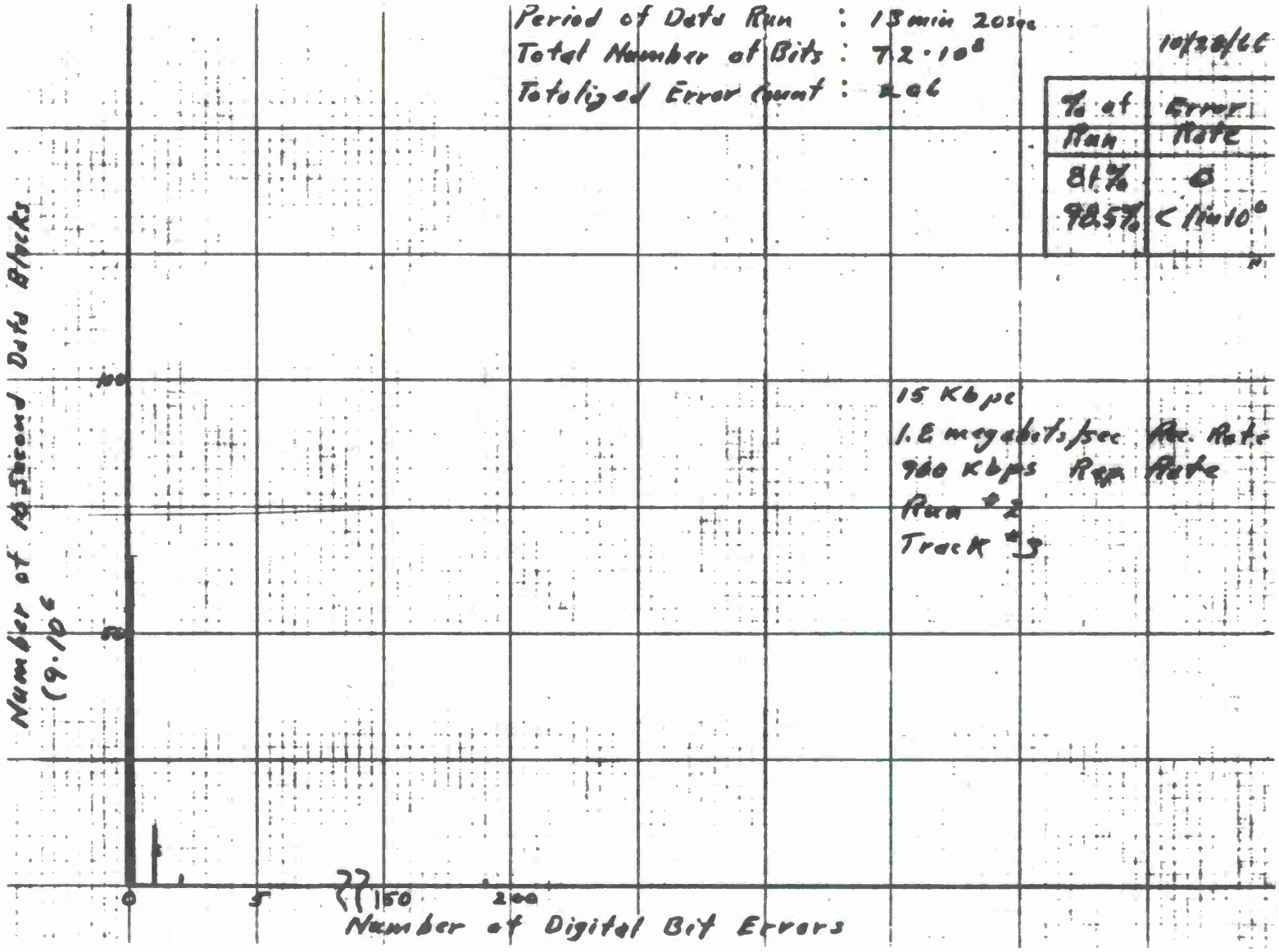
Period of Data Run : 15 min 20 sec
Total Number of Bits : 7.2 · 10^8
Totalized Error Count : 2.06
10/28/66
% of Run
Error Rate
81%
0
98.5%
< 1 in 10^6
15 Kbps
1.2 megabits/sec Rec. Rate
960 Kbps Run Rate
Run # 2
Track # 3
Number of Record Data Blocks (9.10^5)
0
5
77
150
200
Number of Digital Bit Errors

Fig. 29

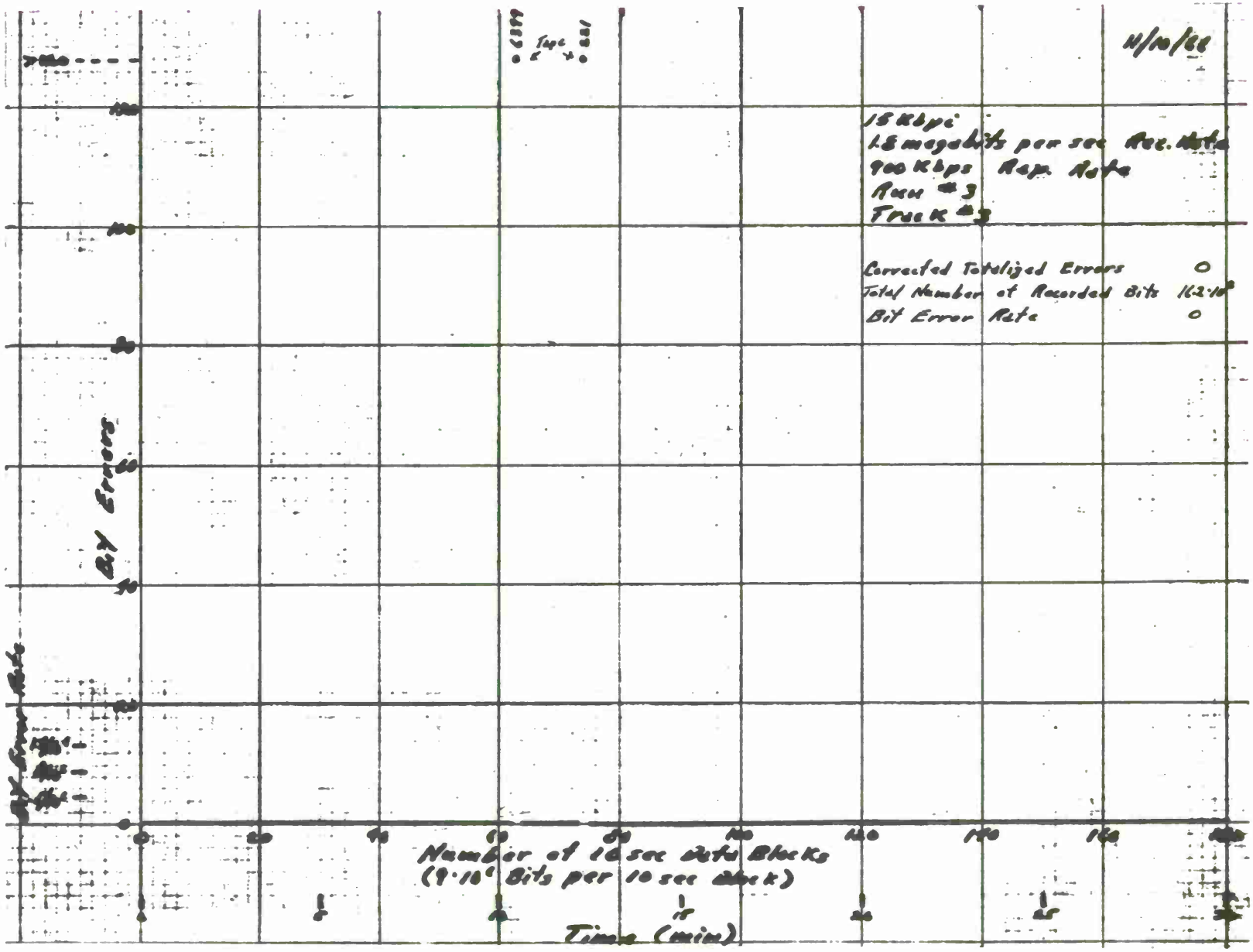
11/10/66
15 Kbps
1.8 megabits per sec Rec. Rate
900 Kbps Rep. Rate
Area #3
Track #3
Corrected Totalized Errors 0
Total Number of Recorded Bits 16.2·10⁹
Bit Error Rate 0
Bit Errors
Bit Error Rate
Number of 10 sec data Blocks
(9·10⁶ Bits per 10 sec block)
Time (min)

Fig. 30

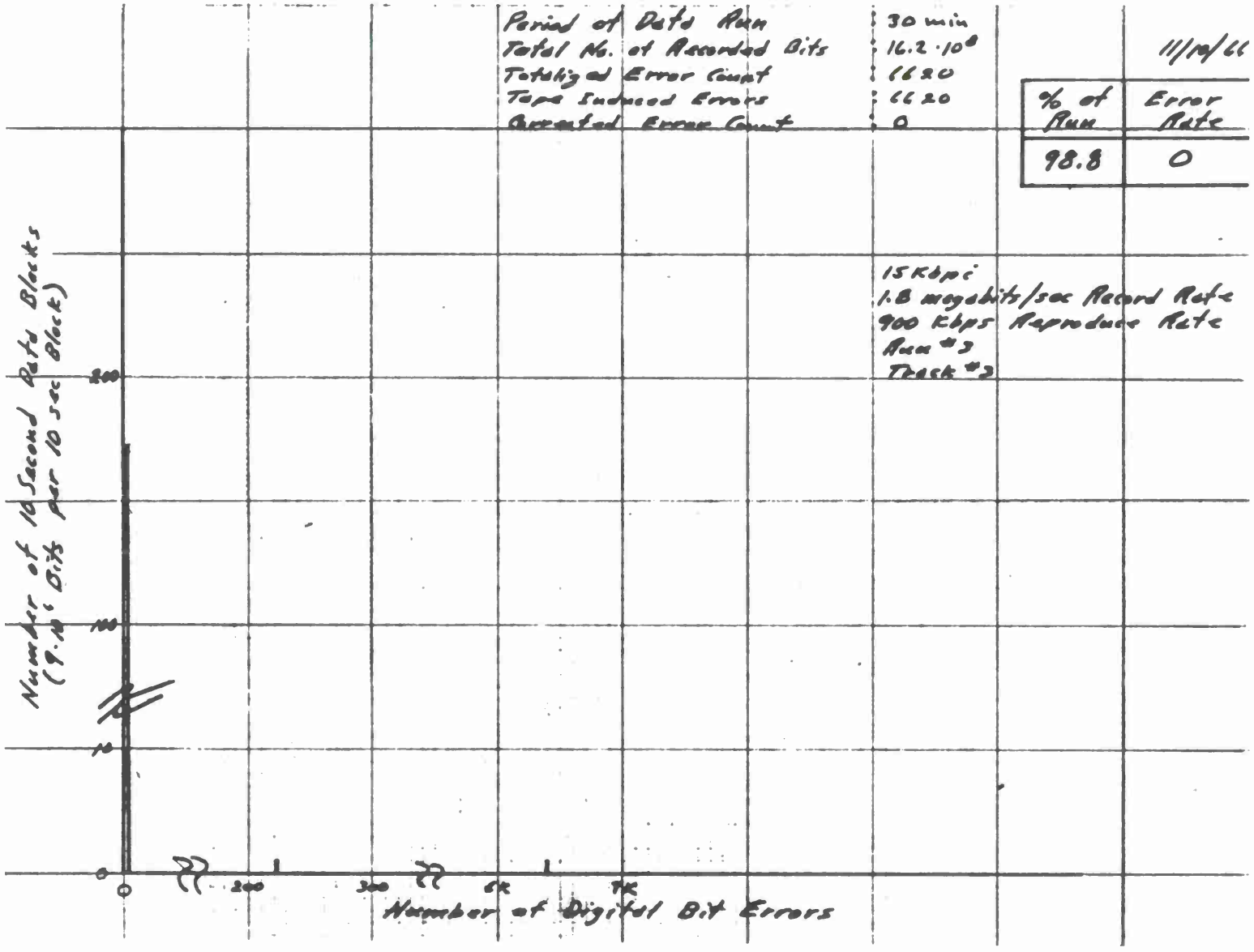
Period of Data Run
Total No. of Recorded Bits
Total Digital Error Count
Tape Induced Errors
Corrected Error Count
30 min
16.2 · 10⁸
6620
6620
0
11/10/66
% of Run
Error Rate
98.8
0
15 Kbpi
1.8 megabits/sec Record Rate
900 Kbps Reproduce Rate
Run #3
Track #2
Number of 10 Second Data Blocks
(1.44 Bits per 10 sec Block)
200
100
10
0
200
300
6K
7K
Number of Digital Bit Errors

Fig. 31

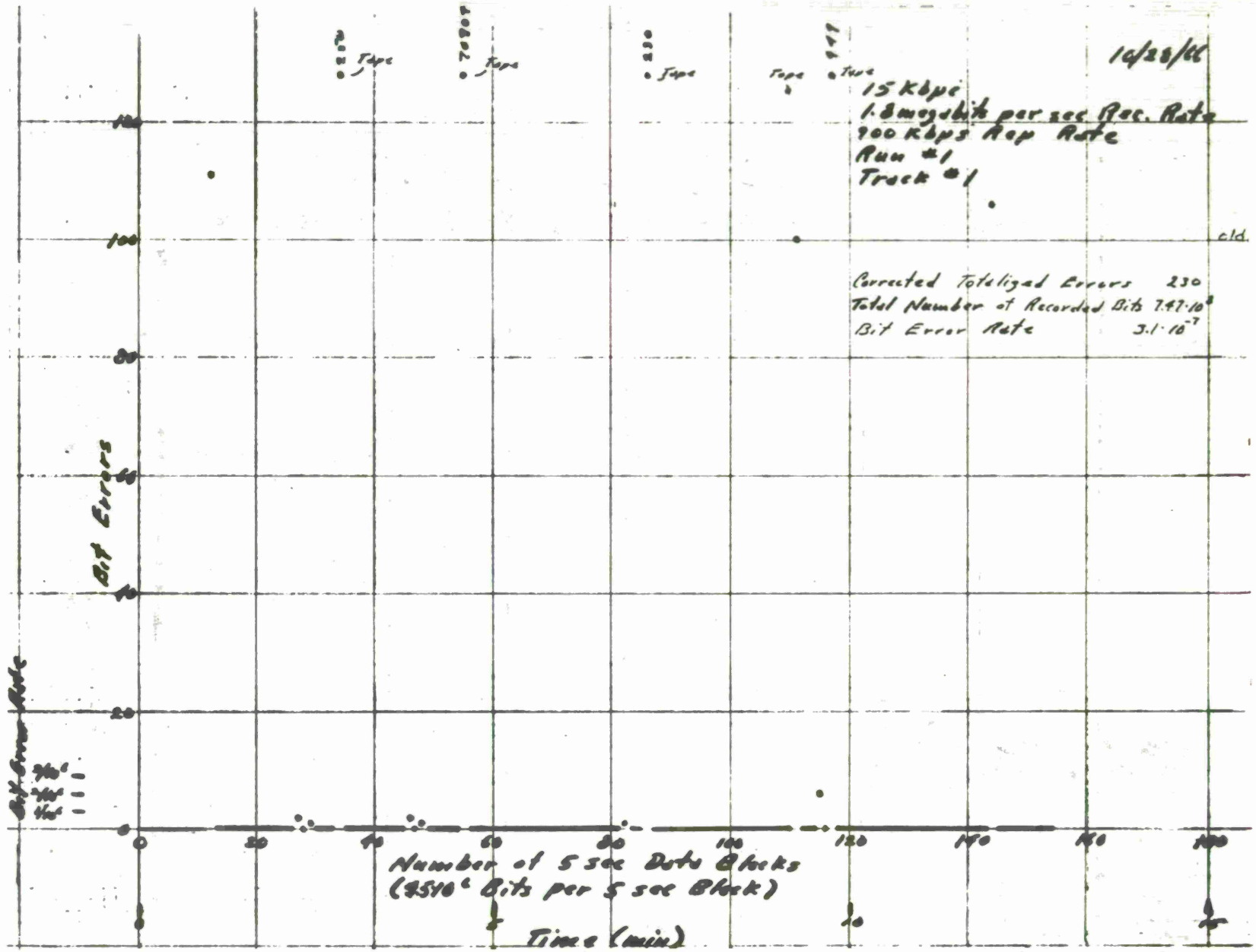
10/28/66
15 Kbpi
1.8 megabit per sec Rec. Rate
900 Kbps Rep Rate
Run #1
Track #1
cld.
Corrected Totaliged Errors 230
Total Number of Recorded Bits 7.47·10⁸
Bit Error Rate 3.1·10⁻⁷
Bit Errors
Bit Error Rate
Number of 5 sec Data Blocks
(2510⁴ Bits per 5 sec Block)
Time (min)

Fig. 32

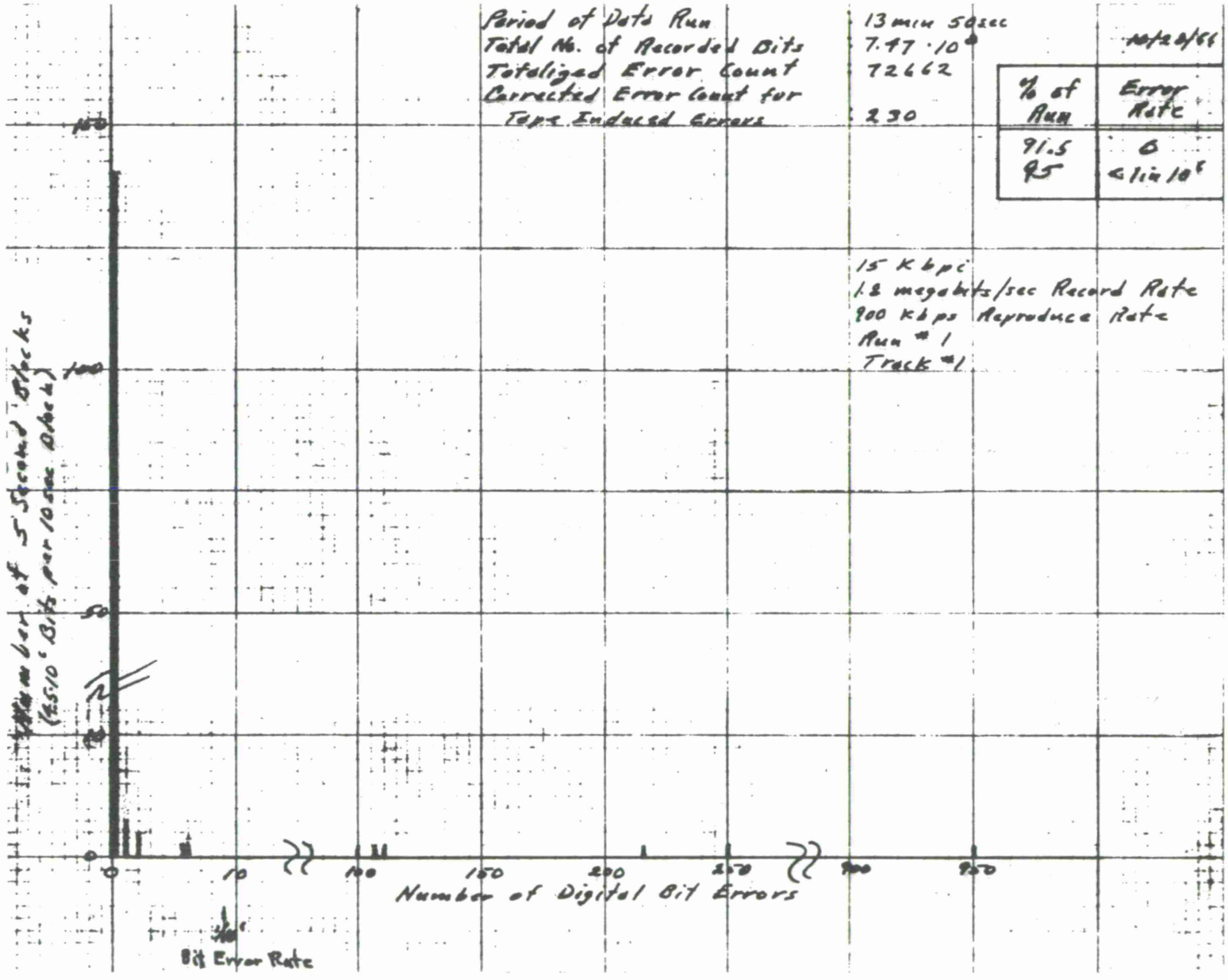
Period of Data Run
13 min 50 sec
Total No. of Recorded Bits
7.47 · 10⁸
Totaliged Error Count
72662
Corrected Error Count for
Tape Induced Errors
230
% of Run
Error Rate
91.5
0
< 1 in 10⁸
15 K bpi
1.2 megabits/sec Record Rate
900 kbps Reproduce Rate
Run # 1
Track #1
Number of Digital Bit Errors
Bit Error Rate

Fig. 33

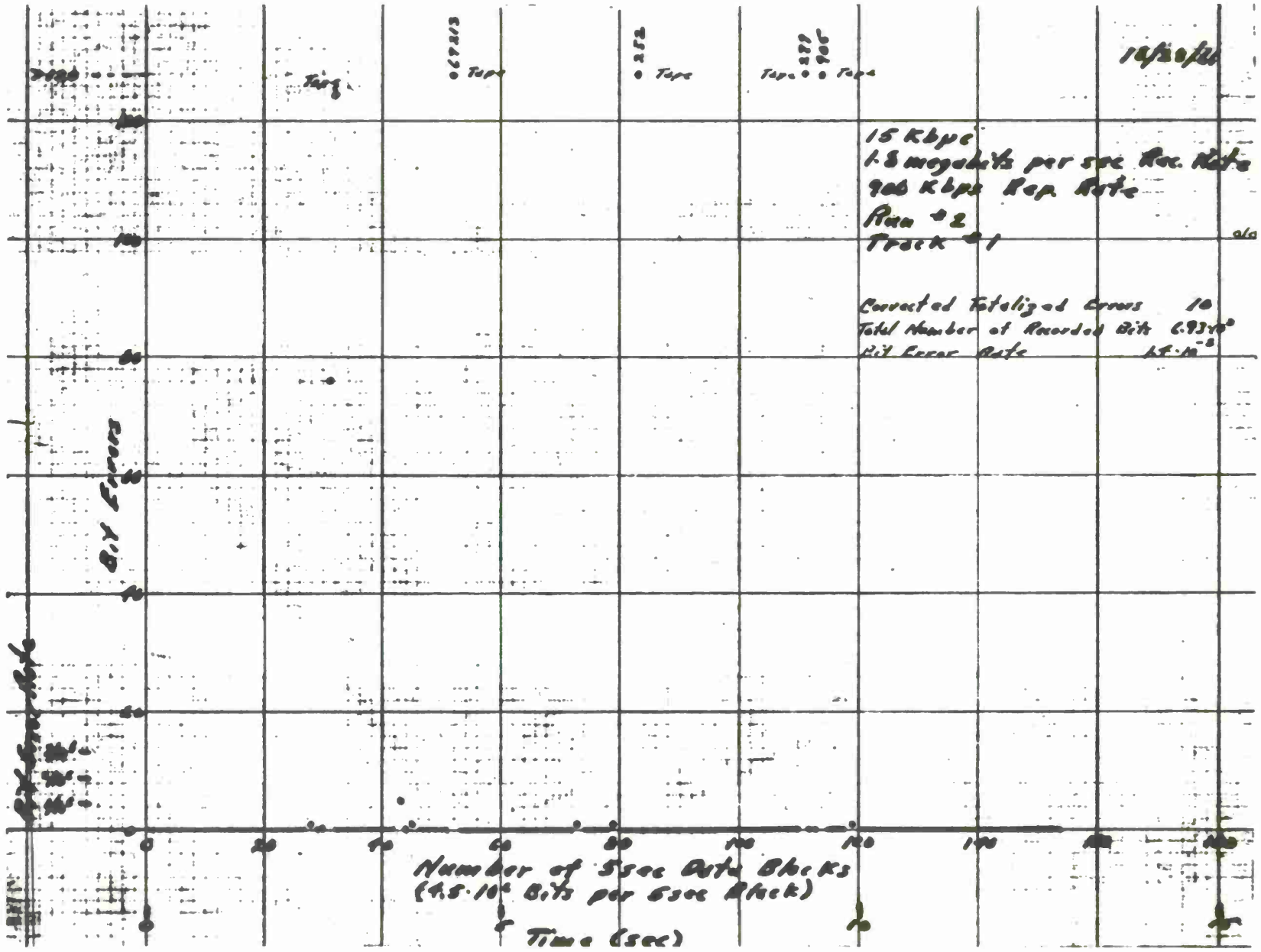
15 Kbps
1.8 megabits per sec Rec. Rate
900 Kbps Rep. Rate
Run #2
Track #1
Corrected Totalized Errors 10
Total Number of Recorded Bits 6.93x10^8
Bit Error Rate 1.4x10^-8
Number of 5 sec Data Blocks
(4.5·10^6 Bits per 5 sec Block)
Time (sec)

Fig. 34

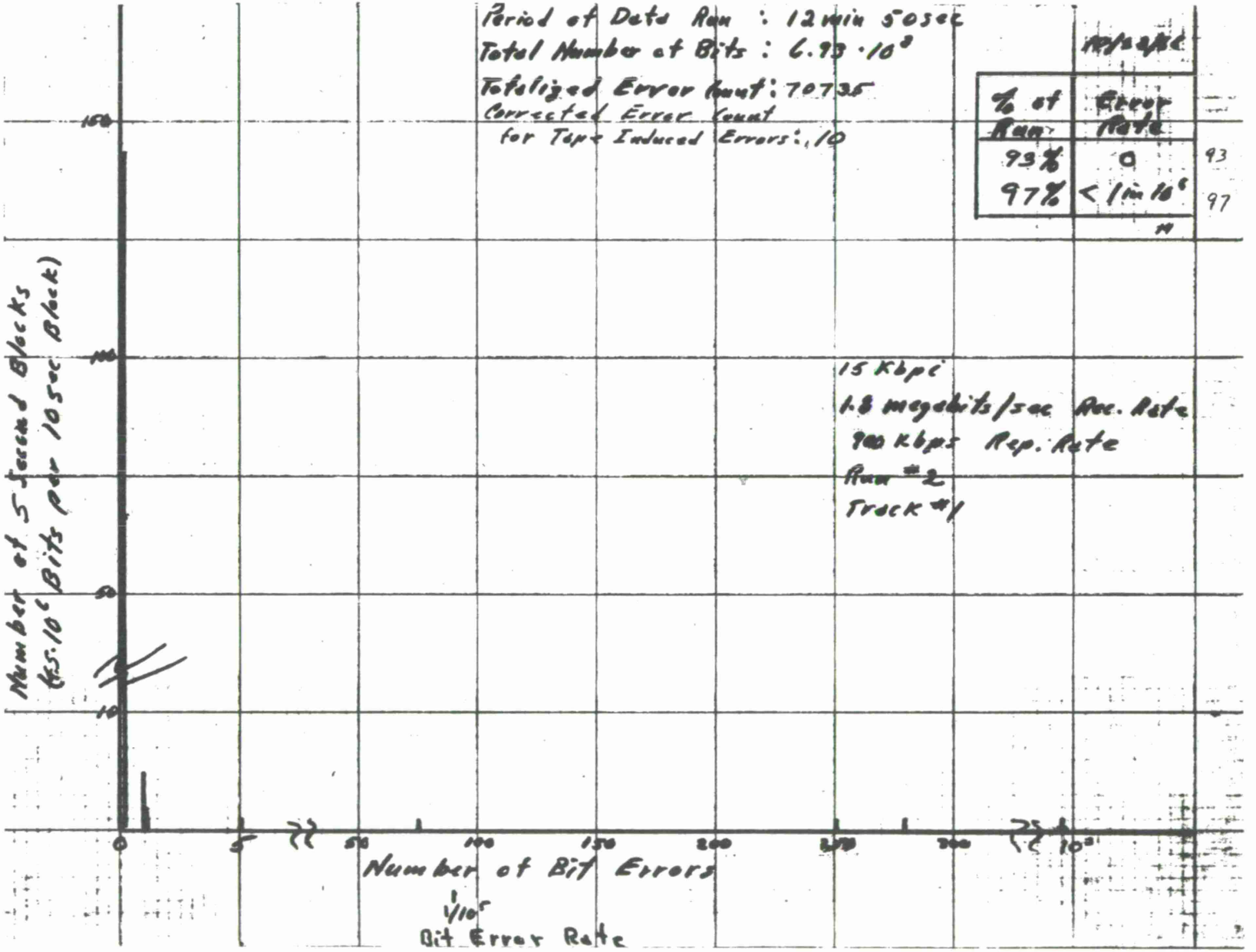
Period of Data Run : 12 min 5.0 sec
Total Number of Bits : 6.93 · 10⁸
Totaliged Error Count: 70735
Corrected Error Count
for Tape Induced Errors: 10
% of Run
Error Rate
93%
97%
0
< 1 in 10⁶
93
97
15 Kbpi
1.8 megabits/sec Rec. Rate
900 Kbps Rep. Rate
Run #2
Track #1
Number of 5 second Blocks
(Ks. 10⁶ Bits per 10 sec Block)
Number of Bit Errors
1/10⁵
Bit Error Rate

Fig. 35

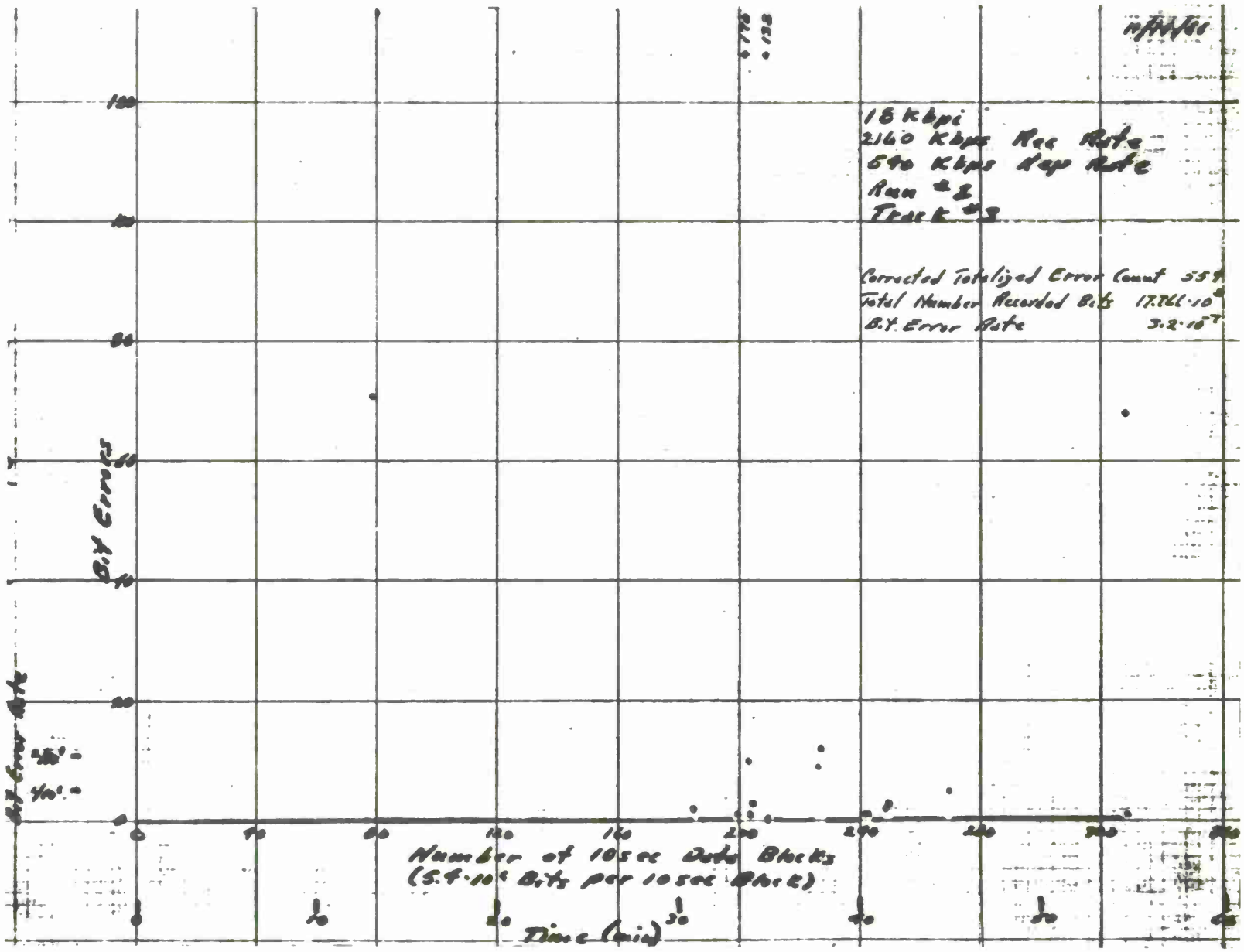
18 Kbpi
2160 Kbps Rec Rate
540 Kbps Rep Rate
Run #1
Track #3
Corrected Totalized Error Count 55
Total Number Recorded Bits 17.66·10⁸
B.E. Error Rate 3.2·10⁻⁷
B.E. Errors
B.E. Error Rate
Number of 10 sec Data Blocks
(5.4·10⁶ Bits per 10 sec Block)
Time (min)

Fig. 36

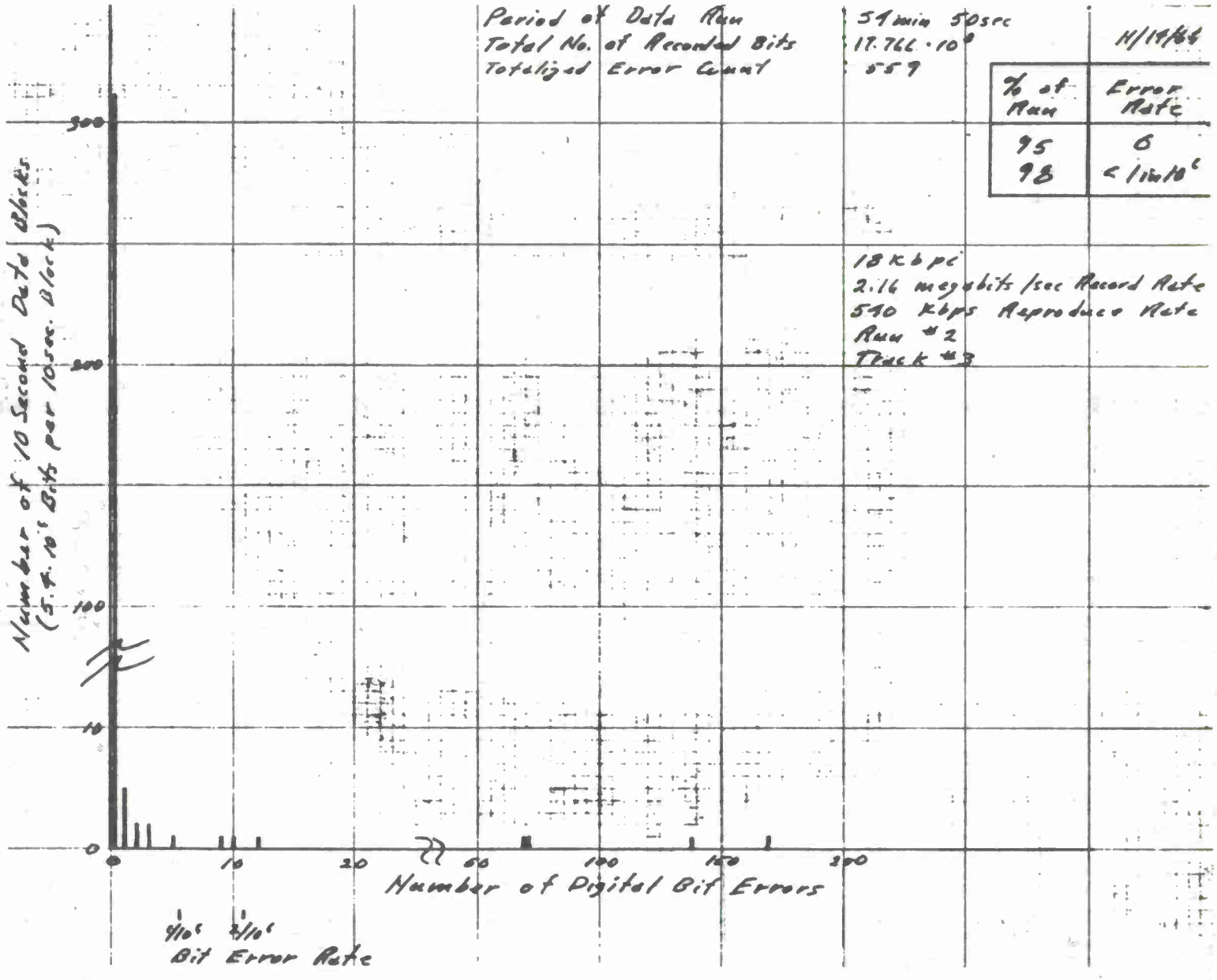
Period of Data Run
Total No. of Recorded Bits
Totalized Error Count
54 min 50 sec
17.766 · 10⁹
559
11/19/66
% of Run
Error Rate
95
98
6
< 1 in 10⁶
18 Kbpc
2.16 megabits/sec Record Rate
540 Kbps Reproduce Rate
Run #2
Track #3
Number of 10 Second Data Blocks
(5.4 · 10⁵ Bits per 10 sec. Block)
300
200
100
10
0
0
10
20
50
100
150
300
Number of Digital Bit Errors
1/10⁶
2/10⁶
Bit Error Rate

Fig. 37

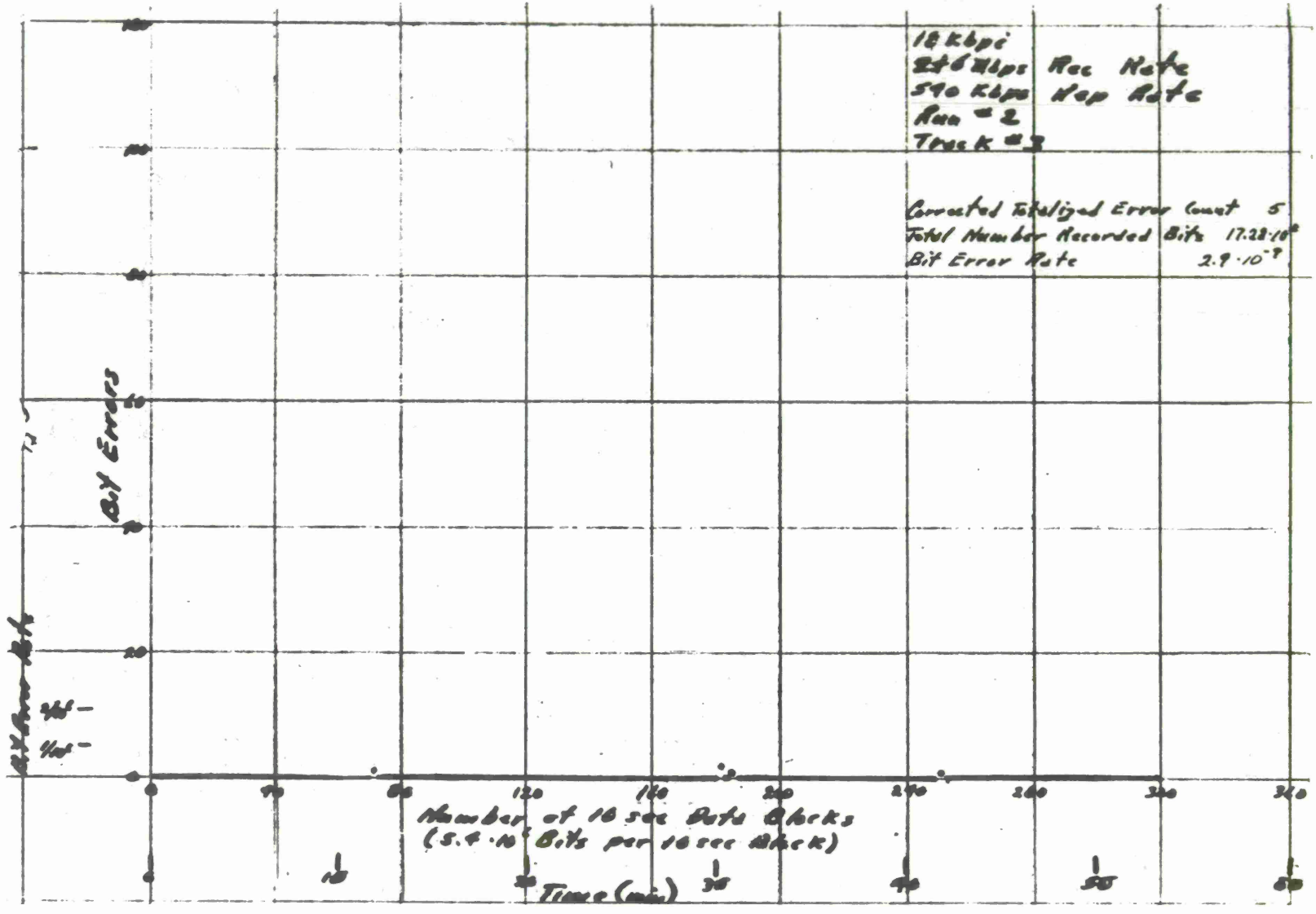
18 Kbpi
246 Kbps Rec Rate
590 Kbps Nop Rate
Run = 2
Track = 3
Corrected Tolerized Error Count 5
Total Number Recorded Bits 17.28·10⁹
Bit Error Rate 2.9·10⁻⁹
Bit Errors
Number of 10 sec Data Checks
(5.4·10⁶ Bits per 10 sec Block)
Time (min)

Fig. 38

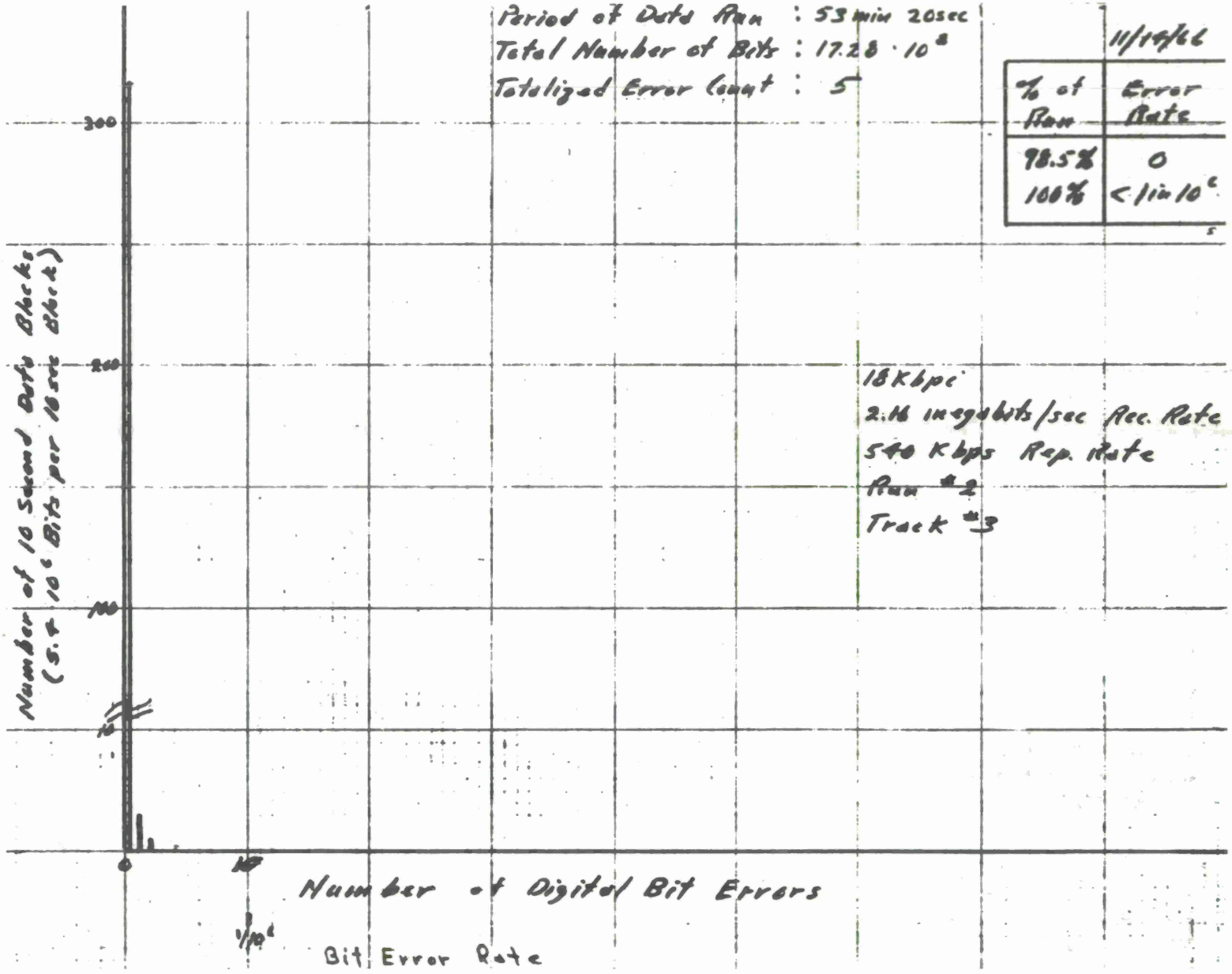
Period of Data Run : 53 min 20 sec
Total Number of Bits : 17.28 · 10⁸
Totalized Error Count : 5
11/19/66
% of Run
Error Rate
98.5%
0
100%
< 1 in 10⁶
5
18 Kbps
2.16 megabits/sec Rec. Rate
540 Kbps Rep. Rate
Run #2
Track #3
Number of 10 Second Data Blocks
(5.4 · 10⁶ Bits per 10 sec Block)
300
200
100
10
1
0
Number of Digital Bit Errors
1/10⁶
Bit Error Rate

Fig. 39

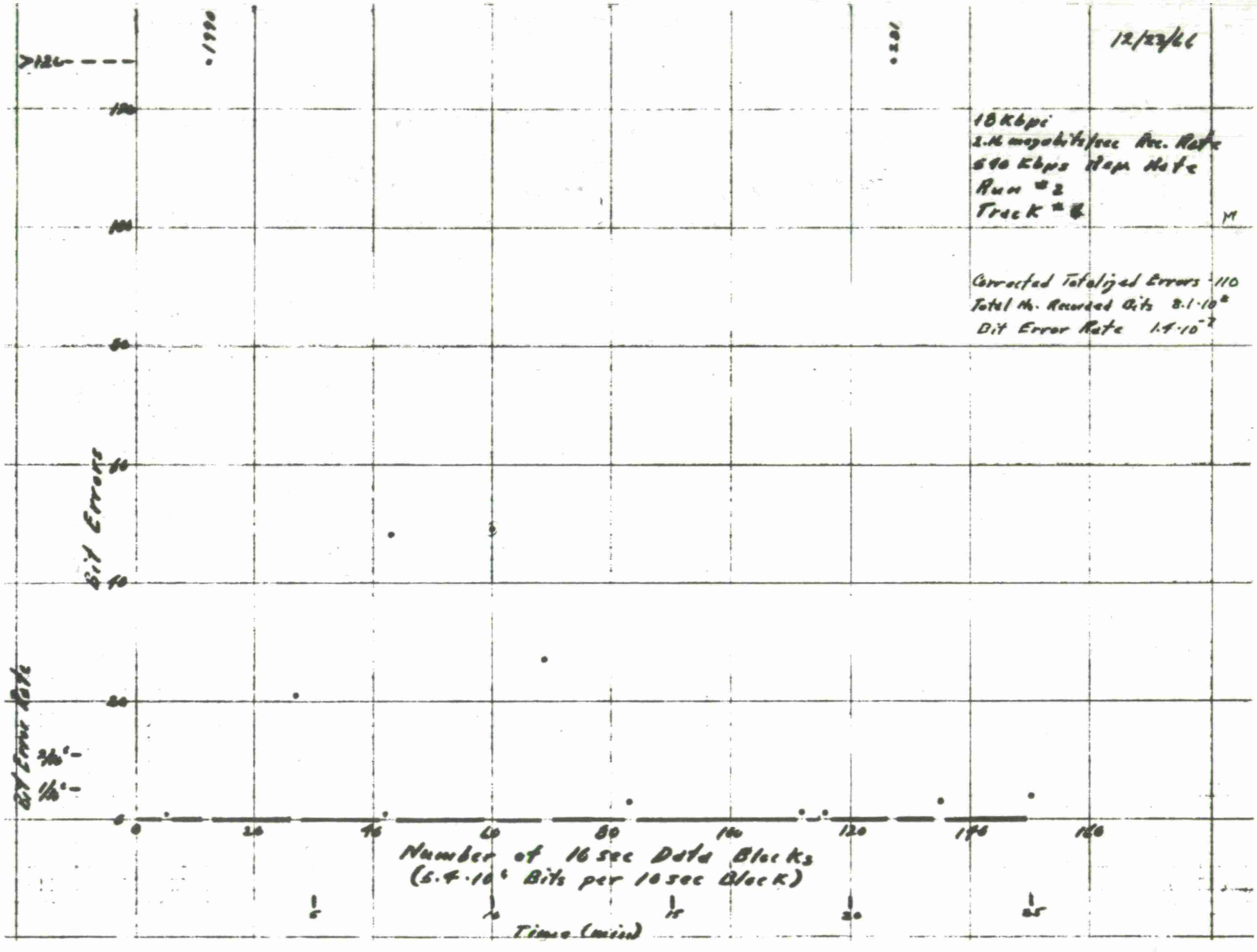
12/23/66
18 Kbpi
2.4 megabits/sec Rec. Rate
540 Kbps Dump Rate
Run #2
Track #6
Corrected Totalized Errors 110
Total No. Recorded Bits 8.1·10⁸
Bit Error Rate 1.4·10⁻⁷
Bit Errors
Bit Error Rate
Number of 16 sec Data Blocks
(5.4·10⁶ Bits per 16 sec Block)
Time (min)

Fig. 40

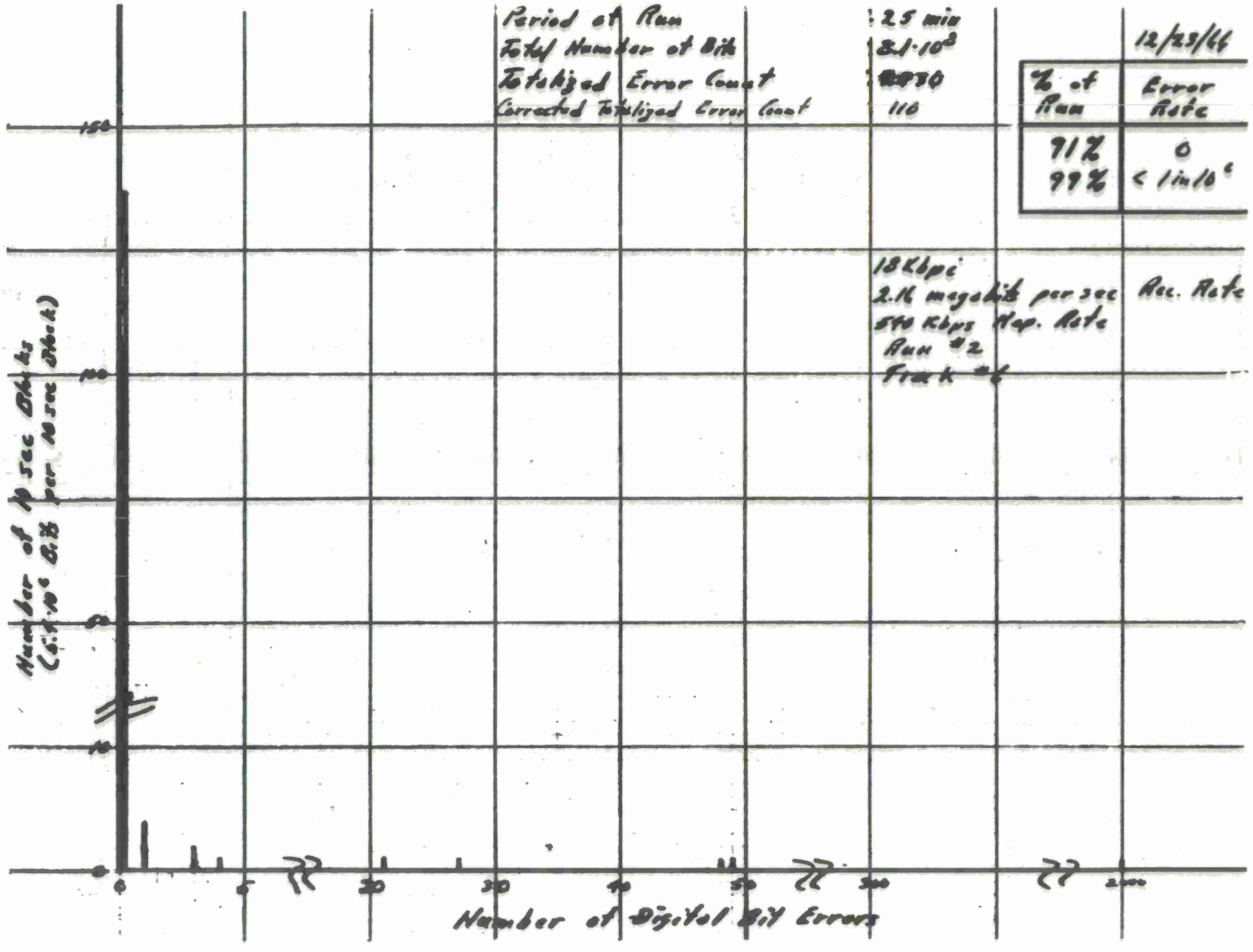
Period of Run
Total Number of Bits
Totalized Error Count
Corrected Totalized Error Count
25 min
2.1·10⁸
8970
110
% of Run
Error Rate
91%
99%
0
< 1 in 10⁶
12/23/64
18 Kbpi
2.4 megabits per sec
540 Kbps Rep. Rate
Run #2
Track #6
Rec. Rate
Number of Digital Bit Errors

Fig. 41

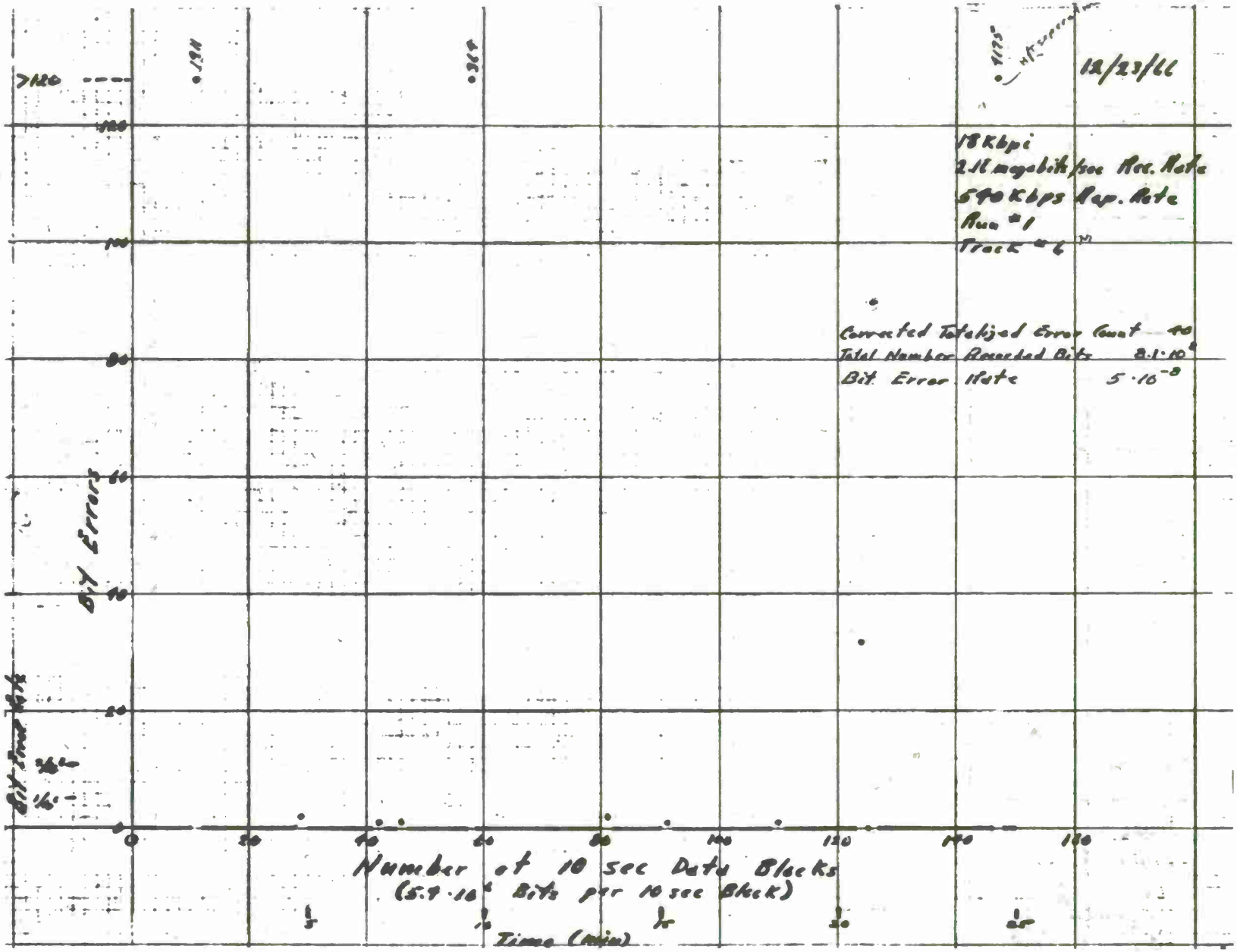
12/23/66
18 Kbpi
2.16 megabit/sec Rec. Rate
540 Kbps Rep. Rate
Run #1
Track #6
Corrected Tabulated Error Count 40
Total Number Recorded Bits 8.1·10^8
Bit Error Rate 5·10^-8
Bit Errors
Bit Error Rate
Number of 10 sec Data Blocks
(5.9·10^6 Bits per 10 sec Block)
Time (Min)

Fig. 42

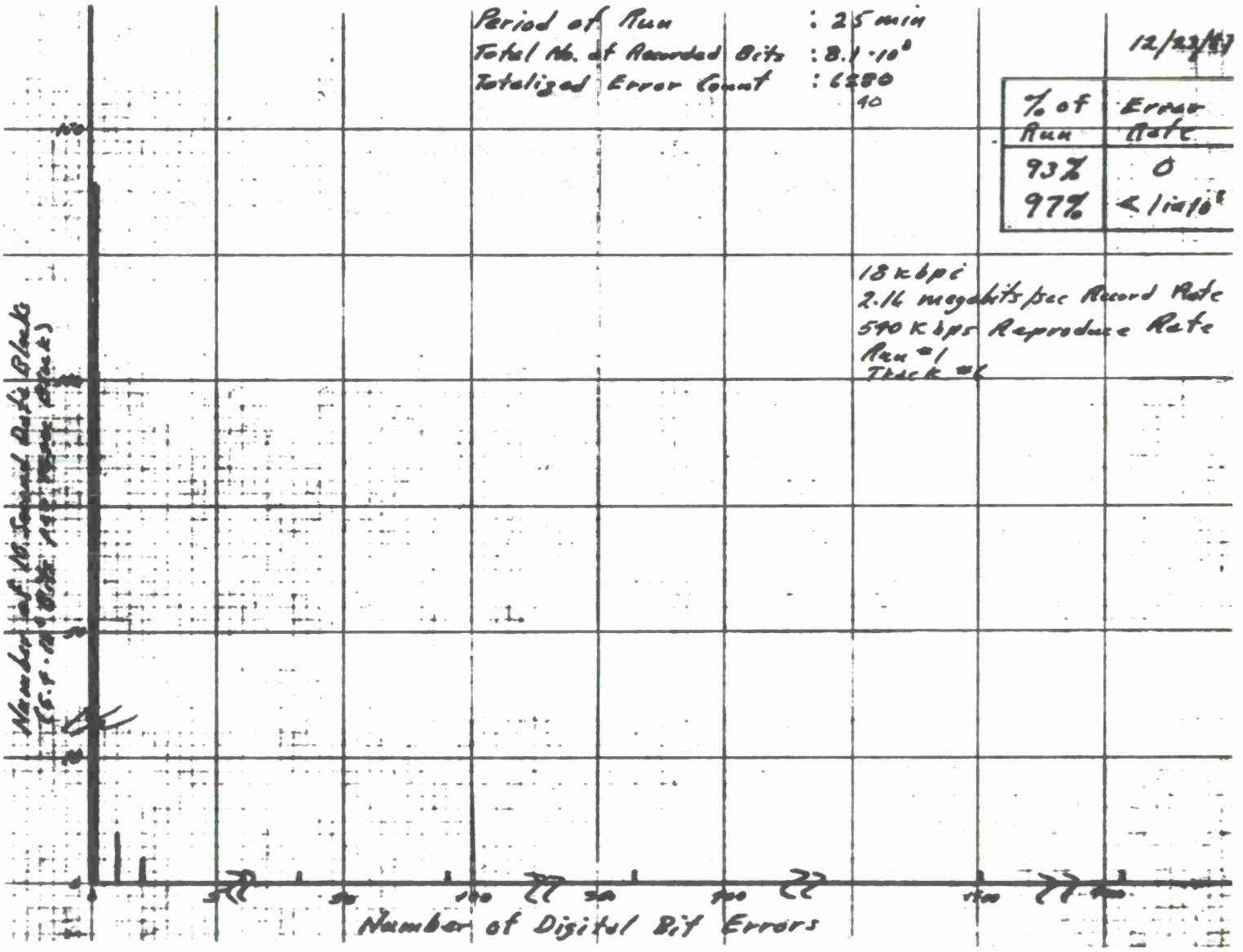
Period of Run : 25 min
Total No. of Recorded Bits : 8.1 · 10^8
Totalized Error Count : 6280
40
12/23/63
% of Run
Error Rate
93%
0
97%
< 1 in 10^8
18 kbpi
2.14 megabits/sec Record Rate
540 kbps Reproduce Rate
Run #1
Track #
Number of Digital Bit Errors

Fig. 43

1/17/67

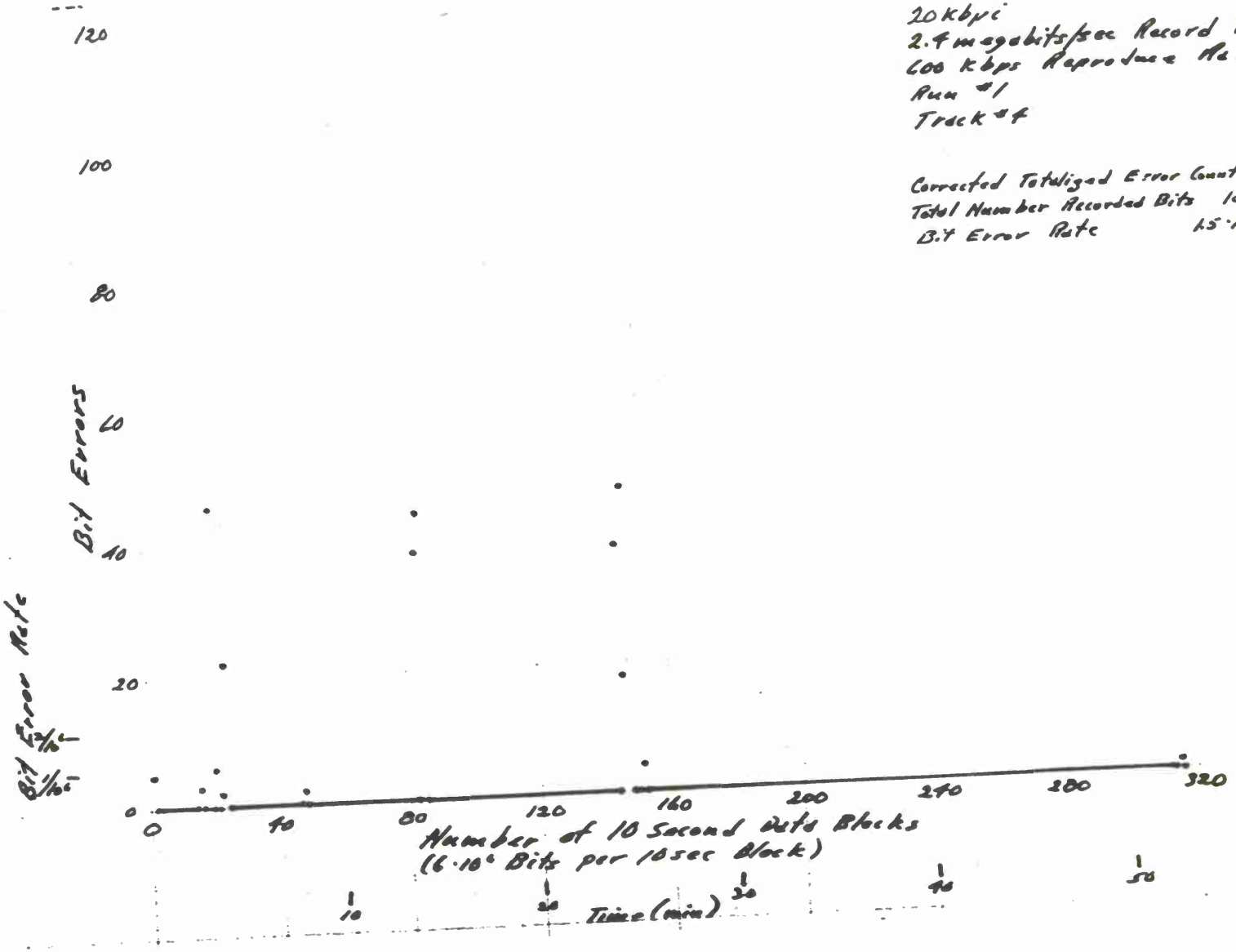

20 Kbyte
2.4 megabits/sec Record Rate
600 kbps Reproduce Rate
Run #1
Track #4

Corrected Totaliged Error Count 281
Total Number Recorded Bits $18.96 \cdot 10^8$
B.E Error Rate $15 \cdot 10^{-7}$

Fig. 44

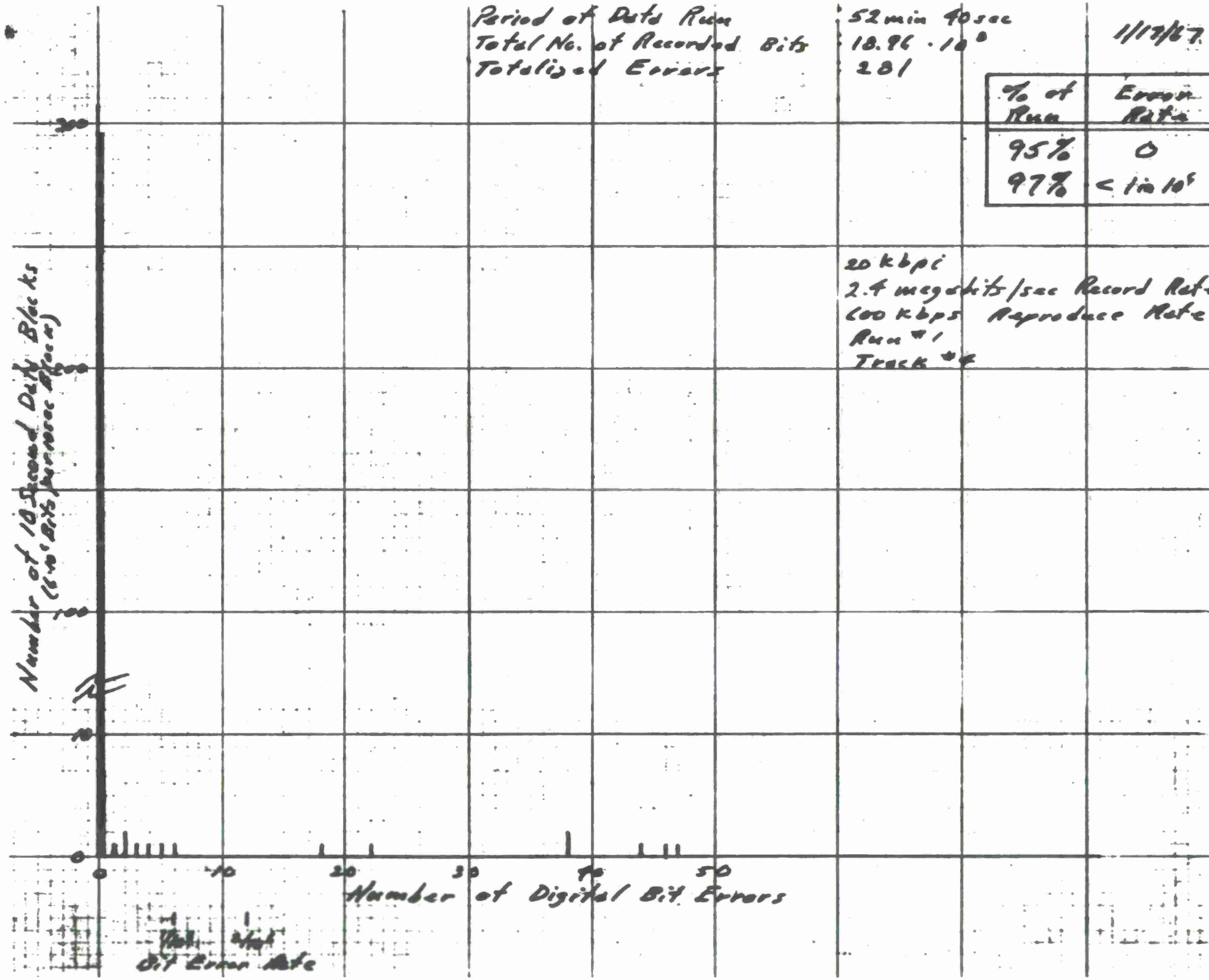
Period of Data Run : 52 min 40 sec
Total No. of Recorded Bits : 18.96 · 10⁹
Totalized Errors : 281
1/17/67
% of Run | Error Rate
95% | 0
97% | < 1 in 10⁸
20 kbpi
2.4 megabits/sec Record Rate
600 kbps Reproduce Rate
Run #1
Track #4
Number of 10 Second Data Blocks
(6·10⁶ Bits per 10 sec Block)
300
200
100
10
0
10
20
30
40
50
Number of Digital Bit Errors

Fig. 45

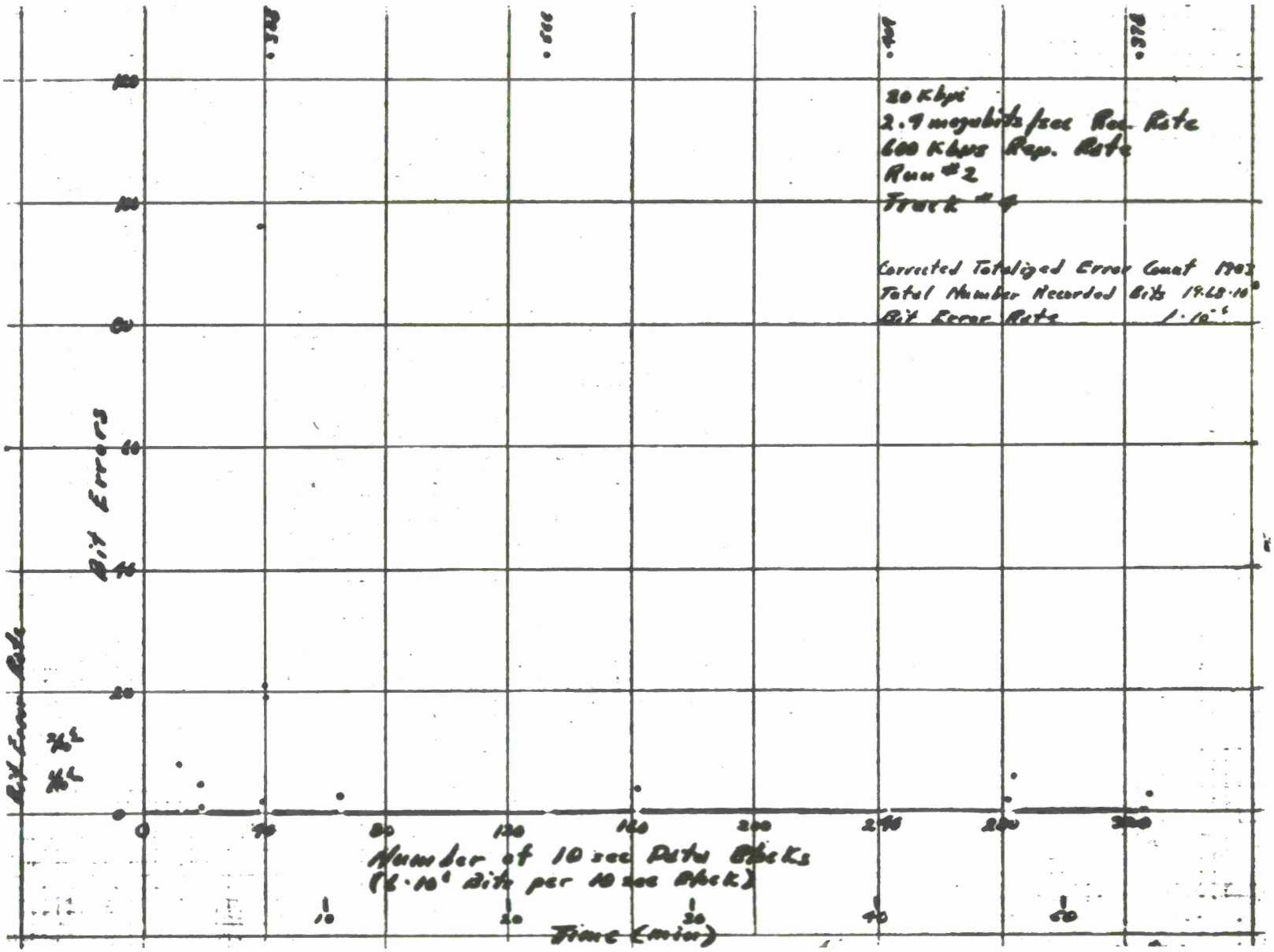
20 Kbps
2.4 megabits free Rec. Rate
600 Kbps Rep. Rate
Run #2
Track #4
Corrected Totalized Error Count 1903
Total Number Recorded Bits 19.48·10⁹
Bit Error Rate 1·10⁻⁶
Bit Errors
Bit Error Rate
Number of 10 sec Data Blocks
(1·10⁶ bits per 10 sec Block)
Time (min)

Fig. 46

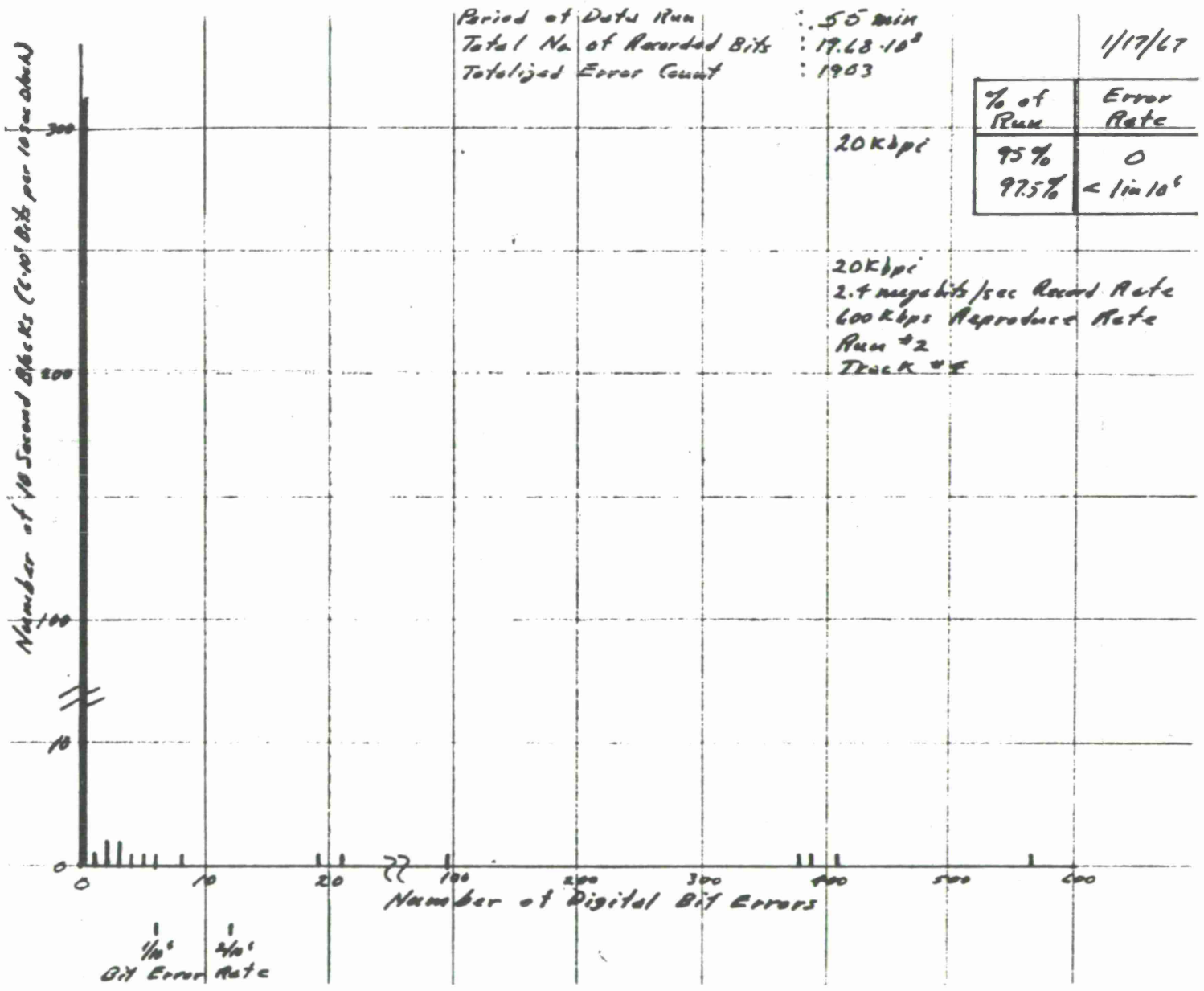
Period of Data Run : 50 min
Total No of Recorded Bits : 17.68·10⁹
Totalized Error Count : 1903
1/17/67
% of Run
Error Rate
95%
0
97.5%
< 1 in 10⁶
20 Kbpi
20 Kbpi
2.4 megabits/sec Record Rate
600 Kbps Reproduce Rate
Run #2
Track #F
Number of 1/10 Second Blocks (5·10⁴ Bits per 1/10 sec block)
300
200
100
10
0
0
10
20
100
200
300
400
500
600
Number of Digital Bit Errors
1/10⁴ Bit Error Rate
2/10⁴

Fig. 47

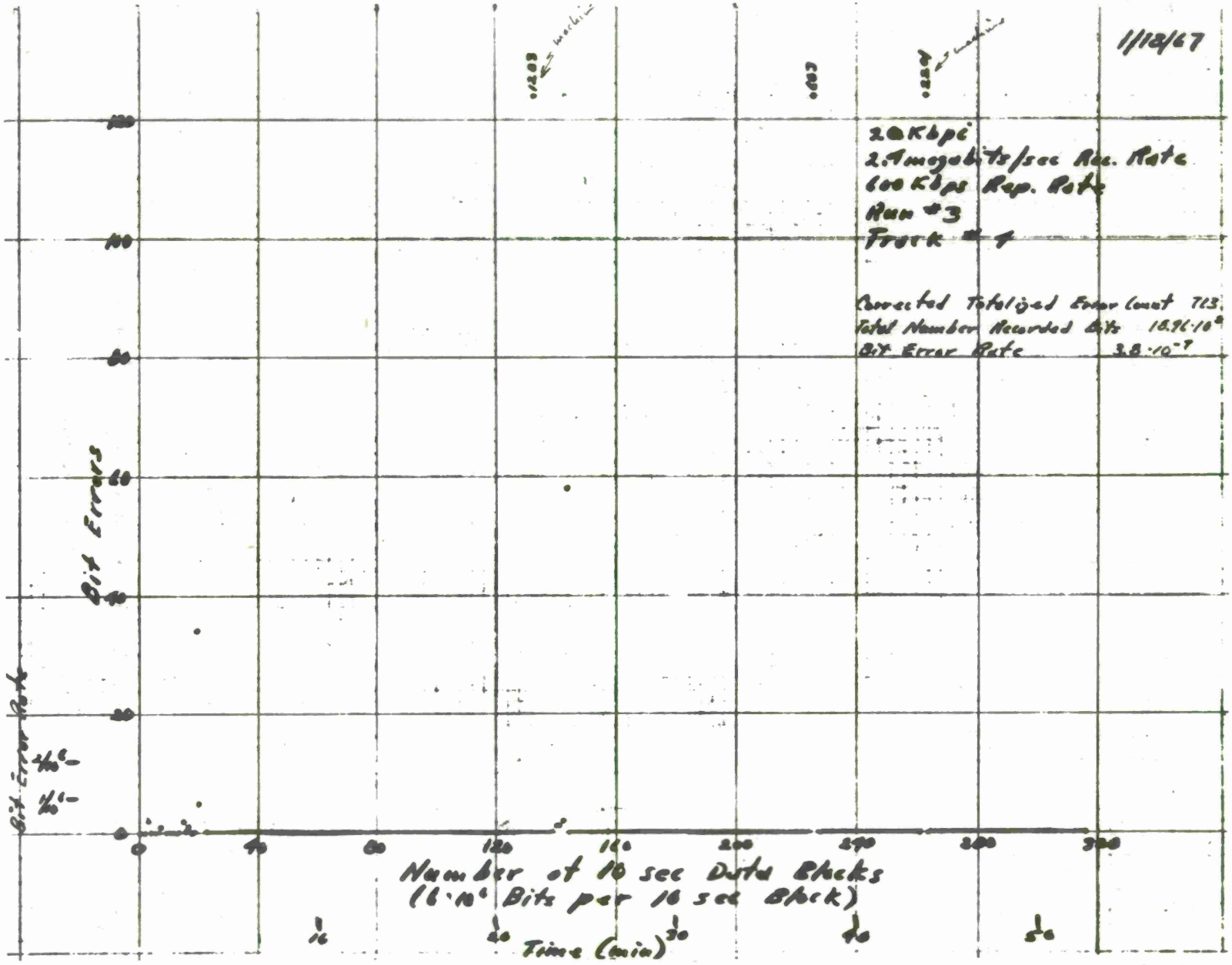
1/12/67
200 Kbpi
2.4 megabits/sec Rec. Rate
600 Kbps Rep. Rate
Run #3
Frame = 4
Corrected Tabulated Error Count 713
Total Number Recorded Bits 18.96·10⁹
Bit Error Rate 3.8·10⁻⁷
Bit Errors
Bit Error Rate
Number of 10 sec Data Blocks
(1.8·10⁶ Bits per 10 sec Block)
Time (min)

Fig. 48

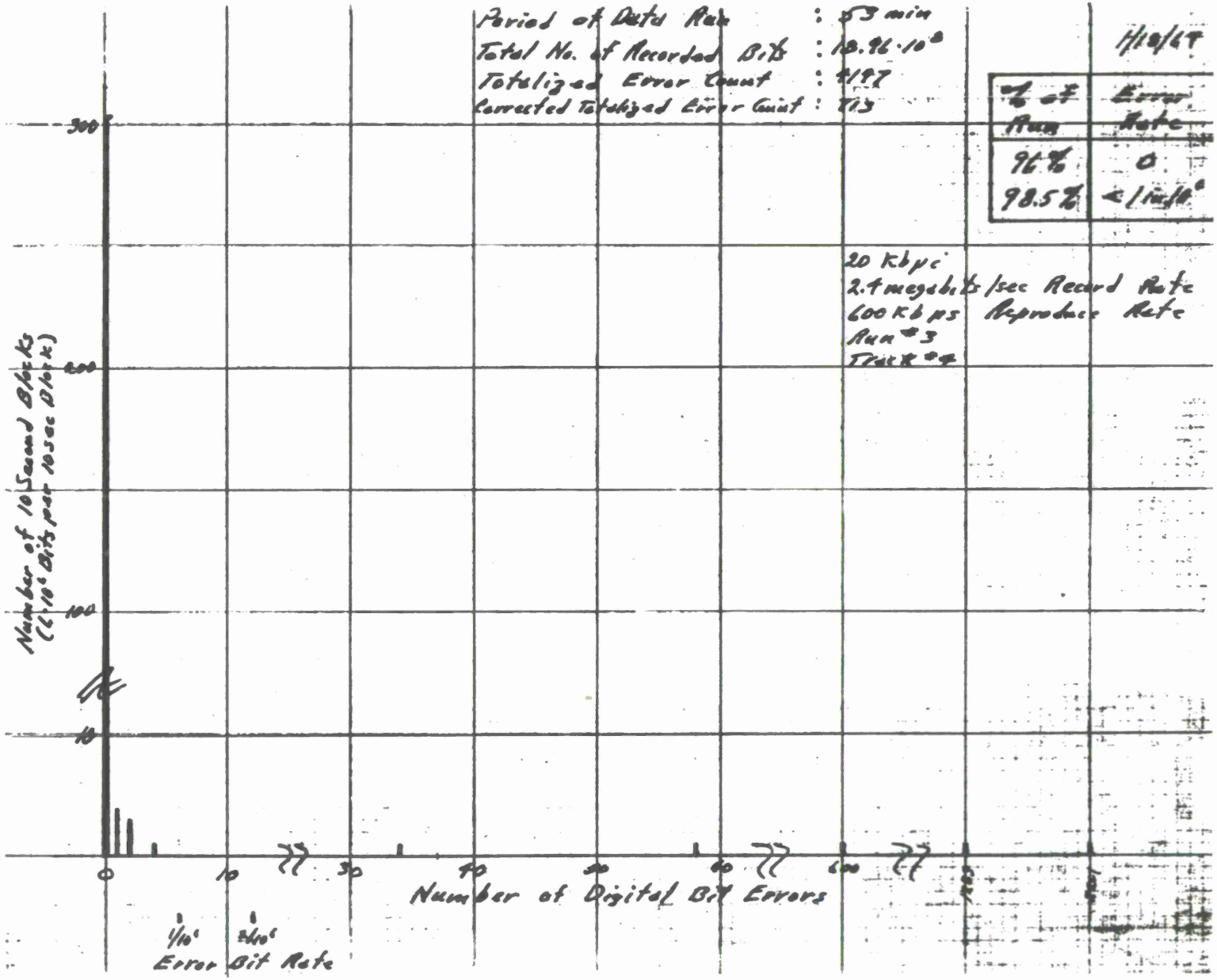
Period of Data Run : 53 min
Total No. of Recorded Bits : 18.96·10⁸
Totalized Error Count : 1197
Corrected Totalized Error Count : 713
11/10/67
% of Runs
Error Rate
96%
0
98.5%
< 1/10⁸
20 Kbps
2.4 megabits/sec Record Rate
600 Kbps Reproduce Rate
Run #3
Track #4
Number of 10 Second Blocks (1/10⁶ Bits per 10 sec Block)
300
200
100
10
0
10
30
40
60
Number of Digital Bit Errors
1/10⁶ Error Bit Rate
2/10⁶

Fig. 49

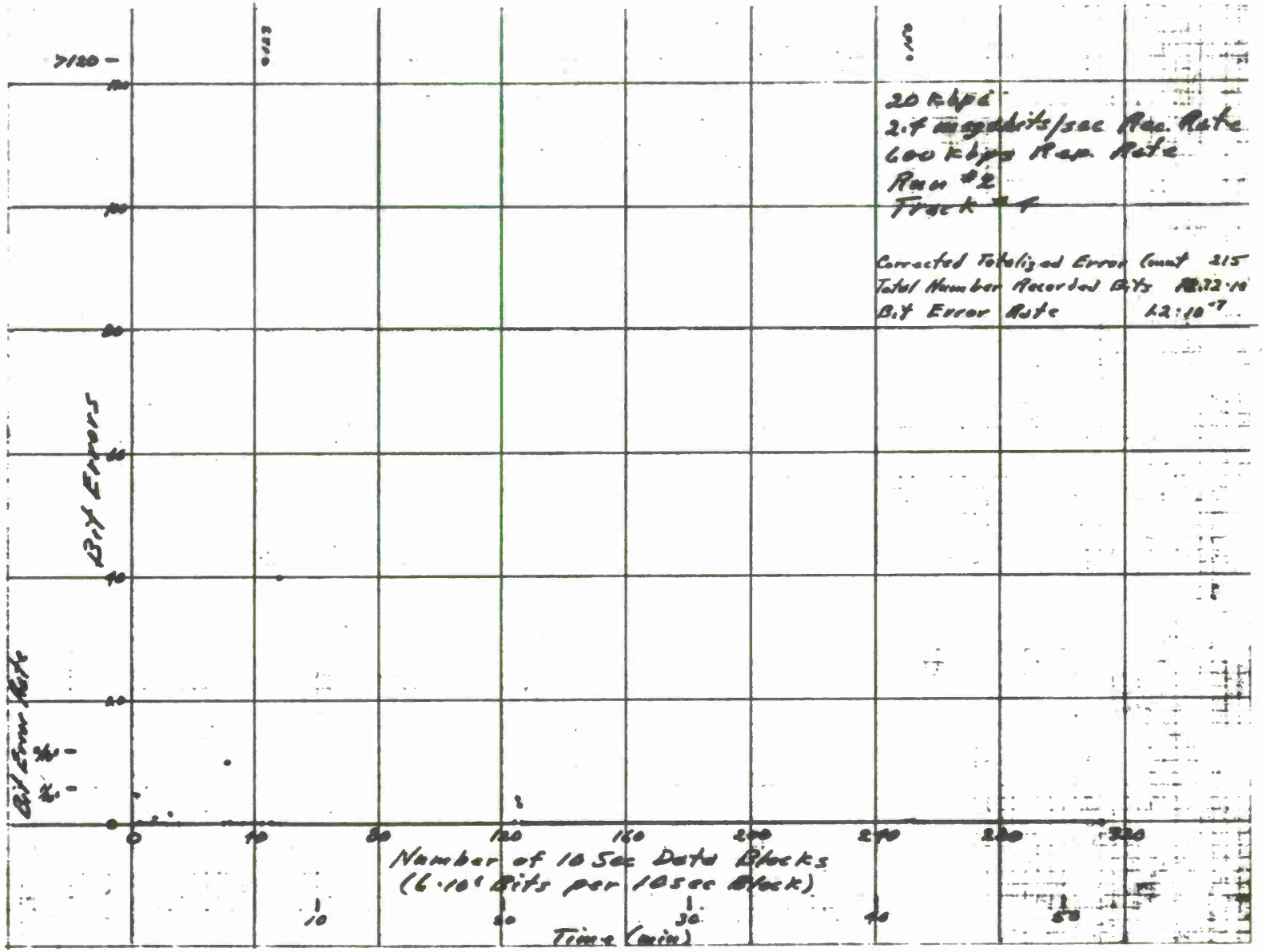
20 kbps
2.4 megabits/sec Rec. Rate
600 kbps Rec. Rate
Run #2
Track #4
Corrected Tabulized Error Count 215
Total Number Recorded Bits
Bit Error Rate
Bit Error Rate
Number of Errors
Number of 10 Sec Data Blocks
(6·10⁶ Bits per 10 sec Block)
Time (min)

Fig. 50

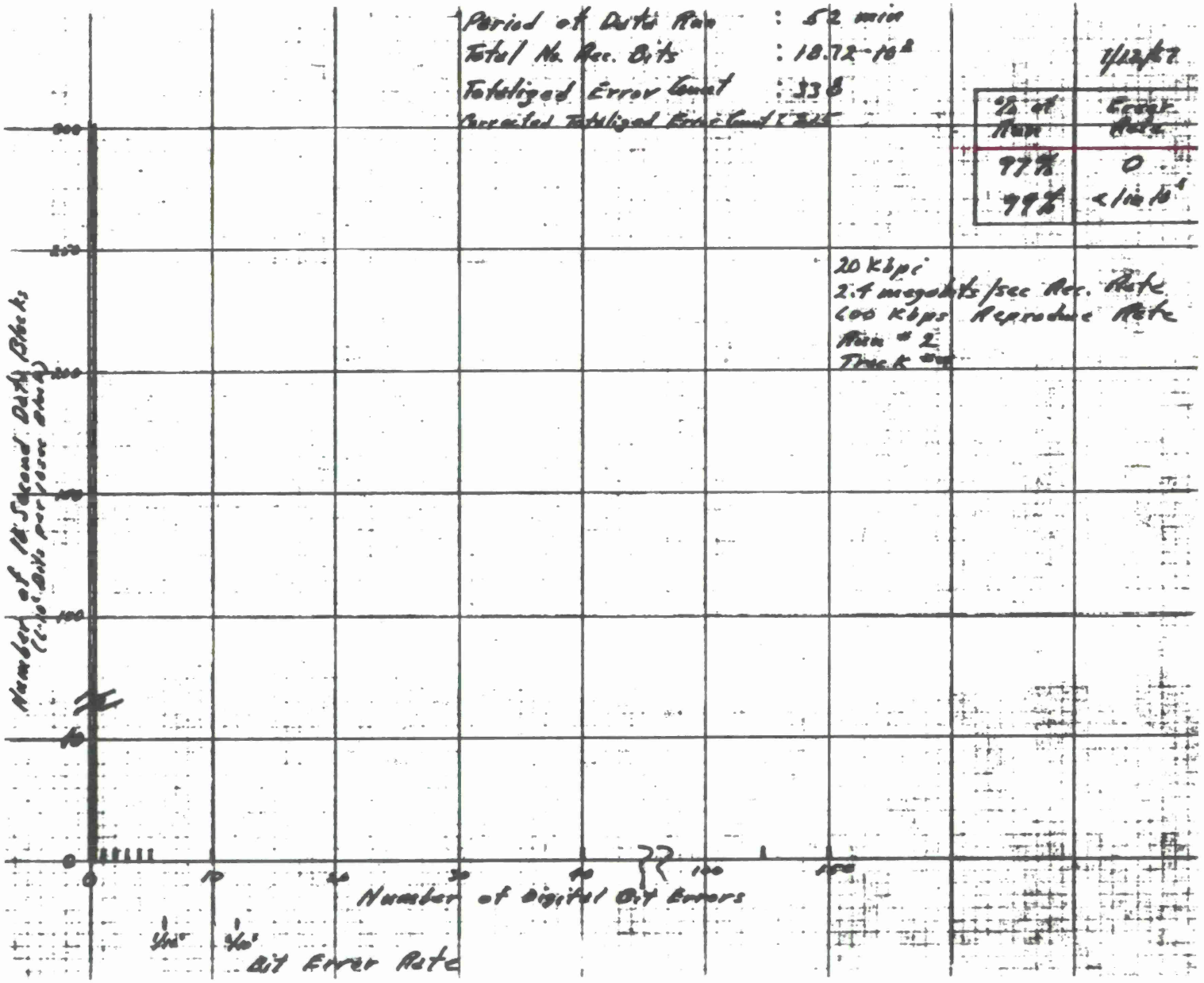
Period of Data Run : 52 min
Total No. Rec. Bits : 10.72-10^8
Total Digital Error Count : 33
Corrected Total Digital Error Count : 25
% of Runs
Error Rate
97%
0
99%
< 1 in 10^8
20 Kbps
2.4 megabits/sec Rec. Rate
600 Kbps Reproduce Rate
Runs = 2
Number of Digital Bit Errors
Bit Error Rate

Fig. 51

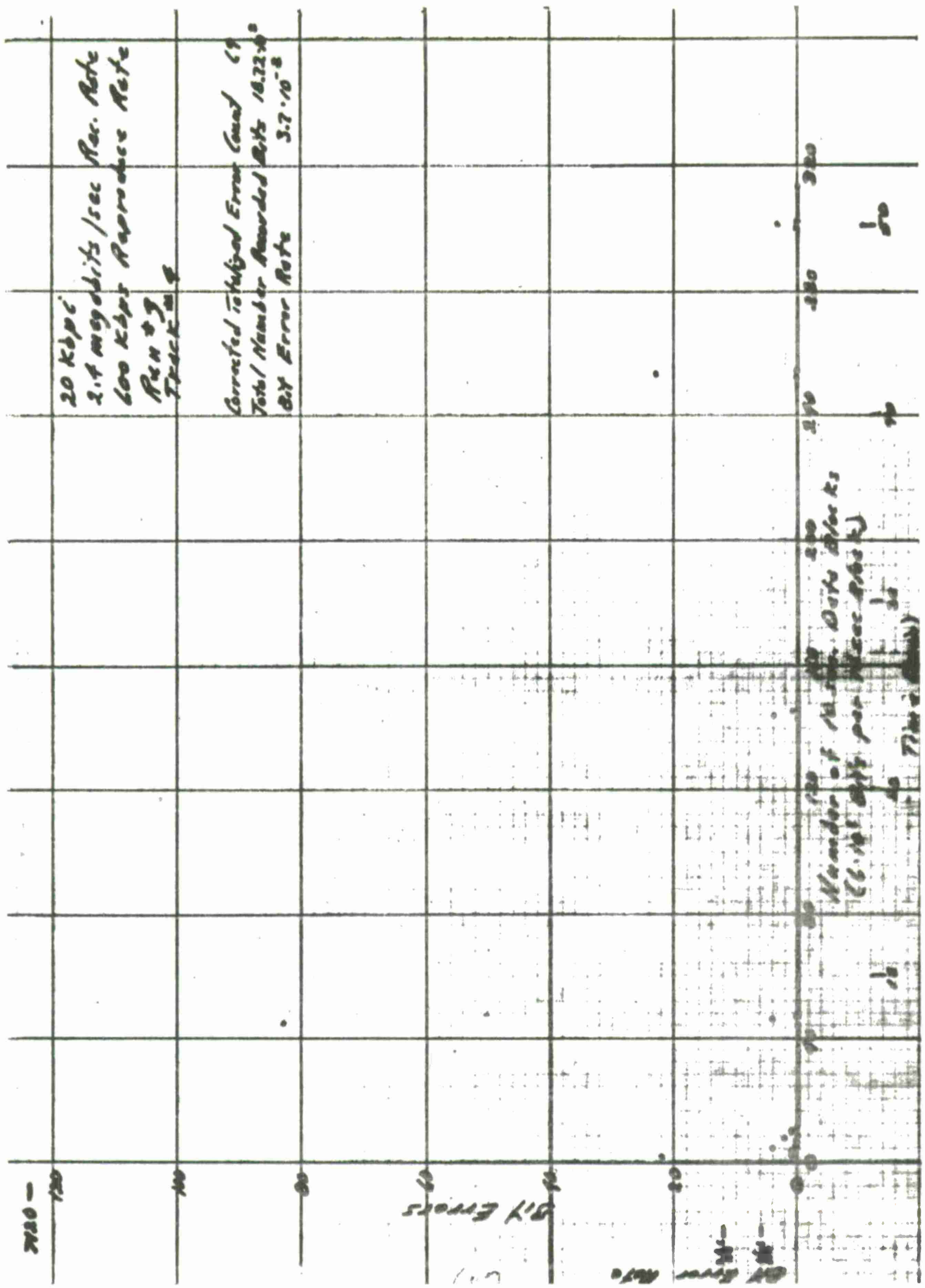

Fig. 52

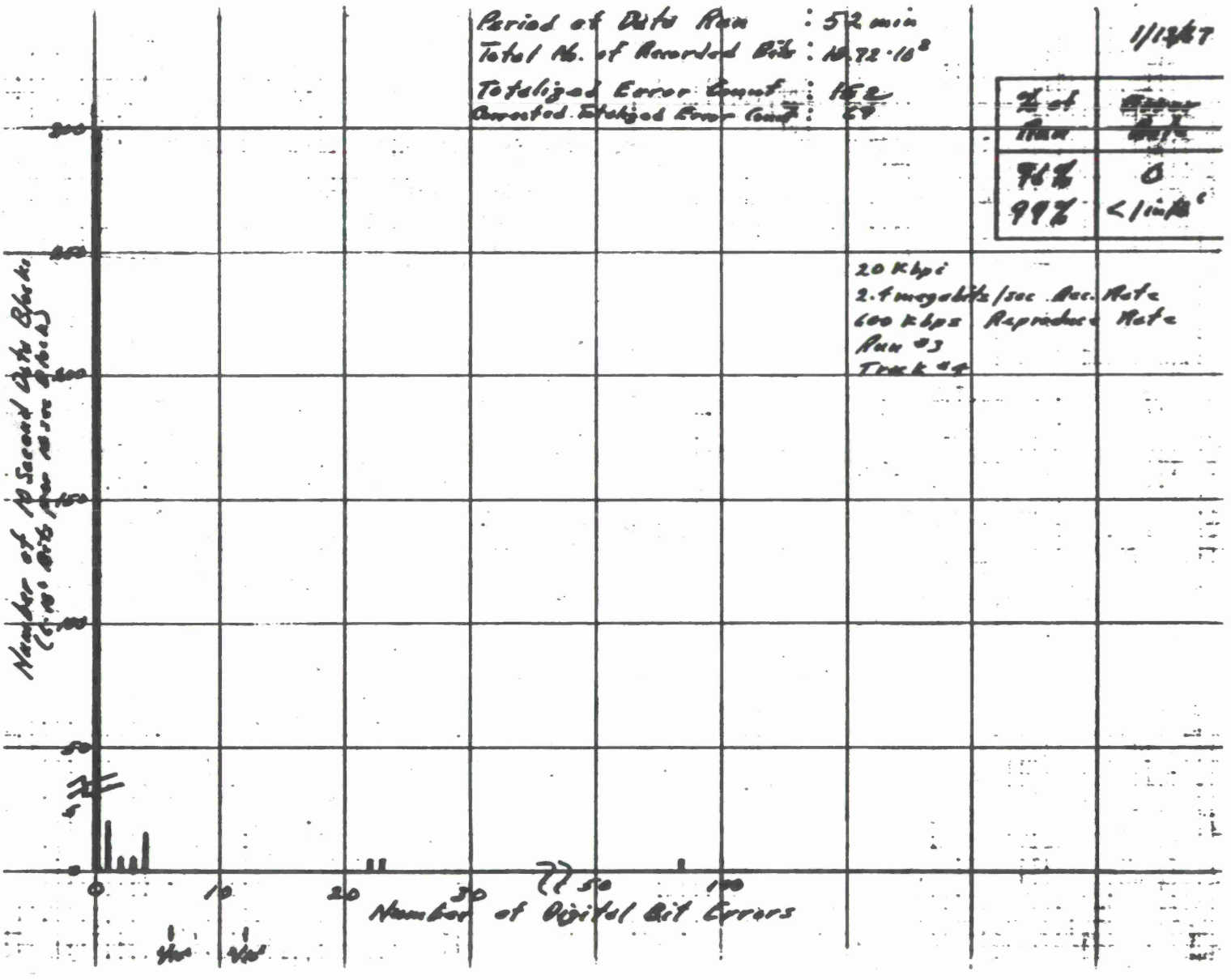
Period of Data Run : 5.2 min
Total No. of Recorded Bits : 10.72·10⁸
Totalized Error Count : 152
Corrected Totalized Error Count : 27
1/12/67
% of Run
76%
99%
0
< 1 in 10⁸
20 Kbpi
2.4 megabits/sec Rec. Rate
600 kbps Reproduce Rate
Run #3
Track #4
Number of Digital Bit Errors
0
10
20
30
50
100

Fig. 53

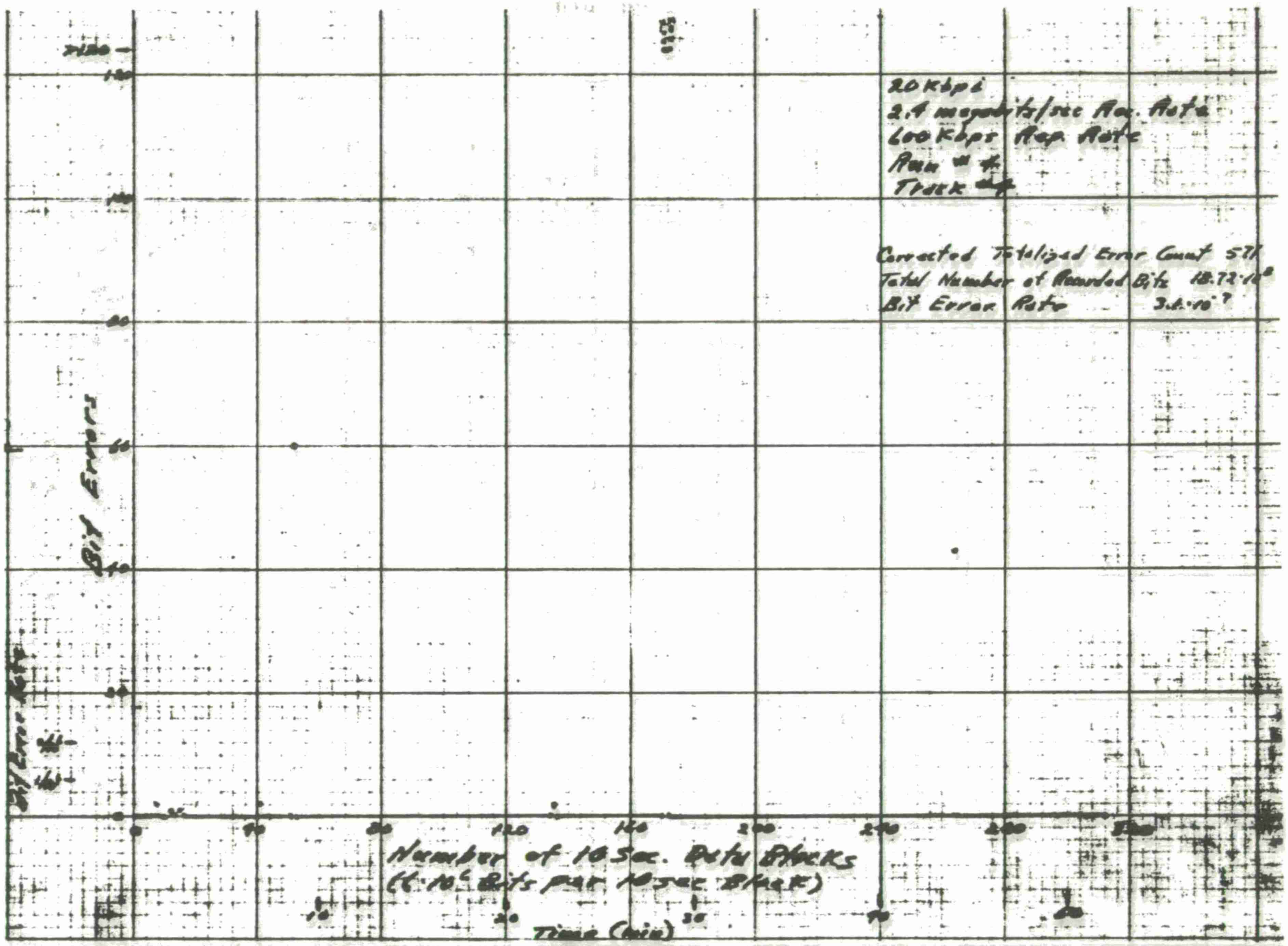
20 Kbpi
2.4 megabits/sec Rec. Rate
600 Kbps Rep. Rate
Corrected Totalized Error Count 571
Total Number of Recorded Bits 18.72·10^8
Bit Error Rate 3.1·10^-7
Bit Errors
Number of 10 Sec. Data Blocks
Time (min)

Fig. 54

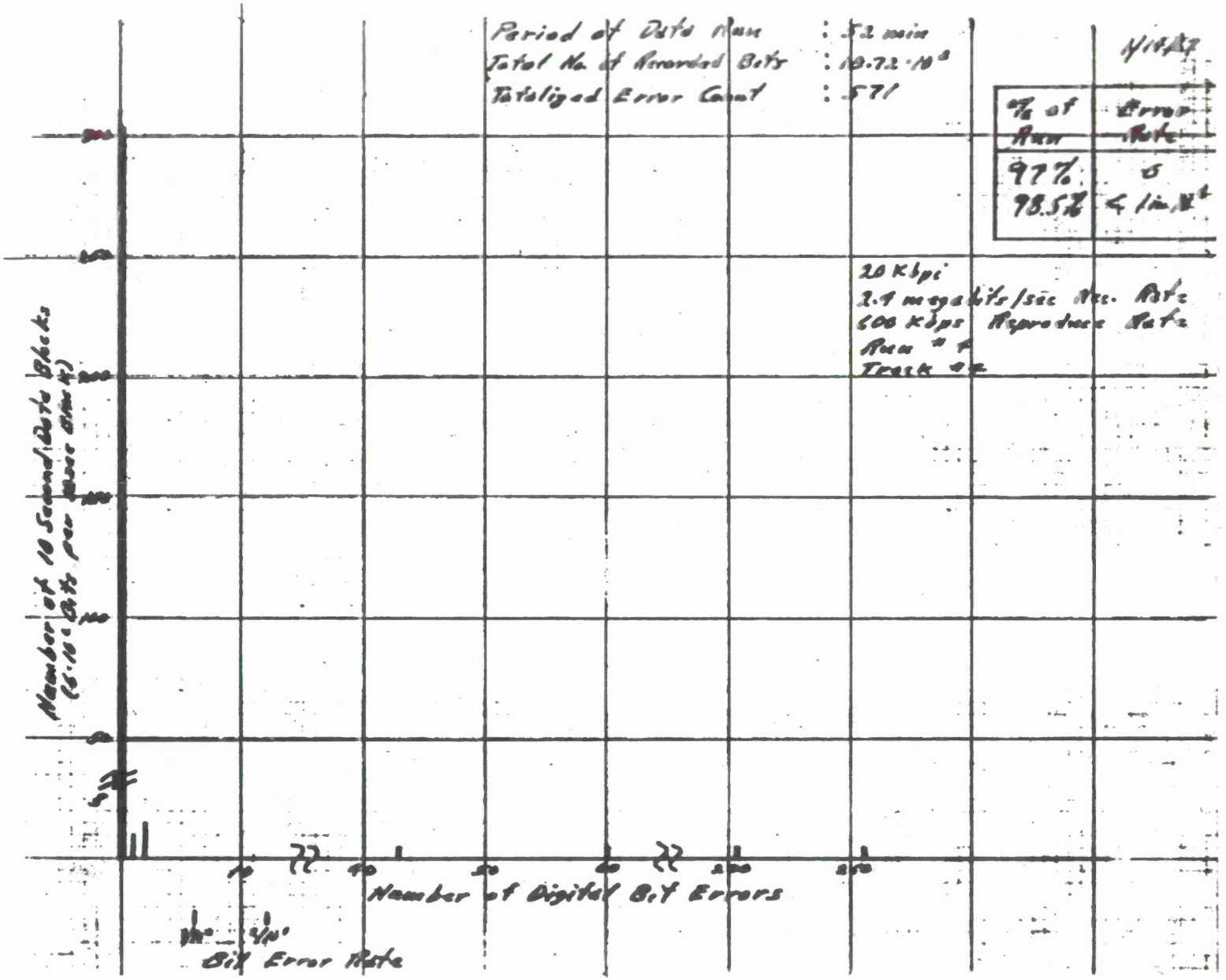
Period of Data Run : 52 min
Total No. of Recorded Bits : 19.72 · 10^9
Totaliged Error Count : 571
% of Run
Error Rate
97%
98.5%
< 1 in 10^9
20 Kbpi
2.4 megabits/sec Rec. Rate
608 Kbps Reproduce Rate
Run # 1
Track # 2
Number of 10 Second Data Blocks
Number of Digital Bit Errors
Bit Error Rate

Fig. 55

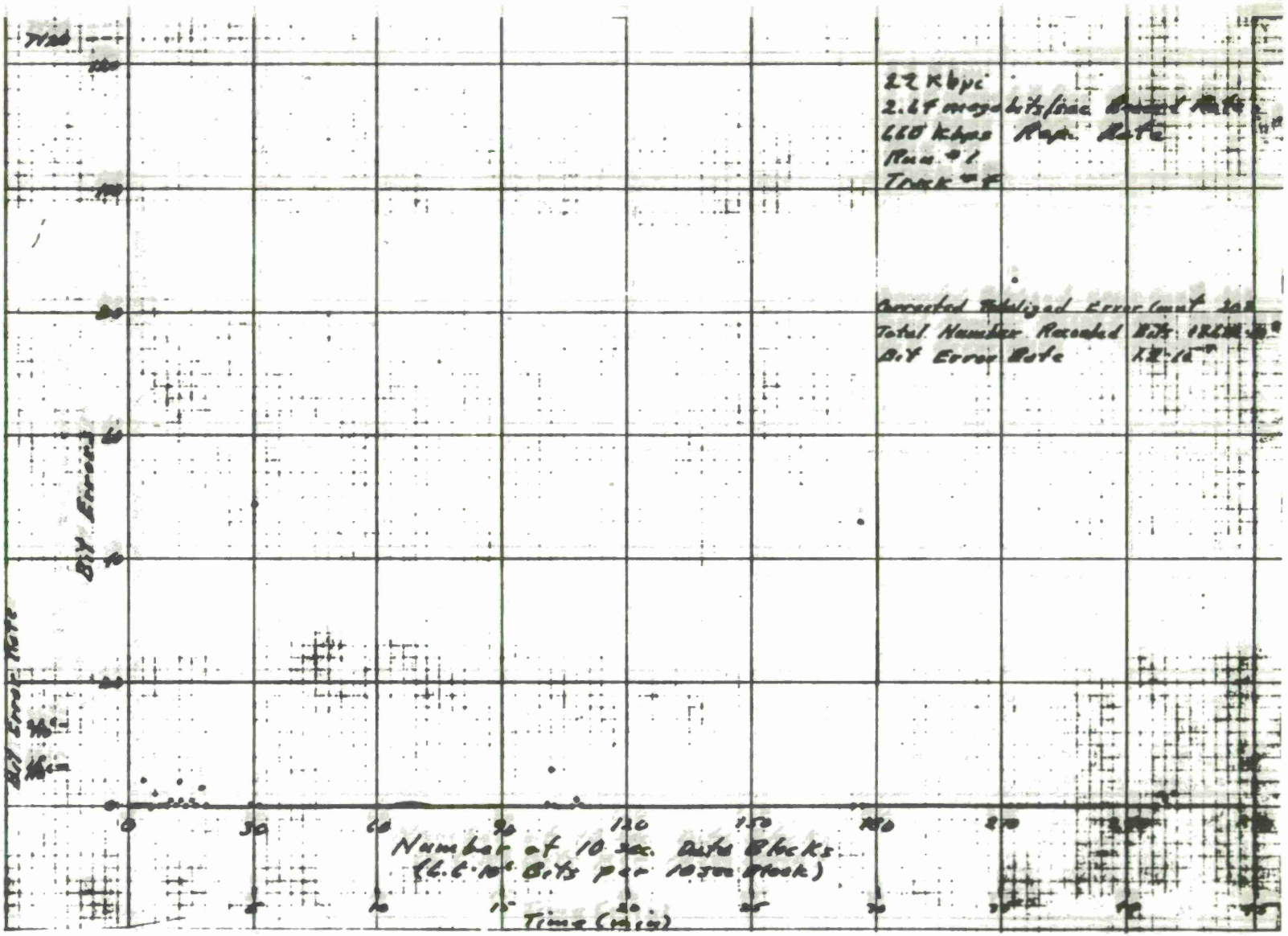
22 Kbps
Track #F
Number of 10 sec. Data Blocks
(6.6·10⁶ Bits per 10 sec Block)
Time (min)

Fig. 56

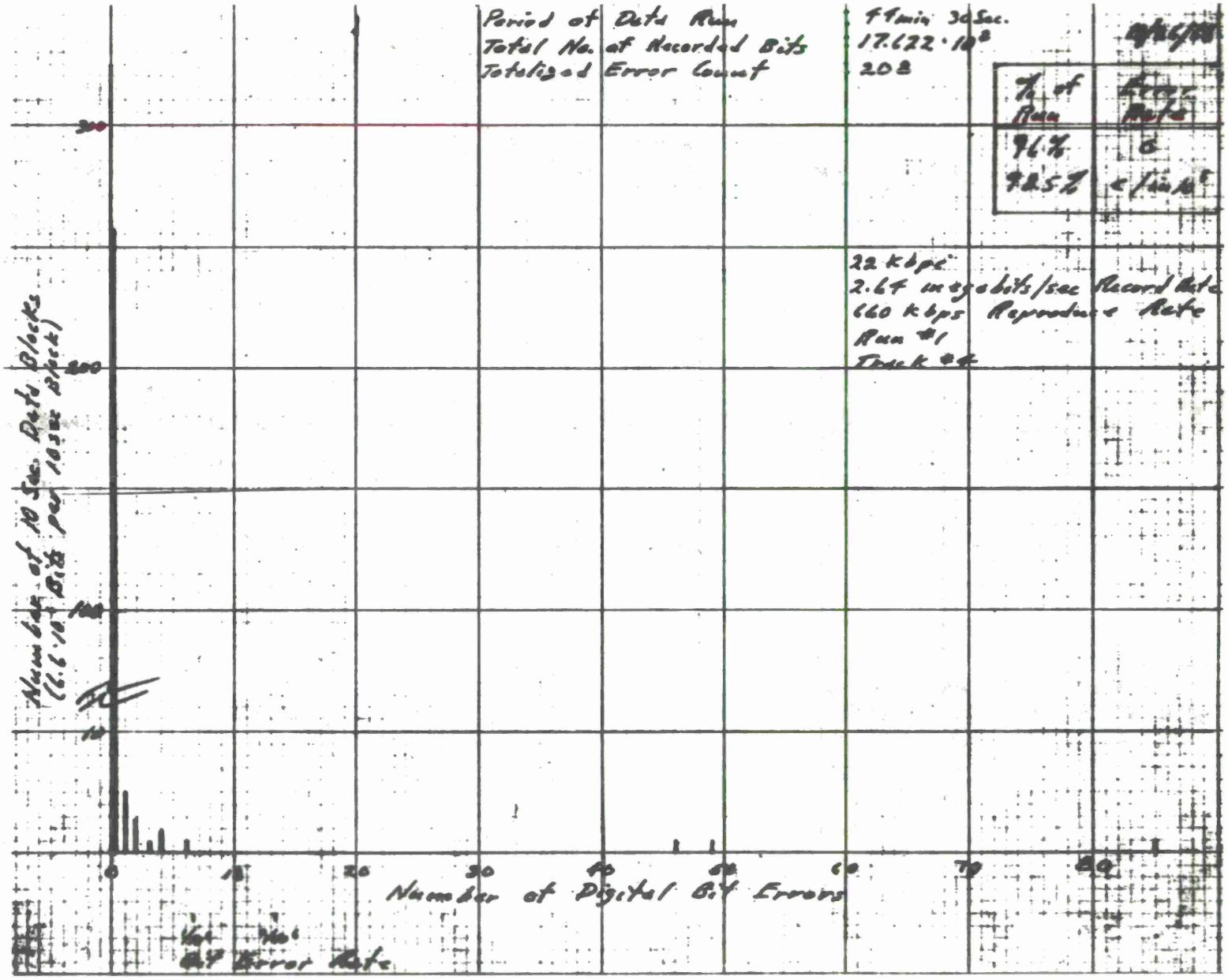
Period of Data Run
Total No. of Recorded Bits
Totalized Error Count
11 min 30 sec.
17.622 · 10⁸
208
% of Run
Error Rate
96.7%
2.5%
22 kbpc
2.64 megabits/sec Record Rate
660 kbps Reproduce Rate
Run #1
Track #4
Number of Digital Bit Errors
0
10
20
30
40
50
60
70
80
100
200
300

Fig. 57

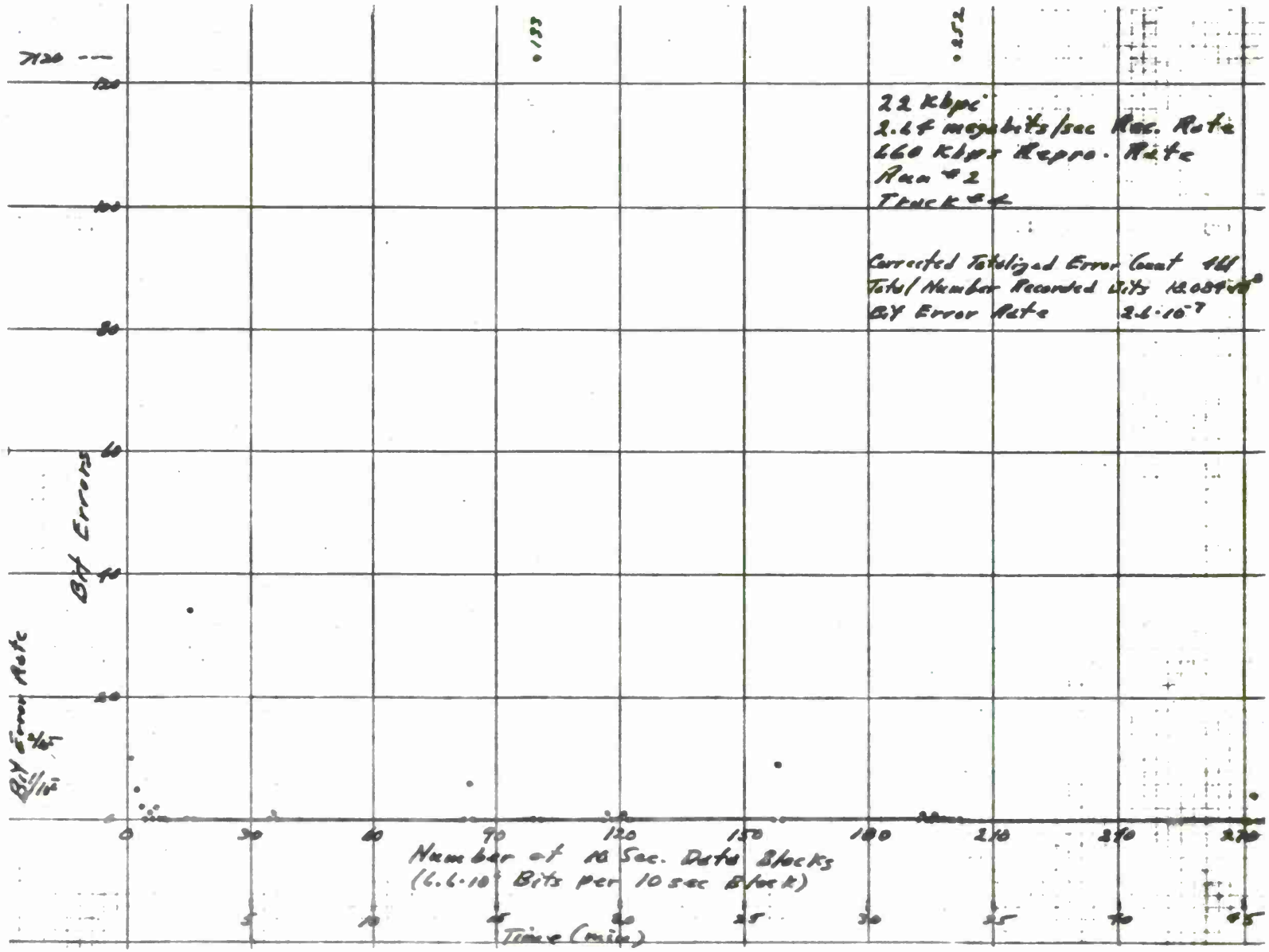
22 kbps
2.4 megabits/sec Rec. Rate
660 kbps Repro. Rate
Run #2
Track #2
Corrected Totalized Error Count 44
Total Number Recorded Bits 12.08
Bit Error Rate 2.6·10⁻⁷
Bit Errors
Bit Error Rate
Number of 10 Sec. Data Blocks
(6.6·10⁶ Bits per 10 sec Block)
Time (min)

Fig. 58

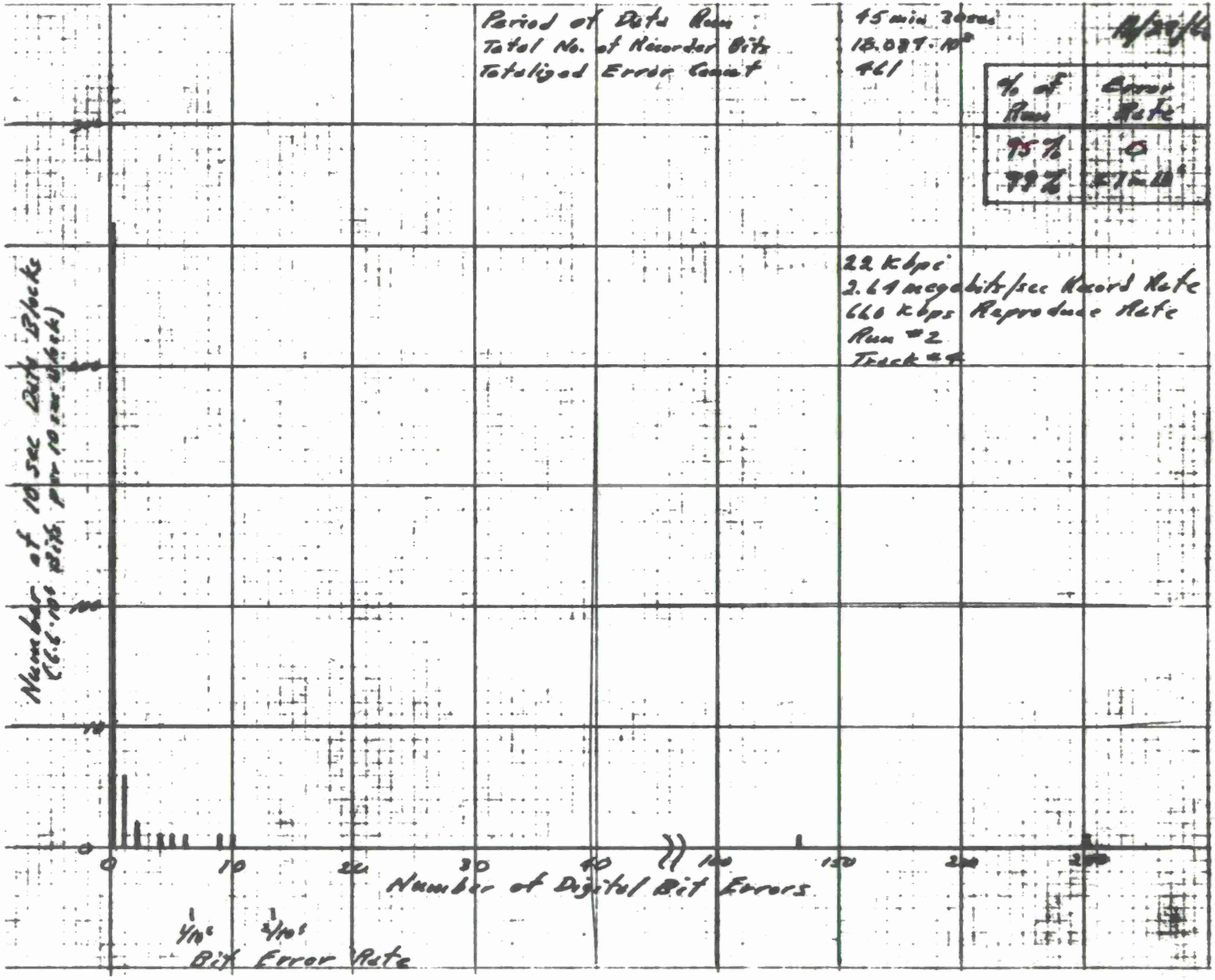
Period of Data Run
Total No. of Recorder Bits
Totaliged Error Count
45 min 30 sec
15.027 · 10⁹
461
% of Runs
Error Rate
75 %
79 %
0
2.7 - 4
22 kbpi
2.64 megabits/sec Record Rate
66 kbps Reproduce Rate
Run = 2
Track = 4
Number of 10 sec Data Blocks
(1.5 · 10⁶ bits per 10 sec block)
0
10
20
30
40
50
100
150
200
Number of Digital Bit Errors
1/10⁵
1/10⁴
Bit Error Rate

Fig. 59

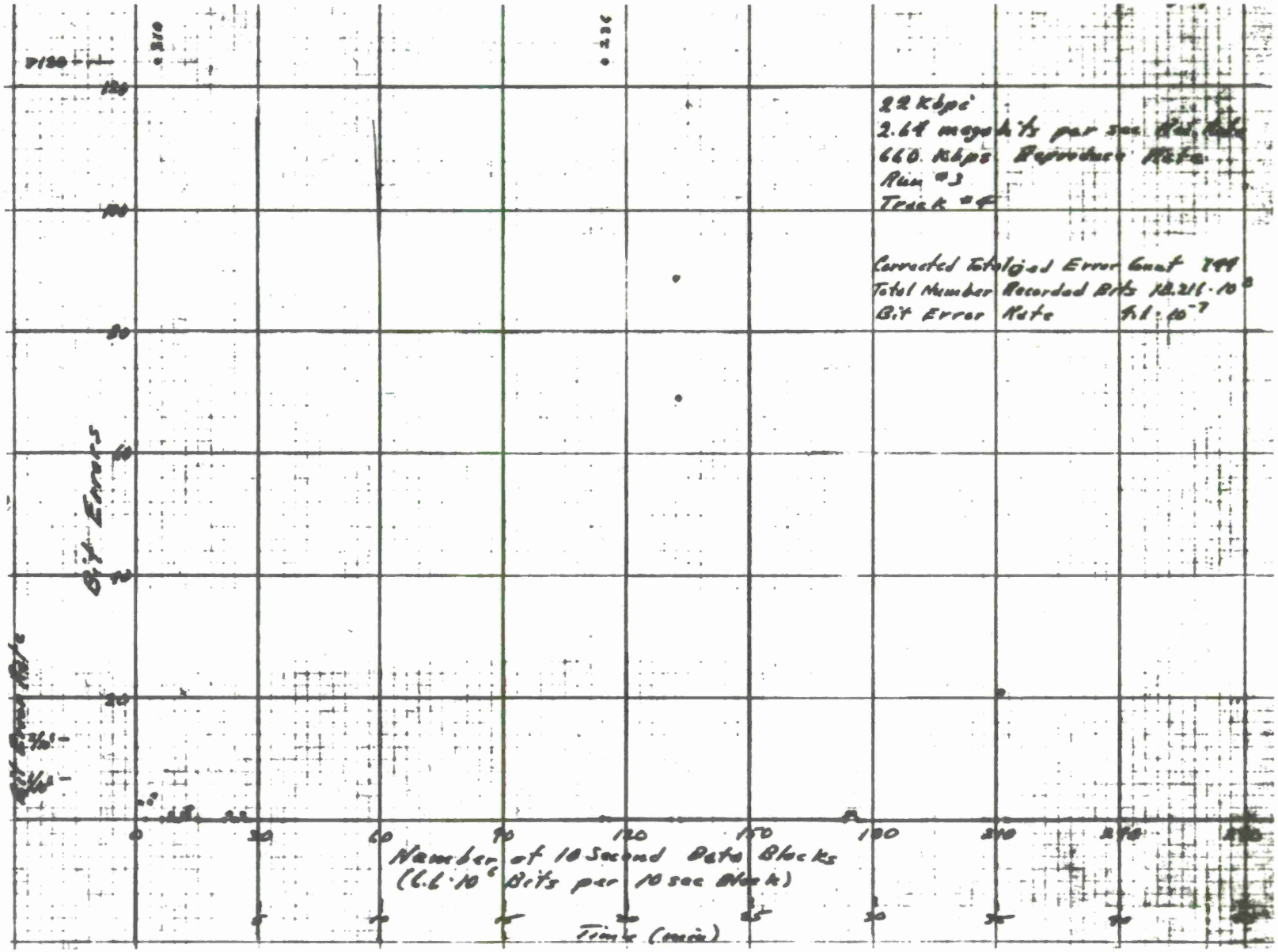
22 Kbps
660 Kbps
Run #3
Track #4
Corrected Total Error Count 744
Bit Error Rate
Number of 10 Second Data Blocks
(6.6·10⁶ Bits per 10 sec Block)
Time (min)

Fig. 60

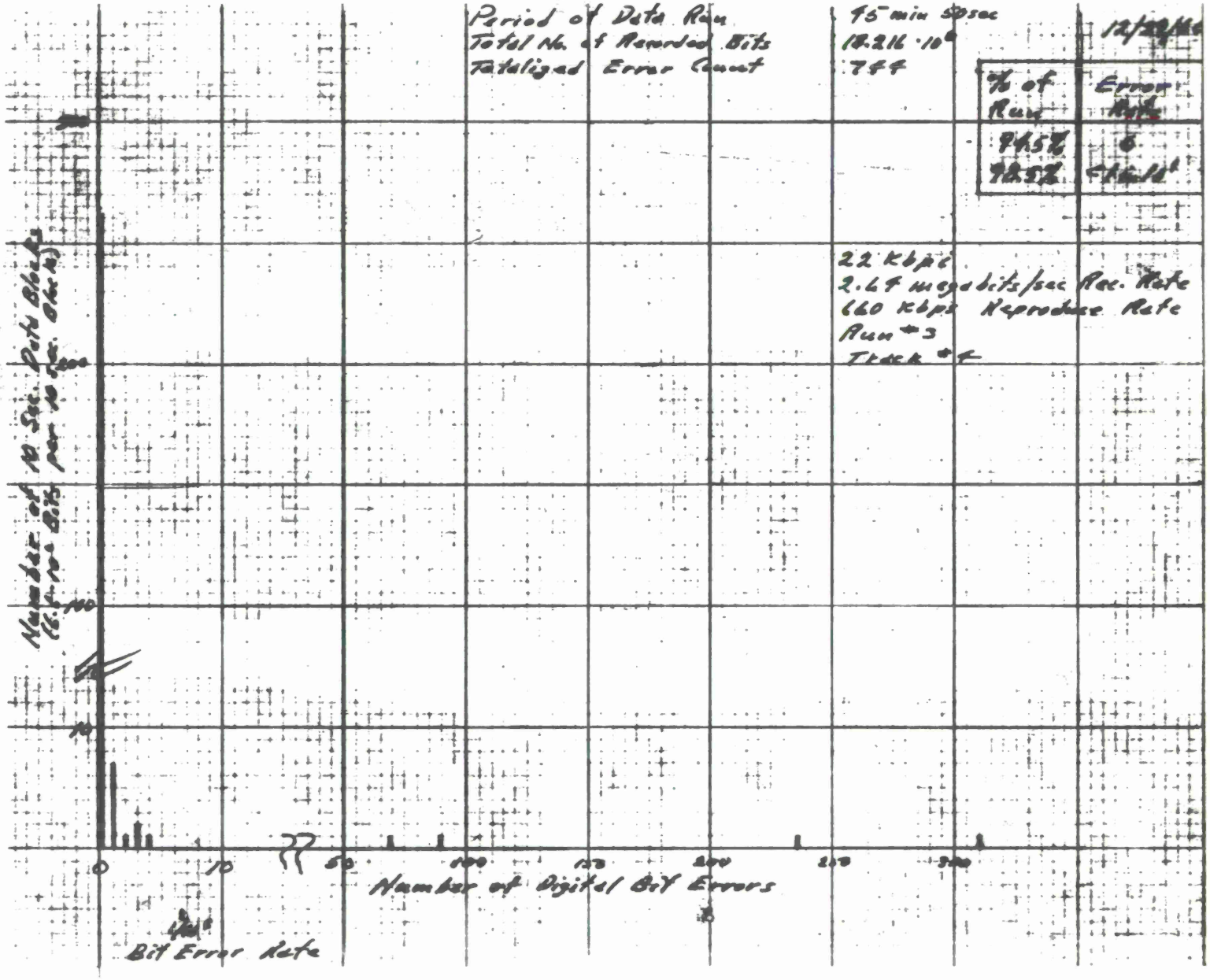
Period of Data Run
Total No. of Recorded Bits
Tabulated Error Count
45 min 9 sec
18.216 · 10⁶
744
% of Run
Error Rate
22 kbpi
2.64 megabits/sec Rec. Rate
660 kbpi Reproduce Rate
Run #3
Track #4
Number of Digital Bit Errors
Bit Error Rate

Fig. 61

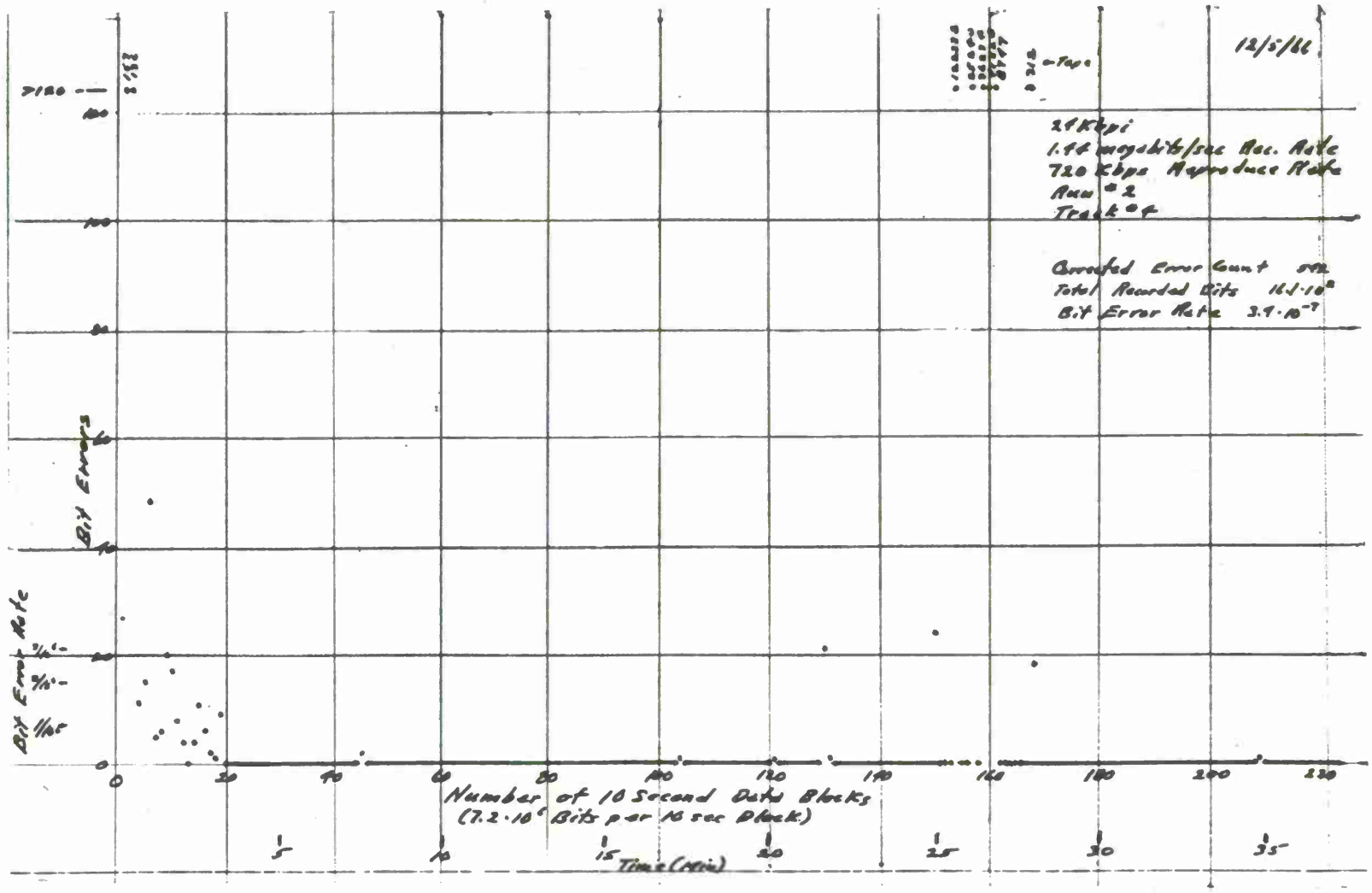
12/5/66
24 Kbpi
1.44 megabit/sec Rec. Rate
720 Kbps Reproduce Rate
Run #2
Track #4
Corrected Error Count 0
Total Recorded Bits 16.1·10⁹
Bit Error Rate 3.9·10⁻⁷
Bit Errors
Bit Error Rate
Number of 10 Second Data Blocks
(7.2·10⁶ Bits per 10 sec Block)
Time (min)

Fig. 62

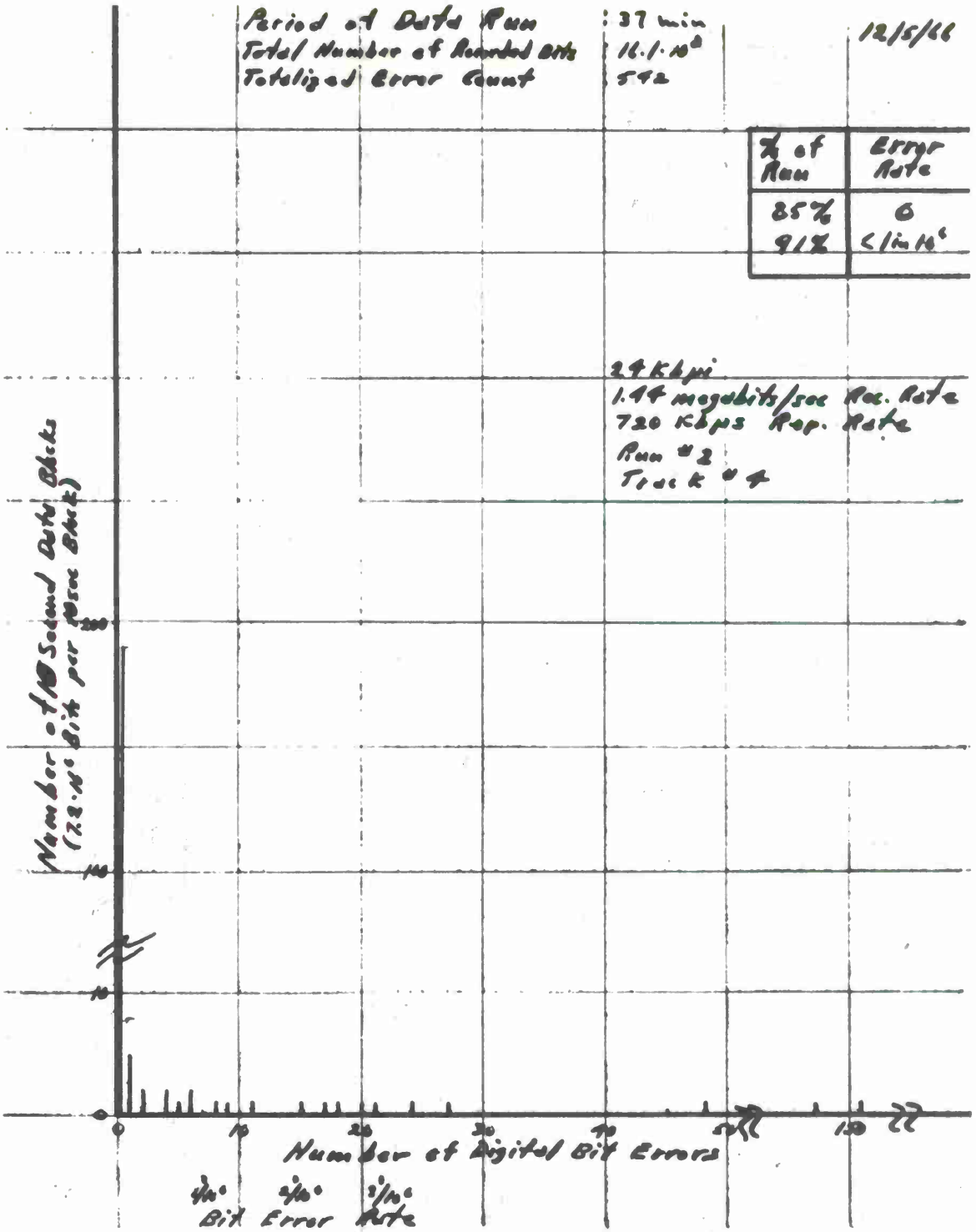
Period of Data Run
Total Number of Recorded Bits
Tabulated Error Count
37 min
11.1·10⁹
542
12/5/66
% of Run
Error Rate
85%
91%
6
< 1in 10⁶
24 Kbps
1.44 megabits/sec Rec. Rate
720 Kbps Rep. Rate
Run #2
Track #4
Number of 1/10 Second Data Blocks (128 Bit per Block)
100
10
0
10
20
30
40
50
100
Number of Digital Bit Errors
1/10⁶
2/10⁶
3/10⁶
Bit Error Rate

Fig. 63

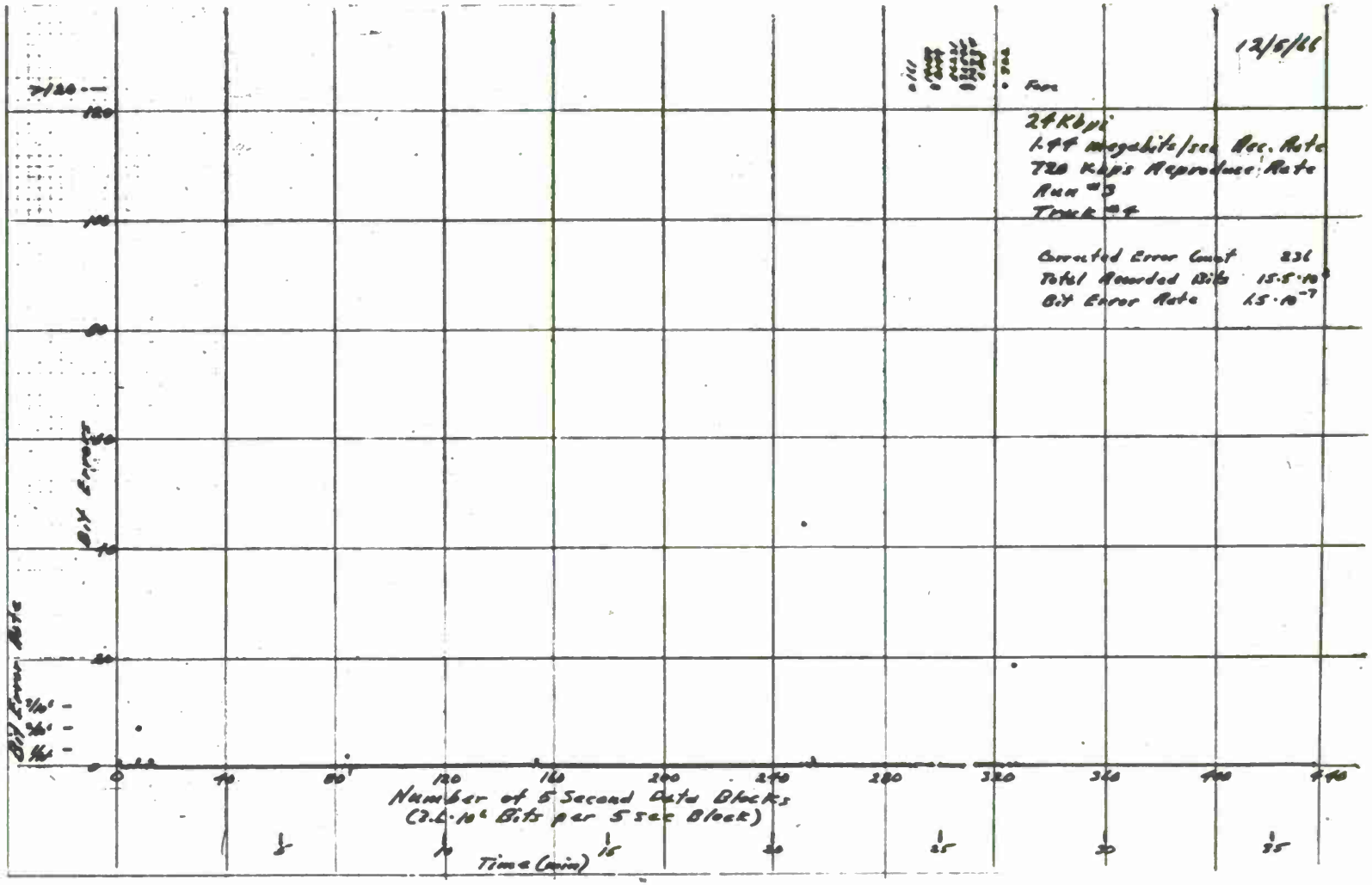
12/6/66
24 Kbps
1.44 megabits/sec Rec. Rate
720 kbps Reproduce Rate
Run #3
Track #4
Corrected Error Count 236
Total Recorded Bits 15.5·10⁹
Bit Error Rate 1.5·10⁻⁷
Number of 5 Second Data Blocks
(3.6·10⁶ Bits per 5 sec Block)
Time (min)

Fig. 64

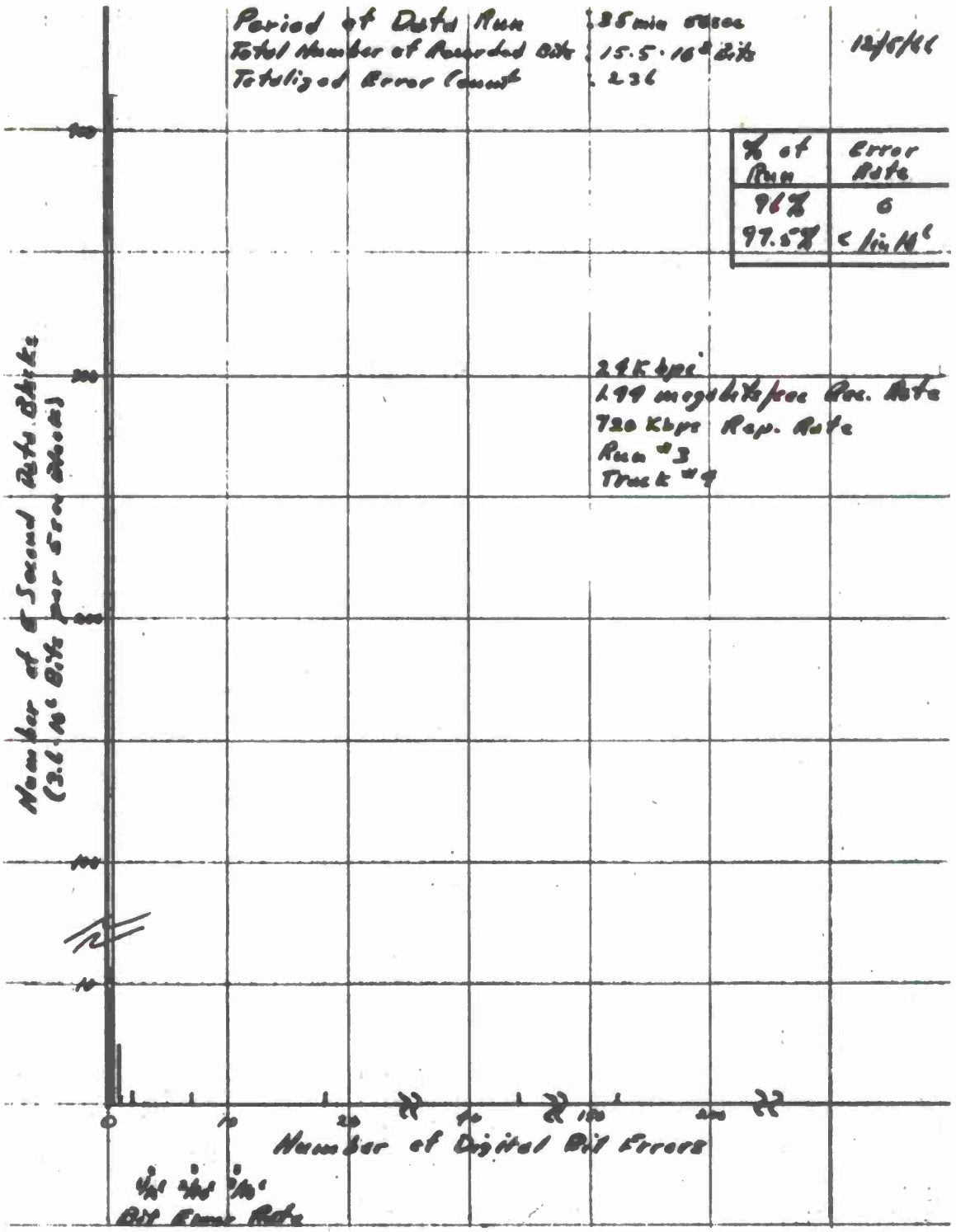
Period of Data Run
Total Number of Recorded Bits
Totaling of Error Count
35 min each
15.5 · 10⁹ bits
236
12/5/66
% of Run
Error Rate
96%
0
97.5%
< 1 in 10⁹
295 kbps
1.99 megabits/sec Rec. Rate
720 Kbps Rep. Rate
Run #3
Track #4
Number of 4 Second Data Blocks (3.6 · 10⁶ Bits per Each Block)
Number of Digital Bit Errors
Bit Error Rate

Fig. 65

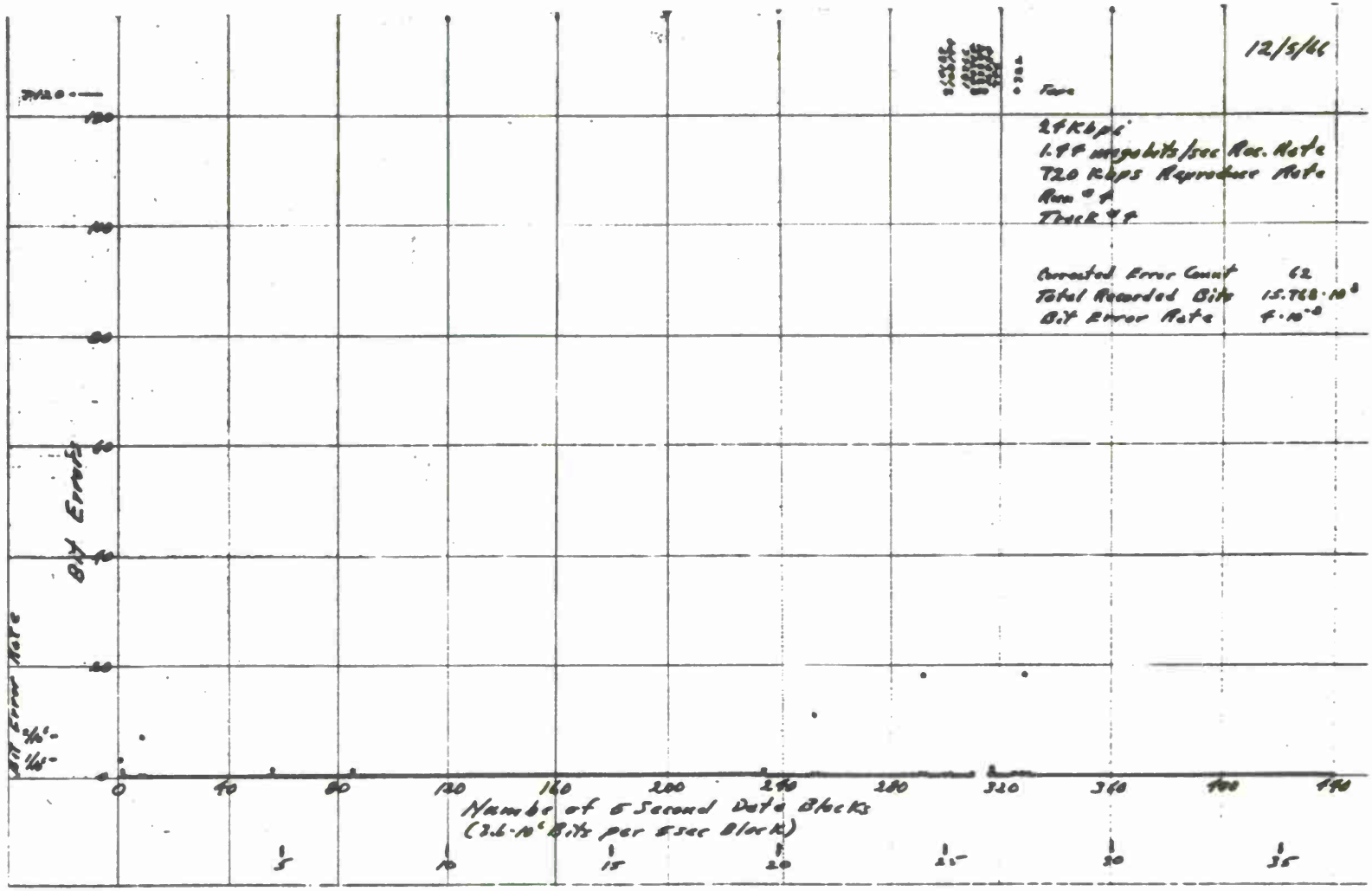
12/5/66
24 Kbps
1.44 megabits/sec Rec. Rate
720 Kbps Reproduce Rate
Run # 4
Track # 8
Corrected Error Count 62
Total Recorded Bits 15.768·10⁸
B.E Error Rate 4·10⁻⁸
Error Rate
Bit Error Rate
0
40
80
120
160
200
240
280
320
360
400
440
Number of 5 Second Data Blocks
(3.6·10⁶ Bits per 5 sec Block)
1/5
10
15
20
25
30
35

Fig. 66

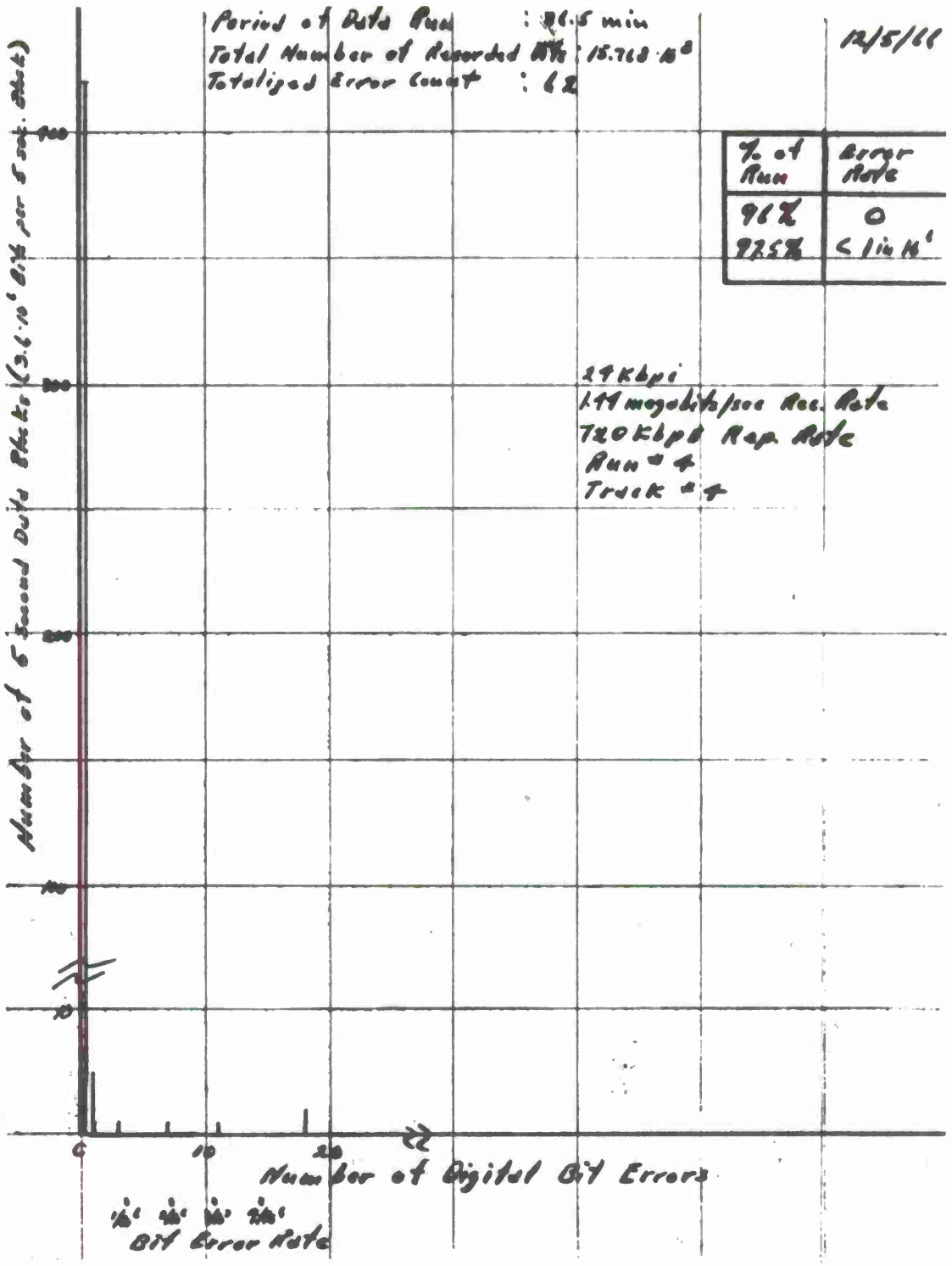
Period of Data Run : 26.5 min
Total Number of Recorded Bits : 15.768 · 10⁶
Totalized Error Count : 62
12/5/66
% of Run
Error Rate
96%
0
99.5%
< 1in 10⁷
24 Kbpi
1.44 megabits/sec Rec. Rate
720 Kbps Rep. Rate
Run = 4
Track = 4
Number of 5 second Data Blocks (3.6·10⁶ Bits per 5 sec. Block)
Number of Digital Bit Errors
Bit Error Rate

Fig. 67

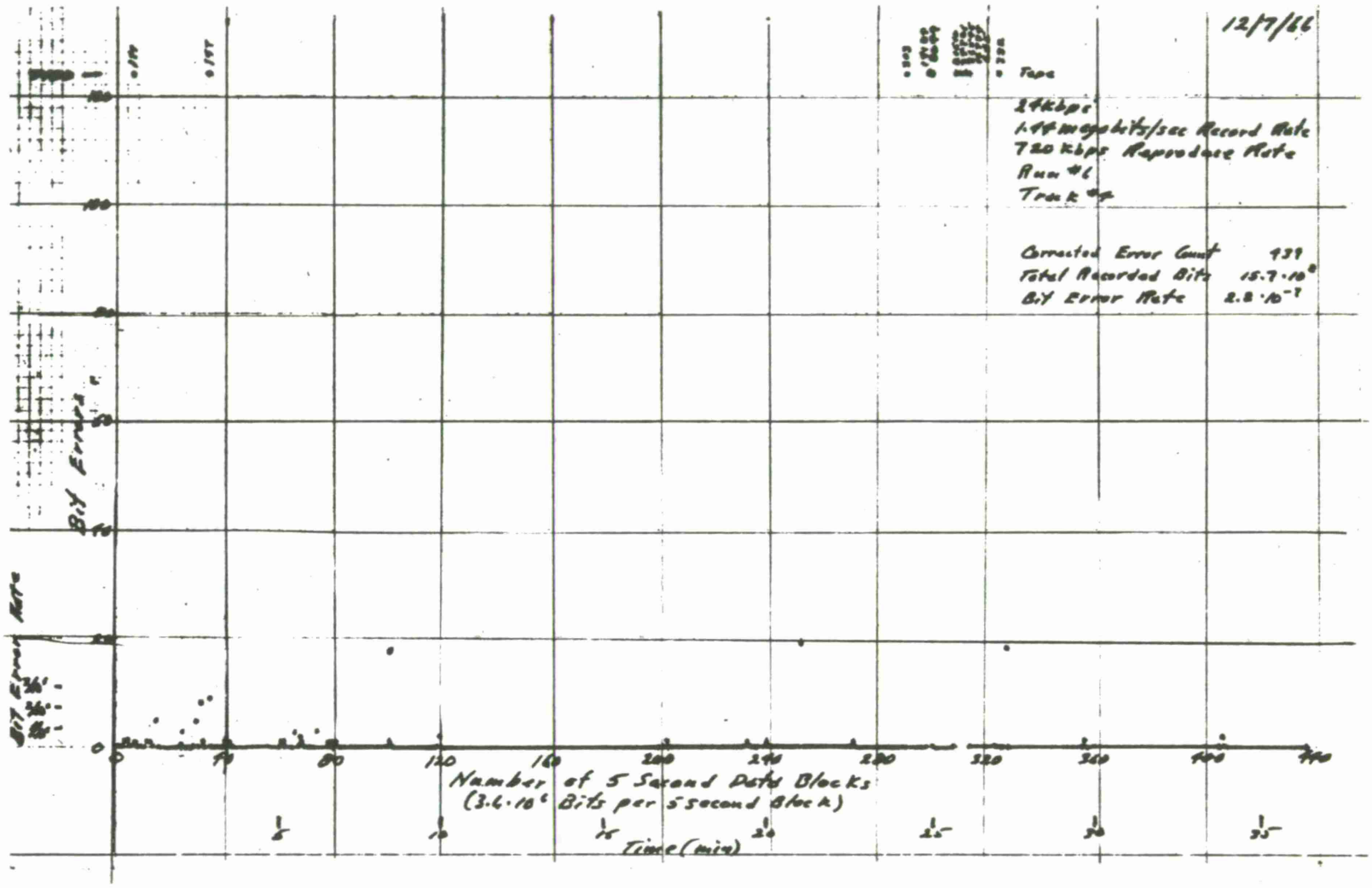
12/7/66
Tape
24 kbps
1.44 megabits/sec Record Rate
720 kbps Reproduce Rate
Run #6
Track #p
Corrected Error Count 939
Total Recorded Bits 15.7·10⁸
Bit Error Rate 2.8·10⁻⁷
Bit Errors
Bit Error Rate
0
40
80
120
160
200
240
280
320
360
400
440
Number of 5 Second Data Blocks
(3.6·10⁶ Bits per 5 second block)
1/8
1/4
1/16
1/20
1/25
1/30
1/35
Time (min)

Fig. 68

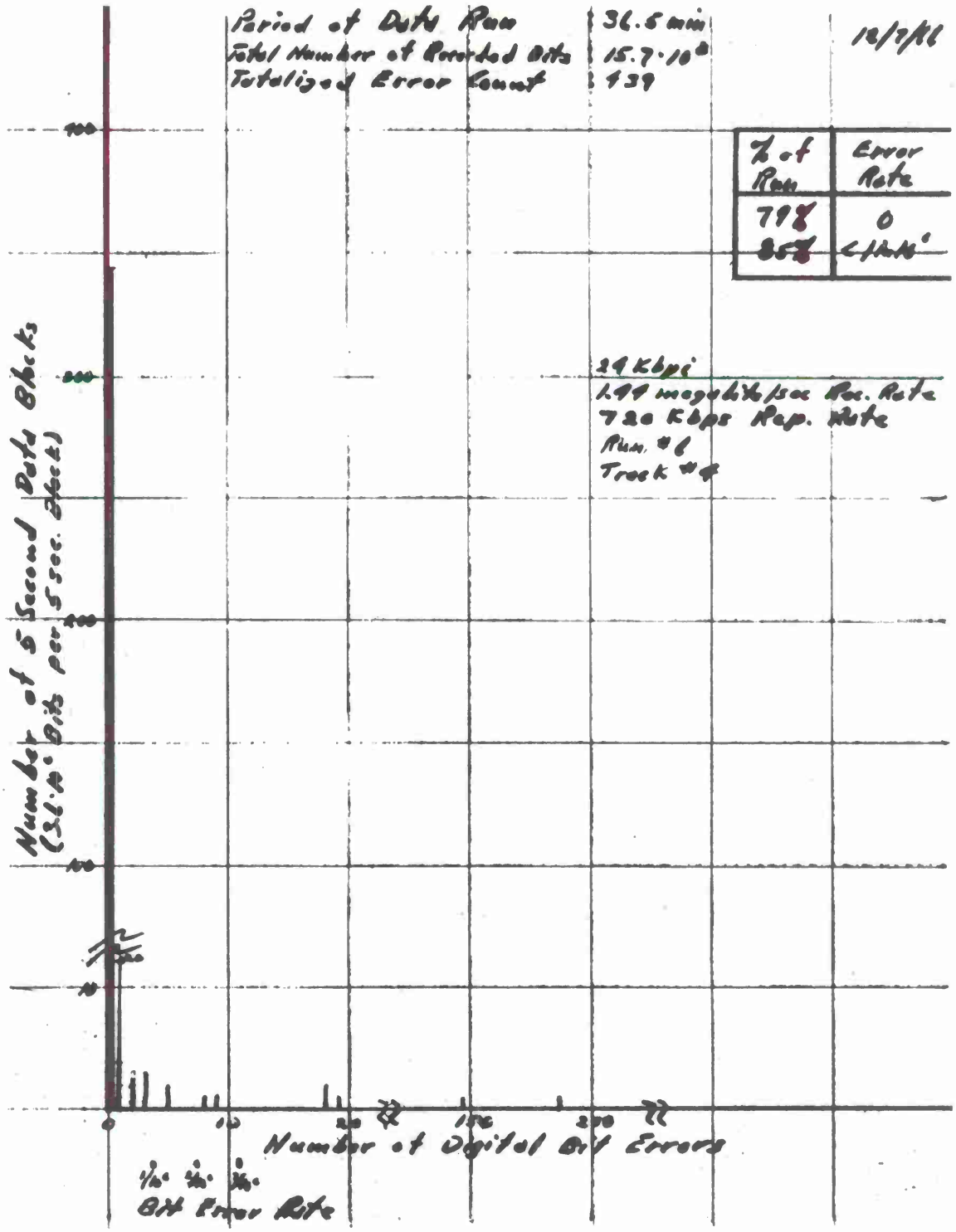
Period of Data Run
Total Number of Recorded Bits
Totalized Error Count
36.5 min
15.7·10⁸
139
12/7/71
% of Run
Error Rate
79%
0
24 Kbpi
1.44 megabits/sec Rec. Rate
720 Kbps Rep. Rate
Run #1
Track #4
Number of 5 Second Data Blocks (31.6 Bits per 5 sec. Block)
Number of Digital Bit Errors
Bit Error Rate

Fig. 69

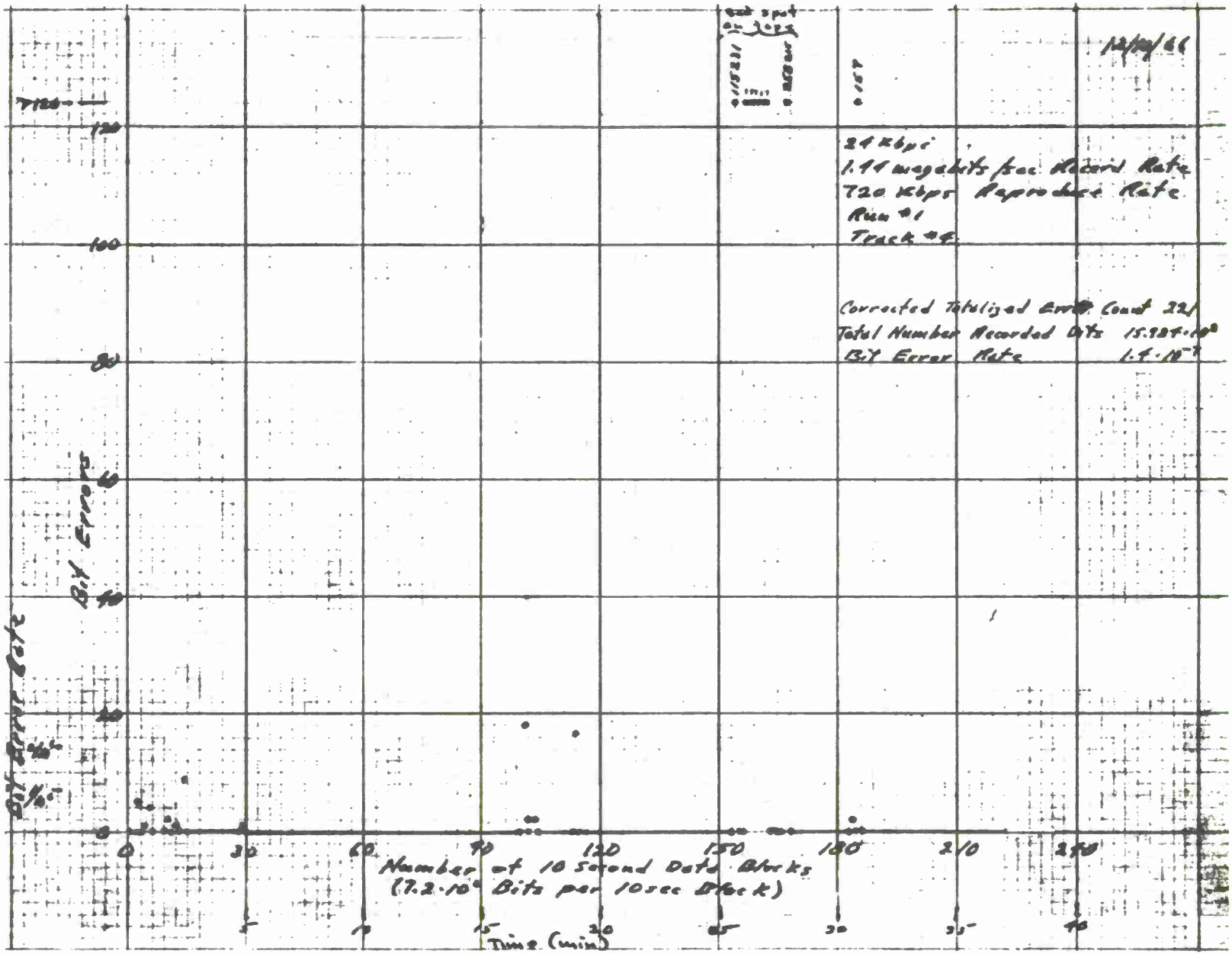
12/14/66
24 Kbps
1.44 megabits/sec Record Rate
720 Kbps Reproduce Rate
Run #1
Track #8
Corrected Tabulated Error Count 22
Total Number Recorded Bits 15.984·10⁹
Bit Error Rate 1.4·10⁻⁹
Error Count
Bit Error Rate
Number of 10 Second Data Blocks
(7.2·10⁶ Bits per 10sec Block)
Time (min)

Fig. 70

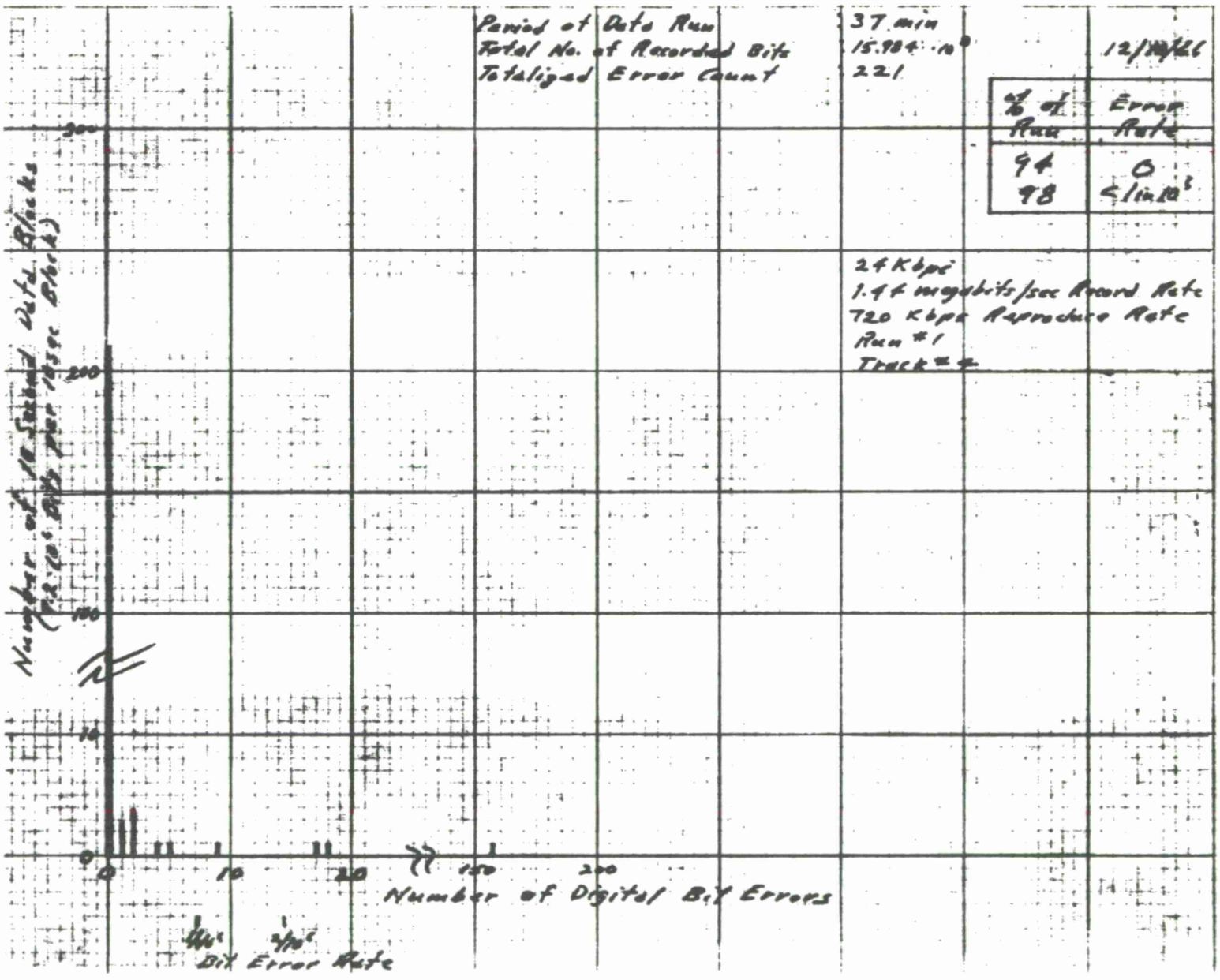
Period of Data Run
Total No. of Recorded Bits
Totaliged Error Count
37 min
15.984 · 10⁹
221
12/
% of Run
Error Rate
94
98
0
< 1 in 10⁸
24 Kbpi
1.44 megabits/sec Record Rate
720 Kbpe Reproduce Rate
Run #1
Track #
Number of Digital Bit Errors
Bit Error Rate

Fig. 71

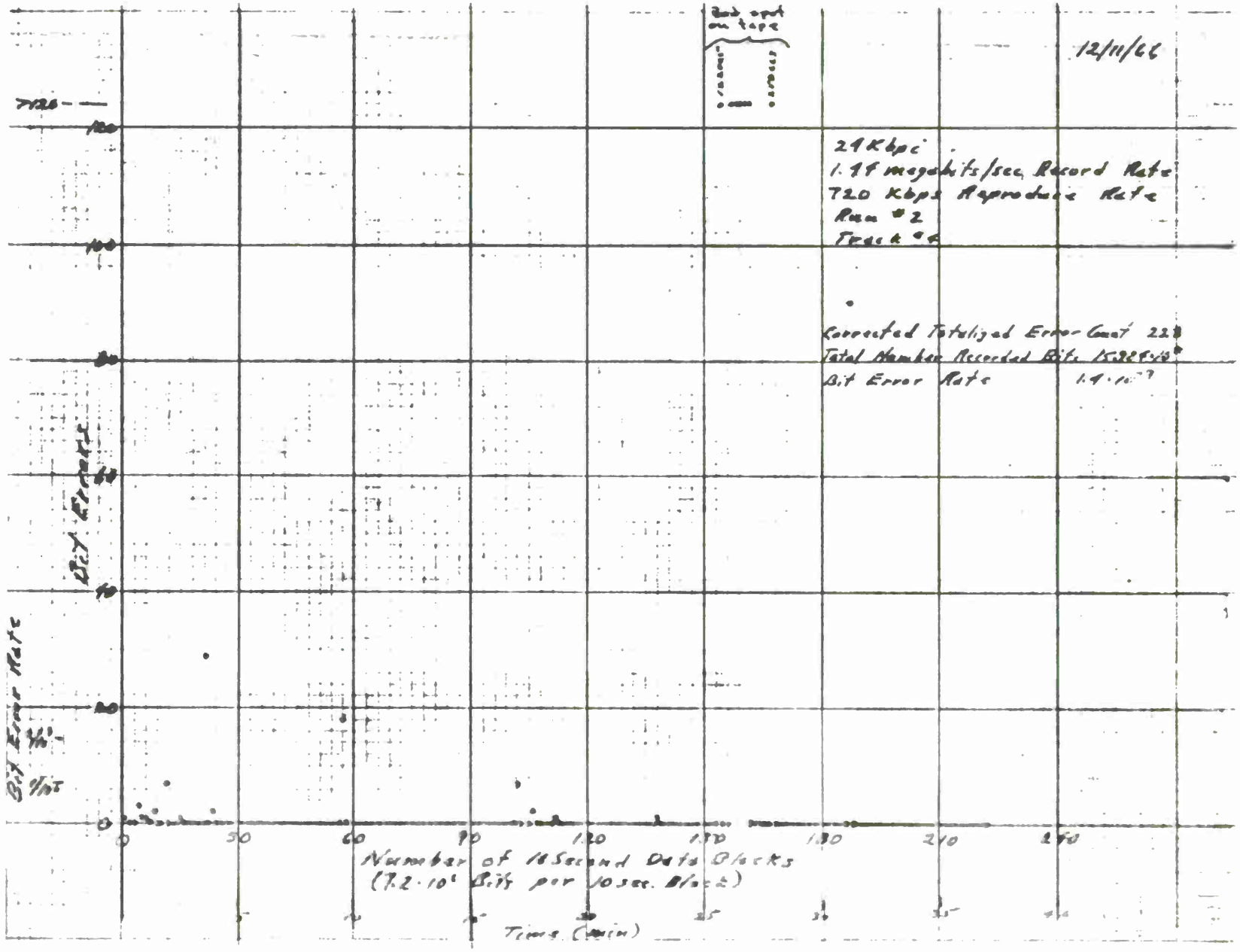
12/11/66
24 Kbpc
1.44 megabits/sec Record Rate
720 Kbps Reproduce Rate
Run #2
Track #6
Corrected Totalized Error Count 228
Total Number Recorded Bits 1532548
Bit Error Rate 1.4·10⁻⁷
Bit Error Rate
Number of 10 Second Data Blocks
(7.2·10⁶ Bits per 10 sec. Block)
Time (min)

Fig. 72

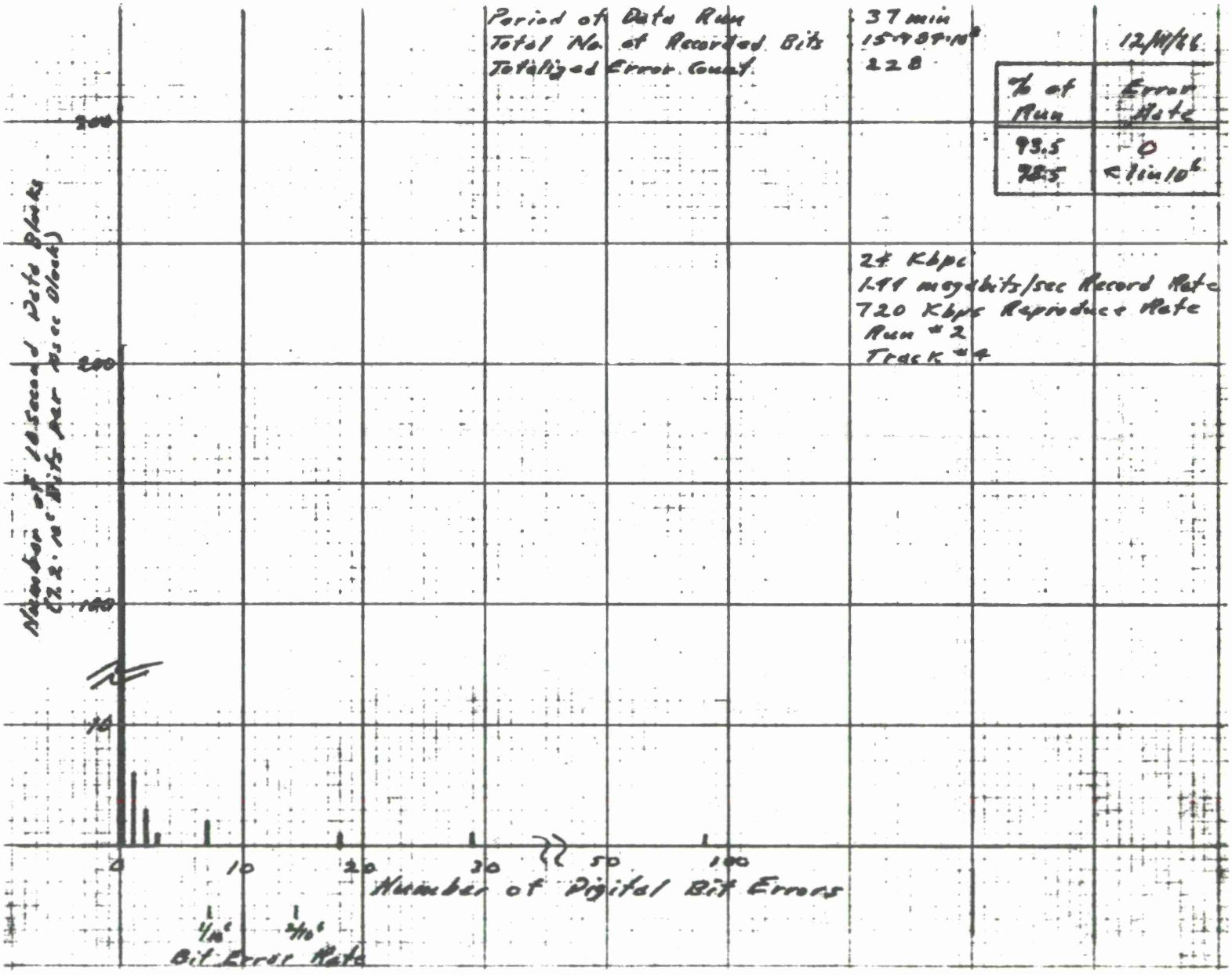
Period of Data Run
Total No. of Recorded Bits
Totalized Error Count
37 min
15·10⁸
228
12/11/66
% of Run
Error Rate
93.5
7.5
0
< 1 in 10⁶
24 Kbpc
1.44 megabits/sec Record Rate
720 Kbps Reproduce Rate
Run #2
Track #4
Number of 10 second Data Blocks
(72 x 10⁴ Bits per 10 sec Block)
200
100
10
1
0
10
20
30
50
100
Number of Digital Bit Errors
1/10⁶
2/10⁶
Bit Error Rate

Fig. 73

TABLE 2

Fig.	Page	Bit Packing Density (Kbpi)	Total Number Recorded Bit (TB) X 10^8	Data Record Rate (Kbps)	Corrected Errors (Totalized Errors - Tape Induced Errors) (CE)	Digital Bit Error Rate $\left(\frac{CE}{TB}\right)$
14	54	10	6.06	1200	0	0
16	56	10	5.7	1200	0	0
18	58	10	9.36	1200	0	0
20	60	10	9.66	1200	0	0
22	62	10	9.54	1200	0	0
24	64	10	9.72	1200	0	0
26	66	15	7.56	1800	321	$4.3/10^7$
28	68	15	7.2	1800	206	$2.8/10^7$
30	70	15	16.2	1800	0	0
32	72	15	7.47	1800	230	$3.1/10^7$
34	74	15	6.93	1800	10	$1.4/10^8$
36	76	18	17.766	2160	559	$3.2/10^7$
38	78	18	17.28	2160	5	$2.9/10^9$
40	80	18	8.1	2160	110	$1.4/10^7$
42	82	18	8.1	2160	40	$5/10^8$
44	84	20	18.96	2400	281	$1.5/10^7$
46	86	20	19.68	2400	1903	$1/10^6$
48	88	20	18.96	2400	713	$3.8/10^7$
50	90	20	18.72	2400	215	$1.2/10^7$
52	92	20	18.72	2400	69	$3.7/10^8$
54	94	20	18.72	2400	571	$3.1/10^7$
56	96	22	17.622	2640	208	$1.2/10^7$
58	98	22	18.084	2640	461	$2.6/10^7$

TABLE 2 (Cont)

Fig.	Page	Bit Packing Density (Kbpi)	Total Number Recorded Bit (TB) x 10^8	Data Record Rate (Kbps)	Corrected Errors (Totalized Errors - Tape Induced Errors) (CE)	Digital Bit Error Rate $\left(\frac{CE}{TB}\right)$
60	100	22	18.216	2640	744	$4.1/10^7$
62	102	24	16.1	1440	542	$3.4/10^7$
64	104	24	15.5	1440	236	$1.5/10^7$
66	106	24	15.768	1440	62	$4/10^8$
68	108	24	15.7	1440	439	$2.8/10^7$
70	110	24	15.984	1440	221	$1.4/10^7$
72	112	24	15.984	1440	228	$1.4/10^7$

TABLE 3

Digital Bit Packing Density: 10 Kbpi

Digital Bit Error Rate	% of Error Test Run for Figures					
	#1	#2	#3	#4	#5	#6
Zero Errors	99	98	99	99	99	99
≤ 1 in 10^6	99	99	99	99	99	99

Digital Bit Packing Density: 15 Kbpi

Digital Bit Error Rate	% of Error Test Run for Figures					
	#1	#2	#3	#4	#5	
Zero Errors	93	81	98.8	91.5	93	
≤ 1 in 10^6	97.5	98.5	98.8	95	97	

Digital Bit Packing Density: 18 Kbpi

Digital Bit Error Rate	% of Error Test Run for Figures					
	#1	#2	#3	#4		
Zero Errors	95	98.5	91	93		
≤ 1 in 10^6	98	100	99	97		

Digital Bit Packing Density: 20 Kbpi

Digital Bit Error Rate	% of Error Test Run for Figures					
	#1	#2	#3	#4	#5	#6
Zero Errors	95	95	96	97	96	97
≤ 1 in 10^6	97	97.5	98.5	99	99	98.5

Digital Bit Packing Density: 22 Kbpi

Digital Bit Error Rate	% of Error Test Run for Figures					
	#1	#2	#3			
Zero Errors	96	95	94.5			
≤ 1 in 10^6	98.5	99	98.5			

Digital Bit Packing Density: 24 Kbpi

Digital Bit Error Rate	% of Error Test Run for Figures					
	#1	#2	#3	#4	#5	#6
Zero Errors	85	96	96	79	94	93.5
≤ 1 in 10^6	91	97.5	97.5	85	98	98.5

TABLE 4

	Mean Average ($\sum_{1}^{i} n/i$) %					
Bit Packing Density	10 Kbpi	15 Kbpi	18 Kbpi	20 Kbpi	22 Kbpi	24 Kbpi
Zero Errors	100	91.4	94.4	96	95.2	90.6
$\leq$ 1 in 10^6		97.4	98.5	98.3	98.7	94.6

Mean Average Derived from Figures obtained in Table

Mean Average ($\sum_{1}^{i} n/i$) of % Error Test Run Containing Zero Errors and Error Rates $\leq$ 1 in 10^6

TABLE 5

BIT PACKING DENSITY (Kbpi)	PERIOD OF ALL TEST RUNS APPROX. (min)	SUM TOTAL OF RECORDED BITS OF ALL TEST RUNS (10^8)	SUM TOTAL OF ALL BIT ERRORS (CORRECTED) OF ALL TEST RUNS	ERROR RATE (BIT ERRORS/ 10^7)
10	139	50.04	0	0
15	84	45.36	767	$1.7/10^7$
18	158	51.246	714	$1.4/10^7$
20	315	113.76	3752	$3.3/10^7$
22	136	53.929	1413	$2.6/10^7$
24	183	78.936	1728	$2.2/10^7$

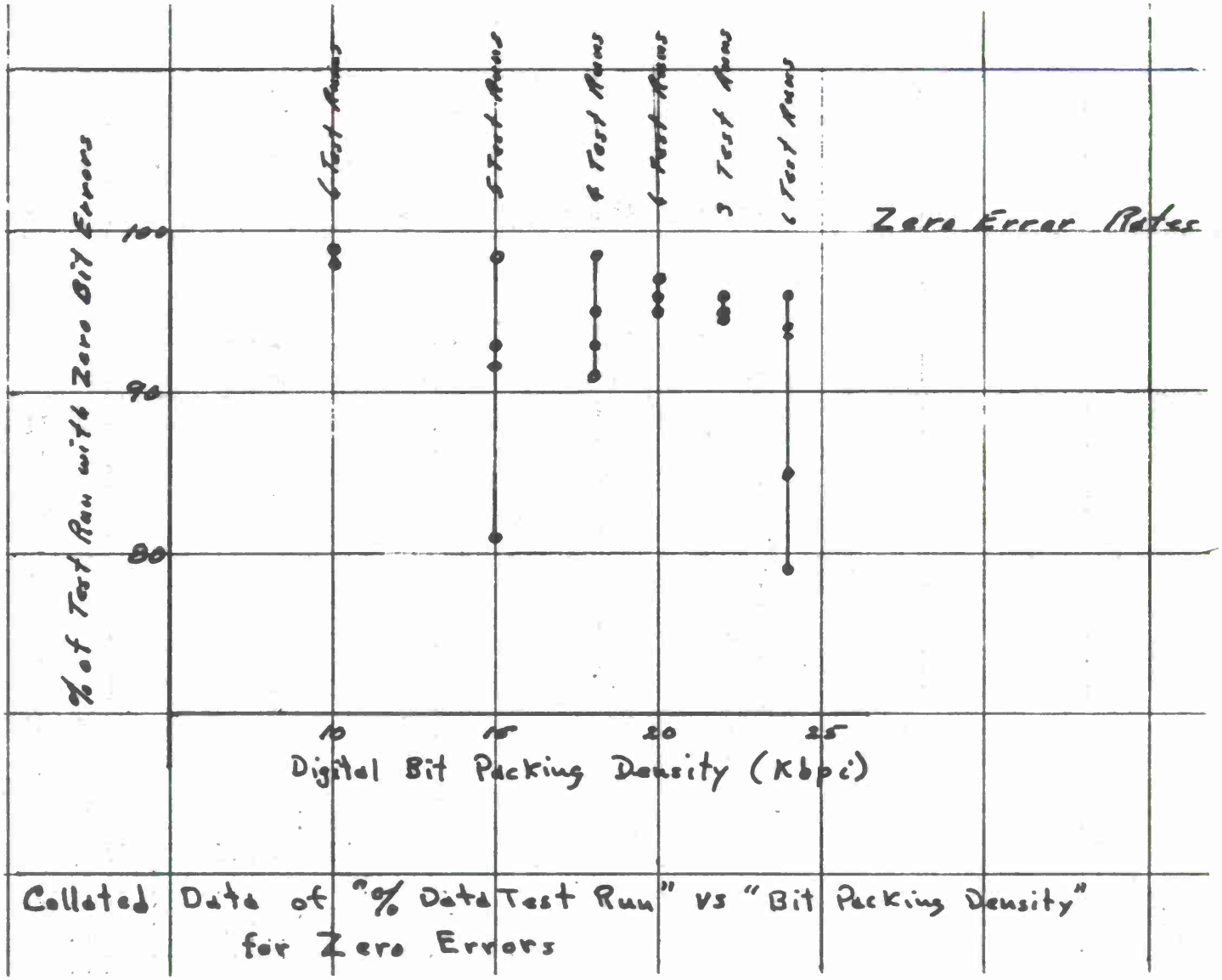
4 Test Runs
5 Test Runs
4 Test Runs
4 Test Runs
3 Test Runs
4 Test Runs
Zero Error Rates
% of Test Run with Zero Bit Errors
100
90
80
10
15
20
25
Digital Bit Packing Density (Kbpi)
Collated Data of "% Data Test Run" vs "Bit Packing Density"
for Zero Errors

Fig. 74

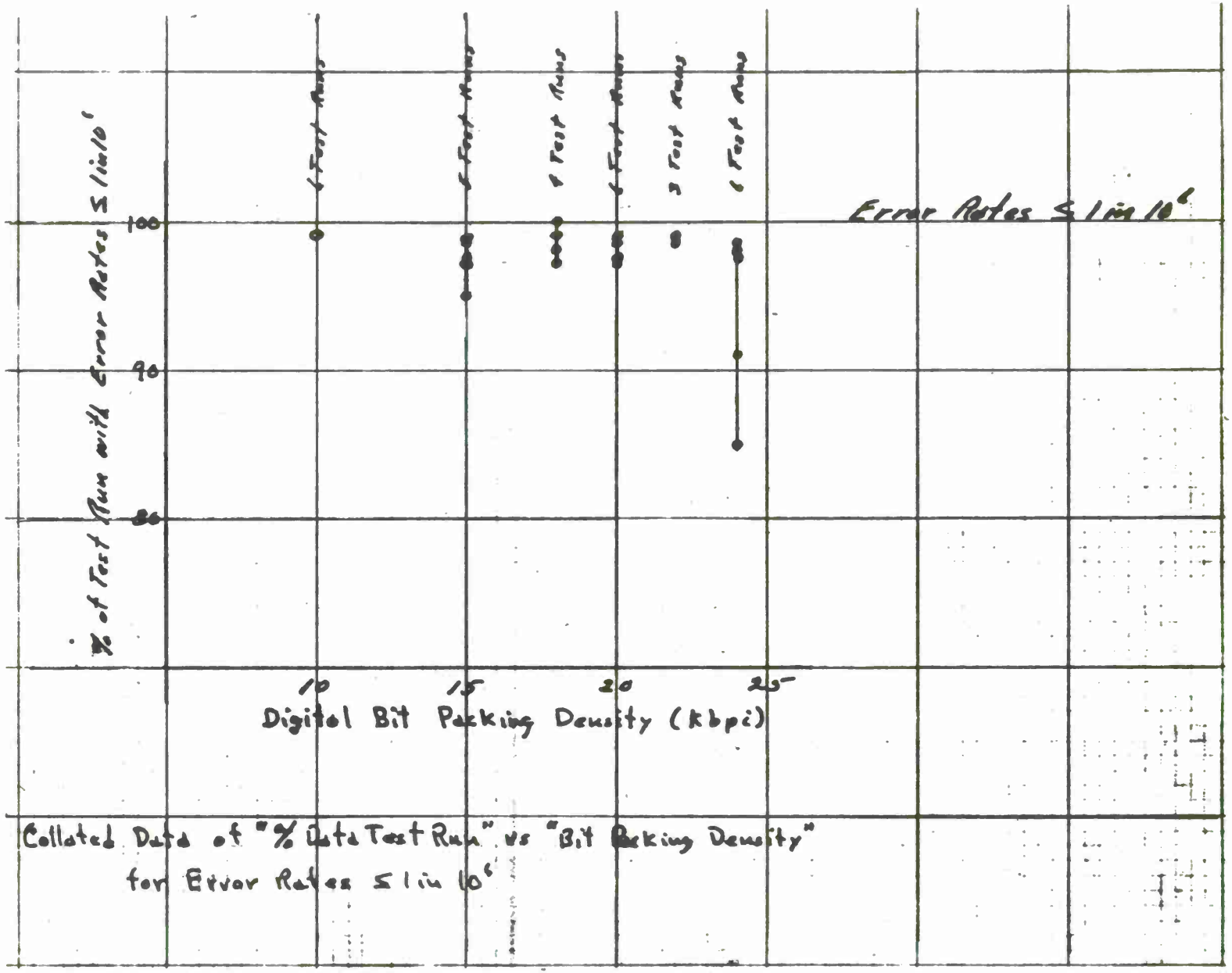

Collated Data of "% Data Test Run" vs "Bit Packing Density" for Error Rates ≤ 1 in 10^6

Fig. 75

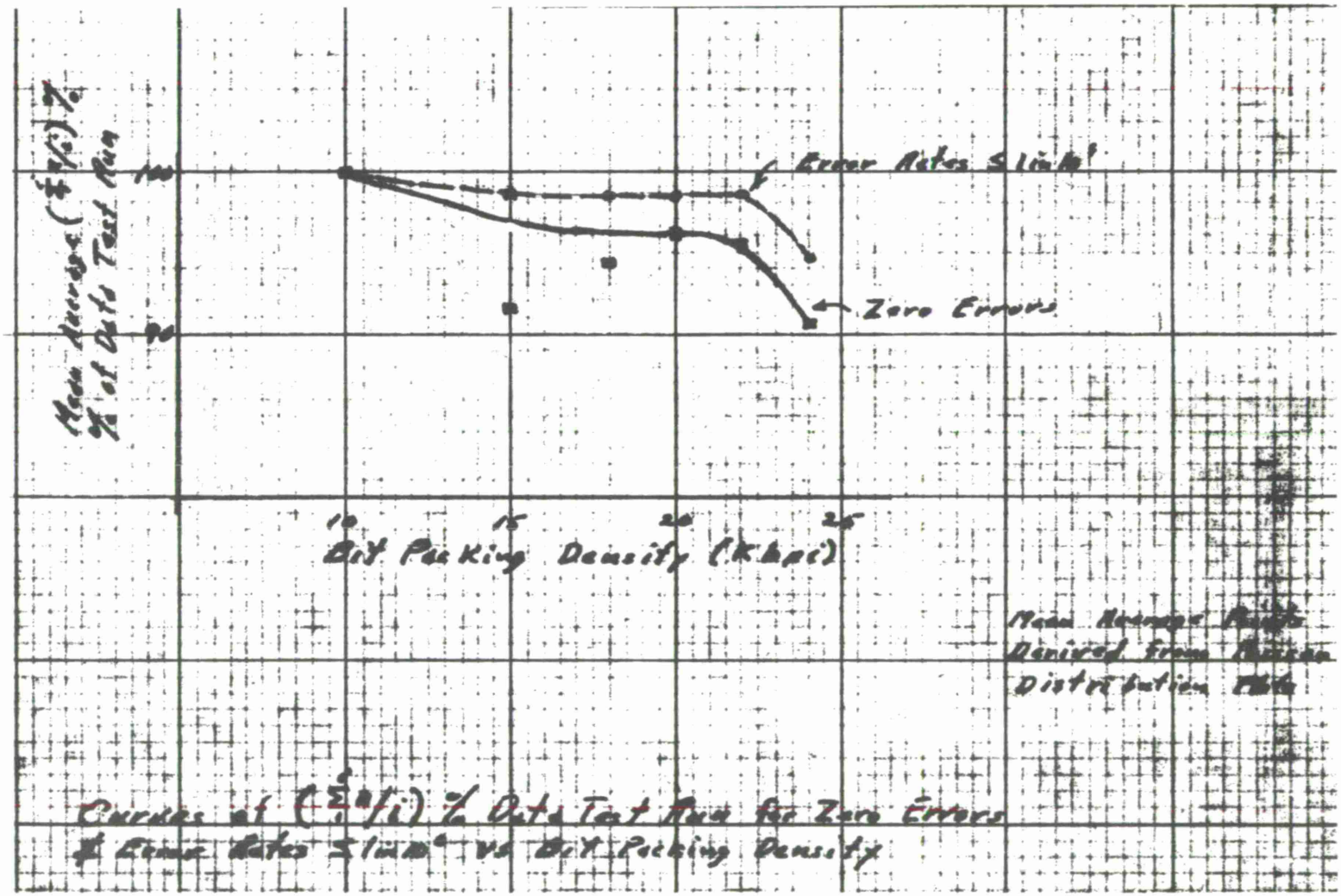

Curves of $(\sum_{i=0}^{2} f_i)$ % Data Test Runs for Zero Errors & Error Rates $\leq 1 \times 10^{-4}$ vs Bit Packing Density

Fig. 76

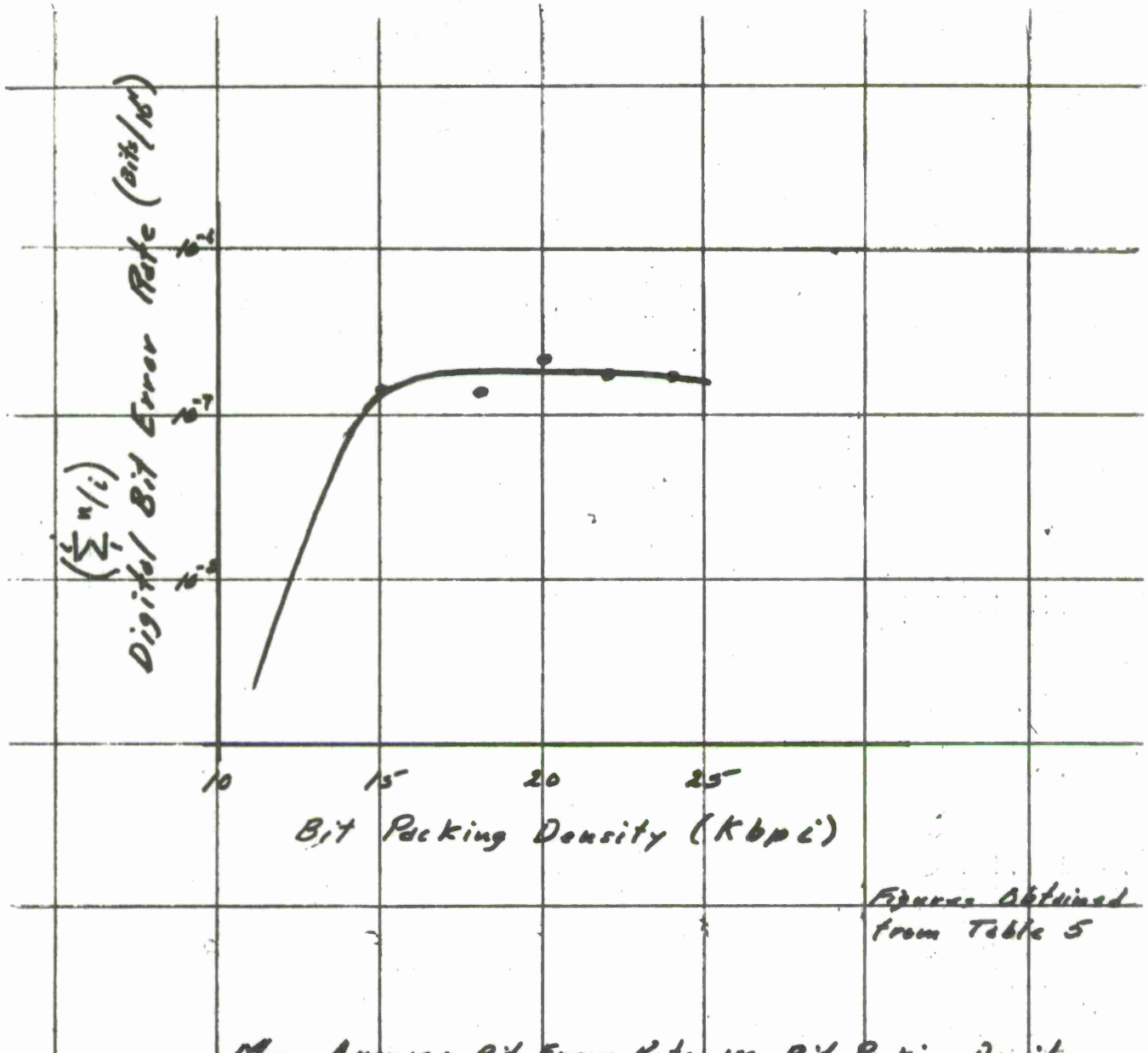
Digital Bit Error Rate (bits/bit)
$(\sum_i n/i)$
10^{-2}
10^{-3}
10^{-4}
10
15
20
25
Bit Packing Density (Kbpi)
Figures Obtained from Table 5
Mean Average Bit Error Rate vs Bit Packing Density

Fig. 77

CONCLUSIONS

Meaningful conclusions relative to this digital high packing density NB/PM Encoding/Decoding scheme must consider both the total system involved in the test setup and the test procedures.

Several factors pertaining to some of the critical components in the test setup as well as testing procedures must be noted. Accumulating test data to a finite degree of accuracy of any system made up of composite pieces of equipment is usually an engrossing task at best. However when a magnetic tape recorder as well as magnetic tape become key items of the composite equipment then the task becomes absorbing. This is particularly true when attempting to maintain consistence of test results on successive tests.

The tape that was used for these tests was obtained from three primary sources: 3M, CEC and Memorex. It was of standard instrumentation-grade tape: Memorex tape 62L, 3M type 888 and CEC type W-1. No precautions were taken in the selection of tape to guarantee that it was dropout free. Of the reels we obtained, not one was completely free of tape imperfections. We attempted to localize those imperfections on each reel of tape and whenever possible make error test runs that were continuous, excluding those localized bad spots. Where bad areas were unavoidable during an error test run, we then confirmed and documented that the detected bit errors were directly attributable to tape surface blemishes.

We continued to use the same reel of tape until the wear rate of the oxide surface became excessive as manifested by complete loss of signal (dropouts occurring at -20db or greater). The results of some error rate test runs on tape that was known to contain excessive dropouts are included in the test results.

In the accumulation of test data several methods were tried. The primary system parameter under evaluation was of course, digital bit-error rates. This parameter, a dimensionless proportion between two numbers, has in the past been an arbitrary figure. In order for it to be meaningful, we not only had to define just how the numbers were obtained but we should graphically display, in a quantitatively manner, their rate of occurrence.

The detected errors were totalized over time increments of either five second or ten second. It was observed that the nature of the errors, when they were detected, usually occurred in consecutive order within the incremental totalizing period. That is to say, if in any ten second period 20 bit errors were detected the odds were, in approximately 75% to 80% of the cases, that they occurred consecutively rather than in a series of 20 or less bit periods spread out over the ten second totalizing period. Therefore if we were to totalize bit errors and record them every 0.5 second or 1 second the bit error dropout profile curves would remain relatively the same in all cases. The total number of error totalizing sample increments would increase proportionately.

However the Poisson distribution plots showing the "Number of N Second Data Blocks" vs "Number of Digital Bit Errors"

would exhibit a rather dramatic change. This picture would reflect, in a most favorable manner the overall qualitative results of the tests if one were to use correspondingly shorter error totalizing increments. As an example in Fig. 29 if one second error totalizing increments were used instead of 10 seconds 98% of the total error test run would have shown to contain zero errors rather than the calculated 81%. As an ultimate example, if just the sum total of the bit periods of all the detected bit errors had been used relative to the total error test run to determine this percentage figure the percent of the error test run that contained zero errors would be even higher than 98%. Thus, it is apparent that the final figures obtained must be carefully considered in order to draw the appropriate conclusions.

In the final analysis the overall performance of the digital high packing density NB/PM Encoding/Decoding system under evaluation here has proved to be eminently successful. The performance figures as well as a careful analysis of the system tested under rather stringent and comprehensive operating conditions and procedures, show that the system is quite unique in all respects. It is of the opinion that this system when product designed, and operating in conjunction with equipment commensurate with the performance level of this NB/PM Encoder/Decoder, will show at least an order of magnitude of improvement with respect to digital bit error rates and at least a 25% (possibly higher) improvement in digital bit packing density. The results to date as well as a thorough analysis of the system under all operating modes and conditions substantiate this. It is concluded that this NB/PM Encoder/Decoder system will greatly enhance all present digital recording systems as well as opening new possibilities to all future digital data handling systems where magnetic surfaces are used as a medium for the storage of data in a digital format.

TECHNICAL INFORMATION AND DATA OF THE EVALUATION OF VIDEO TAPE WITH THE ORION VTA-101 TAPE ANALYZER

APPENDIX I

ORION PRODUCTS, INC.

VIDEO TAPE ANALYZER VTA - 101

TECHNICAL INFORMATION AND DATA OF THE EVALUATION OF VIDEO TAPE WITH THE ORION VTA-101 TAPE ANALYZER

ABSTRACT

This technical information report discusses the increasing need for an accurate and efficient method of evaluating video tape quality and the consequent development of the Orion VTA-101 Video Tape Analyzer.

The VTA-101 detects, sectionally totalizes, and records video tape imperfections and produces a tape dropout profile as a permanent record. The VTA-101 permits tape quality pre-check, grading to specific requirements, and locating of imperfections for spliceout. Old tapes can be checked periodically to determine the extent of wear; tape performance histories can be studied; and tape life can be predicted accurately.

The report includes specifications for the Orion VTA-101 Video Tape Analyzer and describes accessories for counting and totalizing; for dropout simulation; and for splice, dropout, scratch, and signal-to-noise ratio detection.

INTRODUCTION

Introduction of video tape recording has brought an increased demand for better quality magnetic tape. Tape producers have responded with considerable effort aimed at improving their manufacturing techniques and processes but the complexity of the problem has been so great that most high performance record/reproduce systems are still tape limited. The introduction of video tape systems to the fields of instrumentation and special wide-band recording has also spurred the demand for better quality. As these relatively new applications gain wider acceptance, the demand for quality will be even greater.

Quality Standards Differ

The quality of video magnetic tape depends primarily on these important parameters: 1) the uniformity of the magnetic surface; 2) the characteristics of the magnetic media (including intrinsic coercivity and retentivity); and 3) the coefficient of friction of the tape. The uniformity of the magnetic surface is by far the most unpredictable and the most detrimental parameter. It is to this parameter that most attention is given. Most of the video tape imperfections which are introduced during the manufacturing process are illustrated in Figure 1. These include coated-in oxide clumps and fibers; binder nodules and pin holes caused when the binder-oxide vehicle reaches its boiling point during the manufacturing process; foreign particles; the lack of a homogeneous binder-oxide combination, and backing nonuniformity. Other imperfections, such as low signal-to-noise spots, caused when rotary heads are allowed to scan the same spot on the tape, can be introduced by the user.

The physical size and the rate of occurrence of these various imperfections determines the quality of a tape and, consequently, its usability. The nature of the imperfections on any given tape might satisfy the requirements of one type of information recording and yet be totally inadequate for another type. A tape which exhibits imperfections which are large in size but occur infrequently, for example, might be acceptable for information recorded in digital format but unacceptable for video recorded signals and vice versa. Furthermore, tapes exhibiting both characteristics

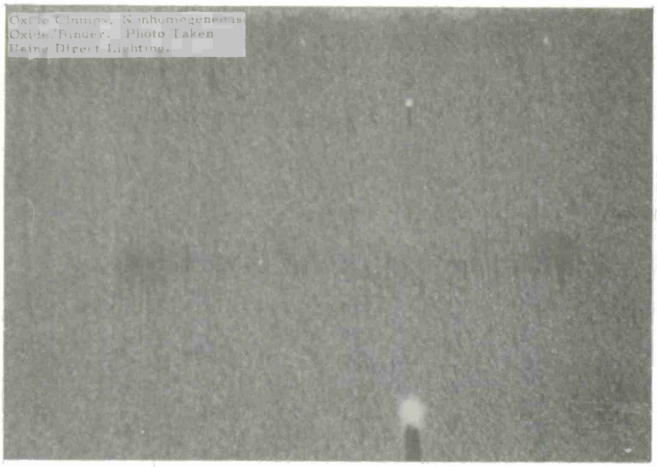
Oxide Clumps, Nonhomogeneous
Oxide/Binder. Photo Taken
Using Direct Lighting.

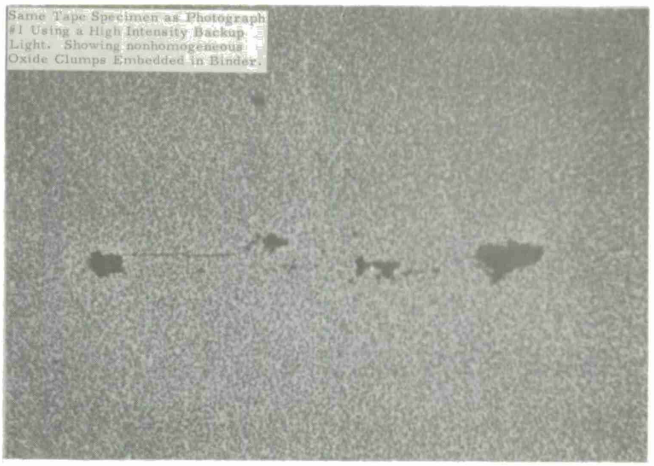
Same Tape Specimen as Photograph
#1 Using a High Intensity Backup
Light. Showing nonhomogeneous
Oxide Clumps Embedded in Binder.

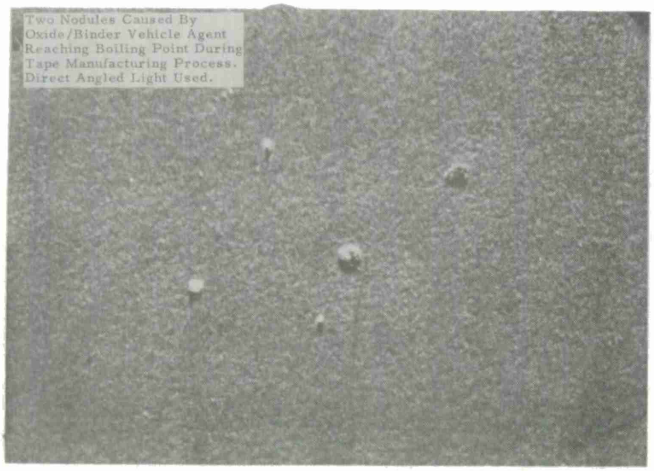
Two Nodules Caused By
Oxide/Binder Vehicle Agent
Reaching Boiling Point During
Tape Manufacturing Process.
Direct Angled Light Used.

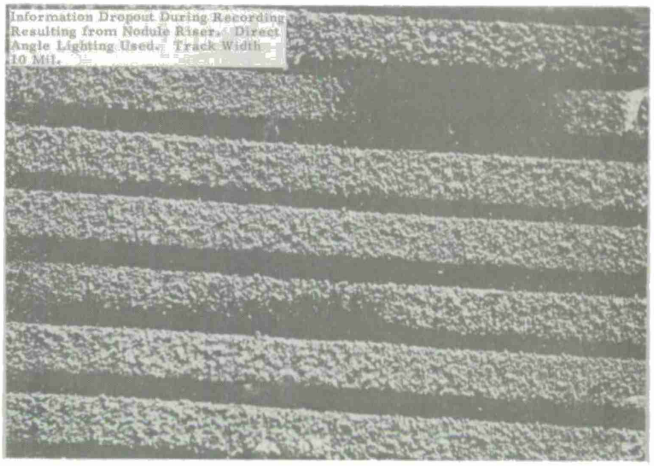
Information Dropout During Recording
Resulting from Nodule Riser. Direct
Angle Lighting Used. Track Width -
10 Mil.

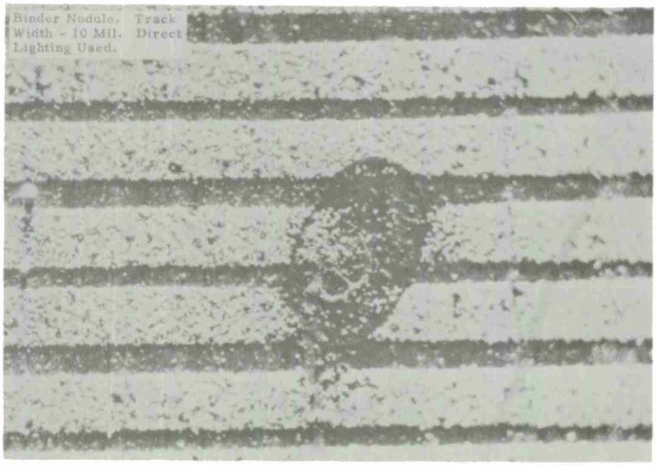
Binder Nodule. Track
Width - 10 Mil. Direct
Lighting Used.

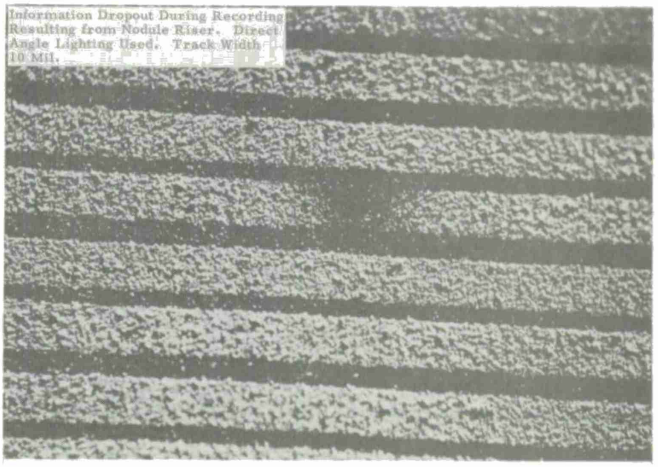
Information Dropout During Recording
Resulting from Nodule Riser. Direct
Angle Lighting Used. Track Width -
10 Mil.

Figure 1

might be acceptable for some TV recordings and unacceptable for others. In short, different applications require different tape quality standards, and the methods for evaluation and grading of tapes can be markedly different.

Imperfections Cause Dropouts

The lack of a uniform tape surface manifests itself as a loss of signal and an introduction of a noise burst during that loss. As the recording transducer passes a point on the tape which exhibits a nonuniform magnetic surface, a separation of the transducer from the surface occurs. When this contact is lost, the fringe flux surrounding the transducer recording gap loses its effective magnetization force on the oxide surface. This loss is either total or partial, depending upon the effective displacement between the transducer gap and the magnetic oxide surface, and results in a discontinuity of the recorded information during that period. During reproduce modes, this discontinuity is further compounded. There is a direct relationship between the effective strength of the flux lines at the gap as a function of the effective separation between the gap and the magnetic surface.

Such discontinuities in recorded information are referred to as dropouts. Dropouts represent a lack of RF signal or a drop in RF signal level. On a television screen, dropouts appear as random black or white streaks and flashes of indefinite duration and intensity. The number of dropouts in any given tape is related to several recorder parameters, such as tip penetration (see Figure 2), but in the main is determined by the manufacturer's ability to produce a product free from physical defects and pollution.

Dropouts can also be introduced by the user during normal handling, dubbing (dubbed tapes will pick up all dropouts in the master and the dubbing process can add others); and by tape wear (see Figure 3). The rate of occurrence and the intensity of dropouts can also be affected by: 1) the nature of the material being recorded; 2) the head-to-tape contact pressure; 3) playback system noise; 4) playback limiting gain (affects dropout depth); and 5) playback system transient response (affects dropout width).

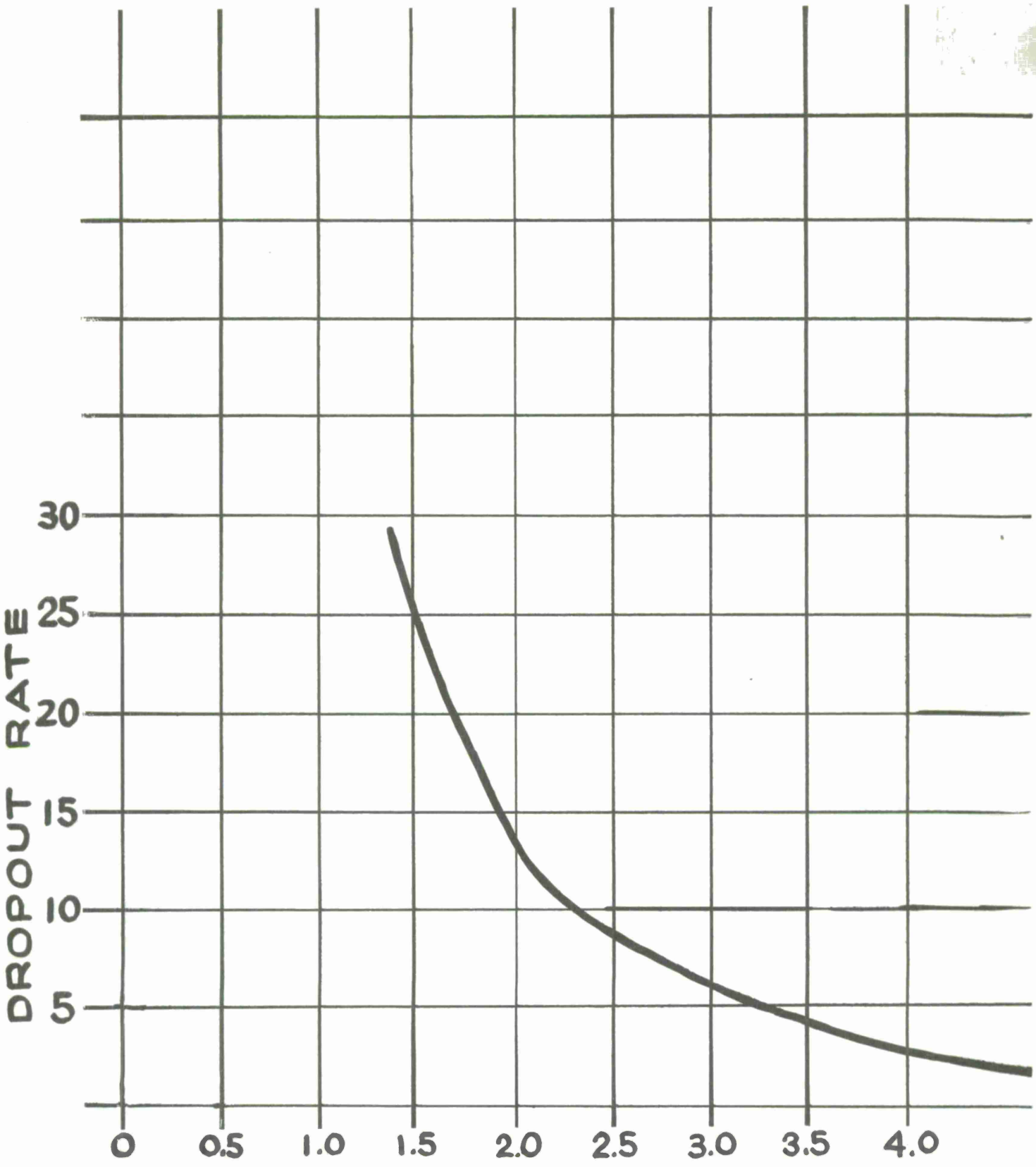

DROPOUT RATE VS. TIP PENETRATION

Figure 2.

The normally constant FM signal shown in the lower portion of Figure 4 becomes an amplitude modulated FM signal (as shown in the upper portion of the figure) due to the imperfections on the video tape. When this degree of amplitude modulation falls below the dynamic gain figure of limiter circuits in playback, then a momentary black or white streak is produced in the reproduced picture.

The upper trace in Figure 5a shows an RF carrier on FM signal with no dropouts. The lower trace in the figure shows the carrier with dropouts. Figures 5b, 5c and 5d show dropouts of various widths and depths. It should be noted that if the carrier is used to inspect the tape, the degree of inspection depends on the upper carrier frequency, i.e., the higher the carrier frequency the greater the increment of inspection. Consequently, tapes which are adequate for low-band recording are not necessarily adequate for high-band use.

The Need for a Versatile Video Tape Analyzer

At the present time, the checking of video tapes is a laborious and costly process which involves tying up expensive tape equipment and highly trained personnel. Tape quality is checked to a minimal level of acceptance in a purely subjective manner, based primarily on visual criteria (see bibliography sources 1, 2, 3 and 4). Although the methods used are acceptable for some television applications, they are totally unacceptable for most instrumentation recording applications.

There is a very real need for an integrated system that will detect, among other parameters, nonuniformity of magnetic tape surfaces and present the results in a form that is both realistic and meaningful.

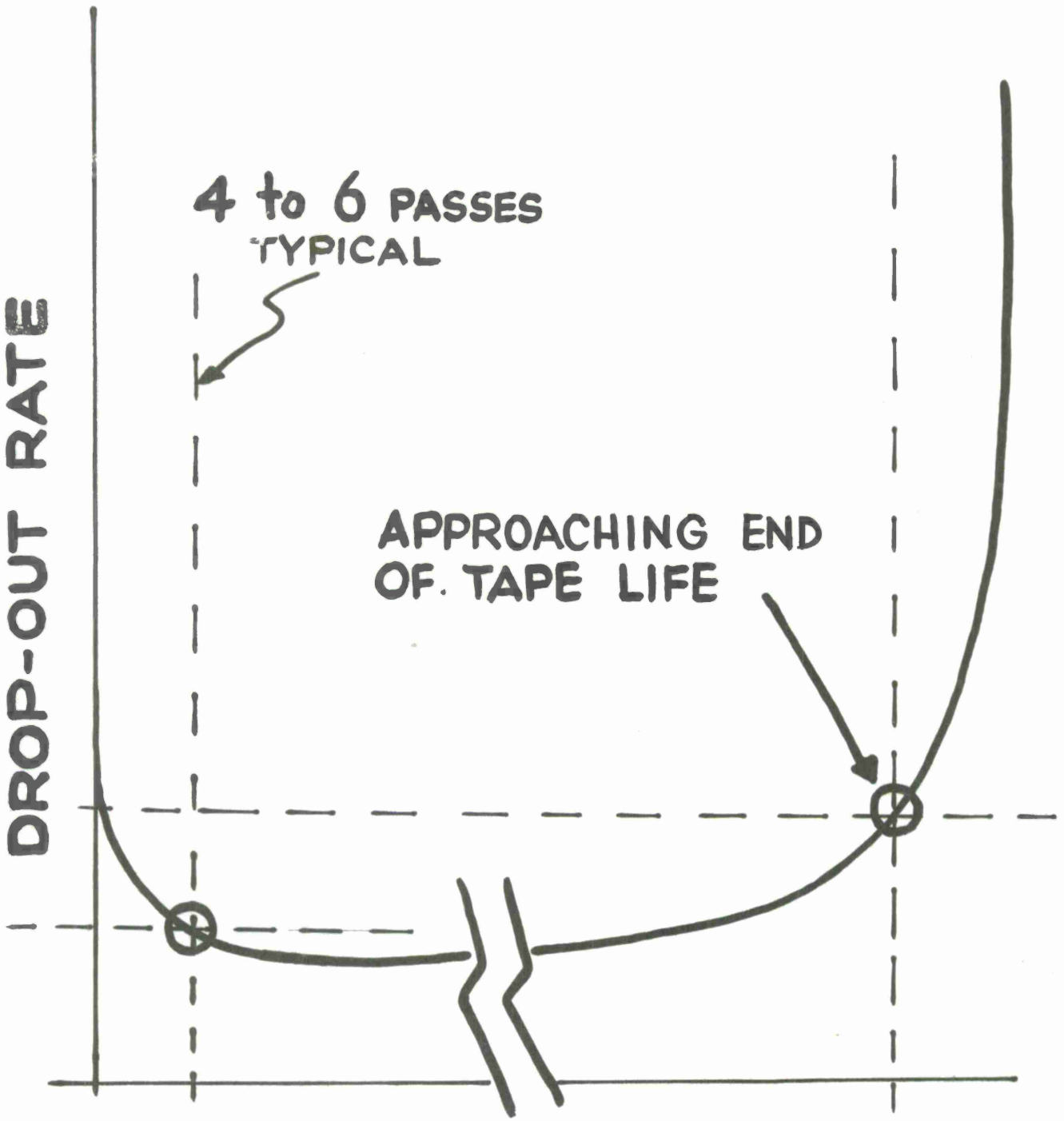

DROP-OUT RATE VS. No. OF HEAD PASSES

Figure 3

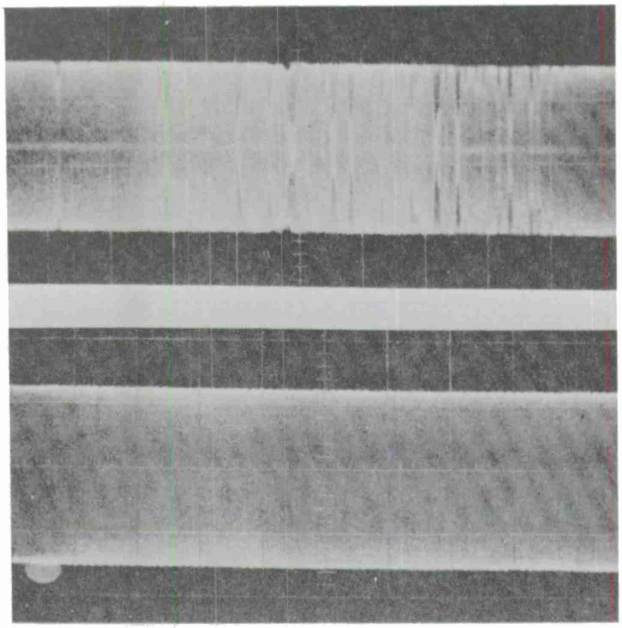

Figure 4

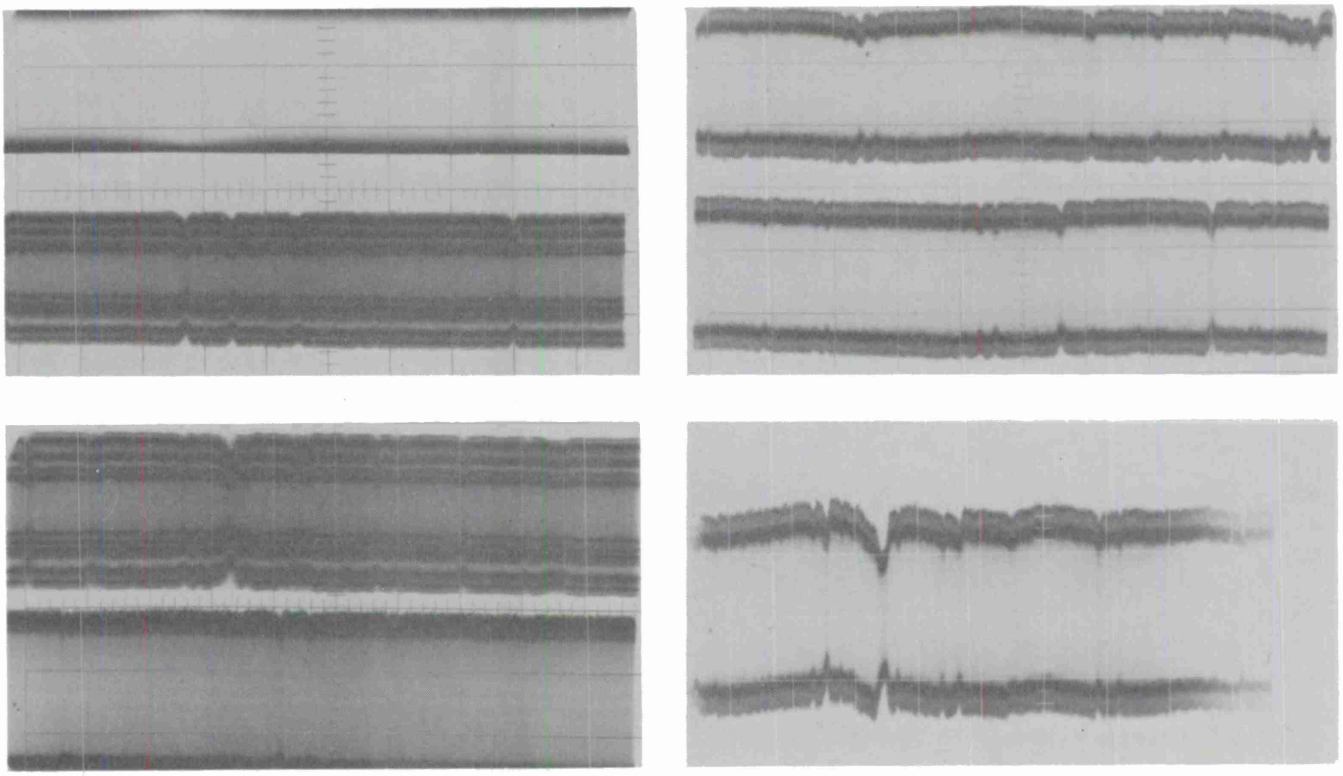

Figure 5

THE KRS/ORION VTA-101 VIDEO TAPE ANALYZER

The KRS/ORION VTA-101 Video Tape Analyzer (Figure 6) detects, sectionally totalizes, and records video tape imperfections and produces a tape dropout profile as a permanent record. The VTA-101 permits tape quality precheck, grading to specific requirements, and locating of imperfections for spliceout -- all before priceless recordings are wasted or lost.

With the VTA-101, users may establish arbitrary standards for tape quality. New tapes may be graded accordingly for subsequent use as masters, dubs, monochrome, low-band and high-band color tapes. Old tapes may be checked periodically to determine the extent of wear. Tape performance histories can be studied. Tape life can be predicted accurately. Tape checking time and labor can be drastically reduced.

Detection and Display

The VTA-101 totalizes the video dropouts in terms of dropout depth and width for a given sampling period. The summation of all of the sampling periods over the entire video tape gives a dropout profile of that tape. Optional equipment can be added to detect and record tape splices and tape scratches and to analyze signal-to-noise ratio, audio tracks and control tracks. With other options the audio track and control tracks on any tape may be checked concurrently with the video track.

Special detection circuitry detects recorded RF carrier envelope irregularities as defined by two parameters -- dropout amplitude and duration. Detection limits are variable over a wide dynamic range and are easily calibrated; thus, any size dropout that can be defined within these limits can be detected (see Figure 7).

A counter totalizes the number of dropouts detected during a predetermined time increment. Detected dropout totals for incremental tape sections are then displayed on a strip chart recorder. The dropout count is visible on the front panel, and the counter can be connected for digital printout.

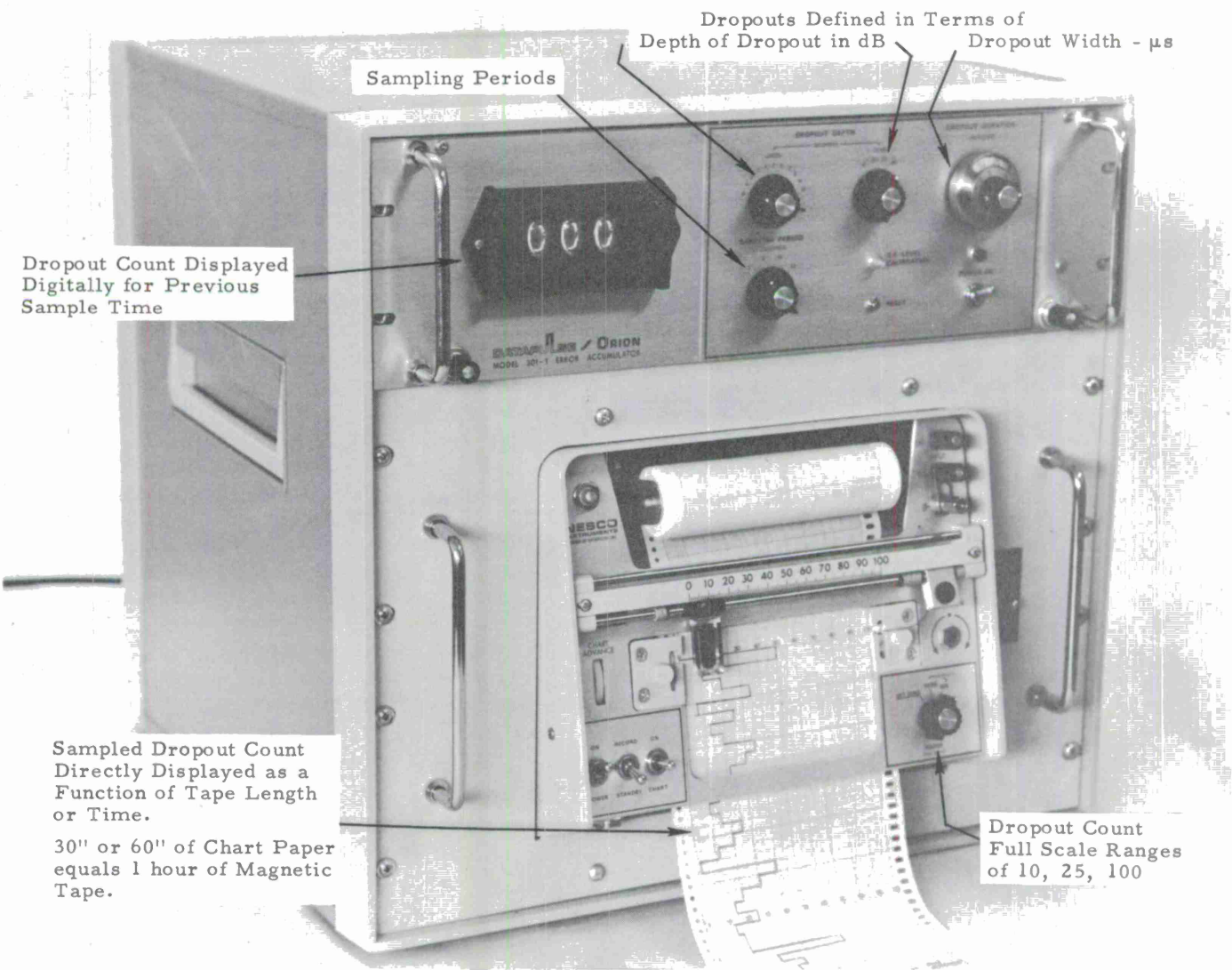
Dropouts Defined in Terms of
Depth of Dropout in dB
Dropout Width - µs
Sampling Periods
Dropout Count Displayed
Digitally for Previous
Sample Time
Sampled Dropout Count
Directly Displayed as a
Function of Tape Length
or Time.
30" or 60" of Chart Paper
equals 1 hour of Magnetic
Tape.
Dropout Count
Full Scale Ranges
of 10, 25, 100

Figure 6

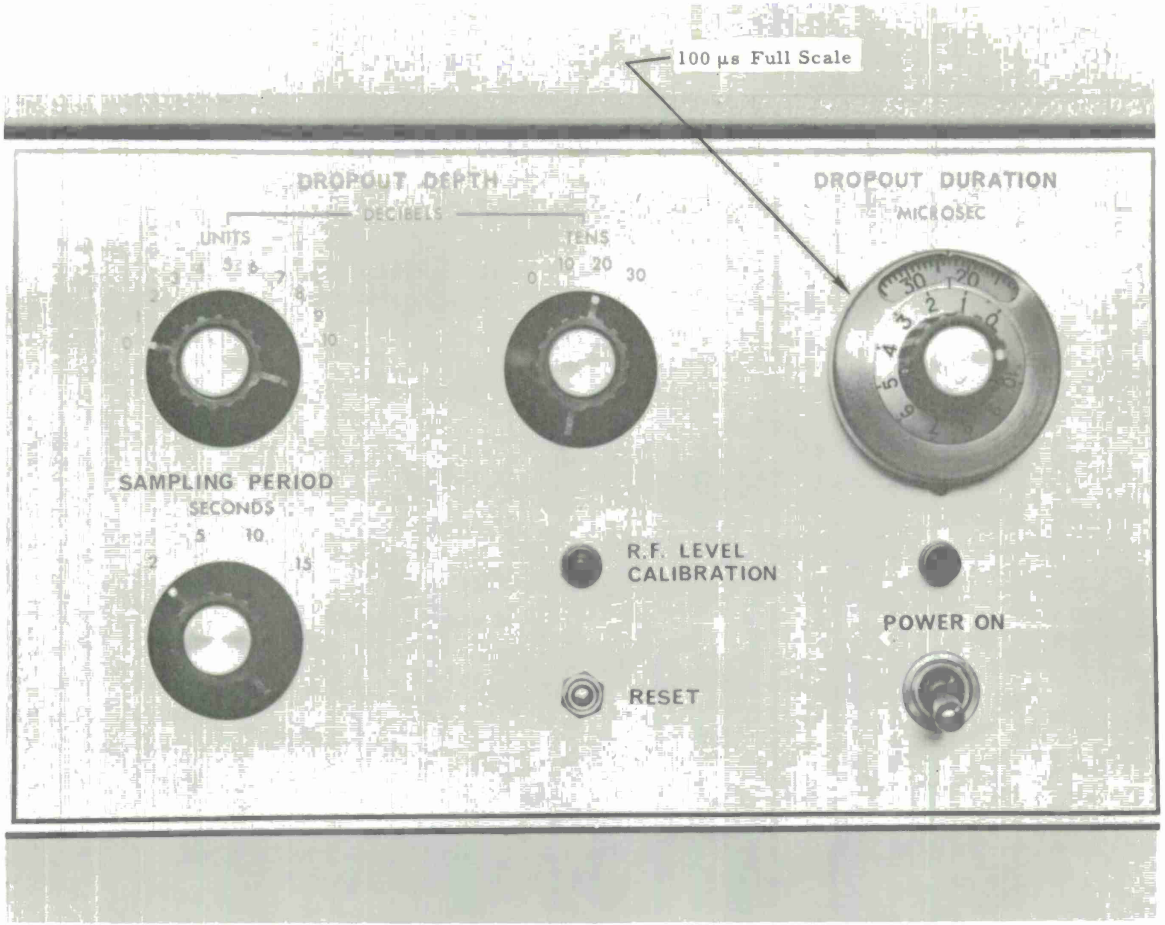
100 µs Full Scale
DROPOUT DEPTH
DECIBELS
UNITS
TENS
DROPOUT DURATION
MICROSEC
SAMPLING PERIOD
SECONDS
R.F. LEVEL
CALIBRATION
POWER ON
RESET

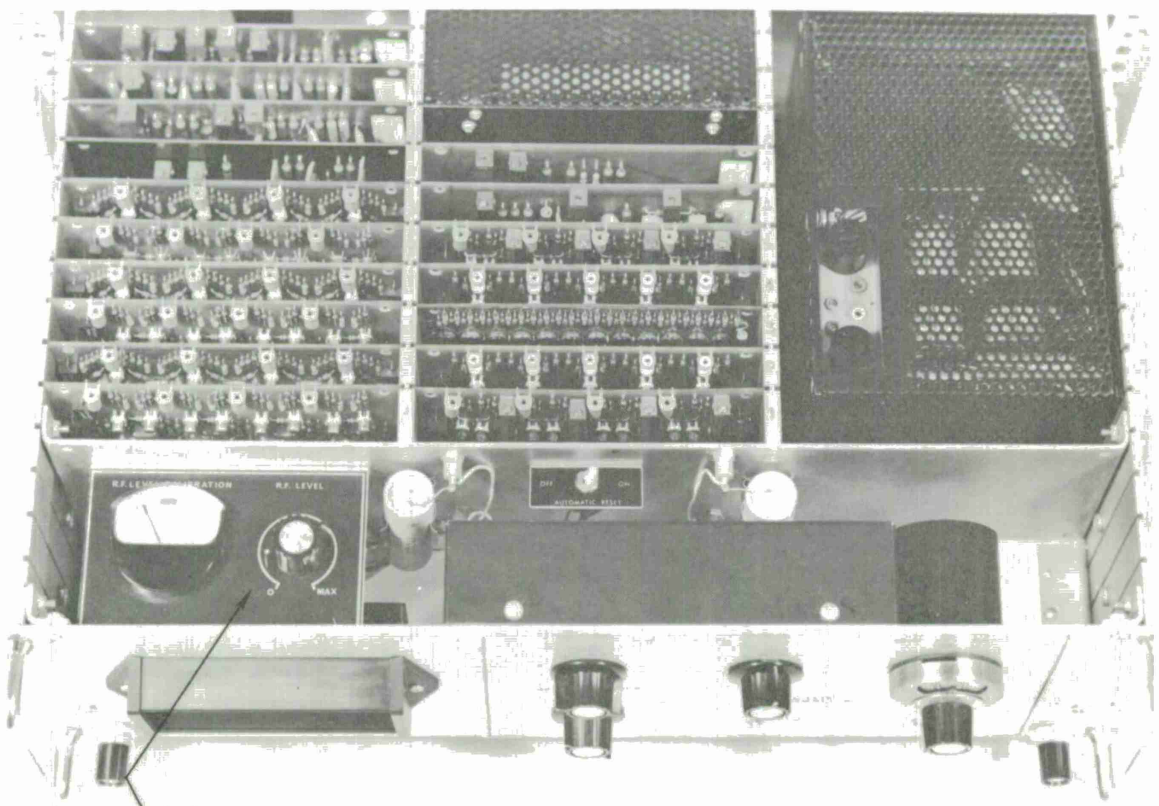
To Set
RF or FM Standard
Level

Figure 7

To add a third dimension to the qualitative dropout profile, a number of dropout detectors may be incorporated to detect, totalize and record various size dropouts. In this case, a multipen strip chart recorder is utilized to present the various dropout profiles.

Special Video Tape Transport

A special purpose video tape transport is being designed to handle video tape on a highly efficient production basis. It will add the following advantages to the KRS/ORION VTA-101 system:

1) automate as many operating functions as possible;
2) eliminate the need for tying up broadcast equipment and personnel;
3) decrease, by at least a factor of four, the time required to check a reel of tape; and
4) condition the tape--clean it, burnish it, and deliver it with a uniform tension profile, ready for use.

Video magnetic tape manufacturers and their customers are presently checking tape with existing rotary head tape transports. This means, in the case of TV recording studios, that operating personnel and a full recording machine are tied up during this period. This is an expensive, time consuming operation which is often very inefficient and ineffective in the actual evaluation of the tape.

Strip Chart Presentation

The length of the chart depends upon the length of the video tape (see Table I). The strip chart speed may be selected as either 30 inches or 60 inches per hour from the front panel. Each time the dropout count is totalized for the chosen sampling period (1, 2, 5 or 10 seconds), the output of the totalizing counter is transferred into a buffer register and displayed for a period of time equal to the sampling period. At the transfer time, the digital-to-analog converter produces an output proportional to the count and causes the chart recorder pen to move to that voltage (see Figure 8).

Dropout Counter Presentation

The dropout counter counts the dropouts during the sampling period as set via the front panel switch position and then resets to zero. It repeats this function for each sampling period.

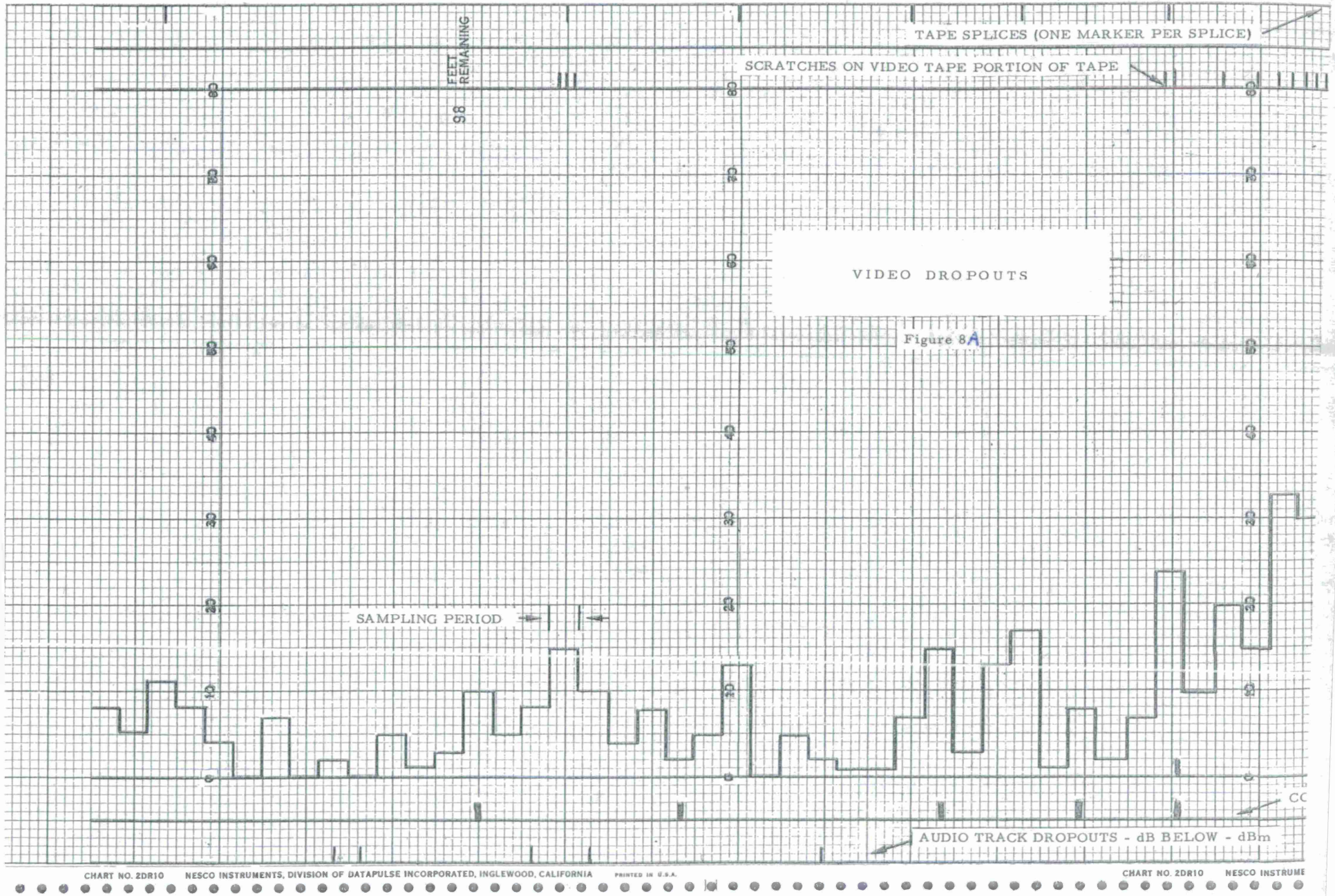
TAPE SPLICES (ONE MARKER PER SPLICE)
SCRATCHES ON VIDEO TAPE PORTION OF TAPE
FEET REMAINING
98
VIDEO DROPOUTS
SAMPLING PERIOD
AUDIO TRACK DROPOUTS - dB BELOW - dBm
CHART NO. 2DR10 NESCO INSTRUMENTS, DIVISION OF DATAPULSE INCORPORATED, INGLEWOOD, CALIFORNIA PRINTED IN U.S.A.
CHART NO. 2DR10 NESCO INSTRUME

Figure 8A

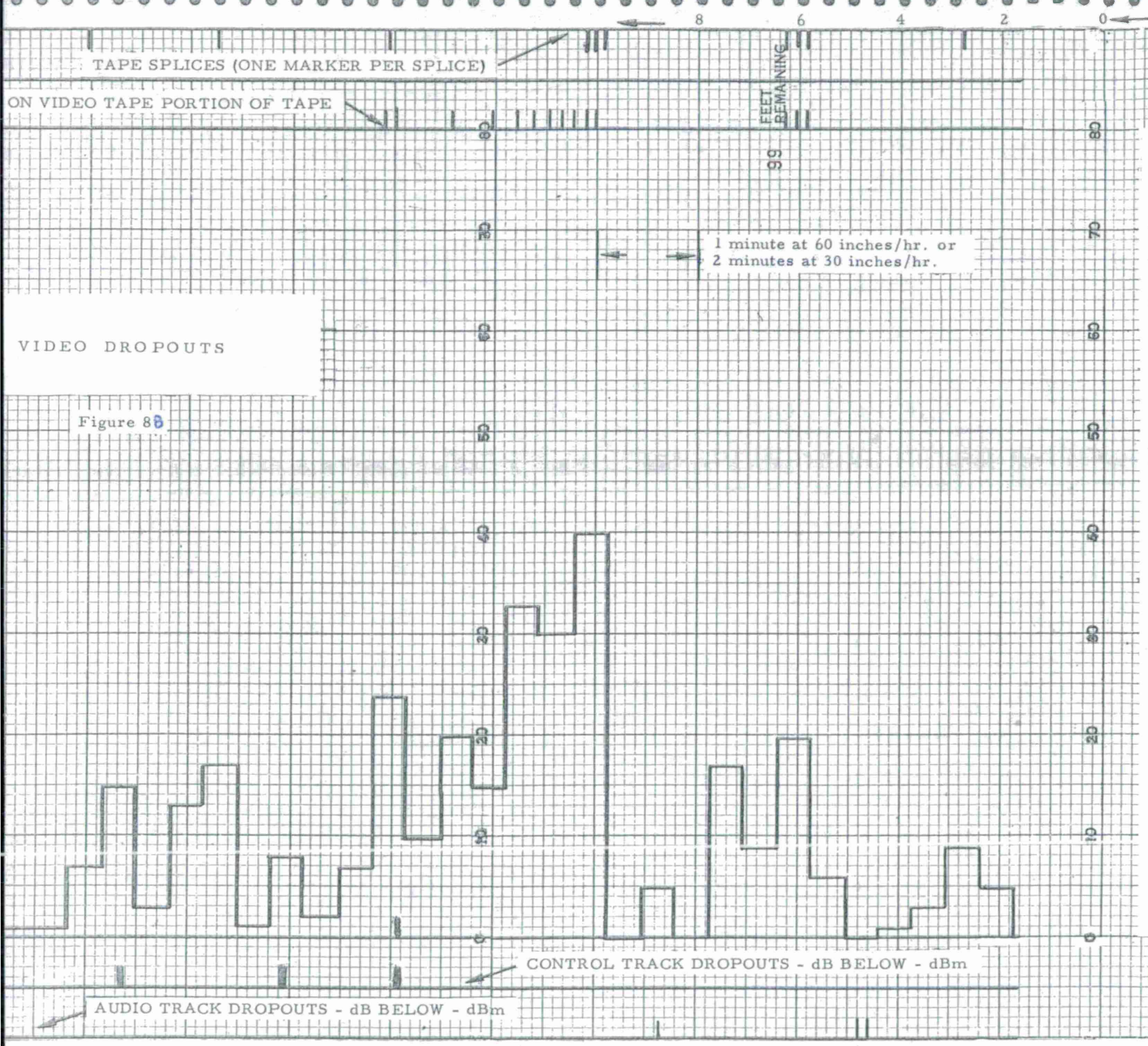

Figure 8

Date _____

TAPE DATA

Manufacturer _____ Reel No. _____

No. of passes to date _____ Reel Size _____

Total No. Dropouts

Video _____ Total

Audio _____ Total

Control Track _____ Total

Splices _____ Total

Video Tape Recorder Data

VTR Model No. _____ Serial No. _____

Rotary Head Ass'y. No. _____

Monochrome _____

Color: _____ highband

_____ lowband

Tip Penetration _____

Dropout Sensor _____ In _____ Out

Video Tape Analyzer Data

Serial No. _____

Depth of Dropout _____ dB

Duration of Dropout _____, _____ µs

Sampling Period _____ Sec.

Chart Paper Data

Chart Speed 30 in/hr. (1 in. = 2 min.)

60 in/hr. (1 in. = 1 min.)

Audio Track _____ dB below

_____ dBm ref.

Control Track dB below

_____ dBm ref.

Video Dropouts Full Scale

_____ 10 _____ 25 _____ 100

The counter readout records the number counted in the previous sampling period and holds that count for the next sampling period. It then resets itself to zero and displays the previous count. The monitor presentation and the counter display are easily correlated. An alternate presentation is available via an internal switch. In this case, the counter does not reset to zero and continues to totalize dropouts. This function is available as the Model 17 dropout totalizer when the dropout counter is used for sampling period totals.

TABLE I.

Correlation of Chart Paper and Video Tape Parameters

Sampling Period (seconds)	No. of Ft. of Video Tape in Sampling Period	No. of Samples in 1 inch of Chart		No. of Samples in "X" Ft. of Tape	
		30"/hr.	60"/hr.	4800 Ft.*	7200 Ft.*
1	1.25	120	60	3833	5749
2	2.5	60	30	1916.5	2874.5
5	5.0	24	12	767	1149.8
10	10	12	6	383.3	574.9

*Video tape recorder longitudinal rate of 15 ips. Tape running time of 1 hour 3.6 minutes for 4800 feet of tape, and 1 hour 35.4 minutes for 7200 feet of tape.

Chart Speed 30"/Hour			Tape Speed 15"/Second		
30"	Chart Paper	=	4500 Ft. of Tape	=	1 hr.
31.9"	Chart Paper	=	4800 Ft. of Tape	=	1 hr. 3.8 min.
47.85"	Chart Paper	=	7200 Ft. of Tape	=	1 hr. 35.4 min.
60"	Chart Paper	=	9000 Ft. of Tape	=	2 hrs.
63.8"	Chart Paper	=	9600 Ft. of Tape	=	2 hrs. 7.2 min.

Chart Speed 60"/Hour			Tape Speed 15"/Second		
60"	Chart Paper	=	4500 Ft. of Tape	=	1 hr.
63.8"	Chart Paper	=	4800 Ft. of Tape	=	1 hr. 3.8 min.
95.70"	Chart Paper	=	7200 Ft. of Tape	=	1 hr. 35.4 min.
120"	Chart Paper	=	9000 Ft. of Tape	=	2 hrs.
127.6"	Chart Paper	=	9600 Ft. of Tape	=	2 hrs. 7.2 min.

The chart paper has 10 small divisions per inch.

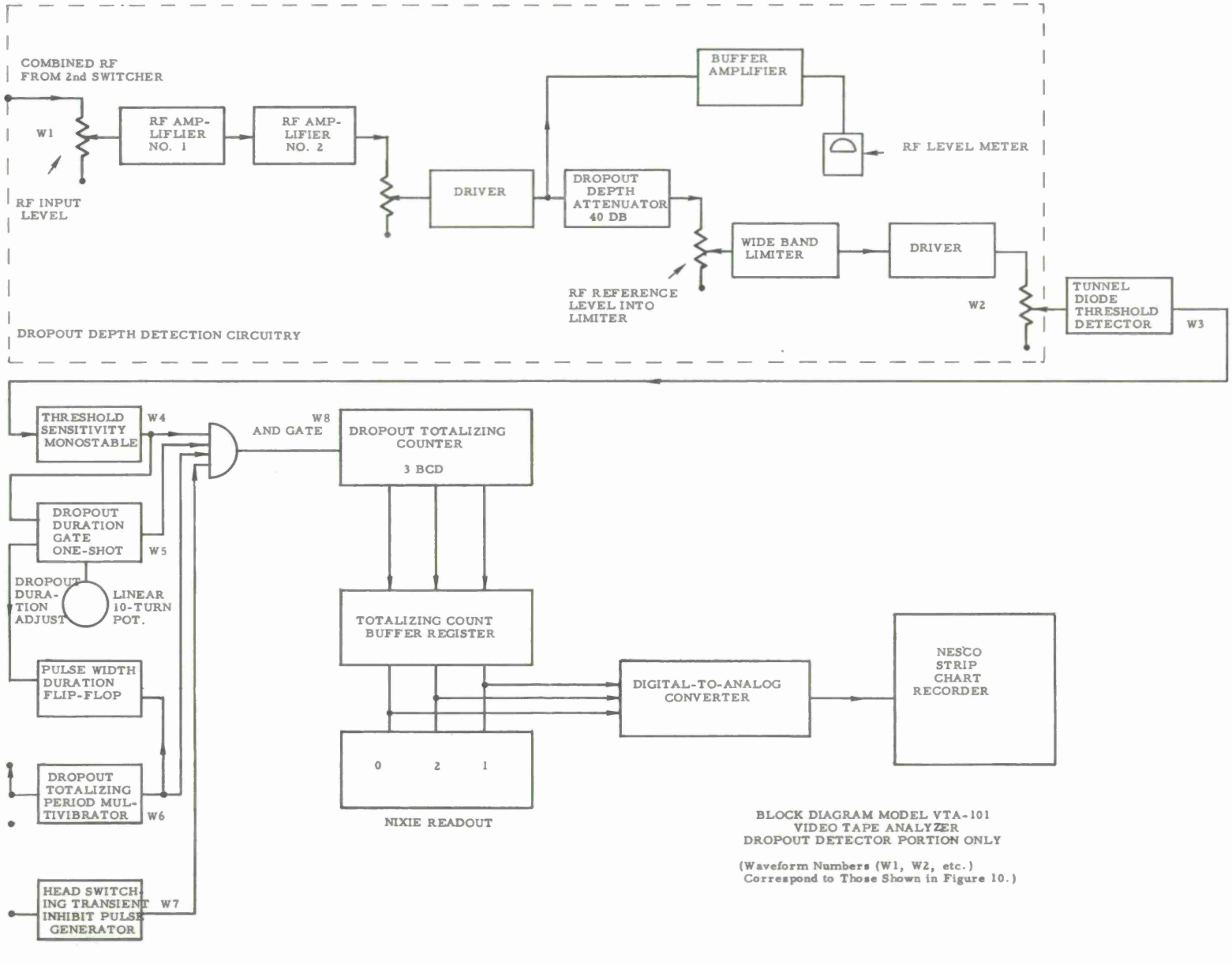

Figure 9

BLOCK DIAGRAM MODEL VTA-101
VIDEO TAPE ANALYZER
DROPOUT DETECTOR PORTION ONLY

(Waveform Numbers (W1, W2, etc.)
Correspond to Those Shown in Figure 10.)

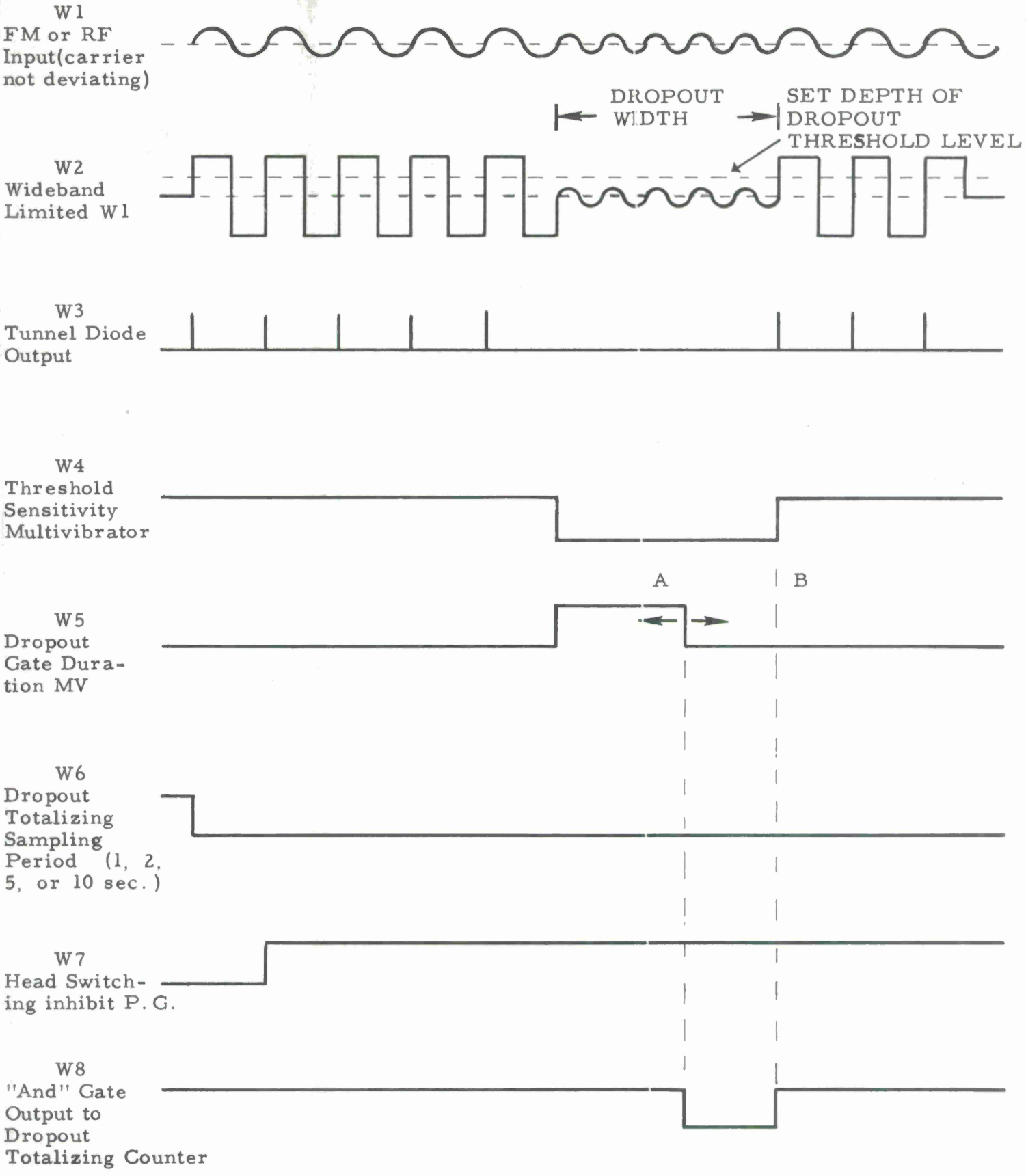

Waveforms Corresponding to Block Diagram
Video Tape Analyzer Model VTA 101

Figure 10

Block Diagram - Model VTA-101 Video Tape Analyzer

The electronics, exclusive of the specialized transport but compatible with that transport, are described below. Note that the electronics are compatible with all existing video tape recorders and many instrumentation recorders. Figure 9 shows the dropout detector and display circuits of the Video Tape Analyzer. The RF signal up to 10 MHz is brought in from the tape transport from the combined RF (2nd switcher). This signal is an FM carrier which may or may not be deviating around its center frequency. The RF input level is varied until the RF level meter is set in its standardized green portion (Reference Amplitude).

For the video tape analyzer to evaluate only that portion of the video carrier which corresponds to the video picture, a 240 cycle input from the transport is required to gate out the overlapped portion of the video signal. If this gate is not used the dropout signals will be about 10% high. This corresponds to the two head overlap period. Industrial video tape recorders use only two heads -- one for video information and the other for sync information so different gating signals are used.

Dropout Depth Circuitry

The objective of the RF amplifiers, driver, and RF level meter is to standardize the RF levels coming in from many different types of video tape recorders. The RF input level is varied to give a standard level (within green area) at the input to the dropout depth attenuator which is calibrated from 0 to 40 dB. The output from the dropout depth attenuator is amplified in a constant gain, wide-band limiter so that the tunnel diode threshold detector always detects at the same level, independent of the attenuator setting.

Detailed Block Diagram and Waveform Correlation (Figure 10)

The combined RF or FM signal, W1, from the 2nd switcher of the video tape recorder is applied to two RF amplifiers. The input level is set to a standardized level by setting the gain levels to the green area of the RF level meter. This also provides a signal input level which can vary over the range of 200 mV to 1 volt. The driver output is applied to a 40 dB attenuator and then to a wide-band limiter driver combination for W2. The output from W2 triggers a tunnel diode threshold detector for W3.

The various potentiometers in this chain of circuits are used to calibrate and preset the levels involved so that the threshold level at the tunnel diode will correspond to the 40 dB attenuator setting and the standardized level input. All circuits employ a generous amount of negative feedback making the level detector linear and a direct function of the attenuator setting.

The tunnel diode output, W3, is fed to the threshold sensitivity monostable. This circuit is kept from triggering by W3. The absence of triggers causes the one-shot to trigger for waveform W4.

It is desired to count only those dropouts which are greater than a fixed (but variable by front panel control) pulse width and to count the dropouts for a fixed sampling time. Also the video data on the tape has overlaps which are eliminated by the head switching transient pulse generator.

Waveforms W5, W6, and W7 are generated by the dropout duration gate generator, period duration generator, and head switching and timing generator.

All of these waveforms are AND'ed together to give an output to be totalized which is greater than the set dropout depth and set dropout duration. Note that if the dropout duration had been set so that it was longer than point B on W5, the AND gate output would not have occurred and no count would go to the totalizing counter.

The dropout count is totalized for the sample gate duration. At the end of the sample period the count in the three stage BCD counter is parallel shifted into the totalizing count buffer register. The Nixie readout then contains the count registered in the previous sample period. The buffer register output is now fed to a digital-to-analog converter giving an output proportional to the digital count. This output is now fed to the Nesco Strip Chart Recorder and a statistical profile of the dropout count is made of the incoming RF signal from the magnetic tape.

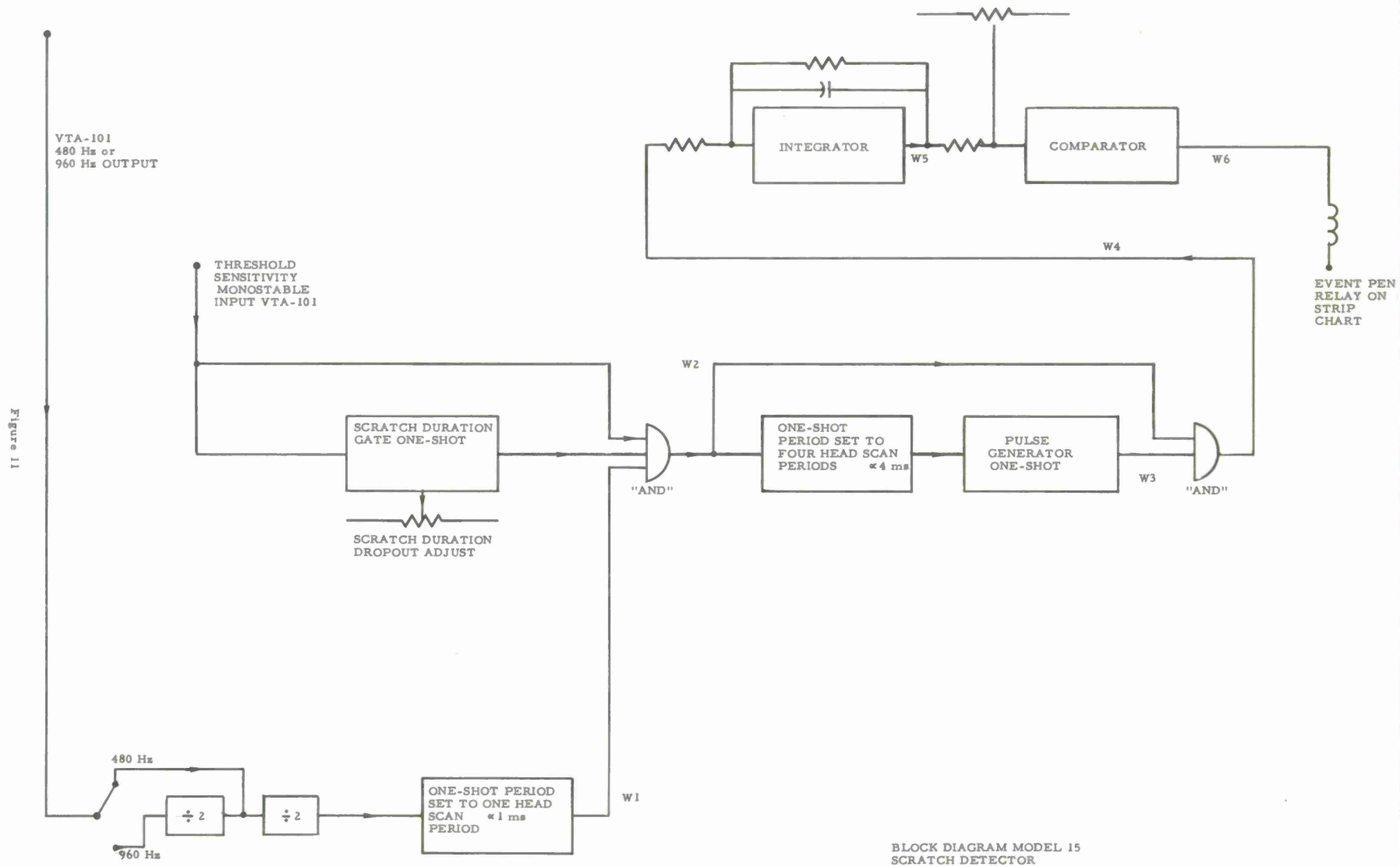

Figure 11

BLOCK DIAGRAM MODEL 15
SCRATCH DETECTOR

(Waveform Numbers (W1, W2, etc.)
Correspond to Those Shown in Figure 12.)

Model 11 Splice Detector and Model 12 Counter

The splice detector consists of a beam light source and a diffused silicon photo duodiode detector. Both the light source and photo diode are mounted in a rigid plate which in turn is mounted on the top plate of the recorder in close proximity to the back side of the magnetic tape. Both the beam light source and the photo diode are directed toward the magnetic tape. Any change in the reflected lighting intensity as a result of a tape splice is detected and indicated by a strip chart event pen. The event marker on the strip chart display indicates the splice's position on the video tape. The total may be obtained by counting the number of event marks on the chart paper. A digital display giving the total number of splices may be obtained at extra cost.

Model 13 Audio Track Dropout Detector

The audio track output is smoothed by an averaging detector and is then applied to a threshold level detector. This detector can be set internally so that an output occurs every time the averaged audio goes below this fixed level. The level is set in dB. The output of this below level detector actuates an event marker on the strip chart display indicating the dropout's physical position on the video tape. The total number of dropouts may be obtained by counting the number of events on the chart paper. A digital display giving the total number of audio dropouts may be obtained at extra cost.

Model 14 Control Track Dropout Detector

The control track dropout mechanism is the same as the audio track circuitry except the averaging detector is omitted.

Model 15 Scratch Detector (Figure 11)

The scratch detector is designed to indicate those scratches in the longitudinal direction and some particular kinds of transverse scratches as shown later. The detector will pick out scratches introduced by guides, dirt, and rotary heads.

Scratch Detector Timing Diagram and Functional Description (Figure 12)

Figure 12.

The scratch detector has two inputs, the 480 Hz head drum sync signal and the output from the RF level threshold detector. The 480 Hz signal is divided down to 240 Hz and this output activates a one-shot monostable whose output is used to activate an AND gate. The duration of this gate is adjusted to one head scan period (approximately 1 ms). The other input to this AND gate is from the scratch dropout detector circuits. Any detected dropout having a dropout duration greater than that of the scratch duration gate one-shot and occurring during the period determined by the head scan gate one-shot simultaneously activates a one-shot whose time constant is slightly less than four head scan periods (<4 ms) and a second AND gate. The output of the one-shot activates a one-shot monostable whose time constant is set to some period greater than the detected scratch duration. The output of this one-shot is fed to the other input of the second AND gate.

If during the successive head scan period a dropout occurs at the same point in time, starting at time zero from the following cycle of the rotary head drum (approximately 4 ms) coincidence is detected at the output of the second AND gate. The output of this AND gate is fed to the input of an integrator circuit. If coincidence is consecutively detected out of the AND gate, the output is integrated and fed to a comparator whose output drives a strip chart event marker. The event marker stays activated during the scratch period and is deactivated after coincidence is lost.

Coincidence is detected if the scratch is longitudinal and is equal to or greater than the period set into the scratch duration gate one-shot. Transverse scratches with a rate of change equal to the ratio of the rotary head drum cycle (approximately 4 ms) to the duration of the pulse into the second AND gate (from the one-shot pulse generator) are detected. Transverse scratches having higher rates of change are not detected.

Dropout Simulator Block Diagram

Figure 13 shows the block diagram of the dropout simulator. The front panel controls are the attenuator controls for depth of dropout in dB, for a variable frequency oscillator control (10 Hz to 0.1 Hz), for the duration of dropout (3, 6, 12, 24 μs and programmed widths) and for a manual burst or continuous control.

Model 18 Dropout Simulator

The objective of the dropout simulator is to allow an operator to simulate and observe on the video monitor the effects of dropouts under conditions of: dropout burst, dropout burst rate, dropout width, and depth of dropout without the use of video tape.

A study of these parameters and a correlation of them with the strip chart and video monitor presentations enables the operator to:

1) Set standards on dropout width and depth, and signal-to-noise ratios for inspection of new prerecorded tapes. Incoming inspection and grading of tapes for use at various quality levels is facilitated.
2) Recognize the effects of video tape defects.
3) Determine the end-of-life quality for any tape. A prerecorded tape is used as the RF input and additional dropouts are added through the simulator. A subjective judgment is made as to end-of-life

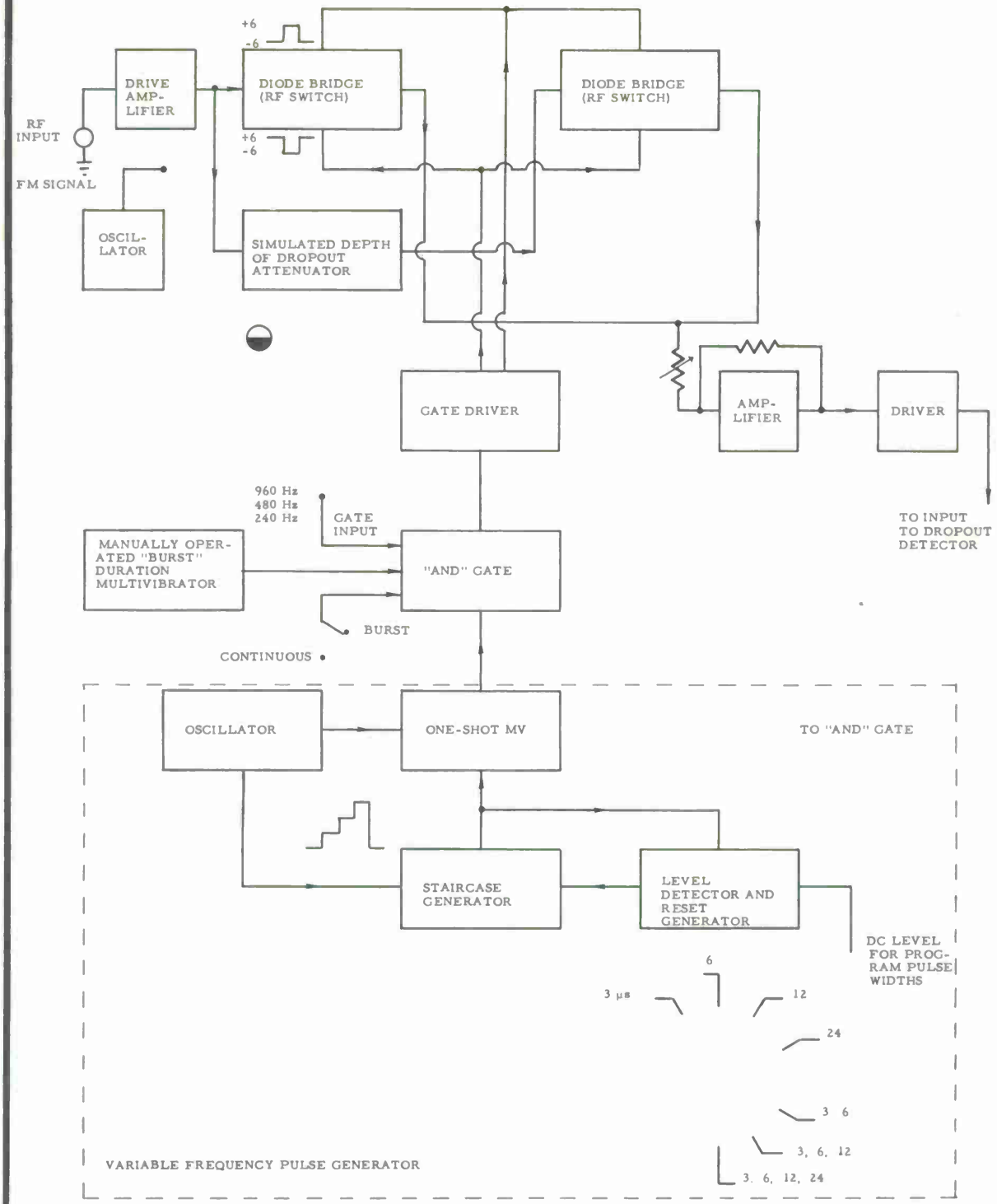

DROPOUT SIMULATOR BLOCK DIAGRAM

Figure 13

Figure 14

VTA-101 Video Tape Analyzer and Ampex VTR-2000 in operation during taping of ABC's Hollywood Palace television show.

by viewing the video monitor and a dropout record is made on the strip chart recorder. If a strip chart record is made and compared with the video tape and kept as part of its record, a comparison of that record and the end-of-life records will give the user an accurate history and record of what went wrong with the tape. It also pins down those sections of tape that have been damaged between quality checks.

A constant amplitude FM signal (FM modulated or not) is applied to a diode bridge gating arrangement such that the amplitude of the FM signal is attenuated at the time of the diode gate input to the level set by the depth of dropout attenuator. The width of dropout is determined by the gated pulse width. The signal is then fed to the RF input of the dropout detector video tape analyzer.

The rest of the circuits develop the diode gating signals. A variable frequency oscillator triggers a one-shot multivibrator and simultaneously triggers a staircase generator. The dc output of the staircase generator determines the width of the pulses from the one-shot multivibrator. This is determined by the staircase generator only during the programmed pulse widths as determined from the front panel (3, 6; 3, 6, 12; 3, 6, 12, 24 μs) control.

The programmed pulse width output on the 3, 6, 12, 24 μs position is 3 μs on the first cycle, 6 μs on the second cycle, 12 μs on the third cycle, 24 μs on the fourth cycle and will recycle thereafter. An input is provided to the AND gate for the rotary head switching input of 960 Hz, 480 Hz, or 240 Hz as may be appropriate. A continuous or burst input is provided along with a manual burst multivibrator whose duration is 1/4 second, 1/2 second or 1 second.

The video tape analyzer is fed FM signals which have dropouts programmed as to depth and duration. The monitor is synchronized from separate synchronizing pulses that are not affected by dropouts.

Model 16 Signal-to-Noise Threshold Detector

The signal-to-noise threshold detector is the measurement of the rms noise figure out of the video recorder's demodulator with the tape having an unmodulated quiescent recorded carrier. With the video recorder's demodulator gain calibrated for 1 volt peak-peak, composite video output (or 0.72 volts noncomposite), the sensitivity of the rms noise detector is calibrated to any desired level. If the rms value exceeds this level, the output of the one-shot multivibrator level detector triggers. The output is mixed with the analog output corresponding to the totalized count. The strip chart recorder then indicates the time start on the tape in which it exceeds the acceptable signal-to-noise ratio.

Model 17 Dropout Totalizer

A second presentation which is of interest is to allow the counter to totalize the number of inputs for the entire reel of tape giving a presentation on the graph paper as follows:

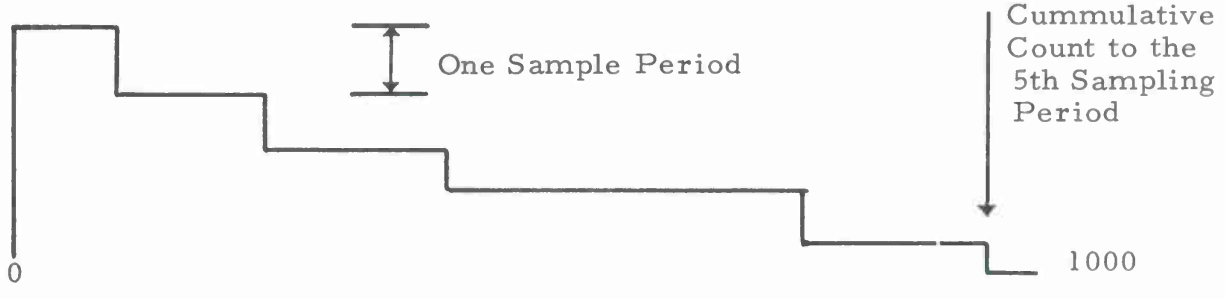

Model 101 Video Tape Analyzer

SPECIFICATIONS

INPUT SIGNALS

RF or FM Signals -- 200 mV to 1 volt rms.

Amplitude -- Adjustable from front panel control for standard input corresponding to the GREEN area on the input meter. Input is available from any video tape recorder.

Impedance -- 100 kΩ, ac coupled.

Drum Track -- Ac coupled into 10 k.

Gating Input -- 240 Hz or 480 Hz square wave or sine wave signal for gating the RF or FM signal to record only those dropouts occurring during the picture portion of the video signal.

Amplitude -- 1 volt square or sine wave.

Impedance -- 2 kΩ, ac coupled, 22 μF.

OUTPUT SIGNALS (Rear Panel Only)

Cummulative Dropout Count

Amplitude -- 3.5 volts min.

Impedance -- Approximately 5 kΩ. Digital-to-analog signal representing the dropout count as an input to the analog chart recorder.

DROPOUT PARAMETERS

Dropout Depth

Dropout Threshold -- Adjustable from 0 dB to 40 dB signal loss in 3 dB steps.

Dropout Duration -- Adjustable from 1 μs to 100 μs with 1000 division helical potentiometer.

Counter Readout -- 3 digit Nixie.

Sampling Period -- Switch selection of 1, 2, 5 and 10 second periods.

Front Panel Controls and Readout

RF or FM Amplitude Adjust -- Potentiometer to adjust the signal to the GREEN area of front panel meter.

Dropout Depth (dB) -- Variable in 10 dB and 3 dB steps to 40 dB.

Dropout Width (μs) -- Ten turn helical potentiometer with full scale of 100 μs.

Dropout Counter Readout -- Nixie readout with 3 digits. Counter counts all dropouts below the set threshold dropout level and whose dropout duration is above that set by the dropout width circuits.

Dropout Sampling Periods -- Switch selection of periods of 1, 2, 5 and 10 seconds.

Power Input -- 105-125V, 50 or 60 Hz. Furnished with line cord with NEMA 3-prong (grounded) plug. Can be furnished at 220V at no extra cost.

Physical Size -- 5-1/4" high x 19" wide x 16" deep.

Optional Equipment

Model 10 Chart Recorder -- Modified Nesco Model JY160A-2.

Chart Speeds -- 30 inches/hour and 60 inches/hour.

Chart Paper -- 10 inches wide, 8 inches for video dropout data, 2 inches for optional event markers. Type 1DR10 chart paper, Time Scale ruling 1/10 inch.

Reference System -- Zener diode.

Event Markers -- Up to 4 event markers for the following options: audio track control, track scratch indicator, and splice indicator.

Pen System -- Gravity feed pen system.

Power Requirements -- 105-125V, 60 cps (approx. 35 watts). Specify Option J for 115V, 50 cps, Option K for 230V, 50 cps. Line cord with NEMA 3-prong (grounded) plug is furnished.

See Nesco Instruments Technical Bulletin JY100A-10 for further information regarding specification and supplies.

Model 11 Splice Detector -- Photo cell detector is mounted on video tape transport to detect splices. Each splice actuates an event marker on the Nesco Chart Recorder and is tallied simultaneously on the splice counter.

Model 12 Splice Counter -- 3 digit mechanical counter.

Model 13 Audio Track Dropout Detector

Input Signal Trans-audio -- $\frac{0.5}{3}$ volts min. / volts max.

Input Impedance -- 10 kΩ.

Output -- Each output "X" dB below a reference output is detected and actuates an event marker on the Nesco recorder. Reference may be set between 0.5 volts and 3.0 volts by internal adjustment. Detector level "X" dB below reference may be set 0-10 dB below reference by an internal adjustment.

Model 14 Control Track Dropout Detector --

Input Signal from Control Track -- 240 Hz pulse, 20 volts max.

Input Impedance -- 10 kΩ.

Output -- Each output "X" dB below a reference output is detected and actuates an event marker on the Nesco recorder. Reference may be set between 20 volts and 1 volt by internal adjustment. Detector level "X" dB below reference may be set 0-10 dB below reference by an internal adjustment.

Model 15 Scratch Detector -- Will detect a scratch which causes dropouts below the set video threshold level, providing the scratch is parallel to the direction of tape travel. A scratch will be presented on the strip chart only if it is long enough to be detected for four head scan periods.

Model 16 Signal to Noise Threshold Detector -- (Deviation of FM carrier due only to system noise.)

Input -- Constant FM carrier with only noise deviation.

Input Impedance -- 100 kΩ. System noise will be measured at output of VTR demodulation circuit.

Output -- Indicated by chart recorder event marker.

Model 17 Totalized Video Dropout Counter -- 3 digit BCD counter with Nixie readout. Indicates the total number of dropouts in a complete run.

Model 18 Dropout Simulator -- Dropout simulator is inserted in series between the output of the second switcher and the input to the demodulator.

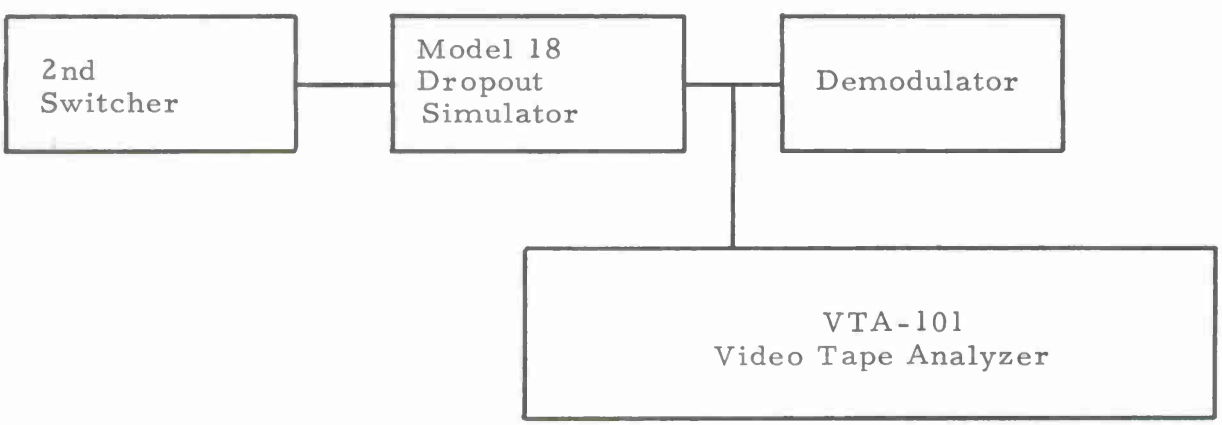

Simulator Dropout Depth -- Adjustable from 0 dB (with respect to reference level) to 40 dB in 1 dB steps.

Dropout Duration -- Fixed 3, 6, 12, 24 μs selected by front panel switch. Fixed sequenced pulses 3, 6; 3, 6, 12; 3, 6, 12, 24 μs. Sequence changes each repetition rate. Sequence selected by front panel switch.

BIBLIOGRAPHY

1. Carson, R. H.: Dropouts in Magnetic Tape Recording Systems. Washington, D.C., U.S. Naval Research Labs. From a paper presented at the I.R.E. Convention, New York, 1962.

2. Homberg, Berten A. and Irving Moskovitz: Compensation for Dropouts in Television Magnetic Tape Recording. Minnesota Mining and Manufacturing Company, (n.d.).

3. Geddes, W. K. E.: "Dropouts in Video Tape Recording." B.B.C. Engineering Monograph No. 57, Part I and Part II. London, June, 1965.

4. Stubbe, M.: "On the Measurement and Valuation of Dropout Errors in Video Tape Recording." Conference Record. I.E.E. International Conference on Magnetic Recording, July, 1964, p. 9.

5. Homberg, Berten A.: A Standard Tape for Evaluating Magnetic Video Recorder Dropout and Noise Immunity Factor. Minnesota Mining and Manufacturing Company, (n.d.).

NRZ DATA

CLOCK

SHIFT

NB/PM DATA TO RECORDER INPUT

HIGH HEAD CURRENT

TO HEAD CURRENT MODULATOR

LOW HEAD CURRENT

NOTE: ALL LU315, PIN 6 TO +4.5V
PIN 1 TO GRD.

ENCODER

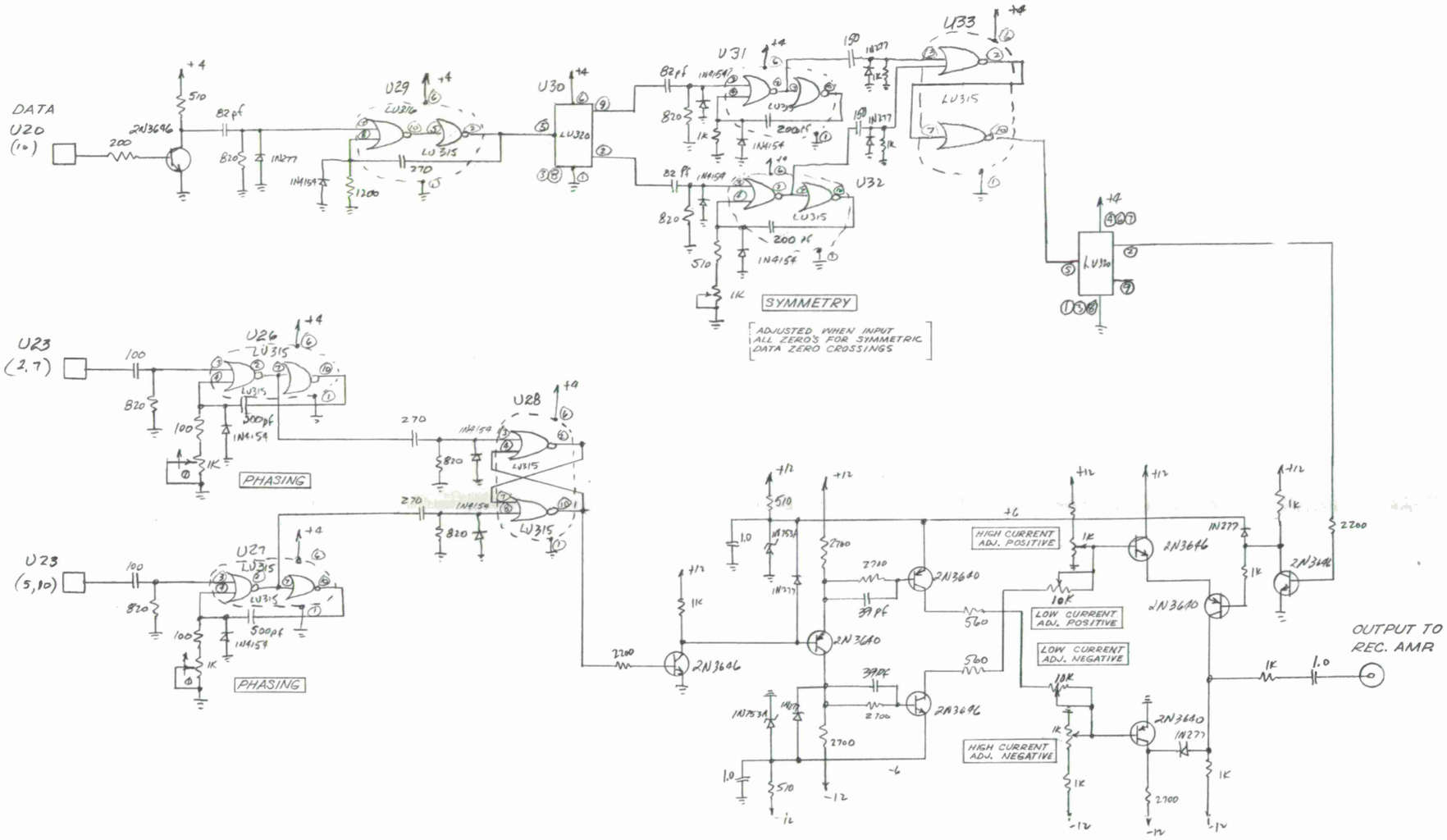

HEAD CURRENT MODULATOR

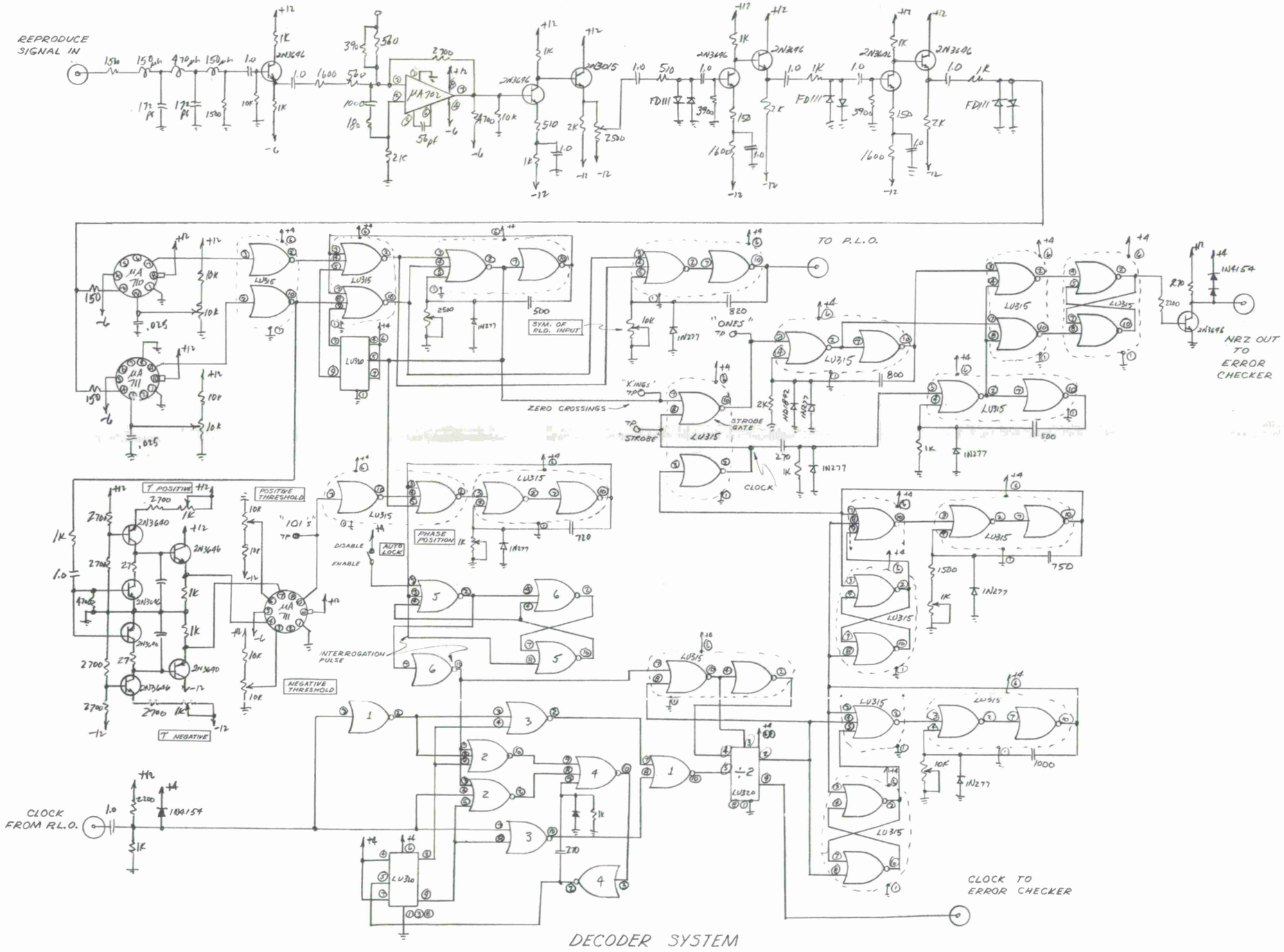

DECODER SYSTEM

DOCUMENT CONTROL DATA – R&D

(Security classification of title, body of abstract and indexing annotation must be entered when the overall report is classified)

1. ORIGINATING ACTIVITY *(Corporate author)* Orion Products Inc. under Purchase Order No. CC-975 to M.I.T. Lincoln Laboratory	2a. REPORT SECURITY CLASSIFICATION Unclassified 2b. GROUP None

3. REPORT TITLE

Study of High Packing Density and High Transfer Rate Encoder/Decoder

4. DESCRIPTIVE NOTES *(Type of report and inclusive dates)*

Final Report

5. AUTHOR(S) *(Last name, first name, initial)*

Wood, John

6. REPORT DATE	7a. TOTAL NO. OF PAGES	7b. NO. OF REFS
None given	180	5

8a. CONTRACT OR GRANT NO. AF 19(628)-5167 b. PROJECT NO. 627A c. d.	9a. ORIGINATOR'S REPORT NUMBER(S) Final Report 9b. OTHER REPORT NO(S) *(Any other numbers that may be assigned this report)* ESD-TR-67-318

10. AVAILABILITY/LIMITATION NOTICES

This document has been approved for public release and sale; its distribution is unlimited.

11. SUPPLEMENTARY NOTES	12. SPONSORING MILITARY ACTIVITY
None	Air Force Systems Command, USAF

13. ABSTRACT

The report covering the narrow band/phase modulated (NB/PM) digital encoding/decoding technique deals primarily with the evaluation of this system in terms of digital bit error rates as a function of digital bit packing density. The evaluation is based on a series of comprehensive tests conducted by controlled procedures.

The collated results of all the tests are presented in graphical form to show quantitatively the overall performance of this system in a statistical manner.

14. KEY WORDS

data storage
errors
magnetic tape
digital systems
data processing